UNITED KINGDOM • CHINA • MALAYSIA

PERFORMANCE EVALUATION AND MODELLING OF A SMALL-SCALE BIOMASS GASIFIER

By

HUSSEIN KISIKI NSAMBA

Thesis submitted to the University of Nottingham, (UK) for the Degree of Doctor of Philosophy (Chemical Engineering)

October, 2017

Dedication

I dedicate the efforts of my dissertation and content to my late mother Najjemba Tijarah with a special feeling of gratitude to my father Hajj. Kaluuma Muhammadi.

Dear mum, your last words of wisdom, encouragement and support remain my source of motivation at all times. My sisters Namuyiga, Nakachwa and brothers Lubyayi, Yiga, Jengo,Muyiga and Sagala, let this education remain an eye opener, a source of inspiration and gratitude that we remain solid and breed a generation of children that will keep the Najjemba fraternity shinning!

I also dedicate this dissertation to the entire Kisikifamily where this scholarly attainment becomes the first highest qualification since the history of our family. Special dedications to the Invention Plus Group, Limited for granting me a study leave to obtain this highest academic qualification from the UK.

I profoundly dedicate this work to my wonderful wife and children Raudha, Tijarah and Tariq for the joy you bring to my life. May you always live to embrace and value education! It is my greatest recommendation for you my children. To my wife Hajarah, your immeasurable support can't be quantified! To the World, you are single individuals but to me, you are the World!

Abstract

Many parts of the World have remained underdeveloped due to the lack of access to electricity. Developing and promoting alternative energy sources from renewable materials would assist to mitigate the energy crisis in many parts especially in the World.

This research examined the possibility of using a 10KW power pallet as a sustainable energy generation system especially for energy poor areas. This was achieved through the gasification of woodchips at varying moisture content, varying gasification times and at varying electrical loads while investigating the numerous changes in the major factors affecting gasification such as temperature, fuel consumption rate, equivalence ratio (ER), quality of the producer gas, heating value, carbon conversion efficiency as well as the cold gasification efficiency of the gasifier. Experimental data was analysed and interpreted by one way Analysis of Variance (Anova) to establish a relationship on the effect of the major factors affecting gasification as investigated in this study.

It was discovered that the gasifier is an autothermal system that maintains a steady state of thermodynamic equilibrium for longer hours as long as the gasifier is constantly supplied with a drier fuel. The gasifier stably and optimally operates with woodchips of moisture content less than 10% to produce an energy rich gas for gasification times longer than six hours to yield a gas rich in Hydrogen (H_2), Carbon monoxide (CO) and methane (CH_4) at a respective concentration of up to 18.1%, 25.3% and 2.2% with a corresponding Higher Heating Value (HHV), Cold Gas Efficiency (CGE) and gas production rate of 6.4MJ/m^3, 75.8% and 2.34m^3/kg respectively. The reactor takes longer time to attain thermodynamic equilibrium once operated with woodchips of moisture content above 15%. This subsequently affects the quality of producer gas yielding a gas of low calorific value that would even clog

the engine. The moisture content of the wood chips was found to play a very significant role in determining the values of temperatures attained and subsequently determining the quality of producer gas. The gasifier was found to produce the required energy up to the design capacity of 10KW required for several industrial applications. Increasing the engine throttle valve increased the frequency of the engine and subsequently the voltage. The designed energy output of up to 10KW could only be produced if the engine frequency was 60HZ and could be lower if the engine operated at a lower frequency.

A thermodynamic equilibrium model was further developed to predict the composition of producer gas going to the engine. The thermodynamic equilibrium model yielded a gas composition of 25.99%, 23.92%, and 0.42% for CO, H_2 and CH_4 respectively that was in good agreement with the experimental results at 850 ºC and ER of 0.27. Similarly, the modelled gasification temperature of 870.85ºC corresponds with a minor deviation of 2.5% with the experimental gasification temperature of 850ºC. The exhaust stream composition contained Carbondioxide (CO_2) of upto 20% which is on the higher side because air was used as the gasifying agent and the gasifier was completely autothermal. Such CO_2 concentration ought to be lowered if the gasifier is to be adopted as a sustainable renewable energy system. The gasifier was found to operate better with wood chips in the size range between 1.3cm – 4.0cm as very fine wood chips would block the flow of air hence compromising on the sustainability of the exothermic reactions and bigger wood chip particles would not be easily broken down by the auger hence resisting the flow of the woodchips into the reactor. Operating the gasifier at optimal conditions yields a gas of high calorific value good enough to make it a reliable standalone system that could be integrated into sustainable bioenergy systems.

ACKNOWLEDGEMENTS

With due respect, I thank the Almighty Allah for having assisted me attain this highly sought qualification in academia. Special thanks are extended to the Islamic Development Bank Group for sponsoring my PhD studies under the Merit Scholarship Program together with the University of Nottingham. I thank you for having identified my potentials and for considering me as a potential candidate for selection and sponsorshipup to this stage.

Special thanks are extended to Professor Hao Liu and Professor Colin Snape who have mentored me during this academic tenure. Thank you so much for the much celebrated cooperation we have had since I joined Nottingham whose results are reflected under this piece of literature. I must sincerely and vehemently thank you for all your tireless support dear Prof Hao Liu. Your support towards my doctorate candidature is greatly appreciated. I appreciate the technical assistance offered by Dr Andrew Rollinson for the training and induction especially during the initial stages of my PhD. Special thanks to my other colleagues Rashid Mijumbi, Muniirah Mbabazi, Twaha Sennoga, Wenbin Zhang, Andrew Stone, Nassanga Shamim, Ivan Kirunda, and all my colleagues from Derby UK for the numerous support you offered towards my PhD journey. I say thank you to everyone out there.

Lastly but not least, I duly extend my heartiest appreciation to my father Hajj. Kaluuma Muhammad for educating and nurturing me with the best morals that have made me survive against all odds. My late mum, may the Almighty Allah forgive your soul for all the struggles and sacrifices you made for us. Rest in peace mum as I dedicate this piece of literature to you. I will always miss you!

DECLARATION

I hereby declare that this thesis is my ORIGINAL work except for quotations and citations which have been duly acknowledged. I also declare that it has not been previously, and is not currently, submitted for any other degree at University Of Nottingham or at any other Institution.

NSAMBA HUSSEIN KISIKI

DATE: October/05/2017

List of Tables

List of Figures

Nomenclatures

The symbols used in equations in the text are explained immediately below the equation where the symbols appear.

Abbreviations

AC	Ash Content
ASTM	American Society for Testing and Materials
BIGCC	biomass-fired integrated gasifier combined cycle
CDM	Clean Development Mechanism
CFR	Code of Federal Regulations
C2C	Cabazole Char
CEMS	Continuous Emission Monitoring Systems
CER	Certified Emission Reductions
CHP	Combined Heat and Power
DDGS	Distillers Grains
ER	Equivalence Ratio
FBFP	FluidizedBedFastPyrolysis
FBFPCT	FluidisedBedFastPyrolysiswithCatalyticTreatment
FC	Fixed Carbon
FCR	Fuel Consumption Rate
GDP	Gross Domestic Product
GHG	Green House Gas
GR	Gasifying Ratio
ICAFB	internally circulating aerated fluidized bed
ICE	Internal Combustion Engine
IEA	International energy agency
IGCC	Integrated Gasification Combined Cycle
HCCI	Homogeneous Charge Compression Ignition
HHV	Higher Heating Value
LHV	LowerHeating Value
MJ	Mega Joule
MSW	Municipal Solid Waste
PM	Particulate Matter
SGR	Specific Gasification Rate
TMP	Thermo Mechanical Pulp
UNCED	United Nations Conference on Environment and Development
USEPA	United States Environmental Protection Agency
VM	Volatile Matter
VOC	volatile organic compounds
WGS	Water Gas Shift

TABLE OF CONTENTS

CHAPTER 1

1.0 INTRODUCTION

1.1 The need for bioenergy

Energy is one of the core drivers for sustainable development and calls for its adoption if national progress should be achieved. Countries that are endowed with rich energy source reserves such as Saudi Arabia, Iran and the Middle East have experienced robust growth over other regions that are energy source deficient. Conventionally, fossil fuels have been the core drivers of energy supplemented by nuclear and other renewable energy sources. Fossil fuels are not only non-renewable but they are also not environmentally friendly with a highly proposed contribution to global warming and climate change subsequently. Globalefforts have been put in place to mitigate climate change and ensure sustainable energy security by advocating for sustainable energy sources such as bioenergy from biomass.

Biomass can be defined as plant and animal matter of recent origin. The study of biomass as a potential energy source has attracted tremendous progress (Barisano et al., 2014; Bauen, Berndes, Junginger, Vuille, & Londo, 2009; Bruun, Jensen, Khanh Vu, & Sommer, 2014) because it produces carbon neutral emission levels compared to fossil fuels (IEA, 2006; Vinterbäck, 2010). Biomass as a source of energy has been studied in depth(ZEF 2014; Chutichai et al. 2012; Doherty et al. 2009; Bauen et al. 2009) and reveals growing evidence that biomass will continue to be on the battle front as a source of energy globally (IEA, 2012).

Biomass is also widely distributed and, relatively easy to access from season to season which makes it a renewable resource compared to fossil fuels which replenish with time when ever used(Roethlisberger & Favrat, 2002). The wastes generated as bio agricultural residues arising from the consumption of biomass form a core component in completing the bioenergy cycle if used efficiently. However, the management of biomass solid wastes continues to be a major challenge in the developing world today. Poor management of these wastes arises from low or poor financial resources to promote modern technology that can avert the risks related with the ancient waste management. Presently, commonly exercised methods include land filling (Hau & Ray, 2008) but consumes up space that would otherwise have been used for construction or other development projects. By considering the exponential increase in human population, the rise in land value and real estate management as well as the need for infrastructural development, it is not a logical decision to promote technologies such as land filling that would otherwise compromise development. Incineration as a means for biomass waste deposition (Deydier, Marias, Bernada, Couture, & Michon, 2010)(Hau & Ray, 2008) has been in addition exercised but its dependency is not sustainable due to its associated pollutant sources if not well controlled. However, biomass-fired integrated gasifier combined cycle (BIGCC) technology is a promising alternative for handling organic wastes (Andri *et al.*, 2001).

The energy produced from biomass wastes has the potential to meet a large portion of the world's energy demand, given its abundant availability on a sustainable basis.It is motivating to produce energy from biomass because it produces less greenhouse emissions compared to fossil fuels(Moroń & Rybak, 2015), it is widely distributed, relatively easy to collect and it usually contains reduced air pollutants than coal or oil (Ndibe, Grathwohl, Paneru, Maier, & Scheffknecht, 2015; C. Wang, Zhang, Chang, & Pang, 2015).Interest in the energy from

biomass has been enhanced because of its potential to be generated locally and could make many countries less-dependent on foreign petroleum resources through technologies such as gasification.

Gasification is the thermal conversion of solid material into a gaseous product in a limited air supply at higher temperatures. Biomass gasification is a promising technology that can produce the green, high efficiency, and eco-friendly gas fuels, such as H_2, CO, CH_4 and other hydrocarbons (Chiang, Lu, Lin, & Chien, 2013). The use of biomass as a starting feedstock for gasification can provide a more positive solution through the provision of energy including electrical energy, heat, and transportation fuels which can reduce emissions, sulphur and heavy metals from the environment, while potentially improving rural income and energy security through the substitution of coal, oil and natural gas.

1.2 Statement of the problem

The lack of access to electricity especially in developing countries has led to low industrialisationmaking many parts of the World under developed.Additionally, biomass fuel which could be used as an alternative energy source is characterised by its bulky, high moisture, fibrous content and low-energy-density which makes it difficult for transportation to processing plants. The costs involved in moving biomass subsequently increase the costs of energy generation. Biomass if processed from the source could be a cheaper energy option but this has been limited by a lack of access to small scale mobiletechnologies that can effectively process it to compliment the energy demands. There is need to test mobile energy technologies that could be transported to the biomass source to offer sufficient energy

solutions and increase access to electricity especially to energy poor areas. Providing such a solution could help in managing wastes, reducing greenhouse emissions, providing alternative stand-aloneenergy solutions and reducing on the cost incurred during biomass transportation.

1.3 Overall objectives

This study aims at investigating the optimum performance of a 10kWe downdraft gasifier as a micro scale gasification system with potential to provide independent energy systems which can be integrated into energy poor areas.The goal of this study was to investigate fixed bed downdraft gasification as a potential alternative to the production of producer gas and subsequently electricity from biomass residues with potential to improve on the energy disparity of energy remote areas.

The research work is conducted to achieve the following specific objectives

1. To operate the gasifier under varying electricalloads (2,4,10kWe)and determine the effect of airflow rate on the overall gasification process through the quantification of the feed and co-products in terms of

    i. Temperature profile of the gasifier
    ii. Incoming air velocity and temperature
    iii. The mass flow rate of the gasifier
    iv. The ER of the gasifier
    v. The variation of product gas composition (CH_4,H_2,CO,CO_2,NO_X)

vi. the calorific value of the producer gas

vii. Carbon Conversion efficiency

viii. Cold Gas Efficiency of the gasifier

2. To run the downdraft gasifier with wood chips at a constant load (10KWe)at varyinggasification times (2hrs, 4hrs, and 6hrs) and determine

   i. Temperature profile of the gasifier

   ii. Incoming air velocity and temperature

   iii. The mass flow rate of the gasifier

   iv. the ER of the gasifier

   v. The rate of char formation

   vi. The variation of product gas composition (CH_4,H_2,CO,CO_2,NO_X)

   vii. the calorific value of the producer gas and its energy density

   viii. Carbon Conversion efficiency

   ix. Cold Gas Efficiency of the gasifier

   x. Monitor the composition of the exhaust stream

3. To run the downdraft gasifier with woodchips of varying moisture content at a constant gasification time (6hrs)and load (10KWe) and evaluate its performance in terms of

   i. Temperature profile of the gasifier

   ii. Incoming air velocity and temperature

   iii. The mass flow rate of the gasifier

   iv. the ER of the gasifier

   v. The variation of product gas composition (CH_4,H_2,CO,CO_2,NO_X)

   vi. the calorific value of the producer gas

vii. Carbon Conversion efficiency

viii. Cold Gas Efficiency of the gasifier

4. To develop a thermochemical equilibrium model and predict producer gas composition in the down draft gasifier and used to validate the experimental findings at optimal conditions

5. To recommend the best operating conditions and possible system improvement

CHAPTER 2

2.0 LITERATURE REVIEW

2.1 Introduction

The close and unavoidable fossil fuels exhaustion, the energetic dependence on traditional energy sources, the environmental problems associated with their exploitation and the increasing energy demand are reasons more than enough to think that it is imminent that a change on the worldwide energy system has to occur (González et al., 2008). All over the World, Governments, scientists as well as independent International bodies are sourcing for alternative ways of sustaining the next generation of fuels. Gasification of biomass is seen as a promising technology (Andri et al.,, 1997; Saravanakumar et al.,2007; Yoon et al., 2012; Kumar, Jones, & Hanna, 2009; McKendry, 2002) due to its potential to mitigate climate change. Gasification is one of the attractive technologies for alternative fuel from biomass and the equipment used in the gasification process is commonly referred to as a gasifier. Gasification is the conversion of biomass to a gaseous fuel by heating in a gasification medium such as air, oxygen or steam (McKendry, 2002). Biomass gasification is accompanied by the evolution of lesser emissions, making use of waste biomass that would otherwise decompose to generate greenhouse gases. Harnessing of biomass and urban wastes via thermochemical route is not only environmentally benign but also economically viable (Rao, 2003). In tropical countries such as Uganda, biomass grows more productively, which can be converted efficiently into modern energy carriers such as biomass to gaseous fuels via gasification, biomass to liquid fuels through the fisher tropsch method and biomass to electricity via the Integrated Gasification Combined Cycle (IGCC) which can all be implemented more affluently into society. The feasibility of IGCC largely depends on the

composition and quality of syngas channeled to the engine. Thus, the composition and quality of syngas determines the engine performance as well as the gasification efficiency hence syngas must be produced under optimal conditions to maximize its efficiency as well as the engine performance. Critical factors such as feedstock chemical composition, its moisture and ash content, gasifier configuration, feedstock size and density, equivalence ratio (ER), reaction temperature profile and turn down of power that positively influence the reaction kinetics and subsequently affect the calorific value of gas as well as the overall efficiency of conversion must be optimized for a high yield syngas. Understanding the chemistry of heterogeneous and homogeneous reactions taking place in the biomass gasifier and specifically in the reduction zone assists in the optimization of the process. Processes such as biomass physical pre-treatment which include drying assist in the attainment of dry samples which work well in the gasifier. The presence of high biomass moisture content would lower the gasification temperatures as some heat is lost during quenching which lowers the gasifier performance since more biomass must be burnt for longer hours before the system attains the state of thermodynamic equilibrium. While making selection on the choice of the gasifier, a downdraft gasifier is a preferable method for carrying out biomass gasification because the produced gas has viable heating value with low tar content and can be cleaned to high purity, suitable for Internal Combustion Engine (ICE) usage and chemical processing applications (Nisamaneenate et al., 2014).Out of different gasifier design, downdraft gasifier produces relatively low content of tars in the gas (~ 0.1%) (Thomas and Markson, 1983). As the feedstock proceeds through the different section of a downdraft gasifier the following physical, chemical and thermal processes may take place simultaneously or sequentially depending on the properties of feedstock and the design of the gasifier(Chawdhury & Mahkamov, 2010). The major processes leading to the formation of syngas in an autothermal downdraft gasifier occur in the order that combustion is the initial process where the carbon

matter inherent in biomass reacts with oxygen to form CO_2 and heat. These combustion reactions are highly exothermic and cause a rapid temperature increase up to 1100-1500 ^oC creating a burning zone in the section where air is supplied. Generally, a small amount of air introduced into the reactor allows some of the organic material to be burned to produce CO_2 and heat.

$C+O_2 \rightarrow CO_2$ (+ 393 MJ/kg mole) (2.1)

$2H_2 + O_2 \rightarrow 2H_2O$ (+ 242 MJ/kg mole) (2.2)

The produced heat initiates the pyrolysis at temperatures above 250 ^oC, pyrolyzing of the biomass feedstock (Chawdhury & Mahkamov, 2010). Large molecules (cellulose, hemi-cellulose and lignin) are broken down into carbon (char) and medium size molecules (volatiles)

Dry feedstock + Heat $\rightarrow$ Char + Volatiles (2.3)

Drying occurs as the biomass is introduced into the downdraft gasifier from the top due to the heat transfer from the lower part of the gasifier that subsequently dries the incoming biomass.

Moist feedstock + Heat $\rightarrow$ Dry feedstock + 2 H_2O (2.4)

Following the formation of products from both the combustion as well as the pyrolysis zones, the reaction products flow downwards into the reduction zone. Thus, water vapour flows downwards and adds to the vapour formed in the oxidation zone which partly reduces to hydrogen while the rest ends up as moisture in the gas. Carbon is an initially put reactant in

the reduction zone of the downdraft gasifier but continues to be produced as a pyrotic product. Via the reduction process, charcoal helps in the formation of CO, CH_4 andH_2 while the sensible heat of the gases and charcoal is converted into the chemical energy of the producer gas. Subsequent reactions occur when the formed CO and residual water react to form CH_4 and excess carbon dioxide while the temperature of the reduction zone can reach upto 800 -1100 °C.

By considering the rapid increase in human population, the rise in industrialization activities as well as the need for alternative energy to mitigate climate change due to fossil fuels, there is a need to harness energy from biomass which could offer solutions to majority of the challenges experienced as a result of over dependence to fossil fuels as well as address the energy disparity challenge faced in many parts of the World. The energy produced from biomass wastes has the potential to meet a large portion of the world's energy demand, given its abundant availability on a sustainable basis. Interest in the energy from biomass has been enhanced because of its potential to be generated locally and could make many countries less-dependent on foreign petroleum resources. Biomass gasification is a promising technology that can produce the green, high efficiency, and eco-friendly gas fuels, such as Hydrogen (H_2), Carbon monoxide (CO), methane (CH_4) and other hydrocarbons(Chiang et al., 2013)The main intention behind biomass gasification is to generate producer gas rich in H_2, CO, and $CH_4$with a higher calorific value for its integration into energy production mix. Because of its relevance, different biomass feedstocks such as wood chips, barks, olive pomace and hazelnut shells have been tested for their energy potential (Olgun, Ozdogan, & Yinesor, 2010).

The use of biomass can provide a more positive solution through the provision of energy services including electrical energy, heat, and transportation fuels which can reduce emissions, sulphur and heavy metals from the environment, while potentially improving rural income and energy security through the substitution of coal, oil and natural gas. Notwithstanding the worldwide research on biomass gasification studies, efforts to optimize energy efficiency from small scale bioenergy systems are still narrow. It is with in this context that this review discusses in details the production of energy from biomass devoted to in-depth analysis of the chemistry of reactions for biomass conversion to energy, technologies involved for biomass conversion to energy generation, factors affecting biomass gasification for energy generation and the effect of production conditions which will clear any uncertainties on the possibility of optimizing energy recovery from biomass.

2.2 The chemistry of reactions during biomass gasification

The chemistry of gasificationis quite a complicated field of study whose extent involves a series of chemical reactions that are responsible for the end product and would bedependent ona number of operating conditions such as, the nature and type of feedstock used, thedesign and type of the gasifier, temperature and pressure, among others. Generally, the use of an oxidizing agent initiates combustion reactions which partially oxides the carbon material to release H_2 and CO and a minor fraction of carbon being completely oxidized to CO_2. The heat generated during partial combustion provides the energy required to complete endothermic reactions within the gasifier. The major chemical reactions inside the gasifier include both exothermic and endothermic reactions as shown in the Table 2.1 below

Table 2.1 Major chemical reactions in an autothermal gasifier

Chemical reaction	Enthalpy of reaction	Type of reaction	Equation number
$C + ½ O_2 \rightarrow CO$	-111 MJ/kmol	Partial oxidation	2.1
$CO + ½ O_2 \rightarrow CO_2$	-283 MJ/kmol	Partial oxidation	2.2
$H_2 + ½ O_2 \rightarrow H_2O$	-242 MJ/kmol		2.3
$C + H_2O \leftrightarrow CO + H_2$	+131 MJ/kmol	Water-Gas Reaction	2.4
$C + CO_2 \leftrightarrow 2CO$	+172 MJ/kmol	Boudouard Reaction	2.5
$C + 2H_2 \leftrightarrow CH_4$	-75 MJ/kmol	Methanation Reaction	2.6

During the process of gasification in autothermal gasifiers, shown in Figure 2.1, the oxidizing agent is passed through the fuel bed and an ignition reaction is initiated and in this process, four different zones develop along the reactor which include drying, devolatilization, oxidation and reduction as shown in Figure 2.1. Generally, when a small amount of air is introduced into the reactor for self-sustaining fixed bed gasifiers, this allows some of the organic material to be burned to produce CO (equation 2.1) and CO_2 and heat (equation 2.2). The produced heat initiates the pyrolysis at temperatures above 250^{o}C (equation 2.3), pyrolyzing the biomass feedstock (Chawdhury & Mahkamov, 2010). Large molecules (cellulose, hemi-cellulose and lignin) are broken down into carbon (char) and medium size molecules (volatiles). Drying occurs as the biomass is introduced into the gasifier from the top due to the heat transfer from the lower part of the gasifier that subsequently dries the incoming biomass. Drying can also be initiated by the waste or exhaust heat which can be recycled as per the system design and configuration. Following the formation of products from both the combustion (equation 2.1 – 2.3) as

well as the pyrolysis zones (equation 2.4 – 2.6), the reaction productsflow downwards into the reduction zone.Thus, water vapor flows downwards and adds to the vapor formed in the oxidation zone which partly reduces to hydrogen while the rest ends up as moisture in the gas. Carbon (Charcoal) can be an initially put reactant in the reduction zone of the reactor but continues to be produced as a pyrotic product during the process of gasification. The charcoal helps in the formation of CO, CH_4 andH_2 while the sensible heat of the gases and charcoal is converted into the chemical energy of the producer gas. Subsequent reactions occur when the formed CO and residual water react to form CH_4 and excess CO_2 while the temperature of the reduction zone can reach upto 800 -1100 °C.

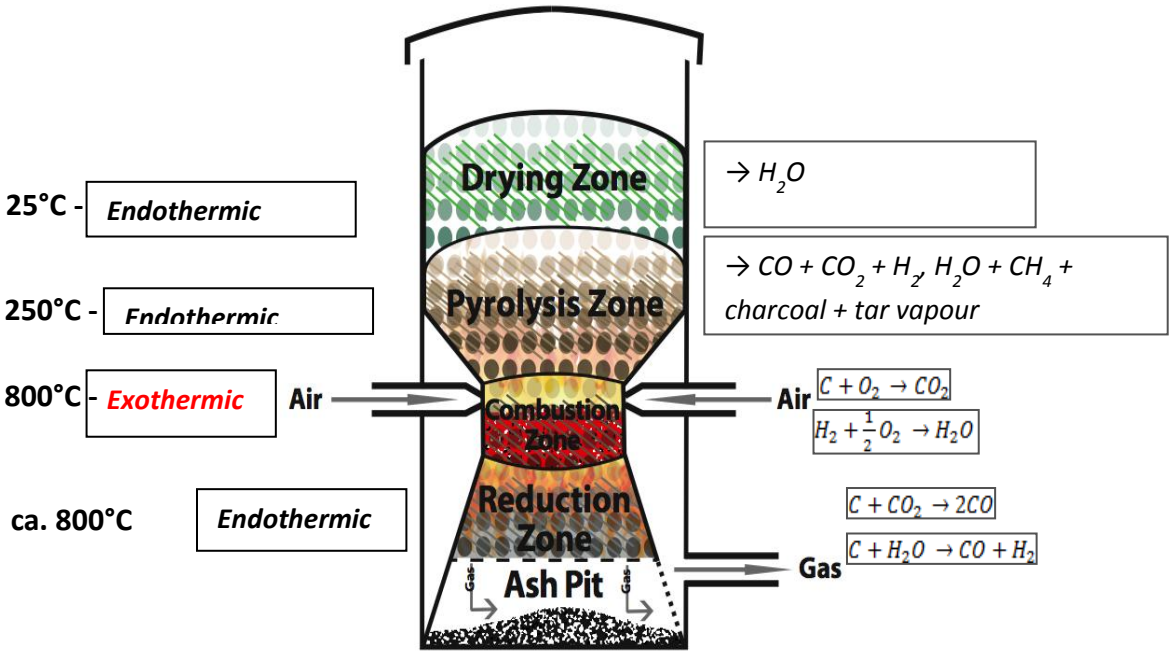

Figure 2.1 Typical gasification reactions in an autothermal gasifier

2.2.1 Application of biomass for combined heat and power generation

Combined heat and power generation (CHP) or cogeneration has been considered as the major alternative to traditionalsystems in terms of significant energy saving and environmentalconservation(Dentice d'Accadia, Sasso, Sibilio, & Vanoli, 2003). Harnessing both heat and power leverages on costs of production and increases system efficiency. In essence, power from biomass can be produced thermochemically through pyrolysis,gasification, combustion or produced biologically via biogas anaerobic digestion or by using the fuel cell technology. However, the biological and fuel cell process of power generation is outside the scope of this review. During the primary biomass gasification or pyrolysis, the generated synthesis gas is burnt in the internal combustion engine to generate the useful energy and for combustion, biomass is burnt directly in a furnace with excess air to generate heat that boils water to form steam which drives a steam turbine that generates electricity. Details of the application of the thermochemical conversion techniques are summarized in Figure 2.2- 2.3 and a detailed application in Table 2.2. Biomass as a source of power has been studied in depth (Liu, Ye, Zhao, & Zhao, 2015) and the progress so far made reveals that biomass will continue to be on the forefront as a source of energy globally (IEA, 2012). While assessing two scales of a 50 MWth facility based on indigenous Willow and a 300MWth facility based at an international port importing woodchip by (Gallagher & Murphy, 2013), their model suggested that eleven 50MWth gasifiers, each requiring 6800 ha of Willow, in a rural environment, with gas grid injection to the distribution grid, would satisfy the shortfall in the 2020 target for renewable energy supply in the heat market in Ireland. Two 300 MW_{th} facilities each requiring importation of 1,000,000 t/yr of woodchip, situated adjacent to an international port satisfied the shortfall. For all these justifications, efforts to harness biomass as a source of energy need to be explored. (Lombardi, Carnevale,

& Corti, 2012) carried out an analysis of two alternative thermo-chemical processes for waste treatment; the high temperature gasification and gasification associated to plasma process. From their results, it was found out that the technological option based on high temperature gasification and energy recovery in a simple steam cycle does not offer any energetic advantage with respect to the traditional Waste-to-Energy option, with quite low efficiency values (13–14%). In the case of plasma gasification process, the energetic performances resulted into higher (two–four percentage points) with respect to traditional waste to energy option. On the other hand, a very promising alternative for wet biomass is the less investigated hydrothermal gasification to produce a hydrogen rich fuel gas (Schmieder et al., 2000). Tao et al., (2015) also carried out a study to use electrochemical catalytic reforming (ECR) technique, known as electric current enhanced catalytic reforming technique to convert the biomass gasification tar into syngas which showed promising capabilities. Despite thetremendous progress made in the study of biomass as a potential energy source(Barisano et al., 2014; Bauen et al., 2009; Bruun et al., 2014), great effort is still desired to achieve maximum process optimization and system energy efficiency because different gasifiers have varying configuration and have differentprocess optimization settings which should be ascertained.

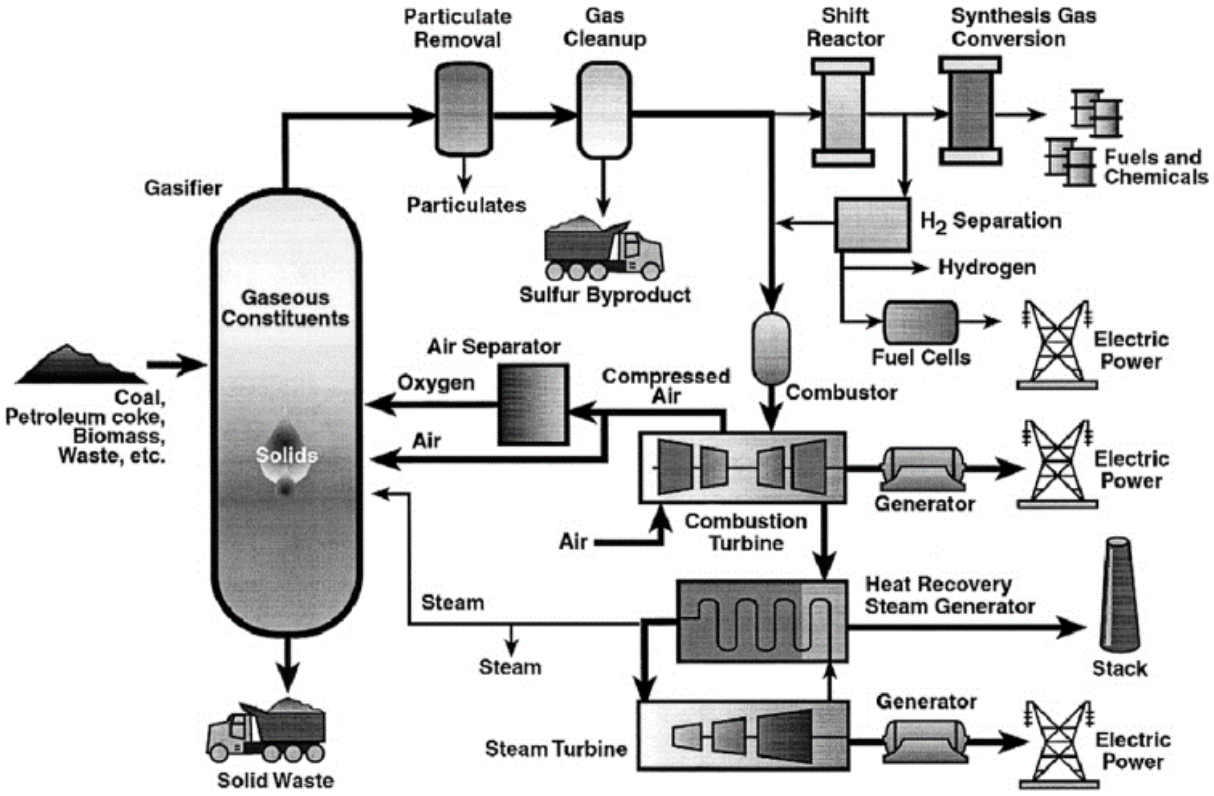

Figure 2.2 Summary of gasification technology for production of liquid fuels and electricity from biomass(Huber, Iborra, & Corma, 2006)

Table 2.2 Application of thermochemical techniques for combined heat and power generation

Primary energy generation	**Technology**	**Description**	**References**
Combustion	Stirling cycle	A stirling engine operates by cyclic compression and expansion of air or other gas at different temperatures, such that there is a net conversion of heat energy to mechanical work.Three major types of stirling engines exist distinguished by the way they move the air between the hot and cold areas.The advantages of the ideal stirling cycle include. (i) The thermal efficiency of the cycle with ideal regeneration equal to the Carnot cycle. (ii) The Carnot cycle is obtained by substitution of two isentropic processes with two constant-volume processes. (iii) The ideal Stirling engine has the maximum possible mechanical efficiency	(Formosa & Despesse, 2010; Kongtragool & Wongwises, 2003, 2006; Stine, 1994)
	Combustion with Organic Rankine Cycle	Rankine cycle is a closed-loop system where a working fluid repeatedly circulates through four components to transform waste heat into mechanical or electrical power. If the selected working fluid is organic in nature, hence Organic Rankine Cycle (ORC).	(Bini & Prima, 2010; Sprouse & Depcik, 2013; Tahani, Javan, & Biglari, 2013; Vaja & Gambarotta, 2010)
	Combustion with steam cycle	In a steam power plant, a steam turbine is used for extracting the heat from the steam and turning it into work. The turbine usually drives a generator that turns the work from the turbine into electricity. The steam, used by the turbine, can be recycled by cooling it until it condensates into water and then return it as feed water to the boiler.	(Declercq, 2006; Lucquiaud & Gibbins, 2011; Soundararajan, Anantharaman, & Gundersen, 2014; Teir, 2002)

Co-firing	Indirect cofiring	Biomass co-firing consists of burning biomass along with coal in coal-fired power plants with a net electric efficiency ranging from 35-44%. It can be classified into : a) Direct co-firing, using a single boiler with either common or separate burners b) Indirect co-firing, in which a gasifier converts solid biomass into a gaseous fuel; c) Parallel co-firing, in which a separate boiler is used for biomass, and its steam generationis then mixed with steam from conventional boilers.	(Scheffknecht and Ndibe, 2015; Service et al., 2012; US DOE, 2004)
Gasification	Fixed bed gasification (updraft, downdraft, crossdraft)	Also known as "moving bed gasifiers", are updraft and downdraft reactors based on the directions of the flows of the fuel and the oxidant (either co- or countercurrent). The gasification process is based on partial combustion of the fuel in order to produce heat required to maintain temperature favorable for gasification reactions.	(Tinaut, Melgar, Pérez, & Horrillo, 2008)
	Fluidized bed gasification(bubbling, circulating, dual)	In such a reactor, the fuel together with inert bed material behaves like a fluid by forcing a gas (fluidization medium) through the solid inventory of the reactor.	(Siedlecki, de Jong, & Verkooijen, 2011)(Makwana, Joshi, Athawale, Singh, & Mohanty, 2015)

	Entrained flow gasification	Fine coal or biomass feed and the oxidant (air or oxygen) and/or steam are fed co-currently to the gasifier which results in the oxidant and steam surrounding or entraining the coal particles as they flow through the gasifier in a dense cloud. Entrained-flow gasifiers operate at high temperature and pressure and extremely turbulent flow which causes rapid feed conversion and allows high throughput. The gasification reactions occur at a very high rate (typical residence time is on the order of few seconds), with high carbon conversion efficiencies (98-99.5%). In this type of reactor, no inert added solid material is present, like it is the case in a fluidized bed. A further details of gasifier types is demonstrated in Figure 2.3	(Senapati & Behera, 2012)

2.2.2 Gasifier types useful for energy generation from biomass.

Biomass gasification can be achieved based on the nature and type of the gasifier. Thus, the quality and quantity of producer gas arising from the gasification process depends on the configuration of the gasifier as well as the operating conditions. These gasifiers can be classified based on the source of heat used to initiate the gasification processes. The source of heat can be external (autothermal gasifier) or internal (allothermal).

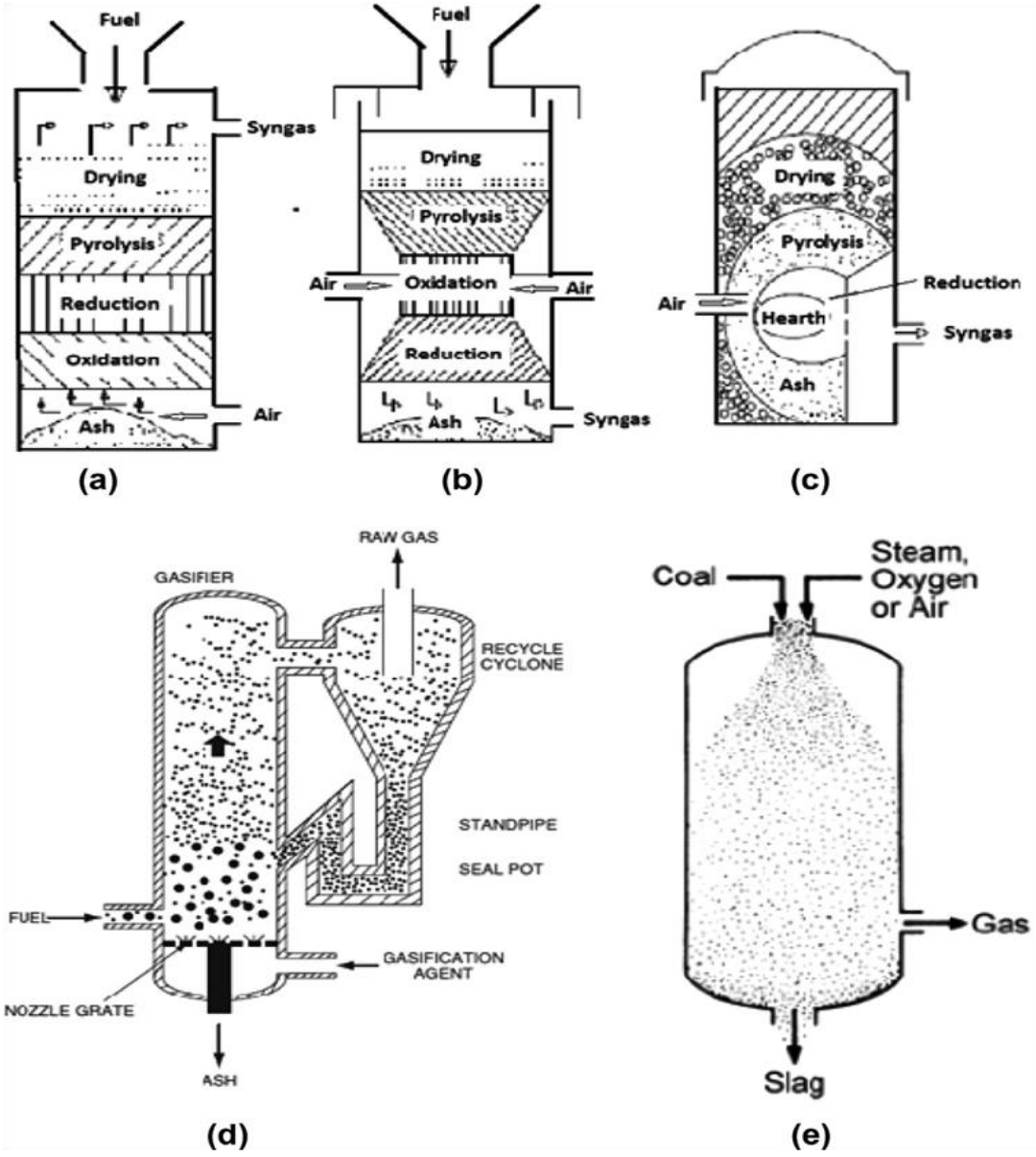

Figure 2.3 Types of gasifiers (a) updraft, (b) downdraft, (c) cross-draft, (d) fluidized, and (e) entrained flow gasifiers (Guangul, Sulaiman, & Ramli, 2012)

2.3 Process parameters and their effects on biomass gasification for power generation

While biomass has been seen as a good substitute for supply of energy, a number of factors affect biomass gasification for power generation and majority of these factors will depend on the design and type of the gasifier. Such factors include; biomass moisture content (Li-ping et al., 2010; Xu, Zhu, & Li, 2012; Yuntenwi, MacCarty, Still, & Ertel, 2008), pressure (Siedlecki et al., 2011), nature of catalyst used (Güngören et al., 2013; Sharma et al.,2008; Ross et al., 2001), particle size (Ryu et al., 2006), biomass composition(Howaniec & Smoliński, 2014), nature of gasification agent (Ghassemi & Shahsavan-markadeh, 2014), gasification temperature (Guo et al., 2009; Karmakar et al., 2013), bed height(Manyà et al., 2006; Xiao et al., 2007), fluidization velocity(Ngo et al., 2015), equivalence ratio (ER)(Kumar et al., 2009; Lv et al., 2004; Ryu et al., 2006), air to steam ratio (González et al., 2008; Kumar et al., 2009) among others.

Understanding the effect of such factors on the overall gasification performance assists in the optimization process of the gasifier as well as maximizing on the system energy recovery.

2.3.1 Effect of biomass moisture content on gasification performance

Moisture content has a significant impact on the burning rate of the fuel as high levels of biomass moisture content cause difficulty in ignition(Yang et al., 2003). The need to dry biomass feedstocks before they can be gasified is thus an important parameter that should not be under estimated as it can place a large energy and capital cost burden on small-to-medium scale biomass gasification plants for the production of heat and power (Brammer & Bridgwater, 2002). As biomass moisture content increases, the quality of the product gas deteriorates along with the overall performance of the whole system. Water that is present in the biomass is considered to have a negative impact on the gasification due to the amount of energy absorbed during the vaporization process which can lead to the decrease of the operating temperature and lowering the calorific value of producer gas (Figiel & Tajner-Czopek, 2006).

Biomass as received has higher moisture content between 10-30% and depending on the type of the gasifier, it may need to be dried before being subjected for gasification purposes. Drying is an energy intensive process that can reduce the heating value of the product gas and temperatures in the range of boiling point of water need to be applied to avoid the devolatilization of the biomass which may lead to low heating values of the product gas. When waste heat produced during gasification is used for drying, it can increase the overall efficiency of the gasification process. Brammer & Bridgwater, (2002) suggested that biomass samples of moisture content in the range less than 10% need not to be dried since they are dry enough to instantly initiate the reactions during the firing process or else drying of the biomass must be ensured where moisture content is greater than 10% if successful gasification should be achieved. Li-ping et al., (2010); Yao et al., (2013) and Xu et al.,

(2012)in their study of the effect of moisture content of sludge in gasification noted thatthe total gas production was increased by decreasing the water content of the sludge hence high moisture content of the feed material affects gas yield from gasification process as the higher the moisture content, the less the gaseous yield. Higher water content in feedstocks would diminish the calorific value of the produced syngas (Figiel & Tajner-Czopek, 2006). Different authors have investigated the effect of moisture content on the product gas composition and their findings are summarized in Table 2.3 below.

Table 2.3 Effect of moisture content on biomass gasification

Study	Operating conditions	Main findings	Reference
Effect of moisture on the gasification process	Air superficial velocity of 0.06 m/s, particle size:2 - 6 mm, Moisture content of 10.62%. flame front velocity = 11 mm/min, ER = 3.2, Specific gasification rate = 125 kg/h/m^2,	Increasing the moisture content of biomass led to reductions in the maximum process temperature, the biomass consumption rate, the equivalence fuel/air ratio and the flame front velocity	(Pérez, Melgar, & Nel, 2012)
Effect of moisture content on the characterization of products from the pyrolysis of sewage sludge	moisture contents of 0%, 31%, 47% and 80% Temperature :1000◦C Reactor type : tubular furnace	The high moisture content of sewage sludge favored the steam reforming reactions of volatile compounds and the steam gasification of solid char, enhancing the production of hydrogen rich fuel gas. The evaporation of water accelerated the evolution of porosity in the solid char and contributed to the devolatilization of sewage sludge, leading to an increase in the gas fraction and a decrease in the solid fraction Increase of moisture content improved the production of light aromatics and decreased the toxic effect of tar	(Xiong et al., 2013)
Effects of various operational parameters on biomass gasification process; a modified equilibrium model	Modified equilibrium model based on Gibbs free energy minimization	Moisture content of biomass has negative effects on cold gas efficiency and higher heating value	(Ghassemi & Shahsavan-markadeh, 2014)
Influence of moisture content on the direct gasification of dewatered	high-pressure autoclave at a constanttemperature of 400 °C residence time of 60 min and by	The total gas production was increased by decreasing the water content, and the gas yield was decreased. The CO_2 yield was significantly affected by water content, whereas H_2, CH_4, and CO yields were slightly reduced.	(Xu et al., 2012)

sludge via supercritical water	adjusting water content by adding distilled water or using air-dried dewatered sludge.	The concentrations of organic matter OM and total phenols increased with a decrease in water content.	
Effect ofmoisture content of dried sewage sludge for the hydrogen production and tar removal	The air gasification of dried sewage sludge was conducted in a two-stage gasifier that consisted of a bubbling fluidized bed and a tar cracking zone.	The gasification of a dried sewage sludge sample containing 30 wt.% of moisture with a combination of calcined dolomite as the bed material and activated carbon in the tar-cracking zone removed the most tar and produced the highest hydrogen concentration.	(Mun & Kim, 2013)
Effect of moisture content on conveying characteristics of pulverized coal for pressurized entrained flow gasification	Conveying pressure up to 4 MPa. The experiments included soft coal and lignite with similar density and particle size.	With the increase in moisture content, the mass flow rate decreased for lignite (3.24% < M < 8.18%) but increased at first and then decreased for soft coal (0.4% < M < 6.18%) at same operating parameters.	(Liang et al., 2011)
Effect of moisture content in sewage sludge on air gasification	External heated downdraft reactor under a stable air flux of 0.05 m^3/h and a constant gasification temperature of 800 ^oC	The contents of CO_2, CH_4, and H_2 in gas, lower heating value (LHV) of gas and aqueous yield increased with increasing moisture content, while content of CO and tar yield decreased.	(Li-ping et al., 2010)
Effects of moisture content and air to fuel ratio	The pyrolysis model took place when drying temperature reached 473 K.	Increasing the moisture content affected the height of drying, and pyrolysis zones while the critical char bed length of reduction zone decreased from 0.53 to 0.25 m.	(Dejtrakulwong & Patumsawad, 2014)

2.3.2 Effect of particle size on biomass gasification

Particle size as a factor affecting gasification was discussed by (Pérez et al., 2012., Guizani et al., 2015., Luo et al., 2010., Mahapatra and Dasappa., (2014) as well as Yin et al., (2012) and their detailed findings summarized in Table 2.4 below. It was observed that dry gas yield increased with a decrease in particle size, and char and tar yield decreased while smaller particle sizes resulted in higher H_2 and CO contents for both pyrolysis and gasification of MSW(Luo et al., 2010). Erkiaga et al., (2014) found out that the difference in particle sizes accounts for different rates of chemical reaction inside the gasifier and subsequently different compositions in gasification products due to the difference in the available space allowing gasification to take place. Larger size particles are hard to operate in the reactor as they block the continuous feeding of the feedstock inside the reactor while smaller particles tend to create resistance to the flow of the gasifying agent which leads to longer residence times inside the reactor. Generally, fuel particle size influences gasification time and plays an important role in all the successive reaction steps (fuel heating, reactant and product diffusion between the particle and the reaction atmosphere, and solid–gas reactions) which occur during the conversion of biomass to product gas. Fuel particle size, along with other fuel properties (moisture content, heating value, ultimate and proximate analysis) and gasifier operating conditions (gasifying agent, temperature, heating rate, biomass/air ratio, etc.), have been reported as one of the main parameters affecting the composition, quality and final quality of the producer gas (Reed, T.B. and Das, 1988). The smaller the fuel particle size, the more effective are mass and heat transfer since the particle external surface area to volume ratio is higher enhancing faster rates of reaction(Chen & Gunkel, 1987). The larger the particle size, the lower its surface temperature and thus more heat is required for the reactions to take place. Reed and Das (1988)in an in-depth work on downdraft fixed bed gasifiers

stated that fuel particle size and shape determine the difficulty of fuel feeding, as well as its behavior inside the reactor. (Tinaut et al., 2008) observed that there was maximum efficiency in biomass burning rate and the process propagation velocity due to smaller particle sizes and lower air velocities, owing to the higher fuel/air ratio in the gasifier. (Lv et al., 2004)revealed that due to smaller biomass size, there was a higher yield of CO, CH_4, C_2H_4 and less CO_2 which resulted in higher yields of the gas composition, higher energy content of the gas and increased carbon efficiency. The higher yield of product gas due to smaller particles was attributed to the higher heat and mass transfer which ensures effective and complete gasification reactions. Smaller biomass particles are thus preferable during gasification because they enhance gas recovery. Given the conflicting information from the different researchers (Guizani, Escudero Sanz, & Salvador, 2015; Luo et al., 2010; Pattanotai, Watanabe, & Okazaki, 2015; Yin et al., 2012), there is still a gap to investigate with concrete evidence the effect of biomass particle size to give a clear understanding of the effect of particle diameter during the gasification process.

Table 2.4 The effect of particle size on gasification products

Study	Operating conditions	Main findings	Reference
Influence of temperature and particle size on the single and mixed atmosphere gasification of biomass char with H_2O and CO_2	Mixed atmosphere experiments i.e. pressure of 0.2 atm or (0.2 atm + 0.2 atm) and temperature ranges from 850^oC to 1100^oC.	Char reactivity decreases when increasing the particle size due to increasing diffusional limitations.	(Guizani et al., 2015)
Influence of particle size on pyrolysis and gasification performance of municipal solid waste (MSW) in a fixed bed reactor	The bed temperature was varied from 600 to 900 ^oC MSW was separated into three different size fractions (below 5 mm, 50–10 mm and above 10 mm).	Dry gas yield increased with a decrease in particle size, and char and tar yield decreased. Smaller particle sizes resulted in higher H_2 and CO contents for both pyrolysis and gasification of MSW.	(Luo et al., 2010)
Influence of particle size on performance of a pilot-scale fixed-bed gasification system	Prunings from peach trees at five different size fractions (below 1cm, 1–2cm, 2–4cm, 4–6cm and 6–8 cm).	With increasing particle size, gas yield increased while tar and dust content decreased. The lower heating value of the gas decreased slightly with particle size. At a smaller particle size, more hydrocarbons were detected in the producer gas. H_2 and CO_2 contents increased with the decrease in particle size, reaching 16.09% and 14.36% at particle size below 1 cm, respectively.	(Yin et al., 2012)
Influence of surface area to volume ratio of fuel particles on gasification process in a fixed bed	Fuel used included wood flakes, coconut shells and wood sphere at aheating rate of about 3 K/s for a 30 mm wood particle and12 K/s with a wood flake thickness of about 4 mm	Particles with higher surface area per volume are subjected to higher pyrolysis rate resulting in fast pyrolysis products	(Mahapatra & Dasappa, 2014)

2.3.3 Effect of gasification temperature on product gas formation and composition

Gasification temperature is a fundamental parameter affecting the composition and distribution of the product gas (Olgun et al., 2010)(Rapagnà et al., 2010)(Jaojaruek, Jarungthammachote, Kathrina, Gratuito, & Wongsuwan, 2011)(Chiang et al., 2013)(Hernández, Ballesteros, & Aranda, 2013)(Azzone, Morini, & Pinelli, 2012). The maximum raised temperature will depend on the type of the gasifier, Equivalence Ratio (ER) as well as the heating source. In their study, Sánchez et al, (2014) discovered that gasification temperature was found to be the most influential factor affecting gasification. They concluded that increasing the temperature resulted in increasedH_2 and CH_4 contents, carbon conversion and energy efficiencies. (Erkiaga et al., 2014) also found out that temperature had a bearing on the gas composition by increasing H_2 content and reducing CO content. In the presence of an oxidizing agent at higher temperatures, biomass polymers decomposes into lighter molecules which finally go to permanent gases of H_2, CH_4, CO, CO_2 as well as lighter hydrocarbons, char, tar, ash and minor traces of contaminants. Higher temperatures yield higher conversion efficiency. The rise in gas yield arises due to the destruction and reforming of the tar content leading to an increase in the gas yield. (Skoulou, Koufodimos, Samaras, & Zabaniotou, 2008) postulates that higher temperatures favor the reactants exothermically and the products endothermically. At temperature above 750-800 °C, the water gas reactions equation and steam reforming equation result into increase in H_2. Steam reforming and Boudouard reactions dominate at temperatures above 850-900 °C and this result into increase in CO content. (González et al., 2008) observed that from 700 to 900 °C in air gasification, contents of H_2 and CO increased while CH_4 and CO_2 decreased. (Kumar, Eskridge, et al., 2009) observed that an increase in temperature (furnace set point from 750 to 850 °C), led to

increase in energy and carbon conversion efficiencies and percent gas compositions of H_2. Chee et al., (1992) reported that with an increase in gasification temperature from 700 to 800 °C, gas yield, gas HHV, energy efficiency, carbon conversion efficiency and H_2 content increased and CH_4, CO and CO_2 contents decreased. The decrease in CO content may have been due to the comparatively lower temperature less than (850-900°C). Generally, all authors seem to agree based on their experimental observations that higher product gas yield is enhanced at higher temperatures especially above 800°C. Such higher temperatures enable biomass conversion and tar cracking with subsequent increase on gas yield and quality. The increase in gas quality reduces the need for gas cleaning that would otherwise compromise its quality. From the above discussion, it can be concluded that increasing the temperature favors product composition thus producing a gas with a higher calorific value. This is because higher temperatures enable the reactions to attain equilibrium hence producing gas yields at maximum concentrations.

2.3.4 Effect of gasifying medium

During high temperature gasification of biomass, a gasifying agent is needed to provide a medium for syngas recovery. Typical gasifying agents include, air, steam, carbon dioxide, oxygen or a combination of these. An experiment carried out by (Y. Liu, Jia, Guo, & Ryu, 2014) demonstrated that the gasifying medium (steam or CO_2) boosts the chemical looping process by reducing the activation energy in the overall reaction and gasification reactions of coal char. However, it was also concluded that the mechanism using steam as the gasifying medium differs from that using CO_2.With steam as the gasifying medium, parallel reactions occur in the beginning stage, followed by a limiting stage shifting from a kinetic to a diffusion regime. It was opposite to the reaction mechanism with CO_2 as the gasifying medium. (Corella, Aznar, Caballero, & Gil, 1999) observed the effect of three different gasification agents of air, pure steam and a mixture of steam and oxygen on composition, yields and lower heating value of syngas and their results revealed higher composition of syngas when steam was used as the gasifying agent. Air as a gasifying agent is the cheapest and easily available but provides a gas with a low calorific value due to the high concentration of nitrogen in air. A detailed chemical process on the effect of each gasification agent is discussed here under.

2.3.4.1 Air gasification

In this process, when air is used as a gasifying agent, its purpose is twofold. It reacts with the excess char during the pyrolysis process within the gasifier and also sustains the combustion reactions if supplied continuously. This is important to sustain thermochemical reactions if no

external source of heat is supplied. The product is a low-energy gas containing primarily hydrogen and carbon monoxide diluted with the nitrogen from the air. The heating value of the produced gas is between the range of 3.5 - 7.8 MJ/Nm^3. Air is cheap but gives a gas of lower calorific value while use of steam increases the costs of production. While choosing a gasification agent, it is important to consider gas quality without compromising production costs. A study on the effect of air on gasification was carried out by (Sarker, Bimbela, Luis, & Kofoed, 2015) and observed that increasing air from 4.16 to 4.99 N m^3/h contributed to the evolution pattern of several parameters such as the rise in gas lower heating value (LHV) and gas yield, the average maximum of which were 4.2 MJ/N m^3 and 1.5 N m^3/kg respectively. Gas composition was mainly boosted by the concentration of CO, as the rest of the combustible components stayed rather unaffected due to the modified air flow rate.

2.3.4.2 Steam gasification

This process requires a heating source and cannot independently sustain the gasification process. Steam reacts with carbon monoxide to produce hydrogen and carbon dioxide. During a modelling study on the effect of gasification agent on the performance of solid oxide fuel cell and biomass gasification systems by (Colpan, Hamdullahpur, Dincer, & Yoo, 2010), their results showed that using steam as the gasification agent yields the highest electrical efficiency (41.8%), power-to-heat ratio (4.649), and exergetic efficiency (39.1%), but the lowest fuel utilization efficiency (50.8%). Bioenergy should be produced while maximizing energy efficiency without compromising fuel utilization efficiency. The principle gas-phase reaction in the steam gasification system is the water gas-shift reaction

$$CO+H_2O \rightarrow CO_2+H_2 \qquad (2.1)$$

2.3.4.3 Oxygen gasification

If pure oxygen is used as a gasifying agent, an oxygen source is required which may elevate the capital cost necessary for the plant installation if the amount of nitrogen supplied to the gasification process is limited. This is because the product gas will not contain nitrogen and thus, have medium energy (approximately 12-21 MJ/Nm^3).

2.3.4.4Carbon dioxide gasification

The use of CO_2as an oxidizing agent has been extensively studied (Garciaet al., 2001).They observed an increase in H_2 and CO when $CO_2$was used as a gasifying agent for gas production from pine sawdust at low temperatures using a Ni/ Al coprecipitated catalyst. Addition of CO_2 decreases the gasification rate as a part of the carbon will be gasified by CO_2 which is slower than the C–H_2O reaction and the net rate would be a combined rate of the C–H_2O gasification and the C–CO_2 gasification (Sharma et al., 2008). Following a study by (Tay, Kajitani, Zhang, & Li, 2013) aimed at investigating the changes in char structure and reactivity during the gasification of Victorian brown coal gasified at 800 °C in a novel fluidized-bed/fixed-bed reactor with three different gasification atmospheres of 15% H_2O balanced with argon, 4000 ppm O_2 balanced with CO_2 and 4000 ppm O_2 + 15% H_2O balanced with CO_2, their findings revealed that the char–H_2O gasification follows a different reaction pathway from the char–CO_2 gasification, at least for the gasification of Victorian brown coal under the tested experimental conditions.

2.3.5 Effect of equivalence ratio on the quality of synthesis gas

Equivalence ratio (ER) is defined as the ratio of the actual oxygen amount in gasification process to the required stoichiometric amount required during the complete oxidation of biomass with air. It indicates the extent of partial combustion. A study carried out by (Kumar, Eskridge, et al., 2009) revealed that increasing ER decreased the hydrogen content but increased carbon conversion and energy efficiencies. In their study, (Xiao et al., 2007) also found out that the ER appeared to have a significant effect on the reactor temperature and other gasification results. The increase of the ER favored the formation of the fuel gas and decreased the formation of the tars and char.(Xiao et al., 2007) also noted a decrease in the hydrocarbons content and the gas heating value with an increase in the ER.

A study carried out by (Makwana et al., 2015) asserted that with an increasing ER, the carbon conversion efficiency decreases because the reaction tends to being more exothermic.Ghassemi and Shahsavan-markadeh., (2014) reported decreasing negative effect on the cold gas efficiency and HHV for higher ER during the gasification processes.Yamazaki et al., (2005) reported that, for indirectly heated gasifiers, air flow rate is the most important factor influencing the product quantity and quality since it affects the burning rate. Gao et al., (2008) showed that when ER was varied from 0-0.3, a hydrogen-rich syngas with a high calorific value was produced, in the range of 8.10-13.40 MJ/Nm^3 and hydrogen yield between 45.05-135.40 g H_2/kg biomass in an updraft fixed bed gasifier. Corella et al., (1999) observed that, there was an increase in gas yield, a decrease in the lower heating values of syngas and a decrease in the composition of H_2, CO, CH_4 and C_2H_2 and tar contents when ER was varied from 0.20 to 0.45. Results obtained by Guo et al., (2009) performed in a cyclone gasifier concept using biomass micron fuel revealed that higher ER

led to higher gasification temperature and contributed to high H_2-content, but too high ER lowered fuel gas content and degraded fuel gas quality.

Hashimoto et al., (2007) observed that with an increase in ER from 0.16 to 0.26, the bed and freeboard temperatures increased giving rise to a higher gas yield and higher heating value (HHV) of the gas, an increase in cold gas efficiency from 57% to 74%, an increase in H_2 yield from 8.5% to 13.9%, and an increase in CO yield from 12.3 to 14%. Such an increasing trend in gas yield with increase in ER implies that an increased airflow increases the biomass conversion rate. However, the effects of ER on the contents of H_2, CO, and CH_4 (%) have been contradictory, which is logical because the percentage compositions of individual gases depend on both the yield of individual gases and the overall gas yield. If the overall gas yield is more pronounced than the yield of individual gas, the percentage composition of individual gas decreases even though the individual gas yield may actually have increased. Effects of ER on the product gas composition also depend upon other operating factors such as temperature, gasifying agent used and particle size.

2.3.6 Effect of biomass feedstock type on producer gas yield

The fuel properties and process conditions affect the combustion characteristics, altering the heat generation, heat transfer and reaction rates in a complicated manner(Howaniec & Smoliński, 2014; Ryu et al., 2006). The properties affect feedstock selection, sizing, transportation, storage; gasification and syngas recovery, and residue or co-product processing and the extent of the effects of feedstock properties depend on gasifier type, operating conditions, and syngas quality product requirements (Haryanto et al., 2009) . Samaras et al., (2014) studied three feedstocks, namely olive, peach and grape kernels for the producer gas and their findings revealed that producer gas from each studied feedstock had much lower calorific value than propane. The difference in the calorific value arose due to the difference in the amount of elemental carbon, hydrogen and oxygen present in the different feedstocks as compared to natural gas as a starting material for propane.(Stolarski et al., 2015a) carried out a study that analyzed the chemical composition of different biomass of willow, poplar and black locust as potential feedstocks in the production of second-generation bioethanol. The highest content of cellulose in the experiment was found in willow biomass obtained from the control plot in the 3-year harvest cycle. On the other hand the highest content of lignin was found in biomass of poplar, both in the 3-year and 4-year harvest cycle. This illustrates that different biomass materials contain varying amounts of cellulose, lignin as well as hemicellulose. Due to these constituents, which vary in composition according to biomass type, the pyrolysis and gasification behavior of lignocellulosic biomass depends upon these main components of cellulose, xylan (hemicelluloses), and lignin(Nsamba et al., 2015).Tinwala et al., (2015) carried out a pyrolysis study of woody biomass, agro-residues and seed performed at 500 ± 10 ^{o}C in a fixed bed pyrolyser. Bio-oil yield was found varying from 20.5% to 47.5%, whereas the

biochar and pyrolysis gas ranged from 27.5% to 40% and 24.5% to 40.5%, respectively. Pyrolysis gas was measured for flame temperature along with CO, CO_2, H_2, CH_4 and other gaseous composition. HHV (29.4 MJ/kg) of biochar and pyrolitic gas (8.6 MJ/kg) of woody biomass was higher analogous to sub-bituminous coal and steam gasification based producer gas respectively, whereas HHV (25.6 MJ/kg) of bio-oil obtained from seed was significantly more than husks, shells and straws. Two Brazilian biomass samples, namely sugarcane trash and Eucalyptus benthamii were evaluated as feedstocks for liquid and solid fuels production by fast pyrolysis, using a fluidized bed reactor and two different sets of process conditions by (Pighinelli, Boateng, Mullen, & Elkasabi, 2014a). By comparing both feedstocks, the eucalyptus yielded on the average, 50% more bio-oil than the sugarcane trash while the trash yielded 50% more permanent gas. Further studies investigating the effect of feedstock type on gasification products are summarized in Table 2.5 and from their findings, it is justifiable to conclude that biomass varies widely in both physical and chemical properties which significantly has a bearing on the reaction rates and more fundamental studies are required to understand the combustion characteristics of different biomass materials(Ryu et al., 2006).

Table 2.5. Effect of biomass feedstock type on yield of producer gas

Study	Operating conditions	Main findings	Reference
combustion in a spark ignition engine operating with producer gas from various biomass feedstocks	feedstock type: olive, peach and grape kernels. Reactor type: A fluidized bed gasifier in a mobile combined heat and power (CHP) production unit. temperature : 700 and 800 °C	Producer gas from every feedstock has much lower calorific value than propane due to the presence of inert gases (N_2 and CO_2).	(Tsiakmakis et al., 2014)
Intermediate pyrolysis of agro-industrial biomasses in bench-scale pyrolyser	Feedstock type: woody biomass agro-residues and seed.Temperature : 500 ± 10 ^{o}Creactor type :Fixed bed pyrolyser	HHV of biochar (29.4 MJ/kg) and pyrolitic gas (8.6 MJ/kg) of woody biomass was higher analogous to sub-bituminous coal and steam gasification based producer gas respectively, whereas HHV of bio-oil obtained from seed (25.6 MJ/kg) was significantly more than husks, shells and straws.	(Tinwala et al., 2015)
Lignocellulosic biomass from short rotation woody crops as a feedstock for second-generation bioethanol production	Biomass composition of willow, poplar and black locust, depending on the method of soil enrichment and harvest cycle (three- and four-year).	The highest content of cellulose was found in willow biomass obtained from the control plot in the 3-year harvest cycle. The average content of cellulosein biomass of black locust harvested in a 3-year cycle was the lowest and the highest content of lignin was found in biomass of poplar, both in the 3-year and 4-year harvest cycle.	(Stolarski et al., 2015b)
Evaluation of Brazilian biomasses as feedstocks for fuel production via fast pyrolysis	Biomass type : sugarcane trash and Eucalyptus benthamii Reactor type : fluidized bed reactor Temperature (°C): 460-556	The eucalyptus yielded on the average, 50% more bio-oil than the sugarcane trash while the trash yielded 50% more permanent gas. Apart from the high ash content associated with biochar from sugarcane trash, biochar produced from both feedstock samples had similarities with bituminous coal in terms of moisture content, fixed carbon content, and heating values.	Elkasabi et al., 2014b)

Effect of woody biomass components on air-steam gasification	Reactor type: fixed-beddowndraft gasifier at atmospheric pressure. Temperature : 1173K Biomass type : Cellulose, xylan, and lignin as model compounds of woody biomass components and Japanese oak and Japanese red pine bark as woody biomass	The gasification conversions in cellulose, xylan, and lignin were 97.9%, 92.2%, and 52.8% on a carbon basis, respectively The product gas composition in cellulose was 35.5 mol% CO, 27.0 mol% CO_2, and 28.7 mol% H_2, and the CO composition was higher than the CO_2 or H_2 compositions, which was similar to that in the Japanese oak, of which the main component was cellulose.	(Minowa etal.,2005)
Effects of feedstock properties on the performance of a downdraft gasifier	Reactor type : Fixed-bed downdraft gasifier Feedstock type : hardwood chips, softwood chips, softwood sawdust, corn cubes, crude glycerol (a byproduct of biodiesel production), and switchgrass,	The downdraft gasifier is suitable for gasifying diverse feedstocks to produce good quality syngas with good low heating value and low tar and particle concentrations. There was no significant differences in gas composition, low-heating value, tar and particle concentrations among the different feedstocks used in the experiments possibly because the properties of selected feedstocks could be of the same range Feedstocks with small sizes, low porosity, or containing high compounds that can caramelize in high temperature could cause problems with bridging, lumping, collapsing, or clogging inside the reaction chamber and could cause the gasifier to fail.	(Haryanto et al., 2009)

2.3.7 Effect of gasifier type on the quality of producer gas

Biomass gasifiers are designed to suit different applications depending on the nature of feedstock to be used, direction of flow of the gasifying agent or based upon the nature of the heating source to be used during gasification All these affect the quality and quantity of the gasification products. (Simanjuntak & Zainal, 2015) carried out a study that aimed to improve the heating value (HV) of gas produced during the gasification of sawdust using a new type of air-blown gasifier based on a two-compartment cylindrical fluidized bed. The gasification process was based on an internally circulating aerated fluidized bed (ICAFB) and consisted of two individual zones; a gasification zone in the annulus and combustion zone in the draft tube and found that the ICAFB gasifier is capable of producing producer gas with higher CO and CH_4 fractions. Other studies have been carried out using different types of gasifiers such as (Seggiani et al., 2012) used an updraft gasifier, (Cho, Choi, & Kim, 2015; Cho, Mun, & Kim, 2013; Mun, Kim, & Kim, 2011; Mun, Seon, & Kim, 2010) used a two stage gasifier, (Karmakar et al., 2013; Mac an Bhaird et al., 2015) used a fluidized bed gasifier, (Luan, Chyou, & Wang, 2013) used a cross type two stage gasifier, (Guangul, Sulaiman, & Ramli, 2014) used a single throat downdraft gasifier and (Jaojaruek et al., 2011; Nisamaneenate, Atong, & Sornkade, 2015; Sheth & Babu, 2009)applied a down draft gasifier and all received the composition of gasification products in variable proportions. Although the effect of operating conditions on gasification products was invested by these authors, there is still a gap to compare the performance efficiency of these gasifiers it terms of the output gasification products so that a more reliable design can be proposed for further development and adaptation especially bearing in mind that the design configuration has a

bearing on the chemistry of reactions that occur inside the gasifier and thus affect on the composition, quality and quantity of the gasification products.

2.3.8 Effect of feed pre-treatment

During conventional air gasification, the feed contains mainly solid biomass with air and or steam. Pretreatment may involve reducing the moisture content of the biomass upto the required range, fractionation of the biomass particle size as well as raising the temperature of the incoming air and would increase on the system efficiency as well as make the reactor more energetically reliant.(McKendry, 2002) recommends that biomass should be dried upto moisture content of about 10–15% before gasification and biomass particle size in the range 20–80 mm is desired. Small particles tend to contain less nitrogen and alkalis and so fractionation into fine and coarse particles helps to produce a gas with fewer impurities. Drying wood to the required level of 10–15% moisture requires the use of driers such as directly heated rotary driers using the flue gas or indirectly heated fluidized bed driers using steam to heat the feed material. The vapors emitted during drying contain a number of volatile organic compounds (VOCs), mainly terpenes and require appropriate air pollution control systems. Use of highly preheated feed air provides additional energy into the gasification process, which enhances the thermal decomposition of the gasified solids. Preheating air increases the yield and lower heating value of the dry fuel gas.(Lucas, Szewczyk, Blasiak, & Mochida, 2004) performed an experiment to investigate gasification of densified biofuels using highly preheated air and steam as a gasifying agent and observed that by increasing the temperature of incoming air from 350- 900°C, the dry fuel gas composition of H_2, CH_4, and CO_2 increased from 10.6 % to 22.3%, 3.2% to 4.4% and 6.0% to 18.6%

respectively while CO reduced from 30% to 20.9%. The increase in methane composition could be probably explained based on the methanation reactions: $2CO+2H_2 \Leftrightarrow CH_4+CO_2$ and $C+2H_2 \Leftrightarrow CH_4$ which take place. The existing moisture content in the feedstock and the presence of CO reacts to produce H_2 via the water–gas shift reaction which increaseson the amount of available H_2 content of the producer gas (McKendry, 2002). (W. Yang, Ponzio, Lucas, & Blasiak, 2006)made similar conclusions during their experimental fixed-bed gasifier utilized to investigate the gasification of biomass using high-temperature air up to 1473 K. Their results concluded that when the temperature of feed gas was increased, a higher gasification rate, a higher ignition front rate, and higher molar fractions of fuel gases (CO, H_2 and C_mH_n), thus a higher LHV were obtained. Generally, it is important to perform pretreatment on both the solid biomass feed and air to increase the system efficiency and subsequently gas production and recovery rate.

2.4 Gasifier energy efficiency and system thermodynamics

Gasifiers should be designed to optimize energy recovery with minimal energy losses to the environment. Loss of energy either through poor insulation or through the end product does not render the system thermodynamically efficient. According to the first law of thermodynamics, energy is neither created nor lost but converted from one form to another. It is thus justifiable to state that energy conversion processes do not have energy losses, except for losses from the process system into the environment. But from the second law of thermodynamics, energy conversion processes are accompanied by an irreversible increase in entropy, which leads to a decrease in exergy (available energy) and thus, even though the energy is conserved, the quality of energy decreases because energy is converted into a

different form of energy, from which less work can be obtained(Prins, 2005).Gasifiers should thus be insulated with materials of good insulation properties to minimize heat losses as well as integrated with devices of high thermal conversion to minimize the energy losses. For self-sustaining gasifiers that have no external heating source, loss of heat from the system reduces on the total amount of heat useful for complete gasification. In return, it yields incomplete gasification reactions which would further lead to higher emissions arising from incomplete gasification reactions. Systems that are not externally heated require initial ignition to kick start the gasification process and thus it is important to minimize the amount of fuel used for startup to make the system more energy efficient. Studies on systems thermodynamic efficiency are detailed in Table 2.6.

Table 2.6.Thermodynamic efficiency of biomass gasification systems

Study objective	**Operating condition**	**Feedstock type**	**Observation**	**Reference**
To predict H_2 production with a gasifier and evaluate system performance through energy and exergy efficiencies for hydrogen production from biomass	Using a quantity of 14.5kg/s from biomass and an amount of 6.3kg/s of steam at500K temperature range of 950–1500K and steam–biomass ratio of 0.17–0.51	wood sawdust	An improvement in exergy efficiency from 33 to 37% was achieved during hydrogen production only. When the temperature went beyond 1000 K, the exergy efficiency increased from 42 to 47% when all of the product gases were taken into consideration and from 47 to 52% when all of the products from the gasification process were taken into consideration.	(Abuadala & Dincer, 2010)
To study the thermodynamic performance of an integrated gasifier–boiler power system for its hydrogen production	Utilized experimental data from literature, especially on the air-blown gasification characteristics of six different biomass fuels	almond shell (ASF), walnut pruning (WPF), rice straw (RSF), whole tree wood chips (WWF), sludge (SLF) and non-recyclable waste paper (NPF)	theexergy efficiencies changed between 4.33% and 11.89%, exergy efficiencies varied from 18.33% to 39.64%. The higher the nitrogen content the lower the efficiency based on an inverse ratio between exergy efficiency and nitrogen content.	(Kalinci, Hepbasli, & Dincer, 2010)
Performance assessment of a novel energy system integrating both biomass gasification and fuel cell systems performed thermodynamically through energy and exergy efficiencies.	Operating at atmospheric pressure, Direct internal reforming solid oxide fuel cell model was introduced integrated with the system for power production.	N/A	The results showed that steam biomass ratio has a significant effect on the hydrogen production efficiency and optimal value of 0.677 was calculated for maximum exergy efficiency at the base case condition	(El-Emam & Dincer, 2015)

To investigate the thermal profiles of a trailer-scale gasifier in different zones during the course of gasification and also to elaborate on the design, characteristics and performance of the gasification system using different biomass feedstock.	Thermal profiles with respect to five different zones in the gasifier and a comprehensive thermal–chemical equilibrium model to predict the syngas composition	pine wood, horse manure, red oak, and cardboard	The thermodynamic efficiencies predicted by the model and backed by the experimental data was in the range of 80% for the four different feedstock used in the study	(Balu & Chung, 2012)
To assess the effects of stove design and fuel type on efficiency and emissions, five configurations of natural-draft, top-lit up-draft (TLUD) semi-gasifier cook stoves	An energy balance model was developed using measured temperature data to identify the major sources of efficiency loss.	corn (Zeamays) cobs wood pellets	The highest measured thermal efficiency was 42%.	(Tryner, Willson, & Marchese, 2014)

NA; not available

2.5 Mechanism of gas filtration before transport to the engine

After successful gasification of biomass, gases are produced alongside solid particles within them which must be removed to increase gas purity before channeling of the producer gas to the engine. Thus, gas filtration is the separation of solids (particulate matter (PM)) from gases and assists to achieve a cleaner gas going to the engine, improves on the engine performance as well as increases on the service life of the engine. PMare always part of the gasification products and should be separated if a clean fuel must be produced. Before the gases are filtered, the dense particles fall off by gravity through cyclones while the less dense particles move alongside the gas.(Heidenreich, 2013) carried out a detailed review of hot gas filtration mechanisms and reported filtration at high temperature, hot gas filter media and filter elements which included the ceramic filter media, metal filter media, hot gas filter elements and catalytically activated hot gas filter elements and categorized them under single tube sheet design, multi stage designs, filter tube design and cross flow filtration. Because of the possible damages to the engine due to the presence of particulate matter (PM) in the fuel gas, reduction in the efficiency of combustion and improving the quality of exhaust gasses, studies have been carried out to improve the filtration mechanisms and possible defects. For gas filtration, there are mainly two ways of gas solid separation which include sedimentation and filtration. During sedimentation, particles in suspension settle out of the fluid in which they are entrained, and come to rest against a barrier. Fine particles in the gas attach themselves to filters to allow a cleaner gas to exit. (Moldavsky, Gutfinger, Oron, & Fichman, 2013) studied the effect of sonic waves on gas filtration by granular beds and found out that application of acoustics reduces particle penetration up to 35% relative to filtration without acoustics. (Ferrer, Templier, Gonthier, & Bernis, 2000)studied the cake formation mechanisms during tangential filtration of dust-laden gases at high temperature.Sibanda et al., (2001)investigated

the cross flow filtration mechanism of particle separation from gases and confirmed that in cross-flow filtration a dynamic equilibrium between deposition and re-entrainment can be reached and that significant particle aggregation occurs on the surface before particle re-entrainment into the through-flow; (Du, Yao, & Lin, 2005; X. Liu, Gao, & Li, 2005) studied particle flow in a gas–solid separator with baffles using Phase Doppler Particle Analyzer (PDPA) and the analysis of the velocity profile indicated that the particle inertia has a significant effect on the behavior of particles in different size groups. The trajectories of the smaller particles were more influenced by the gas stream in relation to the larger, heavier, particles. (Sibanda, Greenwood, Seville, Ding, & Iyuke, 2010)studied the cross flow filtration about predicting particle segregation in cross flow gas filtration and found that significant segregation of particles occurred during cross-flow gas filtration and becomes more marked by the wider the particle size distribution of the primary/feed dust. In the realm of improving hot gas filtration mechanisms, (Macías-Machín, Socorro, Verona, & Macías, 2006) evaluated the use of the Lapilli as granular medium in fixed bed filters and found that the collection efficiency decreased with increasing temperature. Other works(Dou et al., 2012; Meng, De Jong, Pal, & Verkooijen, 2010) have been done that summarize the research progress of hot gas filtration, desulphurization and HCl removal in coal-derived fuel gas and provide critical evidence toconsiderparticle segregation through a filter media. Effective gas cleaning mechanisms generate a cleaner gas and prevent clogging the engine whilereducing on the effect of damaging the gas analyzer sensors during emission monitoring.

2.6 Mechanism of gas ignition and engine efficiency for power production

Engines can be classified based on type of fuel used to run the engine, based on the location of the valves or according to the types of stroke intakes during its operation classified as four stroke cycle engine or two stroke cycle engines orcategorized depending on the type of ignition such as the spark or compression ignition. Several studies have been done to improve engine efficiency (Rakopoulos, Kosmadakis, Demuynck, De Paepe, & Verhelst, 2011; Shadloo, Poultangari, Abdollahzadeh Jamalabadi, & Rashidi, 2015) in order to extract the maximum possible energy from the incoming synthesis gas stream after gasification. In their study, (Papagiannakis, Rakopoulos, Hountalas, & Rakopoulos, 2010)examined the effects of the total air–fuel ratio on the efficiency and pollutant emissions of a high speed, compression ignition engine and found out that the decrease of the total relative air–fuel ratio results into a lower brake thermal efficiency compared to the one under normal diesel operation, thus revealing the deterioration of the engine efficiency under diesel–natural gas dual fuel operating mode.

Papagiannakis et al., (2010) further concluded that dual fuel combustion using natural gas as a supplement for liquid diesel fuel is a promising technique for controlling both NO and Soot emissions on existing diesel engines, requiring only slight modifications of the engine structure. (Cha, Eom, Song, & Min, 2015) further noted improved combustion efficiency using syngas. (Splitter & Reitz, 2014) also studied the efficiency of compression ignition engines applied to gas engines basing on the fuel reactivity effects and operational window and discovered that for fixed cycle thermodynamics, sources of engine inefficiency are functions of the premixed and global equivalence ratios. (Splitter & Reitz, 2014) recommended that losses in such engines can be minimized through proper balancing of the

intake pressure and temperature, which are affected by fuel reactivity differences. In other studies (Bullock & Olfert, 2014)focused on characterizing the particle size distribution, volatility, and effective density of particulate matter emitted from a homogeneous charge compression ignition (HCCI) engine fuelled by port injected compressed natural gas. (Arroyo, Moreno, Muñoz, & Monné, 2013) carried out an experimental study on ignition timing and supercharging effects on gasoline engine fuelled with synthetic gases extracted from biogas and found out that the variation in the ignition timing has an important effect on parameters of combustion such as maximum pressures, mass fraction burned, heat release ratio and cyclic irregularity hence promising improvement in gas engines. From the discussion above, it is important to choose a fuel that would not only improve the engine efficiency but also reduce greenhouse gas emissions like NO_x. This can be made possible by choosing the best air to fuel ratios to optimize energy recovery. Use of gas as a source of fuel to the engine is environmentally friendly with less pollution effects particularly particulate emissions and nitrogen oxides (Bullock & Olfert, 2014)

2.7 Emission monitoring during synthesis gas combustion in the Internal CombustionEngine (ICE)

During the gasification of biomass for energy generation using an internal combustion engine (ICE), the generated synthesis gas channeled to the engine for further combustion reactions provide the necessary energy to run the engine and subsequently produce the useful energy to do work. This generates exhaust emissions alongside whose concentration depends on a number of factors such as the air to fuel ratio inside the engine. Gaseous pollutants also arise from the incomplete gasification reactions or as a result of exhaust emissions from the

combustion reactions during engine performance. Yao et al., (2013) revealed that engine emissions are the main contributors of air pollution gases like CO_2, particulate matter, NO_x, sulphates among others. A number of international bodies such as the Montreal protocol, United Nations Conference on Environment and Development (UNCED), Kyoto protocol, among others have been put in place to curb these emissions which could pose health threats. Studies have thus been conducted geared towards reducing these possible emissions (Mendiara et al., 2014; Yang & Chen, 2014). Mustafi, Raine, & Verhelst, (2013) investigated that specific NOx emissions for dual fueling was always lower than diesel fueling case. Heitz et al., (2015) further evidences the emission of GHG emission from burning syngas while (Lonati & Zanoni, 2013) found mercury emission from MSW gasification plant. Another study by (Le, Kolaczkowski, & McClymont, 2015) noted elevated levels of H_2S emissions during the study of gasification of biomass and refuse derived fuel. Such findings reveal possible emissions alongside synthesis gas production and extra care should be taken to mitigate any possible leakages and manage these emissions efficiently or use sustainable technologies that produce these emissions in least concentrations.

Having identified such problems, studies have been done to reduce the emission effects due to biomass gasification and subsequently synthesis gas combustion with detailed findings summarized in Table 2.7. Part of the efforts to reduce these emissions include co-gasification of biomass with coal (Howaniec & Smoliński, 2014). In their experiment, (Jeong, Park, & Hwang, 2014) noted reduced CO_2 emissions and reduction of fossil fuel dependency during the co-gasification of coal-biomass blended char with CO_2 at temperatures of 900-1100 °C. (Zhu et al., 2015) noted reduced NO_x emissions due to addition of steam in flue gas

combustion. To constantly monitor these emissions, the USEPA has put in place emission monitoring strategies like Acid Rain Program and the Clean Air Interstate Rule, Code of Federal Regulations (CFR), which requires continuous monitoring and reporting of sulfur dioxide (SO_2), carbon dioxide (CO_2), and nitrogen oxide (NO_x) emissions. Other monitoring systems that have been put in place include the Continuous Emission Monitoring Systems (CEMS) (EPM, 2015). The concentrations of these gases should thus be reported for any new or merging technology.

Table 2.7 Emission factor monitoring during biomass gasification

Study	**Operating conditions**	**Main findings**	**Reference**
Combustion and NOx emissions of biomass-derived syngas under various gasification conditions utilizing oxygen-enriched-air and steam	The gasifier and burner are rated at 800 kW and 879 kW thermal, respectively.	Total amount of NOx emissions increase with increasing NH_3 concentration in the fuel stream; the conversion rate of NH_3 to NO_x decreases as ammonia concentration increases in the fuel stream under conditions studied. Among the three feedstock (pine, maple–oak mixture, and seed corn), the highest nitrogen content was found in seed corn which yielded the highest ammonia concentration in syngas, which, in turn, resulted in the highest NOx emissions for all test conditions	(Huynh & Kong, 2013)
Integration of biomass gasification with a Scandinavian mechanical pulp and paper mill - Consequences for mass and energy balances and global CO_2 emissions	existing thermo-mechanical pulp (TMP) mill, co-located with a sawmill	Integration of biomass gasification with a TMP mill results in larger CO_2 emissions reduction than stand-alone operation	(Berntsson et al., 2012)
Effect of waste incineration and gasification processes on heavy metal distribution	Simulated waste used in this study consisted of wood chips and polypropylene (PP), covered with polyethylene (PE) plastic bags. Asolution (1 mL) of $Cr(NO_3)_2$, $Pb(NO_3)_2$, and $Cd(NO_3)_2$ each (0.025 g heavy metal/mL)	Gasification lowers the emissions of heavy metals, but traps more heavy metals in the bottom ash than incineration.	(Wu, Lin, & Zeng, 2014)

Effects of Fe- and Ca-based additives on NO emission during gasification of N-containing model compound under different atmospheres	The carbazole (CZ) was heated in a 150 ml autoclave at 20 ^{o}C/min up to 550 ^{o}C under 7 MPa H_2, held for 3 h. The loaded compounds included $Ca(AC)_2$, $Fe(AC)_2$, $CaCl_2$, FeCl3 and $FeCl_2$ at the ratio of 2 wt% (on metal basis).	The O_2 concentration strongly influenced NO emission during cabazole char (CZC) gasification; suitable O_2 concentration could largely reduce NO emission, but high or low O_2 concentration wasunfavorable to reduce NO pollution. Iron catalysts increased NO emission during CZC gasification in O_2 concentration ranging from 1.2% -20.9% and their catalytic effects strongly depended on O_2 concentration. $Ca(AC)_2$ and $CaCl_2$ increase NO emission under high O_2concentration (such as 20.9%) and decreased NO under low O_2 concentration (such as 1.2%).	(Guan, Chen, & Li, 2005)
Emissions of particles and trace elements from coal gasification	gasification conditions between 1473 K and 1673 K	Particles entrained in syngas from the coal gasification process were confirmed to have bimodal peaks in their particle size distributions. The peak larger than 7.8 μm in the super-micron size range consisted of ash with unburnt carbon, while the smaller peak at 0.5 μm in the sub-micron range consisted of soot with mineral deposits.	(Naruse et al., 2013)

2.8 Tar formation and reduction techniques during biomass gasification

Tars are dark brown or black viscous non -condensable hydrocarbons produced in the form of liquids together with other liquid products during gasification. The type of biomass feedstock largely determines the nature of the tar produced, which is also influenced by the gasification process and the operating conditions. Tar removal during gasification poses technical challenges and must be sustainably removed for efficient commercialization of the gasification technology. Air gasification produces a low viscosity, low reactivity tar, while steam gasification produces a liquid tar with a low molecular weight (McKendry, 2002). Tars are unpleasant in the gaseous products because of their sticky nature on metal surfaces which brings clogging of the gaseous material arising in sticky surfaces. The gasifier design and gasification temperatures determine the extent and the physical properties of the tars. Fixed-bed, downdraft gasifier are the most effective in producing a low tar/ tar-free gas because of their high heat transfer systems in the gasifier. Tar elimination and removal is a critical ingredient in biomass gasification and should be highly prioritized for effective gas production. The product gas thus has to be cleaned in filters to remove any tar products which can be processed into secondary higher value products. A number of methods are employed in the reduction of tars as summarized in Table 2.8 below. It can be concluded that the use of a catalyst achieved the highest degree of tar reduction.

Table 2.8 A Comparison of tar reduction efficiency by hot-gas cleaning methods

Feedstock	**Methods**	**Tar concentration**	**Tar reduction (%)**	**Reference**
Paper-reject sludge	Catalyst and hot-gas cleaning	0.11-0.81 g/m^3	94.1-99.2	(Chiang et al., 2013)
Pine pellets	Honeycomb (Ni-based catalyst) addition	0.44-1.07 g/Nm^3	50-60	(Ran & Li, 2012)
Chicken manure and wood pellets	Electrostatic precipitator	0.465-0.863 g/Nm^3	35.7-67.9	(Van Paasen et al., 2004)
Biomass	Al_2O_3 based catalytic filter candles	0.15-3.83 g/Nm^3	93.5 (max.)	(Rapagnà et al., 2012)
Rice husk	Ab/adsorption scrubber	34.1-92.3 g/m^3	56.4-63.6	(Yoshikawa et al., 2012)
Almond shell	Catalytic filter candles	0.55-3.67g/Nm^3 (dry)	73.0-85.0	(Rapagnà et al., 2010)

2.9 Economics of biomass power generation

It is important for biomass based power to be produced at relatively affordable costs so that the end user can have the potential for its accessibility. Highly priced processes are expensive and cannot be accessed by the end user especially that these technologies are tailored towards rural communities. Costs of bioelectricity from cogeneration plants vary widely and depend upon types of feedstocks, sizes of the plant, availability of feedstock (including transportation), and conversion technologies(Khatiwada et al., 2012). During a study on the optimization and economic evaluation of industrial gas production and combined heat and power generation from gasification of corn stover and distillers grains (DDGS)by (Kumar et al., 2010), the cold gas efficiencies for gas production were 57% and 52%, respectively, for corn stover and DDGS while the selling price of gas was estimated to be $11.49 and $13.08/GJ, respectively, for corn stover and DDGS. They estimated the selling price of electricity to be $0.1351 and $0.1287/kWh for corn stover and DDGS, respectively and further concluded that high net energy efficiencies for gas and combined heat and power (CHP) production from biomass gasification can be achieved with optimized processing conditions. In furtherance, (Bhattacharjee & Dey, 2014) examined the feasibility of harnessing rice husk potential for power generation in the rice mills of an Indian state Tripura in combination with the solar photovoltaic (PV) energy through hybrid technology and suggested that the cost of generating energy from the hybrid configuration was found to be 0.143 $/kWh. They concluded that the grid-connected PV-biomass hybrid power model would conserve over 90% of grid electricity utilized in the typical rice mills of the state where supply of grid electricity was a great concern. During the estimation of the economic costs for CHP generation(Kumar et al., 2010) (Table 2.9), the total grass root capital cost was estimated to be $12.4 million for both feedstocks where the capital cost for the part of

CHP generation, such as turbines and boiler, was approximately three times more than the capital costs for gasification only. Thus, the techno-economic considerations for choosing conversion technologies are determined by the cost of the technology, load factor, efficiency of the system, nature of feedstock type, ease of repair and system maintenance as well system robustness. If the feedstock type requires little or no transportation requirements, this will further reduce on the overall pricing of the electricity. There is need to innovate and promote economic and sustainable small scale technologies if a wider part of the World community should have access to energy. Users will always compare the relative pricing of electricity as compared to other energy sources and will show high willingness to-pay or choose a given energy source if the technology performs with high integrity, reliability, convenience, safety, and availability on addition to being economical. It is important to note that users will pay a great attention to the pricing of electricity per unit cost.

Table 2.9 Economical results for gas production and CHP generation from corn stover and DDGS gasification(Kumar et al., 2010)

Item	Gas production from corn stover	CHP generation from corn stover	Gas production from DDGS	CHP generation from DDGS
Fixed capital investment ($)	3,170, 000	12,400,000	3,170,000	12,400,000
Cost of land ($)	150,000	250,000	150,000	250,000
Cost of Labour ($/year)	150,000	250,000	150,000	250,000
Cost of utility ($/year)	664,355	664,355	1,298,860	1,298,860
Cost of raw material ($/year)	889,089	889,089	1,901,160	1,901,160
Selling price for heat ($/GJ)	6	6	6	6
Revenue from heat ($)	774,749	1,168,474	1,429,566	1,513,210
Revenue from gas or electricity ($)	2,512,431	5,249,770	3,854,530	6,897,290
Selling price for gas ($/GJ)	11.49		13.08	
Selling price for electricity ($/kW h)		0.1351		0.1287

2.10 Biomass based energy versus food security

In a world of about 7.6 billion people, some 2.4 billion rely on traditional fuels such as wood, charcoal, agricultural residues and dung for cooking and heating and the percentage of those depending on biomass will increase to 2.6 billion by 2030(IEA, 2006). Biomass is thusone alternative sources of energy in many parts of the World(Augusto, Nogueira, & Capaz, 2013). However, the consequences of producing power from biomass could result into competition between food production for both animals and humans and power production (Popp, Lakner, Harangi-rákos, & Fári, 2014). A study done by (Okudoh, Trois, Workneh, & Schmidt, 2014) asserted and recommended the use of cassava as the next main source of biomass energy. Cassava as a staple food has so many advantages that other food crops may not possess. These include being more resistant to drought, high starch content, cheap, requiring less labor to cultivate, thrives in soils that are less fertile as evidenced in (Okigbo, 1980). Accordingly, (Ewing & Msangi, 2009), hypothesized that if power production will continue using biomass as the source of fuel, there will be shortage of food production. (Josef Schmidhuber, 2007)anticipated increased prices for food as a result of biofuel production. Thus, if the amounts of available food are hampered with power production without first meeting the world's food demand, the situation would turn out to be catastrophic. It is important to provide energy with no compromise to food security(Alarcon, Joehnk, & Koch, 2013). An even larger concern however is the large production of pollutant gases from power production activities which have rendered the rains acidic (Singh & Madhoolika, 2008) hence depreciation in the productivity of the soils. Acid rain doesn't only pose effects to soils but also to human beings, quality of building, crops, animals, and aquatic ecosystems. Of a concern, is the discovery of corn as the potential source of biofuel (Jeschke & Heggenstaller, 2012). Several studies have been undertaken (Kim, Seo, Kim, & Han, 2015; Tan, Liu, Bliss,

& Tieszen, 2012; Tyndall, Berg, & Colletti, 2011) and they have revealed that corn (stover) is a very good source of biofuel. Use of algae as a raw material in biofuel production has been proposed(Bharathiraja et al., 2015), although currently, biofuels produced from algal biomass is not economical since biomass cultivation, processing and separation of fuel products appears to increase costs of production. In fact (Karp & Richter, 2011) recommended that the use of high-input food crops for liquid transport fuels needs to be phased out and replaced by the use of crop residues and low-input perennial crops with multiple environmental benefits. They(Karp & Richter, 2011)further suggested that more research effort is needed to improve yields of biomass crops grown on lower grade land, and maximum value should be extracted through the exploitation of co-products and integrated biorefinery systems. (Karp & Richter, 2011) further recommended that policies must continually emphasize the changes needed and tie incentives to improved greenhouse gas reduction and environmental performance of biofuels. Therefore there is a need for more research in this area to fully explore the possibility of using algae as a raw material for biofuels with minimal costs. One recent study(Chen & Zhang, 2015) discovered that perennial plant communities like switch grass, bamboo and annual crops have higher biomass yield per hectare, have easy resource management, store more carbon, maintain better water quality, utilize nutrients more efficiently, tolerate more extreme weather events and resist pests better than annual crops like cereal grains, legumes and oil seeds. In the food security perspective of view, this presents a promising alternative for biomass power production while reducing threat on human food availability. (Rosillo-Calle, 2012) suggested three alternatives to avoid conflict between food and energy as shown in Table 2.10

Table 2.10 Alternatives to avoid conflict between food and energy Source: (Rosillo-Calle, 2012)

Solution	Description
Agriculture	• Diversify feedstocks and move away from key food crops (corn, cereals), toward agricultural residues/wastes and cellulose-based feedstocks • Use only the most suitable feedstocks (economically and environmentally) such as sugarcane whose productivity can largely be increased with low investment while providing all energy needed to run a plant + surpluses. • Pay considerable attention to crops that have more drought, heat, pest/pesticide tolerance. • Bring in new and more productive crops (short cycle) so that a second harvest can be achieved and promote intercropping. For example, ongoing work on sweet sorghum which can produce very high biomass yields with less water and fewer chemical inputs and can be grown on land not devoted to food production. • Improve agricultural management practices and renew effort on R&D. • Recognize that a modern and dynamic agricultural sector has to be at the core of biofuel development. • Increasing crop productivity, which in many countries is extremely low for many major food crops; pay greater attention to the development of biorefineries.
Biomass for energy	• Avoid land grabbing for biofuels, particularly in developing countries, at the expense of staple food crops; • Need to be selective of how to use biomass resources for example, perhaps use solid biomass rather than in its liquid forms.
Social and Environmental Issues	• More research to improve the methods for calculating GHG; investigate in detail the GHG implications from livestock • Support fair and freer international bioenergy trade, standard and harmonization; • Ensure that a sustainability criterion applies not only to biomass for energy but to all energy sources.

2.11 Assessment, ranking and evaluation of sustainable technologies

Although a number of technologies have been developed for biomass Integrated Gasification Combined Cycle (IGCC) (Aziz, 2015; Kumar et al., 2010) , only those technologies that are sustainable are likely to attract wider markets and would have a higher degree of acceptability by the end-user. For its essence, different authors have classified the key performance indicators if a given system should be classified as sustainable. In their study,Dewulf and Van Langenhove (2005)performed a technical assessment of sustainable technologies by incorporating industrial ecology principles into a set of environmental sustainability indicators and observed that the sustainability of various technology options is evaluated in a quantitative way by using the second law of thermodynamics. Their findings revealed five sustainability indicators basing on i) the renewability of resources; (ii) toxicity of generated emissions; (iii) input of used materials; (iv) recoverability of the products at the end of their use and (v) technological efficiency. More efforts have been geared towards developing of more standards for sustainable systems(Mainali & Silveira, 2015.,United Nations, 2007., Dikshit et al, 2012) but thereiscurrently no standard baseline for adaptation of sustainablesystems. Notwithstanding, sustainable technology should aim at better efficiency, better resources use, better cost effectiveness, better environment, better energy security, and better design and analysis but for effective sustainability Canan and Ibrahim (2015) suggested that an energy system must meet the following criteria:

(i) Have minimal or no negative environmental or social impact;

(ii) No natural resource depletion

(iii) Being able to supply the currentand future population's energy demand

(iv) Equitable and efficient manner

(v) Air, land, and water protection;

(vi) Have little or no net carbon or other GHG emissions

(vii) Have safety today without burdening future generations.

The possible sustainable energy system options as illustrated in Figure 2.4 should be able to comply with the core (3S) for sustainability generally referred to as source-system-service. By being able to use a feed source that is clean, abundant, cheap as well as available, the system should achieve increased efficiency, have multiple generation streams, able to achieve system integration with minimal waste or reusable waste to generate a service that is dependable, efficient, practical and clean.

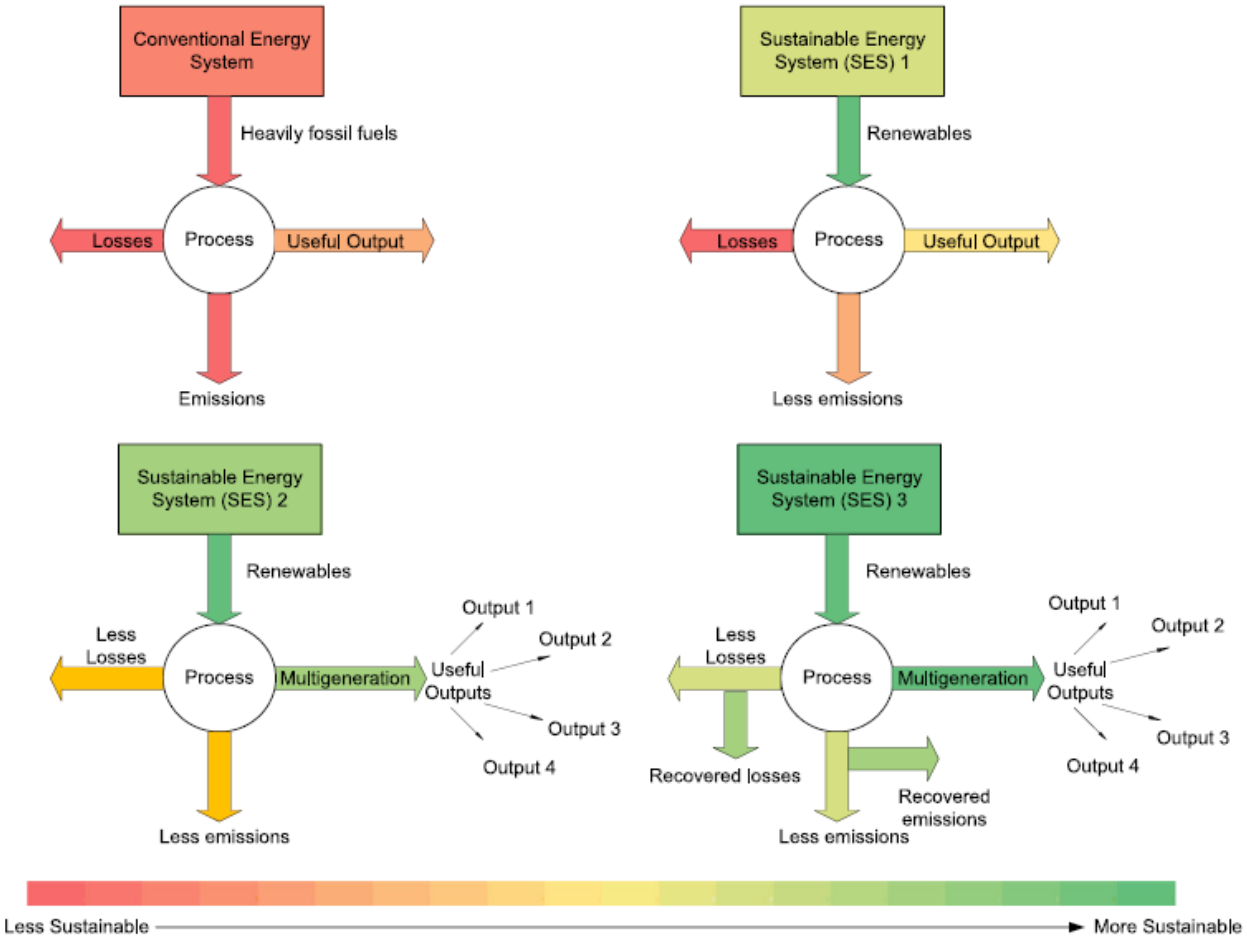

Figure 2.4 Possible sustainable energy system options(Canan, Acar and Ibrahim, 2015)

2.12 Summary for review of literature

Biomass gasification is one promising avenue for clean energy production that could combat the effects of global warming and subsequently climate change. This review discussed in details the production of power from biomass devoted to in-depth analysis of the mechanism of power production from biomass, technologies employed in power generation, factors affecting biomass gasification for power generation, the chemistry involved and the effect of production conditions. This work has thus discussed the whole cycle on the possibility of biomass power production especially for combined heat and power. Gasification temperature, ER, fuel moisture content, particle size, pressure and catalyst addition have been reported to have significant effects on the quality of produced syngas while ER determines the gasification temperature for autothermal gasifiers. There is need to find a balance between the best ER that would produce the optimal gasification temperature without compromising gas quality while catalyst addition has been reported to improve the gasification efficiency.

However, there is still need to understand the economics of small scale biomass power production systems for the different bioenergy systems. In general, there is lack of understanding on how the economics of power generation would vary with the different designs of the gasifier. There is also a need to test and optimize the performance of different small scale bioenergy systems on different biomass feedstocks and match their performance with the needs of the end user. Most theories in literature report findings on the laboratory scale with less data on pilot energy systems. Sufficient data on pilot energy systems would provide a basis for dependency and their reliance as promising bioenergy systems and would further assist to provide sustainable energy solutions especially for the rural communities.

The uniqueness with this work is its ability to discuss the process of biomass power generation from the start of the gasification process (cradle) till the end of energy recovery (grave).This could in furtherance provide understanding on the suitability and application of this technology upto the end user requirement.

Chapter 3

3.0 METHODOLOGY

3.1 Sample preparation before gasification

Biomass wood chips of Scots Pine and Spruce species were supplied by Stones4homes LTD, Riccall Airfield Industrial Estate Market Weighton Road Barlby Selby North Yorkshire YO8 5LDa local supplier company in the UK. The supplied biomass was of size $1.0 \leq cm \leq 4.0$ and matched with the gasifier size specification tolerance of $1.3 \leq cm \leq 3.8$. The woodchips were supplied in a 2 cubic metre polythene bag and stored inside the Energy Technologies Building, University of Nottingham. The wood chips werefirst subjected to sieving before applied for gasification to remove fine particles that would resist the flow of air during gasification. The wood chips were sieved using a parasene garden riddle of 0.64mm mesh (¼ inch). The photographs of woodchips before and after sieving are detailed in appendix A. The woodchips were then dried by indoor air by spreading them on the floor in a closed room. This was aimed at reducing the wood chips moisture content to less than 10%. The moisture content of woodchips was thus tested using a digital moisture content analyzer (Dr. Meter) before the start of every experiment.

3.2 Bulk density determination

Bulk density of woodchips was determined according to ASTM E-873-82 (ASTM. D1762-84, 2013).An empty cylindrical container of known volume was weighed (while empty) using an analytical balance (Sartorius Universal, U6100D). The container was then filled by

pouring sieved woodchips from the top edge of the container and the new weight of the container and sample determined. The bulk density ρ_b (kg/m^3) was determined as the net mass of the material divided by the volume of the container as follows:

$$\rho_b = \frac{W_2 - W_1}{V} \quad \ldots\ldots\ldots\ldots\ldots\ldots\ldots\ldots\ldots\ldots\ldots\ldots\ldots\ldots\ldots\ldots\ldots\ldots\ldots\ldots (3.1)$$

WhereW_2 = weight of the container with sample [kg], W_1= weight of the container [kg], and V = volume of the container [m^3]

3.3 Ultimate analysis

The ultimate analysis was carried out using the Dumas combustion technique (Dumas, 1826 as cited by(Buckee, 1996) using an elemental analyzer LECO CHN628 Series. For the CHN analysis, 0.75 mg of dried and crushed samples were weighed and mixed in a tin capsule then combusted in a primary furnace at 950^{o}C and secondary furnace at 850^{o}C in the presence of pure oxygen. The oxidized products CO_2, H_2O and NO_2 passed through a series of driers to remove moisture, and were homogenized before being carried by a constant flow of carrier gas (helium), and finally CO_2 and H_2O were separated and quantified with a non-dispersive infrared (NDIR) cell. NO_2 gases were passed through a copper reducer, the gas was reduced to N_2 and the quantified with a thermal conductivity cell (TCD). The chromatographic responses were calibrated against pre analyzed standards and the CHN elemental contents are reported in weight percent. Total O was derived by subtraction according to the ASTM method (equation 3.2) as follows: (Enders, Hanley, Whitman, Joseph, & Lehmann, 2012)

$$O\left(\%\frac{w}{w}\right) = 100 - ash\left(\%\frac{w}{w}\right) - C\left(\%\frac{w}{w}\right) - N\left(\%\frac{w}{w}\right) - H\left(\%\frac{w}{w}\right) \ldots\ldots\ldots\ldots\ldots\ldots\ldots\ldots\ldots .3.2$$

For S, the sample was weighed into a combustion boat and placed in the furnace with pure oxygen at 1350 ^{o}C. The oxidized gases in the combustion system flow through an anhydrone tube to remove moisture and are quantified in the sulphur infrared detection cell. The final results for sulphur are given as weight % or parts per million (ppm).

3.4 Process description and assembly of the downdraft gasifier

The downdraft gasifier utilizes solid biomass for power production. The unit combines the technologies of Fixed Bed Gasification (FBG) and Internal Combustion Engine (ICE). The 10KWe downdraft gasifier is a manufacturer supplied product by All Power Labs (USA)(model 7.1.3) with its own built-in safety features consisting of mainly a biomass hopper, a fixed bed reactor, cyclone, particle filter, tar cleaning system and the generator set. It is designed to make gas from waste biomass such as woodchips, agricultural residues, among other biomass materials. The gas then fuels an internal combustion engine, and in turn, generating power. The producer gas from the gasifier is fed into a spark ignition engine of engine power 10Kw and electrical power 5.5 kV A, nominal capacity with output shaft rotation coupled to electric generator providing 220 V at output voltage.

A schematic of the gasification rig is provided in the Figure 3.0 below with a detailed representation shown in Figure 3.1. According to the gasifier experimental rig kit manual (GEK manual, 2012), the rig is a self-contained unit mounted on a pallet of area 1.2m^2 x 1.8m high. It is a closed system and thus not connected to mains electricity, gas, or water. A 12v car rechargeable battery powers all the electrics. The battery is re-charged via an

alternator attached to the engine. The gasifier is made up of a hooper of capacity 30 gallon ($0.1m^3$) where biomass is initially immersed and allowed to fill by gravity before the system is made gas-tight. The wood chips are manually loaded into the hooper and fall into a drying bucket made up of a shell and tube heat exchanger which heats the fuel to ca. 100°C using hot gas that is leaving the reactor. This initial drying allows moist biomass to be accommodated. The gasifier was thus designed to accommodate moist woodchips up to< 30%. From the drying bucket the fuel is auger fed into the pyrocoil situated directly above the gasifier reactor. Here the wood chips are heated in the absence of oxygen ("pyrolysis") by a combination of heat transfer from the reactor and by a pipe which carries waste engine exhaust through the pyrocoil. Air is used to create the initial internal heat of the gasifier reactor. This air enters under negative pressure, driven by the engine demand. Air intake is computer controlled by pressure and temperature sensors to maintain optimum operating conditions and also to monitor system conditions so that safety is ensured.

After gasification, the gaseous products leaving the reactor (CO, H_2, CH_4, CO_2, H_2O, etc) then enter a cyclone particle separator and a packed bed gas filter before entering the engine. Particulate matter and condensate is collected by the cyclone in a container that is emptied after each run and disposed off to the waste collection bucket. Condensate and smaller particles, which are not collected in the cyclone, are trapped within the packed bed filter which comprises charcoal, fabric or sawdust, and oiled foam. The run time for a full hopper of woodchips is between 3 – 10 hours but the actual time depends on engine speed and the intended power output. Engine speed is controlled by a governor attached to the engine throttle, which is fully automated from the Power Control Unit. There are only two outlets for gas. Both are oriented vertically (0.5 metres apart) and have their outlet at the top of the unit. One is an engine exhaust which functions during normal operation. The second is a flare stack which functions for the first 10 minutes during start-up. Gas is initially bypassed to the

flare stack until the reactor gets to the normal operating temperature of about 850 ℃. Bypassing is achieved by the opening and closing of a pipe valve. Once the gasifier performance attains stability, the generator is connected to a local electrical load and the amount of electrical power output can be tested. As a result, producer gas utilization leads to electricity production.

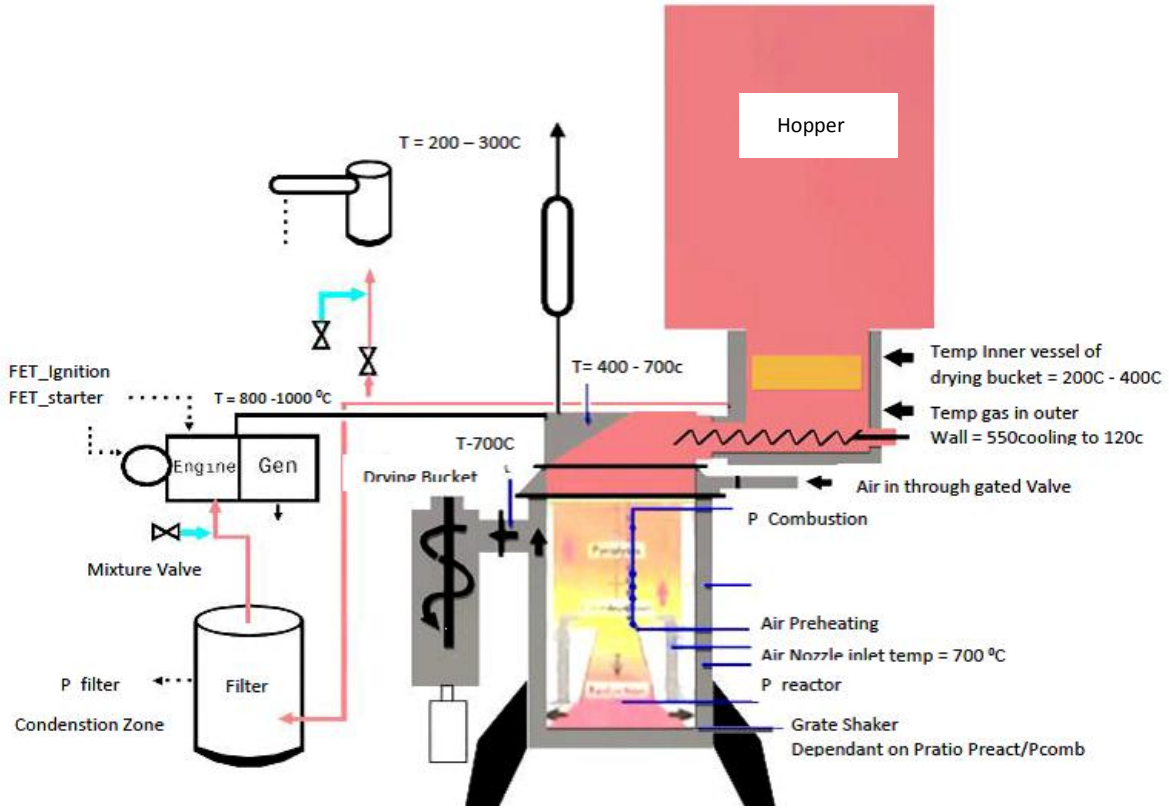

Figure 3.0 Schematic of the experimental set up and assembly of the downdraft gasifier

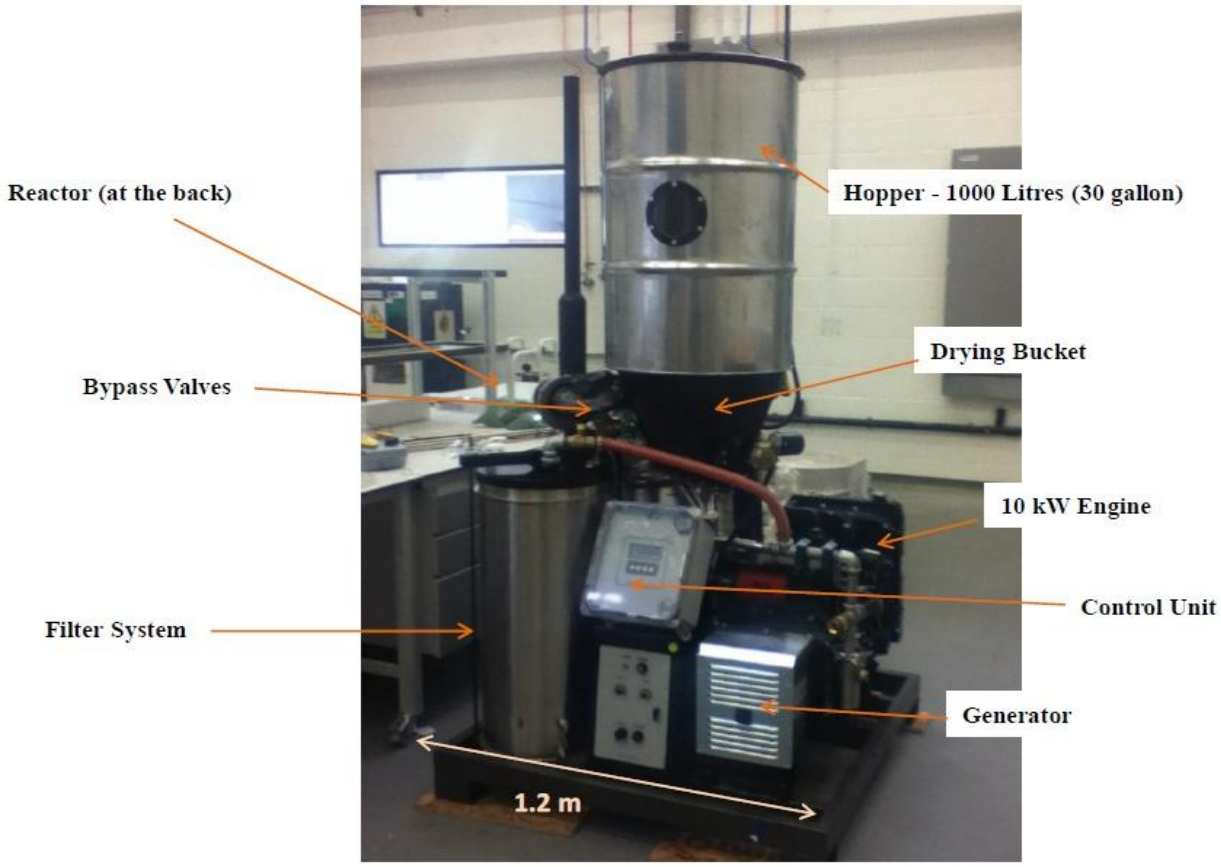

Figure 3.1 Photo of the experimental set up of thedowndraft gasifier comprising of the 10KWe generator set and the gas engine.

3.5 Operating the gasifier

The gasifier was operated by following a well-structured procedure as illustrated in Figure 3.2to minimize performance errors, attain reliable and substantial results as well as minimize the health and safety risks associated with running the gasifier. This involved maintaining a thorough cross checking of standard operating protocols, a step by step procedure for startup of the gasifier, running the gasifier under steady state conditions as well as termination of the gasification experiments at the end of each run.

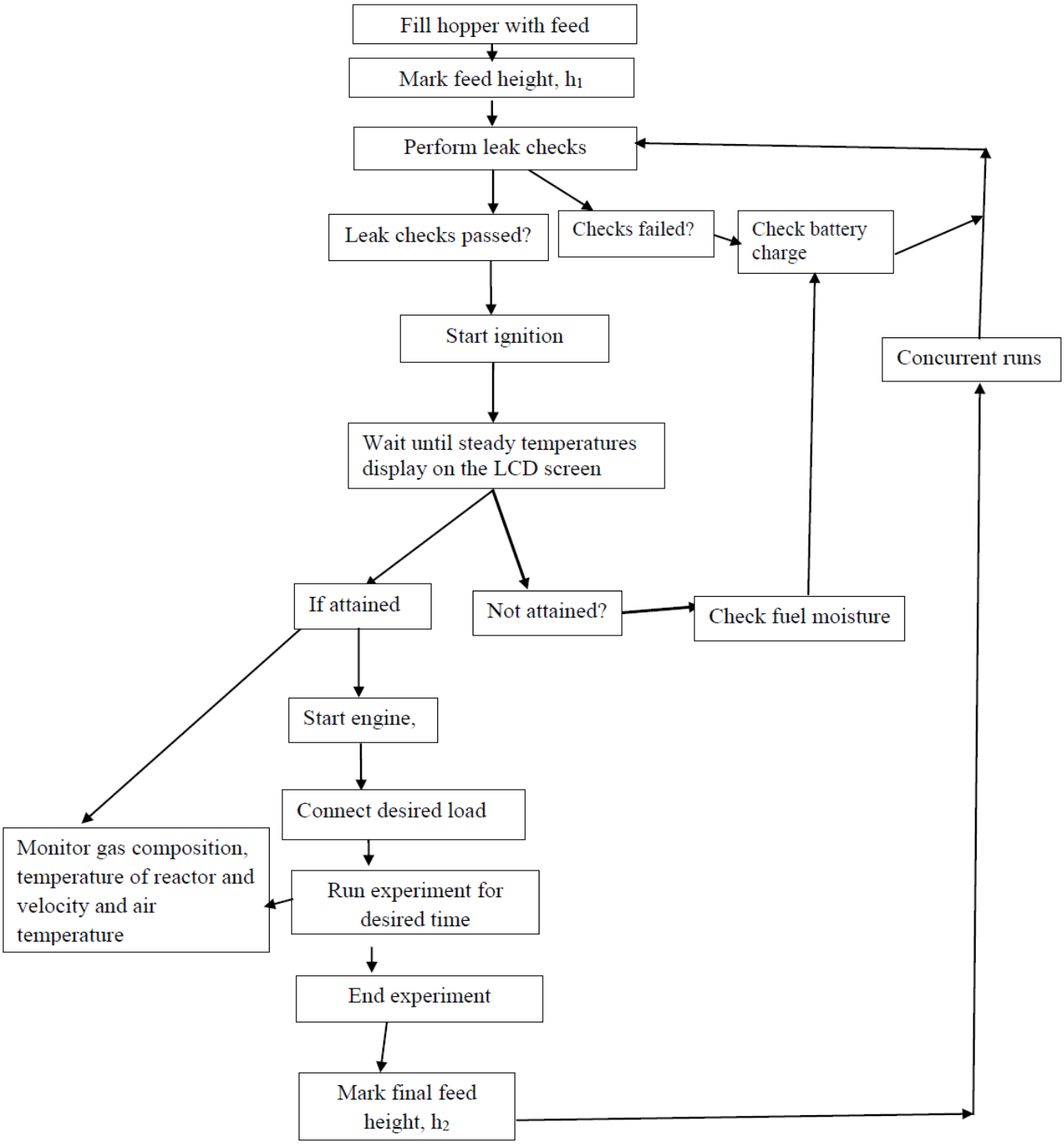

Figure 3.2 The flowchart for the experimental procedure for the study

3.5.1 A step by step experimental procedure for startup of the gasifier

Before startup of the gasifier, the following checklist is done to ensure that everything required for a safer start up is available. The check list and start up procedure are observed according to the system manual (GEK manual, 2012) as detailed below.

i. Ensure that there is enough charcoal in the reactor before start up. This charcoal is useful to initiate the quicker combustion reactions during initial start up as well as being useful in the reduction processes while the gasifier is running.
ii. Fill the hopper with enough woodchips to sustain the gasification runs for a given period of gasification time.
iii. Ensure that gas and air filters are properly checked to ensure their thorough performance and to avoid contamination of the producer gas with particulates which would hinder the effective engine perfomance.
iv. Confirm if the air seals and connections are tight to ensure that all the supplied air does not leak out and is used for the purpose of gasification. This is confirmed by perfoming a step by step leak test as detailed in **section 3.3.2**
v. Ensure if the engine oil coolant is present as this will prevent the engine from over heating.
vi. Confirm if the battery has enough battery to run the gasifier. This is tested from its ability to power the gasifier computer system, as well as its ability to power the fans upto the recommended pressures of atleast 10 inches of waterwhich is the rated suction capacity of the dual fans when deadheaded
vii. Confirm if the CO meter sensor is in place and working properly. This sensor sounds alarm when there is any leakage of CO.

viii. Empty condensate jar, check gaskets, engine condensate jar with longer checks done on filters, cyclone and blowers. This enables working in a cleaner environment as well as assisting to establish a proper material balance of the system

ix. Check if the auger and all blower switches are connected.

x. If all the above is in order, the working space is then cleared and the gasifier can be set to start

3.5.2 Performing the leak test

It is important to do the leak down test every time the gasifier is operated to know that the experimental apparatus is behaving in a constant known pattern and to protect the equipment and personnel during operation. Running the gasifier without a known uniform pattern would affect the service life of the gasifier as well as give false and unreliable experimental results. Before the start of the gasification experiment, the leak test is done to ensure that the supplied air doesn't leak out but specifically reacts with the wood chips without any losses. The procedure for the leak test follows the order below.

a) Place a plug in the air intake check valve
b) Close the engine valve
c) Open the flare valve
d) Turn the gas fans to maximum when the system is cold.
e) A well-sealed system displays a pressure of -100, or 10 inches of water which is the rated suction capacity of the dual fans when deadheaded. This portion of the test reveals two key points as having a functional gas drive system with correctly working

fans and a well charged battery. It also reveals that there are no gross leaks such as hopper lid off, hatches removed among others.

f) The other portion of the leak down test is to initiate a countdown timer with a second hand, phone app, wristwatch, etc

g) Closing the flare valve, turn off the fans, and determine how long it takes the minor leaks in the system to return the pressure display to atmospheric or 0. This is the second leak down number

h) A leak downpressure ratio of -100and 30 seconds, implies that the system has a functional gas drive, and reasonably sealed and that the power Pallet can be well operated

i) A leak down test of 10 inches of water and 5seconds implies that the gas drive is fine, but that there are some significant leak points where air is leaking into the system and so air connection points need to be checked to verify if proper air tight sealing is confirmed.

j) If you begin a run, and rapidly come up to temperature, but only belatedly notice that the flare does not seem to be behaving as it should (roaring powerfully with good gas quality) the reactor could be undergoing secondary combustion of the producer gas via a tiny air leak at the ash clean out hatch gasket or some other low end gasketed area.

k) This small directed jet of atmospheric oxygen acts as an oxy-hydrogen cutting jet on the heat exchanger air lines and creates a pinhole which causes thermal runaway when the pierced airline contributes more oxygen to the secondary combustion, melting more metal, which enlarges the jet and cuts the rest of the airlines as well as possible complete destruction of the reactor.

l) Leaks that can cause secondary combustion in the producer gas path are the most critical and the gasifier should not be operated with that type of leakage

m) A small leak on the pyrocoil lid, or hopper lid gasket, will give less power but will not result in a meltdown.

3.5.3 Startup of the gasifier

Once the gasifier passes the leak test and the system is confirmed to behave according to the performance requirements, the gasifier can now be started according to the startup procedure below as referred to in the GEK manual (2012)

i. Turn on the gasifier power switch
ii. Open the ignitor port
iii. Open the flare gas valve and close the engine ball valve
iv. Turn on gas blower to increase P_{react} to about 15 inches of water
v. Wire up the load bank but don't switch it on.
vi. Light the reactor with propane torch through ignition port
vii. Cap the ignition port if T_tred is climbing and above 80°C
viii. Increase the gas flow rate to about 6 on the dial
ix. Add some air to about 4 on the dial until the flare lights and the flame is pulled down into the burner and not seen above the top of the flare stack.
x. Adjust the air and gas blower settings to manually mix the amounts of air and gas. This is confirmed based on the sound of the flare as too much air will put the

flare out. A proper air to gas mixture is confirmed if the flame is pulled down into the stack with a whoosh sound.

xi. After about 0.25h of preheating with a lighter, bed temperatures rise to around 200°C, at which a small amount of biomass is combusted and rapidly increases the bed temperature to a desired level of ca.750–950°C (T_{tred}) and ca. 675 – 850°C (T_{bred}), high enough to initially sustain autothermal conditions during the gasification step. The heat released in the autothermal conditions with the exception of energy losses isutilized in the endothermic reactions allowing pyrolysis and gasification reactions to endure (Sarker et al., 2015).

xii. Once ideal temperatures are reached, (T_{tred} (750 – 950°C) and T_{bred} (675 – 850°C), close the flare valve, open the engine valve, turn off the air and gas blowers then crank the engine.

xiii. The engine will start when air is purged from the gas line.

xiv. Once the engine is properly running, it is now safe to apply the load in intervals according to the load requirement of a given run and the duration of the experiment.

xv. The load is controlled by a distribution box built with four different connection outlets and four switches which are applied in intervals. Each outlet is connected with a load bank of a known rating. Out of the four loads connected to the distribution box in the four connecting outlets, the two loads are each of 2kWe and the other two other loads are of 3kWe each. These load ratings can be applied indipendently, in pairs or can be varied accordingly but can not exceed 10kWe which is the maximum rated power of the gasifier.

xvi. The syngas composition going to the engine can be monitored once ideal conditions have been attained or when the engine has stabilized. This depends on

the nature and objective of the experiment conducted. The procedure for gas analysis is detailed in section **3.3.3**

xvii. Following the end of the gasification time, the experiment can now be shut down accordingly as detailed in section **3.5.5**

3.5.4 Procedure for gas analysis

Analysis of the producer gas occurs while the experiment is running. The analysis of thegas composition is observed according to the following sequence

i. Press the “on” button of the analyzer for about five seconds for it to power
ii. Plug the connector to the back of the PC into the gas analyzer
iii. Ensure that the gas sampling kit is filled with water (upto 350cc) and connected to the gas sampling line. The detailed connection of the gas sampling line is shown in **Figure 3.3**

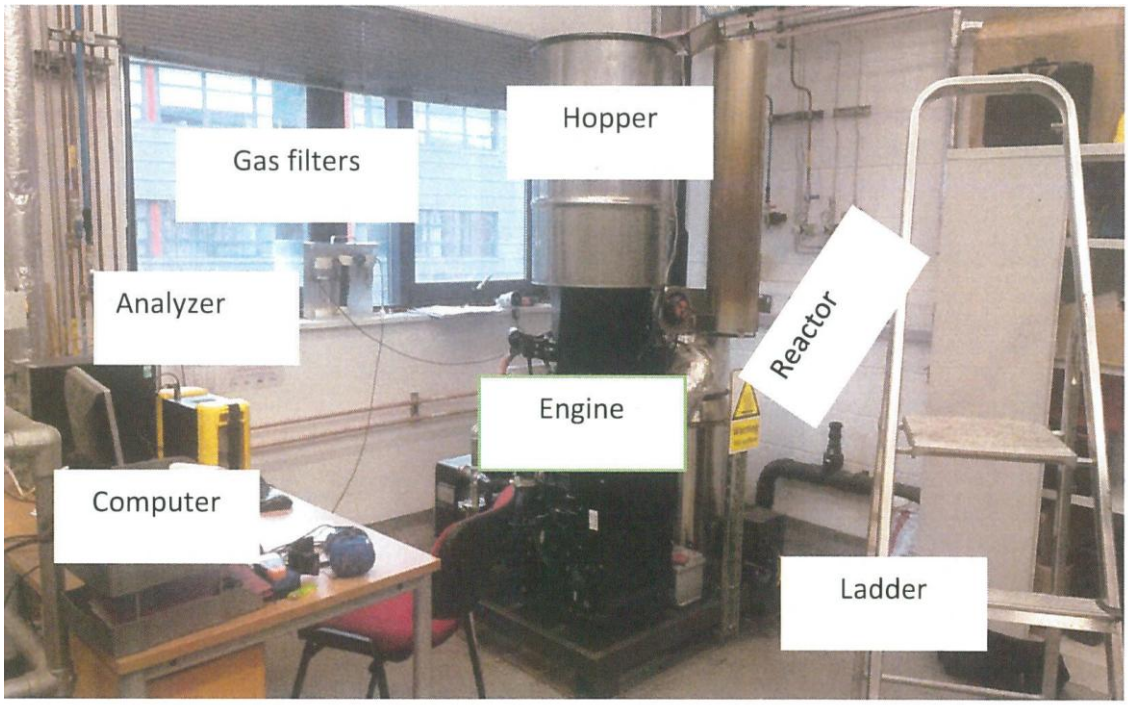

Figure 3.3 Experimental set up with a gas connection line

iv. Verify that the analyzer is well calibrated by checking the previous gas calibration date and subsquently the calibration certificate. The details of gas calibration shall not be reported here as the analyser was operated within its calibration time.

v. Switch on the PC connected to the analyzer and click the gas analyzer icon on the desktop

vi. When the display screen appears, type “COM 5” and press connect

vii. Back to the analyzer, delete all the previous stored memory and set the residence time interval to 5seconds

viii. Press record and key in the password as 9999, set the site number to 1 and enter through the rest.

ix. Press open pump and confirm if its properly working. A properly functioning pump will display two green lights that keep flashing as the analyzer is capturing data.

x. Press the analyzer save button to store all the data into its memory and continue to capture and save data for the duration of the analysis

xi. Once all the required data has been captured,press the data and save button on the screen of the PC to now store data into the computer and saved for further data interpretation.

xii. Data in the analyzer is initially saved as a text file but can be converted to excel file for easy interpretation.

xiii. To achive this, copy and paste the text file into excel data sheets, highlight the first column of datasheet, click the data icon of the excel data sheet and then tick the " delimited icon, click next and choose the delimiters for "coma" and equal sign "=", then next while column data format should be general.

xiv. Data can now be saved as an excel workbook and further interpreted.

3.5.5 Shutdown procedure of the gasifier

Following the completion of the gasification experiment, the experiment can be safely terminated according to the following shut down procedure

i. Disconnect the gas analyser from the contineous monitoring.
ii. Turn off the electrical load as well as the engine
iii. Close the engine gas valve and open the flare valve.
iv. Turn the gas blower knob to low (about 4 on the dial)
v. Turn the air knob until the flare lights.
vi. After about five to ten minutes, the gasifier temperatures drop down and it is safe to switch off the system once the pressure is below negative five (-5).
vii. The system is now left to cool until the start of the next experiment.

3.5.6 Investigating gasification temperature with connection load

To investigate the variation in temperatures with the connection load, electrical loads of various ratings were each connected to the experimental rig via the generator connection point and the system parameters such as temperatures were monitored. Experiments were done in triplicate to verify repeatability of results. The initialsT_{tred} and T_{bred}, respectively indicate the temperatures at the top and bottom of the reduction zone.

3.5.7 Determining the actual amount of power produced from the gasifier

To verify the exact power output of the generator operated on 100% syngas, a universal power analyzer (PM 3000) shown in Figure 3.4 was used which could simultaneously read values for voltage, current and power.

Figure 3.4 A photograph of Power Analyzer (PM 3000)

3.5.8 Computation of the Equivalence Ratio (ER) of the gasifier

The ER is an important parameter affecting the performance of the gasifier. The ER of the gasifier is the ratio of the actual quantity of the air supplied for gasification of fuel wood to the quantity of air required for the complete combustion (stoichiometric) of the fuel wood(Raman & Ram, 2013b). The consideration of the rate of wood supply, rate of incoming air and the gasification time are important parameters to consider in order to minimize the number of parameters upon which the performance of the gasifier depends. Thus, the ER of the gasifier can be computed based on the formulae below (Zainal, Rifau, Quadir, & Seetharamu, 2002b).

$$ER = \frac{Q \times T}{M \times \left(\frac{A}{F}\right)} \ldots\ldots\ldots\ldots\ldots\ldots\ldots\ldots\ldots\ldots\ldots\ldots\ldots\ldots\ldots\ldots 3.3$$

Where:

Q, Rate of air supply, m^3/s

T, Duration of the run, hr

M, Mass input of gasified wood chips, kg

A/F, Air to Fuel ratio at ER of 1, m^3/kg

The A/F at (ER of 1) is computed from the stoichiometric reaction equation between woodchips and air to give carbondioxide and steam as detailed in equation 3.4. The mass flow rate is computed as a ratio of the mass gasified to the time of gasification. The values of M and A/F are subsequently substituted and would vary depending on the experimental conditions. The rate of air supply Q (m^3/s), was computed as a product of the cross sectional area for air inlet, A (referred to in Figure 3.3) and the corresponding incoming air velocity, U (m/s). The incoming air temperature and velocity was measured using a hand held portable Vane Thermo- anemometer / Datalogger (SDL310).

3.6 General empirical formula of wood chips

In order to establish the stoichiometric global equation for complete gasification of woodchips to be used for estimating the ER, it is important to determine the empirical formula for woodchips so that its general formula can be computed based on the average composition. The mole ratio formula, based on the ratio of C,H,O,S and N gives the workable formula for most biomass that can be used in writing conventional equations (Saravanakumar et al., 2007). From literature, the composition of Nitrogen and Sulphur in the woodchips is very small and was ignored in this calculation (Ahmed, Nipattummakul, & Gupta, 2011).A detailed empirical formula calculation is shown in Table 3.0. As determined from the elemental analysis of woodchips, its average elemental composition is detailedbelow.

Table 3.0 Typical woodchips with the following ultimate analysis composition

Material, %	**C**	**H**	**N**	**S**	**O**
Average	48.7±3.9	6.0±0.7	0.0±0.1	0.0	42.1±3.4

Thus the general formula of wood chips can be computed as follows.

$$Consider\ the\ equation\ of\ woodchips\ as\ C_xH_yO_Z\ where\ x, y, and\ z\ are\ subscripts.$$

$$Assume\ x = 1\ and\ by\ using\ the\ formula$$

$$y = \frac{mass\ fraction\ of\ Hydrogen \times Molecular\ weight\ of\ Carbon}{mass\ fraction\ of\ carbon\ \times Molecular\ weight\ of\ Hydrogen}$$

$$y = \frac{6.0 \times 12}{48.7\ \times 1} = 1.5$$

$$z = \frac{mass\ fraction\ of\ Oxygen \times Molecular\ weight\ of\ Carbon}{mass\ fraction\ of\ carbon\ \times Molecular\ weight\ of\ Oxygen}$$

$$z = \frac{42.1 \times 12}{48.7 \times 16} = 0.7$$

The general formula for wood chips is thus $CH_{1.5}O_{0.7}$

3.7 Sample calculation of A/F at ER of 1

From the empirical formula calculation, the reaction between air and woodchips can be established as,

$CH_{1.5}O_{0.7}$+ 1.025(O_2 + 3.76 N_2→ CO_2 + 0.75H_2O + 1.025(3.76N_2) 3.4

$$\text{Grams of woodchips (wc)} = (12 \times 1) + (1 \times 1.5) + (0.7 \times 16)$$
$$= 24.7\text{g}_{\text{wc}} \text{ or } 24.7 \times 10^{-3}\text{kg}_{\text{wc}}$$

$$Grams\ of\ air = 1.025\big((2 \times 16) + (3.76 \times 2x14)\big)$$
$$= 140.712 g_{air}\ or\ 140.712 \times 10^{-3}\text{kg}_{\text{air}}$$

From the ideal gas equation, PV = nRT

$$Density\ of\ air, \rho air = \frac{Mass\ of\ incoming\ air(M) \times Pressure(P)}{Gas\ constant(R) \times Temperature(T)} = \frac{MP}{RT}$$

$$\rho_{air\,26.8\,^{\circ}C} = \frac{\frac{28.97}{1000}\frac{kg}{mol} \times 101325pa}{8.314m^3\frac{pa}{kmol} \times 299.8k} = 1.1777\frac{kg}{m^3}$$

$$Volume\ of\ air = \frac{mass\ of\ air}{density\ of\ air} = \frac{140.712 \times 10^{-3} kg_{air}}{\frac{1.1777 kg}{m^3}}, = 0.1194803 {m^3}_{air}$$

$$Air\ to\ fuel\ ratio\ \left(\frac{A}{F}\right)\ at\ ER_{=1} = \frac{volume\ Air(m^3)}{Mass\ of\ wood\ chips\ (kg)}$$

$$= \frac{0.1194803\ {m^3}_{air}}{24.7 \times 10^{-3}\text{kg}_{\text{woodchi ps}}} = 4.8372608\frac{m^3}{kg}$$

$$\left(\frac{A}{F}\right)\ at\ Q_{=1} = 4.8372608 m^3/kg_{wood}$$

3.8 A detailed calculation of area for air inlet of anemometer

In order to determine the extent of the gasification reactions, air used during gasification is computed and compared to the fraction of woodchips that instantaneously burns with it. Both should burn at a constant ratio for the duration of the gasification experiment and this determines the ER of the gasifier. The space allowing the flow of incoming air is shown in Figure 3.5

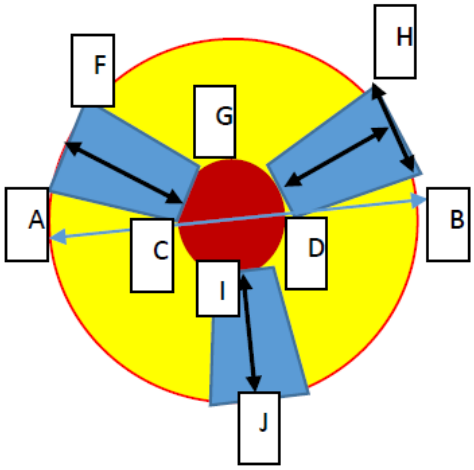

Figure 3.5 Schematic representation of air space in red color

Diameter AB=6.8cm, diameter inner circle, CD = 2.9cm, Length of Trapezium, CG= 0.5cm, AF=0.8cm, Width, IJ= 2cm. Thus, three trapeziums are of equal size hence

$$Area\ due\ to\ air$$

$$= Area\ of\ \ circular\ section\ AB - 3xArea\ of\ trapezium - Area\ of\ inner\ circle$$

$$= \pi \frac{D_{AB}{}^2}{4} - 3\left(\frac{1}{2} \times 2bh\right) - \pi \frac{d^2}{4}$$

$$= \pi \times \frac{0.068^2}{4} - 3\left(\left(\frac{1}{2} \times 2 \times 0.0015 \times 0.02\right)\right) - \pi \times \frac{0.029^2}{4} = 0.00258116\text{m}^2$$

$$or\ A = 2.58116 \times 10^{-3} m^2$$

3.9 Determination of yield of syngas, LHV, carbon conversion and cold gas efficiency

The gasification performance was evaluated based on yield and LHV of syngas, gasifier efficiencies such as carbon conversion and cold gas efficiencies. The overall dry gas yield of syngas was computed based on the formulae below (Guangul et al., 2012)

$$Y_{syngas} = \frac{Q_{air} \times 0.79}{N_2\% \times mb(1 - x_b)} \ldots\ldots\ldots\ldots\ldots\ldots\ldots\ldots\ldots\ldots\ldots\ldots\ldots\ldots\ldots\ldots\ldots\ldots . (3.5)$$

Where

Y_{syngas} is the total syngas yield per kg of biomass, Nm^3/kg

Q_{air} is the flow rate of airNm^3/hr

N_2 is the concentration of nitrogen in the syngas, % v/v

mb is the biomass flow rate (d.b), kg/hr

xb is the ash content in the feedstock

3.9.1 Cold gas efficiency (CGE, %)

The cold gas efficiency of a biomass gasifier is defined as the ratio of energy content in the product gas to the energy content of the fuel. It should be higher than 80% in order to achieve an acceptable electric efficiency of the overall CHP plant (Obernberger & Thek, 2008) and was calculated using the equation below(Sarkar, Kumar, Tumuluru, Patil, & Bellmer, 2014).The efficiency of the gasification process was thus estimated from the energy of the syngas produced in relation to the energy of the biomass feedstock used.

$$CGE = \frac{LHV_{syngas} \times Y_{syngas}}{LHV_{biomass}} x100\% \dots\dots\dots\dots\dots\dots\dots\dots\dots\dots\dots\dots\dots\dots\dots\dots\dots .. (3.6)$$

3.9.2 Determination of the heating values of the fuel

The Higher Heating Value (HHV) or Lower Heating Value (LHV) of a fuel is an important property to be determined before a fuel is combusted because it determines the extent of possible energy released when a fuel is wholly burnt and can be used as a basis for selection of the gas engine. The heating value (HV) of a fuel is a measure of the unit energy per unit mass or volume. The higher heating value (HHV) is the amount of energy released by complete combustion of a mass unit of sample at constant volume in an oxygen atmosphere assuming that the final products of combustion consist of O_2, CO_2, SO_2, and N_2 in gas phase together with water that contained in the sample and that generated from the combined hydrogen in liquid form (Núñez-Regueira, 2001). Based on the work performed by (S. A. Channiwala & Parikh, 2002), their correlation turned out to be the best in the estimation of the HHV of the solid fuel with an average absolute error of 1.45% and bias error of 0.00% with respect to measured values of HHV. The HHV of the solid fuel was thus computed based on a more accurate method below

$$\mathrm{HHV} = 0.3491\mathrm{C} + 1.1783\mathrm{H} + 0.1005\mathrm{S} - 0.1034\mathrm{O} - 0.0151\mathrm{N} - 0.0211\mathrm{A} \left(\frac{\mathrm{MJ}}{\mathrm{kg}}\right) \dots (3.7)$$

Where

$0\% \leq C \leq 92.25\%,$

$0.43\% \leq H \leq 25.15\%,$

$0.00\% \leq O \leq 50.00\%,$

$0.00\% \leq N \leq 5.60\%,$

$0.00\% \leq S \leq 94.08\%,$

$0.00\% \leq A \leq 71.4\%,$

$4.745 \text{ MJ/kg} \leq HHV \leq 55.345 \text{ MJ/kg}$

where, C, H, O, N, S and A represents carbon, hydrogen, oxygen, nitrogen, sulphur and ash contents of material, respectively, expressed in mass percentages on dry basis. Subsequently, the LHV of the solid fuel can be computed as follows(Sarkar et al., 2014),

$$(\mathrm{LHV})\mathrm{d} = (\mathrm{HHV})\mathrm{d} - 2.44(9H_d) \ldots\ldots\ldots\ldots\ldots\ldots\ldots\ldots\ldots\ldots\ldots\ldots\ldots\ldots (3.8)$$

where $(LHV)_d$ corresponds to the lower calorific value of the dry sample (kJ/Kg)

$(HHV)_d$ is the higher calorific value of the dry sample, (kJ/Kg)

H_d the hydrogen percentage of the dry sample, %

The heat of vaporization of water is taken as 2441.8 kJ kg^{-1}, and the water formed during combustion is nine times the hydrogen content(Núñez-Regueira, 2001). Thus, knowledge of biomass chemical composition is necessary for calculation of calorific values and so elementary chemical analysis (C, H, O, N, S, and Cl) were also determined. The higher heating value (HHV) of the dry gas was determined by the following equation:

$$HHV = (CO\% \times 3018 + H_2\% \times 3052 + CH_4\% \times 9500)x0.01 \times 4.1868(\frac{kJ}{m^3}) \ldots . (3.9)$$

where % denotes the volumetric percentages of the specified composition (CO, H_2, and CH_4) in the dry flue gas.

3.9.3 The Carbon Conversion Efficiency, CCE

The percentage of CCE represents the percentage (%) of total carbon in the woodchips converted to product gases which contain carbon (CO, CO_2, CH_4, C_2H_2, C_2H_4 and C_2H_6) and was calculated on the basis of the gas analysis (volumetric percentage of the fuel gas compositions of CO, CO_2, and CH_4) since gas samples were systematically taken using standard and accurate measurements methods. This approach also avoids the difficulties of obtaining representative solid samples and measuring the solid flow rates ((Xiao, Zhang, Jin, Huang, & Zhou, 2006). The same method was used by (Guangul et al., 2012).

$$\mathcal{J}_c = \frac{Y(CO\% + CO_2\% + CH_4\%) \times 12}{22.4 \times C\%} x100\% \ldots \ldots \ldots \ldots \ldots \ldots \ldots . (3.10)$$

Where,

$\mathcal{J}_c$isthe percentage of Carbon Conversion Efficiency

CO, CO_2 and $CH_4$are in % (v/v)

Y is dry gas yield in m^3 per kg of dry feedstock

C% is the mass percentage of carbon obtained in the ultimate analysis of woodchips.

3.10 Determining the power output (Po) of the gasifier

This is the amount of energy released by the gasifier for other mechanical applications. This is computed using the formula. The power output (Po) can be determined as(Guangul et al., 2012):

$$P_o = \frac{FCR \times HHV \times \eta}{3.6}\,(kw) \ldots\ldots\ldots\ldots\ldots\ldots\ldots\ldots\ldots\ldots\ldots\ldots\ldots\ldots . \ldots\ldots (3.11)$$

Where

Po - power output, kW

FCR - fuel consumption rate, kg/hr

HHV is the higher heating value of the feedstock (MJ/kg)

η is the cold gas efficiency of the gasifier.

3.11 Determination of mass flow rate of the feed

To determine the mass flow rate of the feed, the hopper was filled with woodchips upto a given height and the height of the hopper recorded before the start of the experiment. After, running the experiment for a known time interval, the new height is noted and the difference in height calculated. By knowing the circular area of the hopper, the volume of the biomass used for gasification is computed.

By knowing the bulk density of wood chips from above, the mass flowrate of woodchips is calculated as:

$$\dot{m} = \frac{\rho_b \times V}{t} \ldots\ldots\ldots\ldots\ldots\ldots\ldots\ldots\ldots\ldots\ldots\ldots\ldots\ldots\ldots\ldots\ldots\ldots\ldots\ldots (3.12)$$

Where $\dot{m}$ is the rate of mass flow rate of woodchips,$\left(\frac{kg}{hr}\right)$

$\rho_b$is the density of woodchips,kg/m^3

$t$is the gasification time, [hrs]

$V$is the volume of wood chips used during gasification, [m^3]

3.12 Determination of the efficiency of electricity energy generation

To investigate the efficiency of the engine generator set alongside syngas production, a resistor bank was used to simulate the application of the load when the system is running. The loads were of the order 2kW and 3kW each in pairs. A total of 10 kW load would thus be applied under the chosen load bank. These loads could be applied in intervals depending upon the objective of the experiment. To fully evaluate the efficiency of the engine generator set in relation to power generation, the following equations for the specific fuel consumption of biomass (SFC) and specific gas consumption (SGC) were used for analysis applied in the determination of the global efficiency of engine generator set.

$$SFC = \frac{\dot{W}_m}{V_O \times I_O} \ldots\ldots\ldots\ldots\ldots\ldots\ldots\ldots\ldots\ldots\ldots\ldots\ldots\ldots\ldots\ldots\ldots\ldots\ldots\ldots\ldots\ldots\ldots\ldots\ldots\ldots (3.13)$$

$$SGC = \frac{Q_G}{V_O \times I_O} \ldots\ldots\ldots\ldots\ldots\ldots\ldots\ldots\ldots\ldots\ldots\ldots\ldots\ldots\ldots\ldots\ldots\ldots\ldots\ldots\ldots\ldots\ldots\ldots\ldots\ldots (3.14)$$

$$\eta_{E=}\left(\frac{3.6}{LHV_G \times SGC}\right) \times 100\% \ldots\ldots\ldots\ldots\ldots\ldots\ldots\ldots\ldots\ldots\ldots\ldots\ldots\ldots\ldots\ldots\ldots\ldots\ldots\ldots\ldots\ldots\ldots\ldots\ldots\ldots (3.15)$$

Where

$\dot{W}_m$, biomass flow rate,kg/hr

Q_G , syngas gas flow, m^3/hr

V_O, output voltage of electric generator (V)

I_O, output current of electric generator (A)

LHV_G, low heating value of producer gas, MJ N m^{-3}

SGC, Specific gas consumption

SFC, Specific fuel consumption

3.12.1 The engine specifications

In the present study, the engine which is Kubota model DG972-ES with a design capacity of 14.5kW was supplied as an inbuilt component alongside the gasification rig. The engine speed was controlled with an electronic governor rated at 3600 RPM (revolution per minute) while running on 100% syngas. The ignition system of the engine was a distributor-less solid stage type activated by a contact-breaker and a cam-shaft connected to the crank shaft (GEK Manual, 2012). A detailed design configuration of the engine is summarized in Table 3.1 below

3.12.2 Determination of power output from the generator

To determine the current, frequency, voltage and the power output from the generator, a universal power analyzer (PM 3000) was connected across the line of the flow of power from the generator to report a representative output from the engine during the duration of gasification. This was done while the engine was connected at various load banks. The readings were captured at regular intervals and data finally interpreted.

3.12.3 The engine governor

The engine has a centrifugal mechanical governor connected to the throttle valve located at the outlet of the designed fuel intake manifold to regulate the engine speed. The governor activates the throttle in response to the engine speed and thus the engine speed can vary depending on the load applied. When the load increases, the engine speed reduces. This makes the governor to open the throttle valve to a certain degree to increase the flow of fuel mixture into the engine and to maintain the engine at the design speed. In the same way, when the load decreases, the engine speed increases and the governor will reduce the flow of fuel mixture into the engine by closing the throttle valve to a certain degree (Raman & Ram, 2013b). Subsequently, the change in application of the load to the engine could be accompanied by a change in the engine sound. Thus, the engine runs at producer gas designed to run at a speed a maximum of 3600RPM generating power at a frequency of 50HZ. Further details about the engine specifications have been summarized in Table 3.1

Table 3.1 Engine specifications.

Number	Component	Specifications
1	Model	DG972-ES
2	Number of Cylinders	3
3	Type	Vertical, water cooled, 4-cycle Natural Gas engine
4	Bore × Stroke	74.5 x 73.6 mm
5	Total Displacement	962 cm^3
6	ISO / SAE Net Intermittent	17.6 kW / 3600 min-1 (rpm)
7	SAE Gross Intermittent	18.7 kW / 3600 min-1 (rpm)
8	ISO Net Continuous	14.5 kW / 3600 min-1 (rpm)
9	Maximum Bare Speed	3850 to 3950 min^{-1} (rpm)
10	Minimum Bare Idling Speed	1400 to 1600 min^{-1} (rpm)
11	Cylinder Head	Overhead-Valve
12	Ignition System	Distributor-Less Solid Stage Type
13	Governor	Centrifugal Ball Mechanical Type / Electronic Governor
14	Direction of Rotation	Counter-Clockwise (Viewed from flywheel)
15	Spark Plug	NGK BKR4E
16	Ignition Timing	28 ° B. T.D.C.
17	Compression Ratio	9.2 : 1
18	Lubricating System	Forced Lubrication by Trochoid Pump
19	Oil Pressure Indication	Electrical Type Switch
20	Lubricating Filter	Full Flow Paper Filter (Cartridge Type)
21	Cooling System	Forced Circulation with Water Pump
22	Starting System	Electric Starting with Starter
23	Starting Motor	12V, 1.0 kW
24	Charging Alternator	12 V, 480 W
25	Fuel	Natural Gas (100%)
26	Lubricating Oil Capacity	3.4 Litres
27	Weight (Dry)	95.4 kg
28	Application	General Power Source

3.12.4 Electrical generator

The electrical generator is a self-excited three phase synchronous generator equipped with an internal combustion engine (ICE) which automatically regulates the voltage based on the load demand and runs purely on 100% producer gas coming from the gasifier. The three phase alternator coupled to the producer gas engine has a capacity of 15 kVA which works out to be 10 kWe power while working at a compression ratio of 9.2: 1.

3.13 Vibrating grate ash removal system

The gasifier was built with an in built vibrating grate mounted at the base of the reactor for improved ash removal designed to minimize the charcoal fallout from the reactor into the ash pit. The vibrating grate consists of an electric motor coupled with a vibrator, an ash removal grate and a vibration transmitter. The duration of the vibration and frequency of operation of the grate varies depending upon the type of the fuel and operating load of the gasifier. The grate shakes at a regular time interval due to an inbuilt timer which allows the ash to fall off from the charcoal medium. The timer switch is programmed in such a way that it activates the vibrator at desired intervals. The routine shaking of the vibrator allows the ash and dust particles to pass through the grate and avoids the falling of charcoal from the reactor. Minimizing the rate of charcoal fallout from the reactor improves the efficiency of gas production because the removal of ash increases the extent of exposure of the active sites of charcoal and the gaseous phase hence increased heterogeneous reactions.

3.14 Dust particle removal and gas cooling system

Following the successful production of the producer gas from the reactor, the flow of the gas leaving the reactor (CO, H_2, CO_2, H_2O and tar, etc) enter a cyclone particle separator, before the packed bed gas filter (via the drying bucket/heat exchanger). Here, heavier particles fall through the cyclone and the gasproceeds to the packed bed filter where further gas filtration takes place. The filter media is made up of densified particles of wood chips that trap tar particles and a cleaner gas is channeled to the engine.

3.15 Recovery of biochar from the ash pit

Biochar, a cogasification product is formed as part of the products. To verify the amount of char formed at the bottom of the reactor for each run, the char chamber is opened and cleaned before each run to ensure actual material balance for each experiment. Thus the char chamber is opened, cleaned and tightly sealed to avoid any gaseous leakage which would otherwise become hazardous to the working area due to the higher concentration levels of producer gas. The gasification experiment is thus initiated and char collects below the ash grate. It is possible for char to collect below the ash grate because of the presence and availability of the grate shaker that automatically shakes at regular intervals for about 20seconds. This allows part of the formed char inside the reactor to break down into smaller particles and fall through the holes of the grate to the bottom. To investigate the rate of biochar formation during the gasification process, the biochar collected at the bottom of the reactor was weighed using the weighing balance according to the formulain equation 3.16 below

$$Rate\ of\ char\ formation\ = \frac{W_2 - W_1}{GT} \ldots\ldots\ldots\ldots\ldots\ldots\ldots\ldots\ldots\ldots\ldots\ldots\ldots\ldots\ldots\ldots\ldots\ldots\ldots\ldots\ldots\ldots (3.16)$$

Where

W_2 = *Weight of container + biochar*

W_1= *Weight of container*

GT= Gasification Time

3.16 Determination of energy and Mass balance of the gasification system

The energy and mass balance of the gasifier computation is based upon the feed and outlet streams in the reactor as justified in Figure 3.6. Consider the system below with the following feed and exit streams

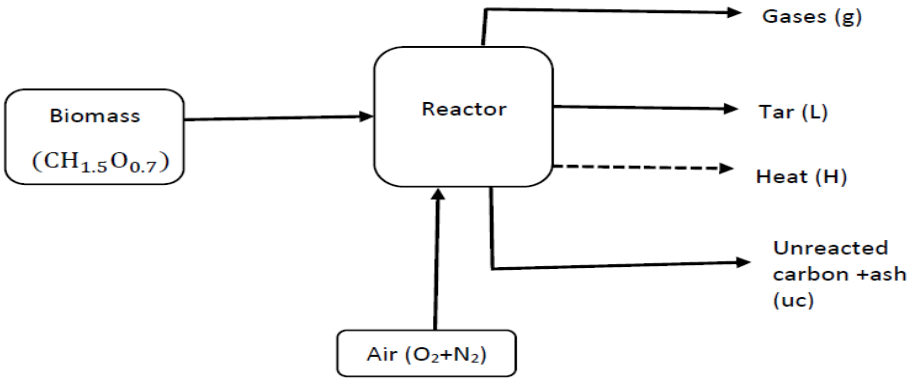

Figure3.6. Schematic of the gasifier flow streams.

3.16.1 Mass balance of the system

Using the mass balance equation, the rate of mass flow into the system should be equal to the rate of mass outflow from the system. Therefore, the in stream components are air and biomass while the exit stream consists of product gases, tar, unreacted carbon and ash. The mass balance equation 3.16 thus becomes:

$$\dot{m}_{biomass} + \dot{m}_{air} = \dot{m}_{gases} + \dot{m}_{tar} + \dot{m}_{uc} + \dot{m}_{ash} \ldots\ldots\ldots\ldots\ldots\ldots\ldots\ldots\ldots\ldots\ldots\ldots\ldots\ldots\ldots\ldots\ldots\ldots (3.17)$$

Where $\dot{m}_{biomass}, \dot{m}_{air}, \dot{m}_{gases}, \dot{m}_{tar}, \dot{m}_{uc}, \dot{m}_{ash}$ denote the mass flow rate of biomass, air, product gases, tar, unreacted carbon and ash respectively.

3.16.2 Energy balance of the system

By considering an energy balance of the system, the downdraft gasifier is an autothermal system with no external heating source. It provides and sustains its own energy required for gasification. The energy from the lighter provided at the start of the experiment for initial combustion is considered to be very small and thus ignored in the overall system energy balance. Similarly, the energy from the battery that powers the control panel is outside the gasification process and not considered as part of the energy balance. The energy balance of the gasifier thus follows the schematic diagram in Figure 3.4 above. Using the law of conservation of energy, the corresponding energy balance equation for the above system can be written as below

$$\dot{En}_{biomass} + \dot{En}_{air} = \dot{En}_{gases} + \dot{En}_{tar} + \dot{En}_{uc} + \dot{En}_{loss} \quad \ldots\ldots\ldots\ldots\ldots\ldots\ldots\ldots\ldots\ldots\ldots\ldots\ldots (3.18)$$

Where $\dot{En}_{biomass}, \dot{En}_{air}, \dot{En}_{gases}, \dot{En}_{tar}, \dot{En}_{uc}, \dot{En}_{loss}$ denote the energy flow rate of biomass, air, product gases, tar, unreacted carbon and energy loss due to heat loss and ash respectively.

But $\dot{En} = \dot{En^{ke}} + \dot{En^{po}} + \dot{En^{phy}} + \dot{En^{ch}}$

Where $\dot{En^{ke}}, \dot{En^{po}}, En^{phy}(or\ sensible), \dot{En^{ch}}$ are the rates of kinetic, potential, physical and chemical energy respectively. By neglecting the rates of potential ($En^{po} = \dot{m}gz$) and kinetic energy $En^{ke} = \frac{\dot{mv}^2}{2}$, the above equation reduces to

$$\dot{En} = \dot{En^{phy}} + \dot{En^{ch}}$$

For combustible gases and tar, the above equation reduces to

$$\dot{En} = \dot{m}(h + HHV) \ldots\ldots\ldots\ldots\ldots\ldots\ldots\ldots\ldots\ldots\ldots\ldots\ldots\ldots\ldots\ldots\ldots\ldots\ldots\ldots (3.19)$$

Where $\dot{m}$, h and HHV represent the mass flowrate, specific enthalpy and high heating value of the stream, respectively. The specific enthalpy of a component can be computed as

$$h = h_O + \int_{T_o}^{T} Cp\,(T)dT \ldots\ldots\ldots\ldots\ldots\ldots\ldots\ldots\ldots\ldots\ldots\ldots\ldots\ldots\ldots\ldots\ldots\ldots\ldots\ldots (3.20)$$

where h_O is the specific enthalpy at standard temperature and pressure, Cp is the is the molar specific heat of species at constant pressure in kJ/kmol K and is a function of temperature, T_o is the temperature at standard conditions and T is the gasification Temperature. The specific enthalpy h_O of gases is shown in appendix B1. Cp can be defined by the empirical equation below with coefficients a–d of constant pressure specific heat capacity of some gases shown in appendix B2. While for unreacted carbon and biomass, the total energy can be computed according to the equation below

$$Cp(T) = a + bT + cT^2 + dT^3 \ldots\ldots\ldots\ldots\ldots\ldots\ldots\ldots\ldots\ldots\ldots\ldots\ldots\ldots\ldots\ldots\ldots\ldots\ldots\ldots (3.21)$$

$$\dot{En} = \dot{m}(HHV) \ldots\ldots\ldots\ldots\ldots\ldots\ldots\ldots\ldots\ldots\ldots\ldots\ldots\ldots\ldots\ldots\ldots\ldots\ldots\ldots (3.22)$$

The high heating value of biomass or unreacted carbon ($HHV_{biomass}$) can be determined experimentally or computed from the proximate (Parikh, Channiwala, & Ghosal, 2005) or ultimate (Channiwala & Parikh, 2002) analysis of biomass. When the LHV of the biomass fuel is known, the HHV can be determined according to the formula (Bilgen, Kaygusuz and Sari, 2004)in MJ kg^{-1}

$$\mathrm{HHV}_{biomass} = \mathrm{LHV} + 21.978\mathrm{H} \ldots\ldots\ldots\ldots\ldots\ldots\ldots\ldots\ldots\ldots\ldots\ldots\ldots\ldots\ldots\ldots\ldots\ldots\ldots\ldots (3.23)$$

Where H is the weight fraction of element Hydrogen in the ultimate analysis.

The Lower heating value (LHV) of biomass fuel is calculated by the Boie formula in (MJ/kg) ((Ngo et al., 2011).

$$LHV_{woodchips\ (MJ/Kg)} = 34.835x_C + 93.870x_H - 10.800x_O + 0.628x_N + 10.465x_S \ldots\ldots\ldots \quad (3.24)$$

Wherex_C, x_H, x_O, x_N, and x_s are the mass fraction of the elements C, H, O, N, and S in biomass on a dry basis respectively.Subsequently, the heating value of dry gas can be estimated from the following equation 3.24. Where, H_2, CO, CH_4 and C_2H_4 indicate the volume or molar fractions of H_2, CO, CH_4 and C_2H_4 in the dry gas in %, respectively.

$$HHV_{dry\ gas} = 12.75H_2 + 12.63CO + 39.82CH_4 + 63.43C_2H_4 + \cdots \ldots\ldots\ldots\ldots\ldots\ldots\ldots\ldots\ldots\ldots\ldots\ldots \quad (3.25)$$

3.17 Calculation procedure for determination of syngas composition from modeling

To establish the actual values of syngas composition, an initial temperature was assumed and used to calculate the equilibrium constants using generic equations developed major reactions that take place during gasification (Zainal et al, (2001). The generated equilibrium constants were finally used to solve the nonlinear simultaneous equations using MatLab software (R2014a) and new values of gas composition and temperature obtained.

CHAPTER 4

4.0 RESULTS AND DISCUSSION

4.1 A summary of results

According to the set objectives and the experimental set up, the experimental rig was assembled according to the user guide (GEK, 2012) and prepared to produce results that could reveal its practical performance based on its standard operating conditions. This results section thus summarizes findings from both the experimental rig and the characterization studies of the biomass species used for this work as detailed hereunder.

4.2 Characterization of wood chips

The wood chips (spruce and Spartan spruce) and their corresponding biocharwere characterized for elemental analysis to investigate the contents of Carbon (C), Hydrogen (H), Oxygen (O), Nitrogen (N) and Ash (A). The corresponding results as summarized in Table 4.0 below reveal that spruce had a lower carbon content of 43.8±0.13% compared to spruce spartan with 46.7±0.09%. The composition of hydrogen (6.3±0.20% and 6.7±0.03%) and oxygen (46.5±0.15% and49.1±0.11%) were lower for spartan spruce compared to spruce respectively. The difference in elemental composition of the woodchips may be attributed by a number of factors such as difference in climate changes and subsquently a difference in soil properties where the wood chips were planted, among other reasons. However, the individual elemental composition (C,H,O,N) for both spartan spruce and spruce woodchips were in the order of the same magnitude. Consequently, the elemental composition of their

corresponding biochar was nearly of the same composition of about 37.0±3.60%,0.6±0.02%,62.0±3.70%, 0.5±0.06% for C,H,O, and N respectively for both spruce and spartan spruce woodchips because it was produced at nearly the same experimental conditions with a gasification time of 6hrs and at steady gasification temperatures of about 850 ºC and from a biomass starting material (feedstock) of nearly the same composition. The composition of the wood chips used in the present research matches well with the composition of other woodchip species such as those detailed in Table 3.1 with an average composition of 48.7±3.9%,6.0±0.7%,0.0±0.1%,0.00%,42.1±3.4% for C, H, N, S and Ash respectively.

Table 4.0 Elemental analysis of woodchips and their corresponding biochar

		Elemental analysis of char				
	Rep	C	H	O	N	Ash
Original wood chips (OWC- spruce biochar)	1	32.85	0.53	66.20	0.39	0.02
	2	39.49	0.57	59.41	0.51	0.02
	3	38.64	0.57	60.28	0.49	0.02
Average	Av	37.0±3.60	0.6±0.02	62.0±3.70	0.5±0.06	0.02±0
New Wood Chip (NWC-spartan spruce biochar)	1	35.05	0.44	64.13	0.37	0.02
	2	39.82	0.48	59.21	0.47	0.02
	3	35.04	0.42	64.11	0.41	0.02
Average		36.6±2.76	0.4±0.03	62.5±2.83	0.4±0.05	0.02±0
		Elemental analysis of wood chips				
Original wood chips (OWC- spruce)	Rep	C	H	O	N	Ash
	1	43.70	6.53	49.17	0.58	0.02
	2	43.95	6.56	48.96	0.51	0.02
	3	43.75	6.60	49.07	0.57	0.02
	Av	43.8±0.13	6.7±0.03	49.1±0.11	0.6±0.04	0.02±0
New Wood Chip (NWC-spartanspruce)	1	46.62	6.42	46.42	0.52	0.02
	2	46.69	6.05	46.69	0.56	0.02
	3	46.81	6.34	46.43	0.41	0.02
		46.7±0.09	6.3±0.20	46.5±0.15	0.5±0.08	0.02±0

4.3 Determination of bulk density

Three trial tests were conducted to obtain an average bulk density of woodchips. The averagebulk density of woodchips was determined to be229±10.6 kg/m^3 as shown in Appendix A2. This value of bulk density compares well with the bulk density of other wood species previously used for gasification such as Birch (Betula pendula) and Oak (Quercus petraea)of 252±3.5 kg/$m^3$and 208 ± 3.2 kg/m^3respectively (Sarker & Nielsen, 2015). With the determined value of bulk density, its important to determine whether the wood specie would be toloreted inside the gasifier as this type of gasifier is sensitive to the particle size of the wood chips used. Smaller particles of high volume block the flow of incoming air and this would limit the extent of initail reactions during start up as well as compromise the speed of gasification reactions during the course of the experiment since this gasifier doesnot depend on an external heating source but only depends on the incoming air to support the combustion reactions and subsquently complete the gasification reactions. Thus woodchips of a high bulk density should be used for the good perfomance of the gasifier.

4.4Monitoring the performance of the gasifier with variation of the electrical load

The gasifier was run with wood chips with nearly the same moisture content 13.4±1.26% and particle density229±10.6kg/m^3while the electrical load connection was varied for different sets of experiments. Gasifier performance was monitored in terms of temperature and velocity for incoming air, gasifier temperature, biomass flow rate, producer gas composition as well as evaluating the CCE, CGE and HHV of the syngas in order to understand the effect of the overall gasifier performance with the connection of loads with different energy

requirement. The loads were thus connected and varied in the order of (2kWe, 4kWe and 10kWe) as each parameter is investigated in details. Resultswere further analyzed in details using one way anova with 0.005 as the level of significance to investigate in details the effect of each parameter as the load was varied.

4.5 Variation of incoming air velocity with power output

The velocity of incoming air was recorded at every start of the new experiment to verify the amount of energy generated as a function of the velocity of incoming air. A typical trend is portrayed in Figure 4.0 where the velocity of air is recorded at steady conditions for a period of one hour. According to results shown in Figure 4.0, it is evident that as the velocity of air increases from 0.7m/s to 0.9m/s, the amount of energy generated from the genset increases from 1.2kW to 6.0kW respectively which implies that higher energy generation from the genset is accompanied with supply of more air as could be observed that an increase of air supply by 28.5% increased energy generationby 400%. Dummy resistive load banks of varying energy ratings were connected at the terminal of the genset to regulate the amount of air entering the gasifier. Correspondingly, an incoming air velocity of 0.9m/s, 0.8m/s and 0.7m/s responded to actual power generation outputof 6.0kW, 4.2kW and 1.2kWrespectively. Analysis of data with one way analysis of variance (Anova) (Appendix A2), confirmed that there is a significant difference in change of velocity (0.9-0.7m/s) with power output. The increase in air velocity as the power output increases may be explained by the increase in the energy potential of the fuel mixture (producer gas +air) and subsequently the engine efficiency as the resistive load increases. When the resistive load increases, factors such as engine efficiency increases (Chaves et al., 2016a) and this makes the gasifier to subsequently respond with a higher air input. Consequently, the specific gasification rate (SGR) of the

gasifier decreases due to a reduction in the velocity of incoming air, because of slower gasification reactions, hence longer gasification times. The decrease in velocity when bigger load is applied leads to slower rates of reaction, increasing gasification time and lower the SGR of the gasifier.

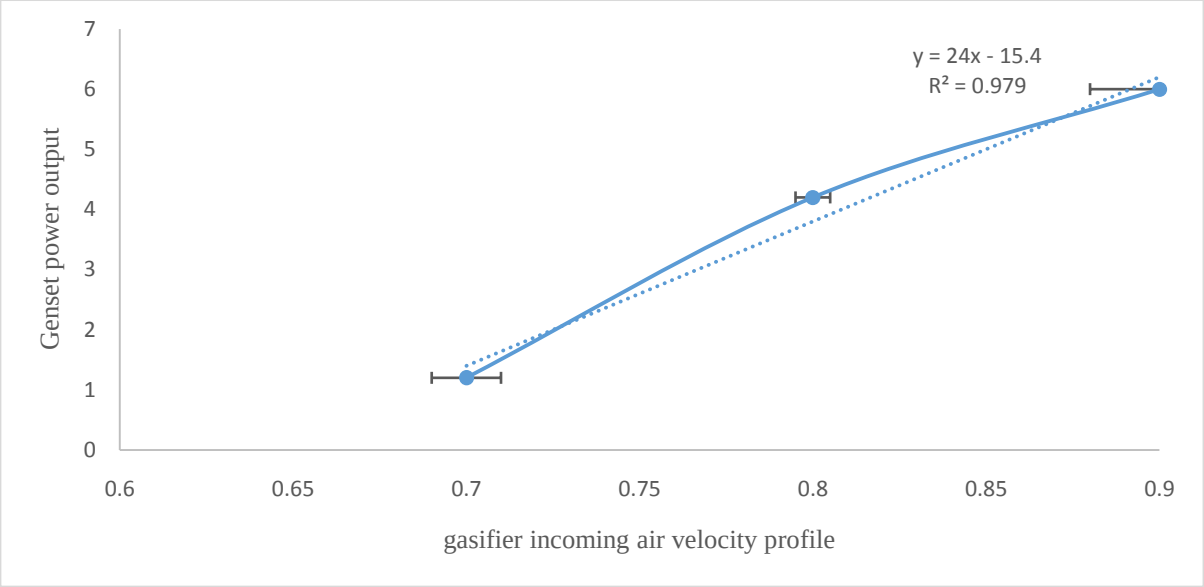

Figure 4.0Variation of gasifier incoming air velocity with generated power output

4.6Effect of changing the connection load with gasification temperature

To effectively monitor the performance of the gasifier as the connection load was varied, data for temperature values were recorded and further interpreted to observe any changes with the connection load. The initials Tt1-n, Tt2-n, Tt3-n, Tb1-n, Tb2-n, Tb3-n, were used to represent the temperatures for the reduction zone at the top (Tt) and bottom (Tb) for replicates 1, 2 and 3 respectively where n represents the corresponding connection load. The Figures 4.1-4.3demonstrate the trend of temperature with changes in connection load. It can be confirmed

that for all the temperatures recorded for the different connection loads for all replicates shown in appendix A-3-1 to A-3-3 with detailed trends in Figures 4.2-4.4, the temperature values at the top of the reduction zone were between 850-950 °C and 715 - 815°C at the bottom of the reduction zone. This indicated that temperatures were hotter at the top of the reduction zone and reduced with decreasing height towards the grate region. As shown in Figures 4.2-4.3, a change in the connected load did not change gasifier temperatures for the duration of the experiment.Analysis of variance (Appendix A.3) for temperature values at the top and bottom of the reduction zone respectively revealed a significant difference in temperature values as the connection load increased from (2 to 10kW) respectively. As shown in Figure 4.4, the temperature values for both at the top (Tt) and bottom (Tb) of the combustion zone are lower with high connection load of 10 kW with a minimum recorded value of 716°C for the bottom reduction zone temperature compared to the lowest recorded value of 741°C for the low connection load of 2kW. It should be noted that for autothermal gasifiers as the one in the present study, the cumulative temperatures inside the gasifier are determined by the amount of air allowed for gasification. The higher the gasification air reflected by the high velocity of incoming gasification air, the higher the temperatures inside the gasifier as more air makes the reaction moreexothermicaccompanied with generation of more heat inside the gasifier. As the connection load increased from 2 to 10 kW, the velocity of incoming air decreased from 0.9m/s to 0.7m/s which justify the subsequent decline in the maximum attainable temperatures inside the gasifier for both Tt and Tb respectively, as shown in Figure 4.1-4.4.

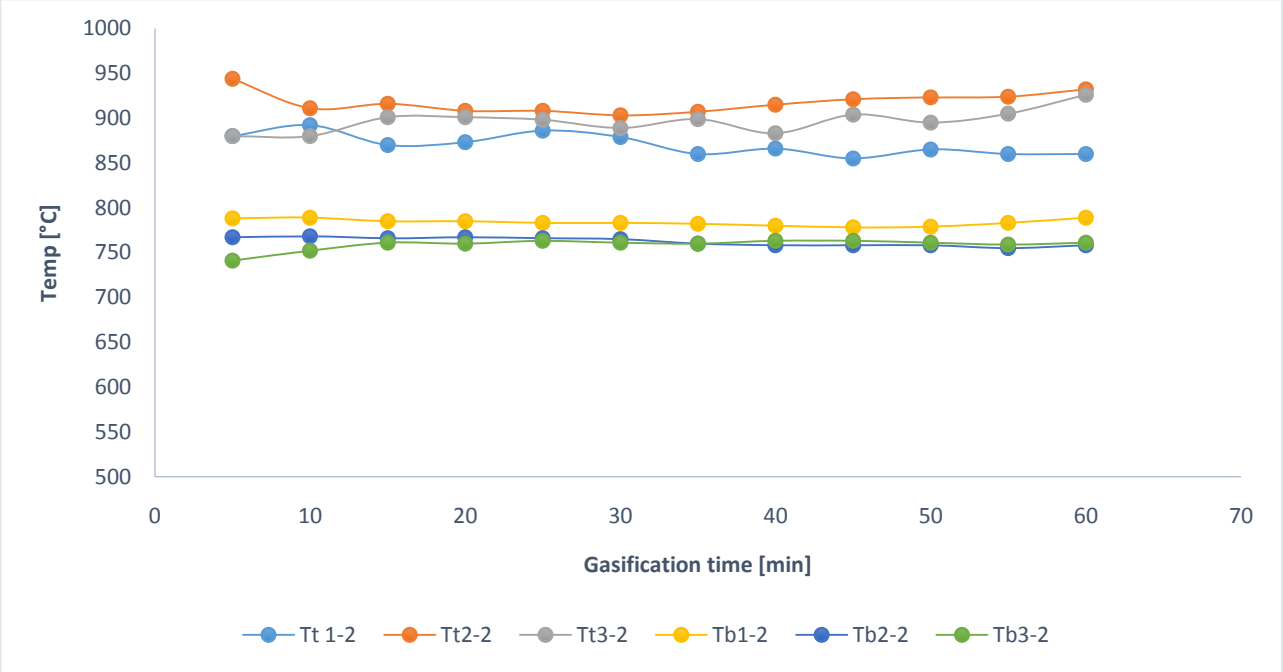

Figure 4.1 Variation of temperature with connection load at 2 kW

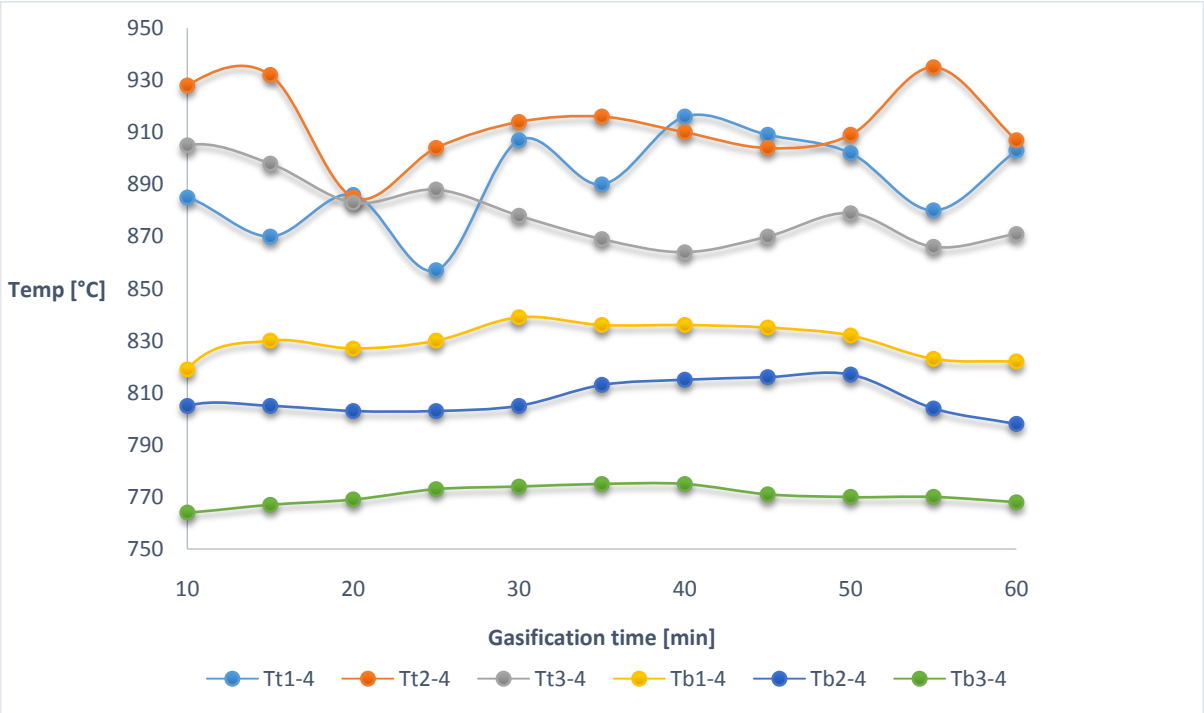

Figure 4.2 Variation of temperature with connection load at 4 kW

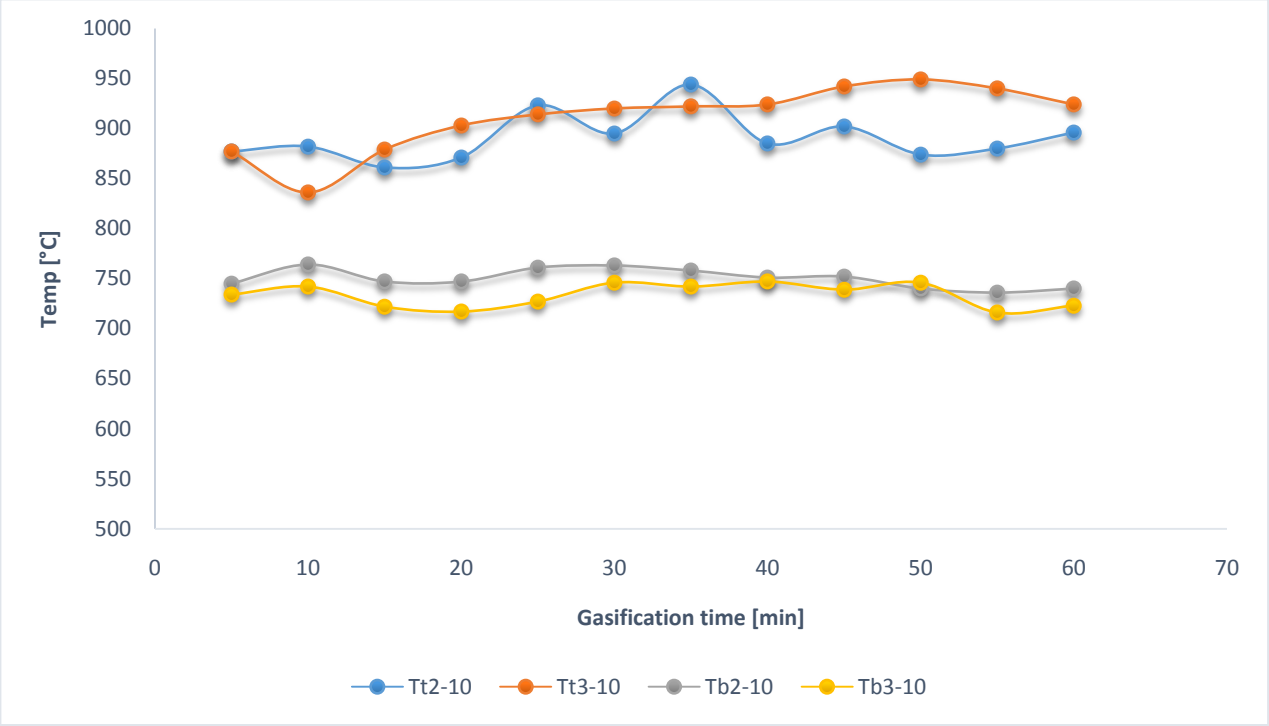

Figure 4.3 Variation of temperature with connection load at 10 kW

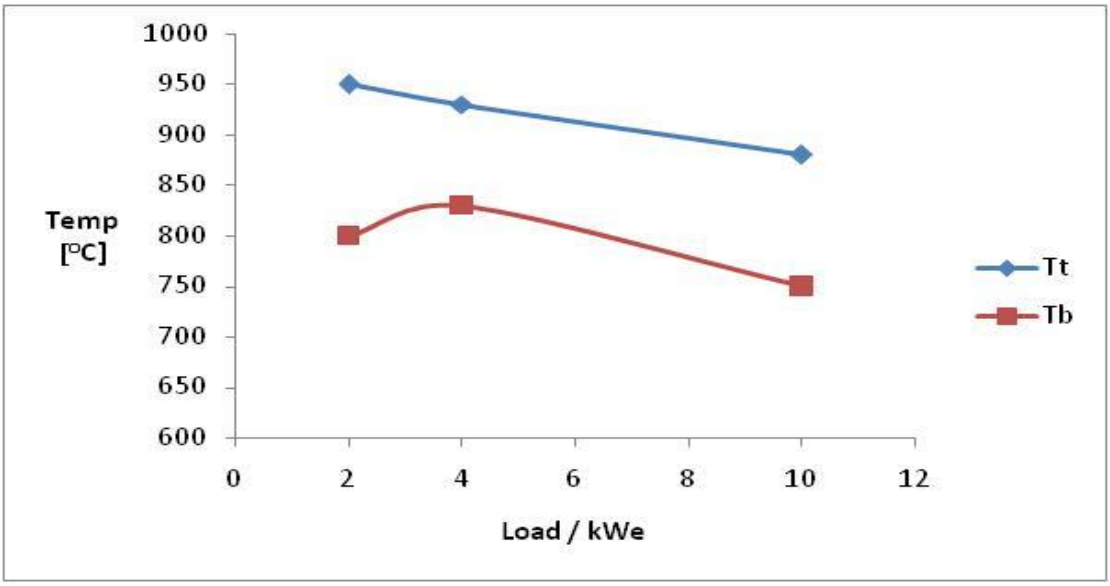

Figure 4.4 Variation of Load with temperature

4.7 Effect of load variation with Fuel Consumption Rate

Generally, an increase of connection with the load from 2 kW to 10 kWe decreased the FCR from 5.0-4.9kg/hr as shown in Table 4.1 below. The decrease of nearly 2.40 % in FCR may be due to the decrease in the velocity of incoming air (0.9m/s - 0.7m/s) which decreases the speed of combustion reactions and subsequently the FCR. Subsequently, the efficiency of the engine increases while working at a higher load producing a more energetic fuel with less dependence on air. This may give rise to decreased fuel demand causing the gasifier to respond at slower rates, decreasing the kinetics of the reactions anddecreasing the fuel consumption rate of the gasifier. The relative change of the feed flow rate depends on the decrease of the flow of air which occurs as the load increases.

Table 4.1 Average values of gasifier operation parameters with load

Initial (h1)/cm	35	29	14.0
Final height (h2)/cm	52	46	31.2
Height difference (h2-h1)/m	0.17	0.17	0.172
Hopper circular area (m^2)	0.2552	0.2552	0.2552
Volume of wood chips gasified ($/m^3$)	0.043	0.043	0.044
Density (kg/m^3)	227.4	227.4	227.4
Total Mass gasified for entire gasification time (Kg)	9.86	9.86	10.00
Total gasification time	2.02	2	2
Mass flow rate (Kg/hr)	4.9	4.9	5.0
LOAD (KWe)	10	4	2
ER	0.2257		

4.8 Effect of load variation with producer gas composition.

When the load was varied from typically (2kWe, 4kWe to 10kWe), themajor composition of producer gas arising from the gasification of wood chips with air is CO (% v/v)and H_2(% v/v)with an average compositionof 21.1±0.48% and 17.7±2.3 % for CO and H_2respectively while 3.31±1.41%, 1.9±0.50%,1.9±2.28% and 54.23±3.10% for CO_2, CH_4 , $O_2$and N_2 respectively. The high concentration of nitrogen in the producer gas was due to the oxidation of wood chips with ambient air which contains 79%nitrogen. The nitrogen in the air remains non-reactive during gasification and forms a major part of the gasification products. During the application of these electrical loads (2kWe, 4kWe and 10kWe) as shown in Figures 4.4-4.8 and subsequently a statistical analysis of the gas composition to establish the impact of changing the load with gas composition, analysis of results with a one way anova with a significance level of 0.05 revealed that the gas compositions for all gases varied significantly as the loads werevaried. Generally, an increase in the load from 2kW to 10kW resulted in a decrease in the concentration of CO from 21.3% (2 kW) to 20.5% (10kWe) (Figure 4.5), H_2concentration from 17.7% (2kW) to 14.8% (10kWe) (Figure 4.6). On the other hand,CH_4increased from 1.2% to 1.8%,(Figure 4.7) while CO_2 (Figure 4.8) and LHV (Figure 4.9) increased and decreased respectively. These significant changes arose due to the difference in air flow and subsequently reduced temperatures. CO and H_2 are favored at higher temperatures and lowering the gasification temperatures would lower their concentrations.

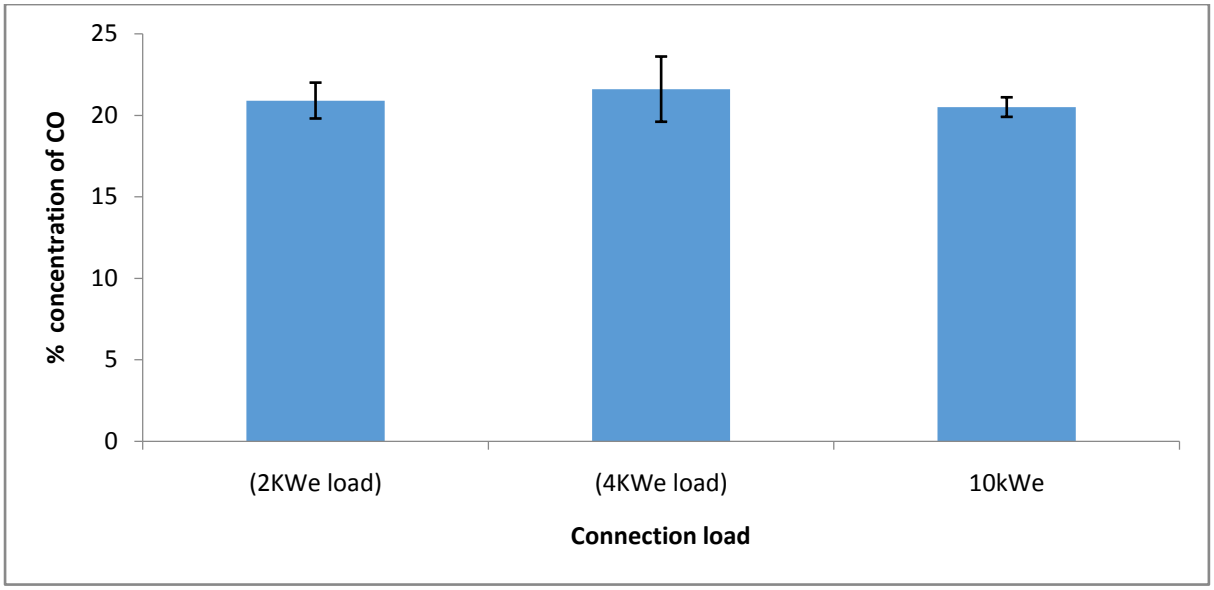

Figure 4.5 Concentration of CO versus varying electrical load

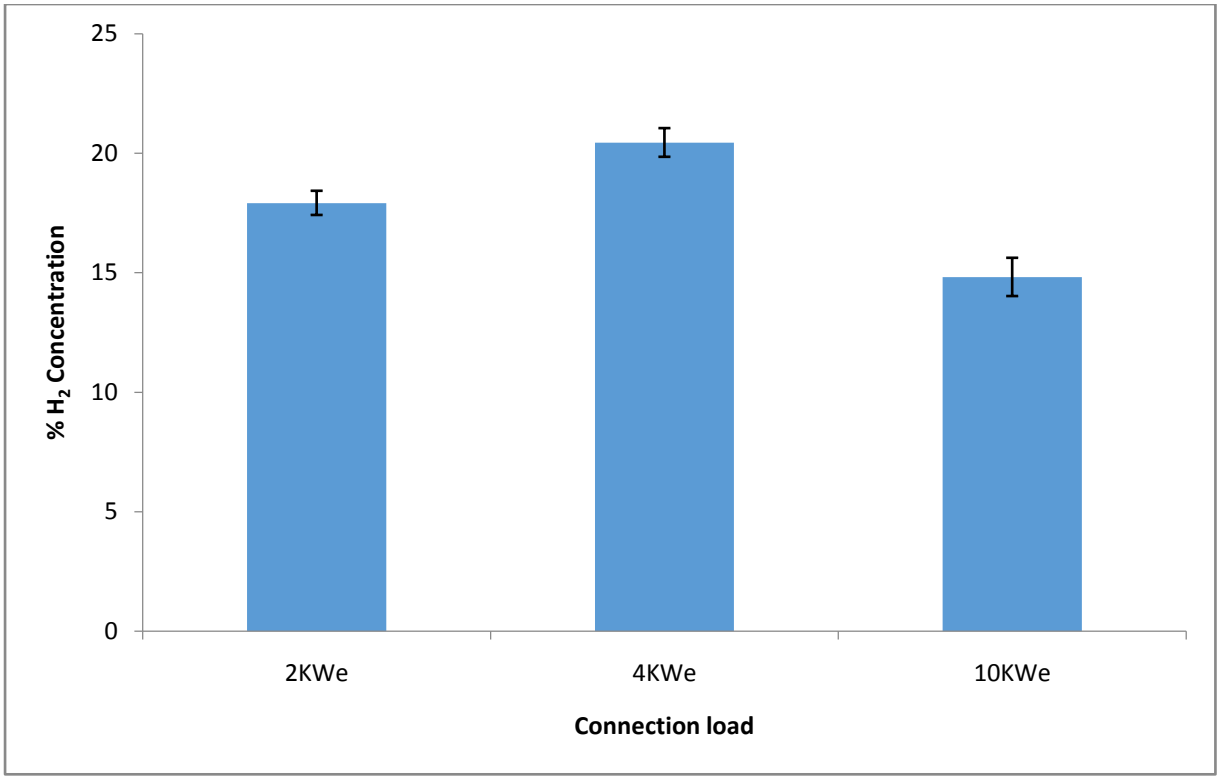

Figure 4.6 Concentration of H_2 versus varying electrical load

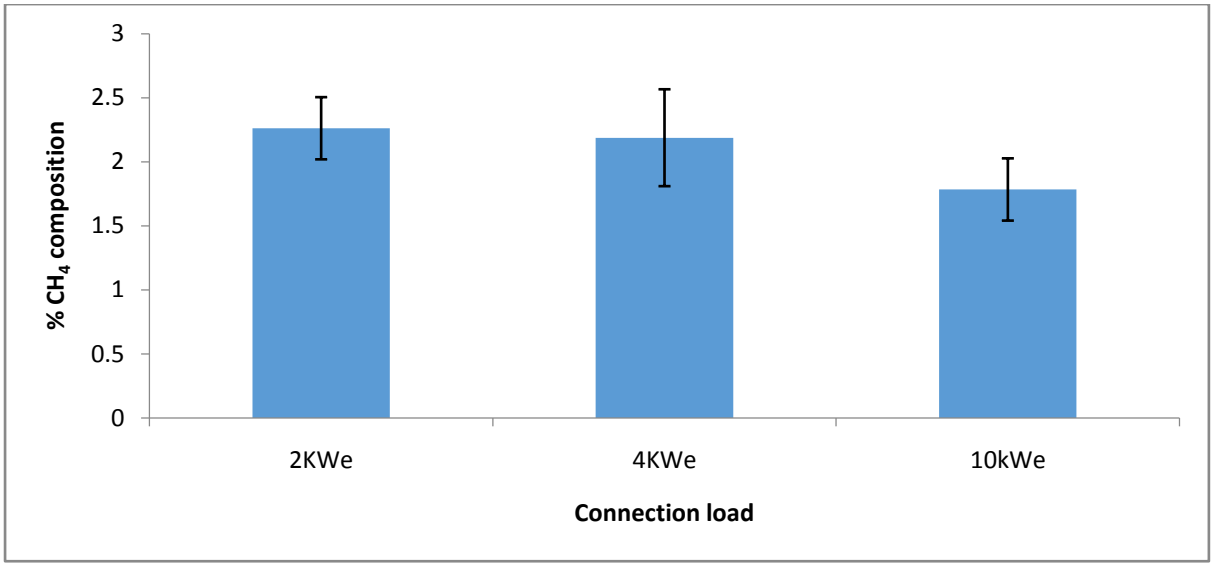

Figure 4.7 Concentration of CH_4 versus varying electrical load

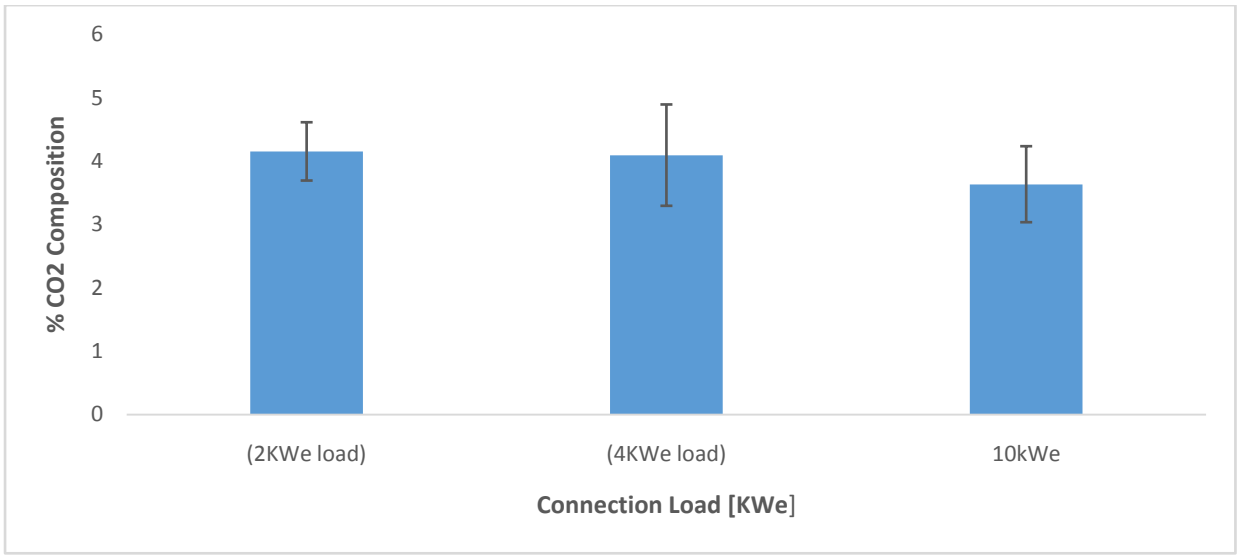

Figure 4.8 Concentration of CO_2 versus varying electrical load

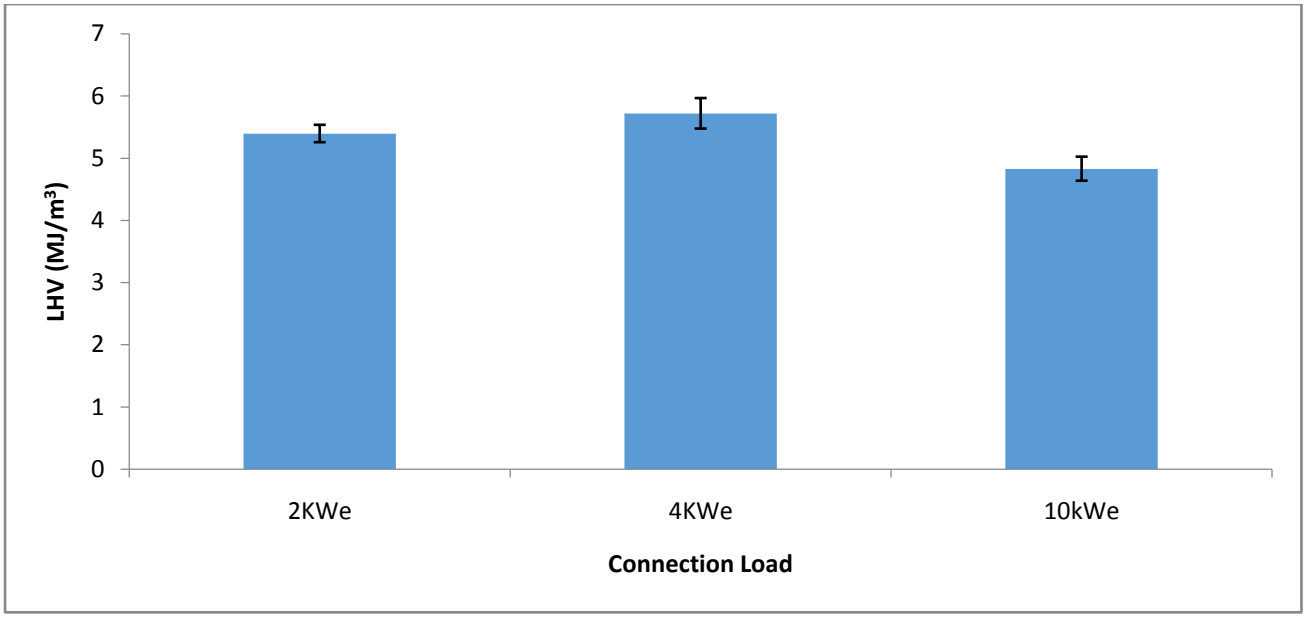

Figure 4.9 Concentration of LHV of the producer gas versus varying electrical load

4.9 Overall efficiency of the engine generator set with variation in electrical load

When the resistive load was varied from 2 - 4kWe as shown in Figure 4.10, the engine generator efficiency increased from 10.5 at (2kW) to - 24.0 % at (4kW). This implied that increasing the resistive load decreases the specific gas consumption (SGC) of the engine and subsequently increases the overall efficiency of the engine. Increase in SGC with decreasing load could be attributed to considerable efficiency loss at low-load condition (Yaliwal, Banapurmath, Gireesh, & Tewari, 2014). The engine generator performance depends upon the thermal efficiency of the Internal Combustion Engine (ICE) as well as depends upon the efficiency of the gasifier. At maximum resistive load, the chemical energy arising from the gasification of the wood chips is converted into mechanical energy via a spark ignition engine (SEI).

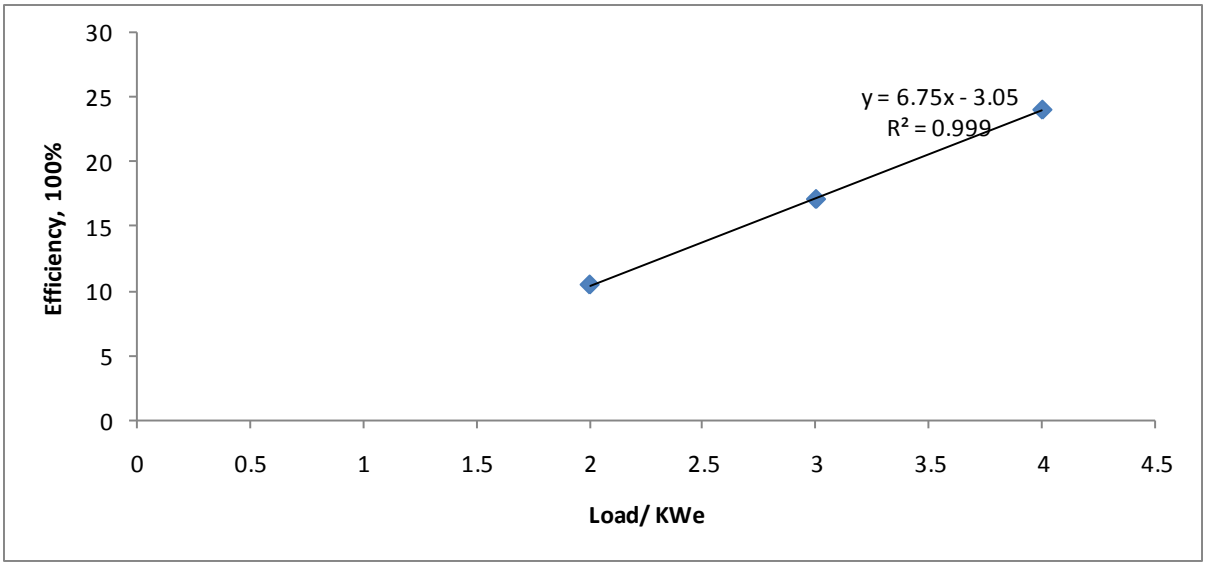

Figure 4.10 Variation of resistive load with engine generator efficiency

4.10 Effect of overall gasifier performance with variation in resistive load

When the resistive load varied from 0-10KWe, the overall performance of the gasifier has been summarized in the Table 4.2. Based on the average results, the overall fuel consumption rate of the gasifier was 4.9±0.07kg/hr with a corresponding syngas composition of 21.1±0.48%,3.3±1.41%,1.9±0.50%,17.7±2.30%, 1.9±2.28% and 54.2±3.10% for CO (% v/v) %,CO_2 (% v/v) CH_4(% v/v) H_2(% v/v) O_2(% v/v) and N_2(% v/v) respectively. This revealed a lower heating valueof 5.2±0.392MJ/$m^3$and a higher heating value of 5.7±0.45 MJ/m^3, a cold gas efficiency of 69.0±11.40%, a carbon conversion efficiency of 69.0±11.40% and a syngas production rate of 2.40±0.31m^3/kg at an equivalence ratio of 0.23. These results tend to agree with the findings of (Chaves et al., 2016b) when they operated a downdraft gasifier with a capacity of upto 150 kWe. From their findings, a gasification yield of 2.5 m^3 kg^{-1}, fuel wood consumption of 5.6 kg $h^{-1}$and a cold gas conversion efficiency of about 60-

70%.Similarly, (Boloy, Silveira, Tuna, Coronado, & Antunes, 2011) attained the same gasification yield of 2.5 $m^3 kg^{-1}$ during the atmospheric gasificationof eucalyptus in a down draft gasifier at an equivalence ratio of 0.25. The overall performance of the gasifier is compared in Table 4.3 with others in literature and the results seem to be in the order of the same magnitude. The deviations in heating values would arise due to the difference in the equivalence ratio of the different gasifiers. A higher amount of air entering the gasifier increases the ER of the gasifier and lowers the concentration of the producer gas and subsequently lowering the gas heating values

Table 4.2 Results for the composition of gasification products

Load/ KWe	CO (% v/v) %	CO_2 (% v/v)	CH_4 (% v/v)	H_2 (% v/v)	O_2 (% v/v)	N_2 (% v/v)	MC% (% w/w)	LHV/ MJ/m^3	HHV/ MJ/m^3	q/ m^3/hr	CGE, %	CCE, %	BMFR/ kg/hr	Y/ m^3/kg
0	21.28	1.18	1.16	17.70	0.15	58.53	14.7±1.50	5.04	5.41	7.69	61.21	58.00	4.84	2.23
2	20.89	4.15	2.26	17.92	2.44	52.34	13.9±1.4	5.39	5.83	7.94	74.25	76.75	4.88	2.56
4	21.57	4.10	2.19	20.45	0.06	51.63	12.7±1.2	5.72	6.21	6.90	69.31	68.25	4.93	2.23
10	20.48	3.64	1.78	14.82	4.87	54.41	12±1.60	4.83	5.19	9.12	72.41	78.48	5.00	2.75
Av	21.1± 0.48	3.3± 1.41	1.8± 0.50	17.7± 2.30	1.9± 2.28	54.2± 3.10	13.4± 1.26	5.2± 0.40	5.7± 0.45	7.9±0. 91	68.0±8. 20	69.0± 11.40	4.9± 0.07	2.4± 0.31

N_2 is calculated by difference, Av; average

Table 4.3 Performance comparison of biomass gasifiers

No	Equivalence ratio	Calorific value of the gas, LHV (MJ/m^3)	Ash removal rate % of mass fraction	Cold gas efficiency % of energy fraction	Ref
1	0.35	4.8	na	72	(Son, Yoon, Kim, & Lee, 2011)
2	na	4.5	4	77	(Dasappa, Subbukrishna, Suresh, Paul, & Prabhu, 2011)
3	0.32	5.3	4.6	52	(Schoeters, Maniatis, & Buekens, 1989)
4	0.38	5.6	na	77.97	(Zainal, Rifau, Quadir, & Seetharamu, 2002a)
5	0.29	5.5	na	57.9	(Plis & Wilk, 2011)
6	0.29	5.2	na	76.7	(Martínez, Mahkamov, Andrade, & Silva Lora, 2012)
7	**0.3**	**5.2**	**less than 1**	**68.019**	**Present study**

na; not available

4.11Effect of charcoal recovery rate with load.

The removal of the formed biocharfrom the ash pit is an important factor as this affects the cold gas efficiency of the gasifier. When all the formed biochar is removed, this implies that the reduction process will be limited as the conversion of carbon to syngas wouldbe hindered and hence incomplete gasification. For instance, for every 3kgs of wood that are gasified, 1kg of charcoal is produced (Raman & Ram, 2013b), this means that the removal of every 1kg of charcoal would increase fuel consumption by a factor of 3. The gasifier system thus requires to be designed to retain a signification proportion of charcoal formed. In this case, the gasifier configuration in the present work was equipped with a grate and a grate shaker designed to operate at regular intervals. The grate shaker has an inbuilt electric motor coupled with a vibrator, and a vibration transmitter(Raman & Ram, 2013a) and could automatically run every about 10 minutes for approximately 30seconds.

The grate had perforated holes that allowed only small char particles to pass though and leave the bigger size charcoal particles inside the gasifier to aid syngas formation via the reduction process. The char recovery rate from the ash pit was less than 1 % of the feed.This made it possible to achieve a cold gas efficiency of 68.0±8.2% as shown in Table 3.1 when the gasifier was operated with resistive loads between 2-10 kW under a mass flow rate of 4.9± 0.07kg/hr. These findings tend to agree with Dasappa et al., (2011) when they run a grid connected 85 ± 6 kWebiomass gasification power plant in Karnataka, India with an efficient ash removal vibration system witha wood consumption rate of 110 ± 10 kg/hr and attained a charcoal and ash extraction in the range of 3.5–4.5%. Their gasifier seemed to be of a higher capacity, with a maxim load tolerance of 100KWe hence higher fuel consumption rate (FCR) of 110 ± 10 kg/hr compared to the one in the present research with a maximum power output

of 10kWe (rated) with a fuel consumption rate of 4.9± 0.07kg/hr. The difference in FCR for both gasifiers may be due to the variation in the operating ER for both gasifiers since FCR depends on ER. It should be noted that the charcoal recovery rate of less than 5% was very low for both gasifiers.

4.12 Variation of equivalence ratio with gasification time

The ER of the gasification system was computed for each run to evaluate the equivalence ratio of the actual woodchips-to-oxidizer (air)ratio to the stoichiometric woodchips-to-oxidizer (air) ratio. A sample of ER calculation is detailed in Table 4.4 and subsequent calculations in the appendix section A5. From the ER value above an equivalent ER 0.227 could be computed from the corresponding air flow rate. This implies that for autothermal gasification systems which largely depend on incoming air to sustain the gasification reactions, the equivalence ratio will be influenced by the air flow rate. The higher the air flow rate, the lesser the gasification time and the higher the fuel consumption rate (FCR) and subsequently the higher the ER. When the airflow rate is low, the fuel consumption rate will also be small and the less the ER as the gasifier would be operated in the sub stoichiometric region. In general, the ER of the gasifier would not significantly vary if air flowing at a constant flow rate as this would create a uniform pattern in the fuel consumption rate and subsequently a uniform pattern in the chemistry of gasification. The ER of the gasifier would thus be uniform at any instant.

Table 4.4 Sample ER computation at a load of 4KWe - for run 2

Time/min	Interval/S	Velocity m/s	Temp air /C	Density, D(Kg/m^3)	Q (m^3/s)=UA	Air Mass flow [kg]= Qxdensityxtime
30	1800	0.8	28.2	1.1726	0.002065	4.358
60	1800	0.7	27.8	1.1726	0.001807	3.814
90	1800	0.7	27.9	1.1726	0.001807	3.814
120	1800	0.7	29.7	1.1726	0.001807	3.814
150	1800	0.6	29.1	1.1726	0.001549	3.269
180	1800	0.6	29.1	1.1726	0.001549	3.269
210	1800	0.6	28.6	1.1726	0.001549	3.269
240	1800	0.6	26.7	1.1726	0.001549	3.269
270	1800	0.6	27.2	1.1726	0.001549	3.269
300	1800	0.6	26.8	1.1726	0.001549	3.269
330	1800	0.6	27.2	1.1726	0.001549	3.269
360	1800	0.6	27.0	1.1726	0.001549	3.269
375	900	0.6	27.0	1.1726	0.001549	1.634
Average Temperature (TºC)			27.9			
Sum of air (Kg)						43.584
Volume of air (m^3)				0.12		
A/F(m^3/kg) at ER = 1				4.858		
ER		0.227				

4.13Variation of gasification temperature with gasification time

It is important to know how the temperature of the gasification zone varies with the connected load over time to investigate the stability of the gasifier after attaining steady state. This helps to depict the thermal stability of the system and its ability to sustainably generate the required gases that power the engine. Typical results of the temperaturesin the reduction zone were recorded and revealed in the appendix A1-A3 with trends shown in Figures 4.11-4.13.Tt1, Tt2, Tt3 and Tb1, Tb2, Tb3 represent the temperatures at the top and bottom of the reduction zone for replicates 1, 2 and 3 respectively. From the results observed in Figures 4.11-4.13, there is no significant variation in the temperature values at the top and bottom of the reduction zone of the gasifier during its operation at steady state. The nearly constant temperature reveals that the rate of flow of the incoming air is nearly constant and that reactions inside the gasifier are taking place at nearly constant ratesunder similar conditions and almost the same biomass fuel consumption rate inside the gasifier. This further implies that syngas is produced at a nearly constant rate and that its composition doesn't significantly change. The incoming air is the primary source of air for the exothermic reactions and is responsible for the maximum amount of temperatures that can be obtained inside the gasifier. The higher the flowrate of incoming air, the faster the exothermic reactions and the higher the temperatures inside the gasifier. Nearly constant temperatures reveal that the reaction equivalence ratio is subsequently constant. The average temperatures at the top of the reduction zone (Tt red) were 897.1± 12.11 °C and 884.7± 27.64°C when a 2KWe and 4KWe and the average temperatures at the bottom of the reduction zone (Tb red) were 762.9± 4.70°C and 824.1±20.22°C for both the 2kW and 4kW respectively. Thus, the change in the load connection from 2kW to 4kW didn't significantly affect the change in temperature because the amount of air required to power both loads were nearly the same and within the

order of the same magnitude. A bigger load would require more energy and this would expedite the rate of gas intake to the engine as well as consume more biomass to sustain the energy supply. However, the temperatures of the reduction zone is higher at the top (Tt red) and lower at the bottom (Tb red) because the reactor is vertically aligned and that the temperature gradient increases with increase in the perpendicular distance from the combustion zone and so gas molecules get cooler as their distance from the combustion zone region increases.

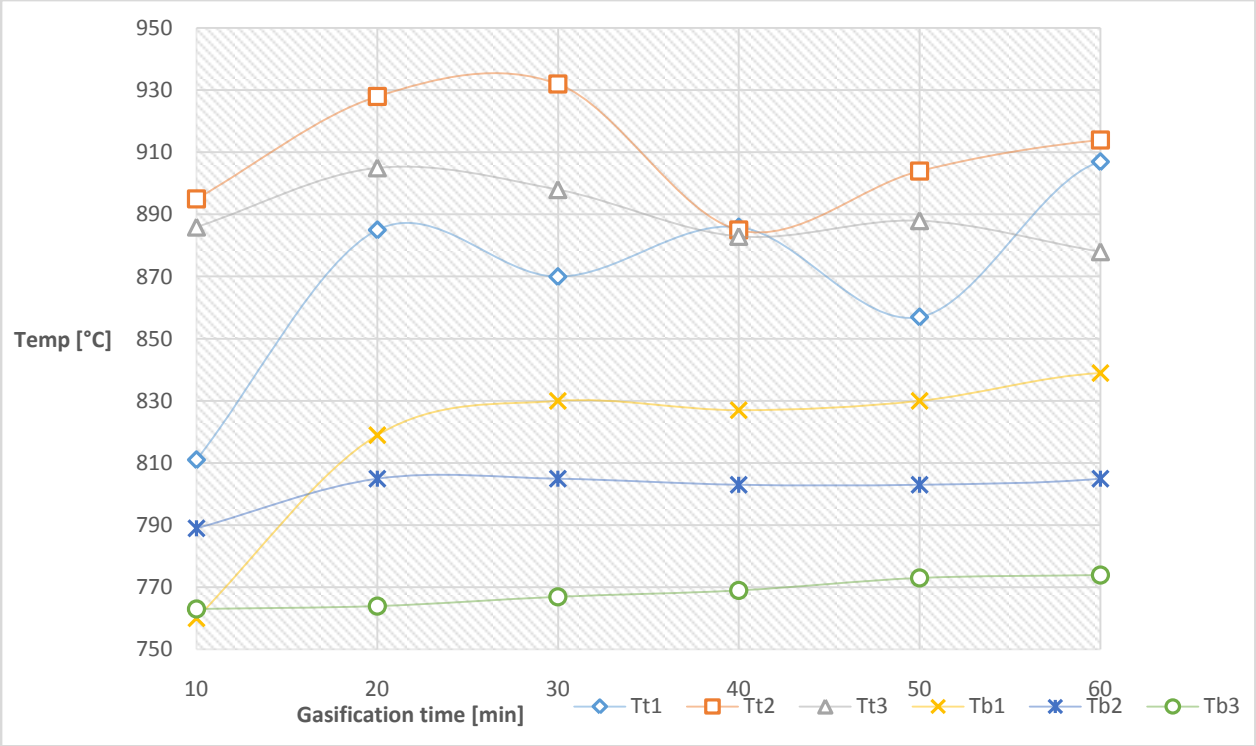

Figure 4.11 Temperature distribution as the gasifier runs on the 4KWe load for 1 hr

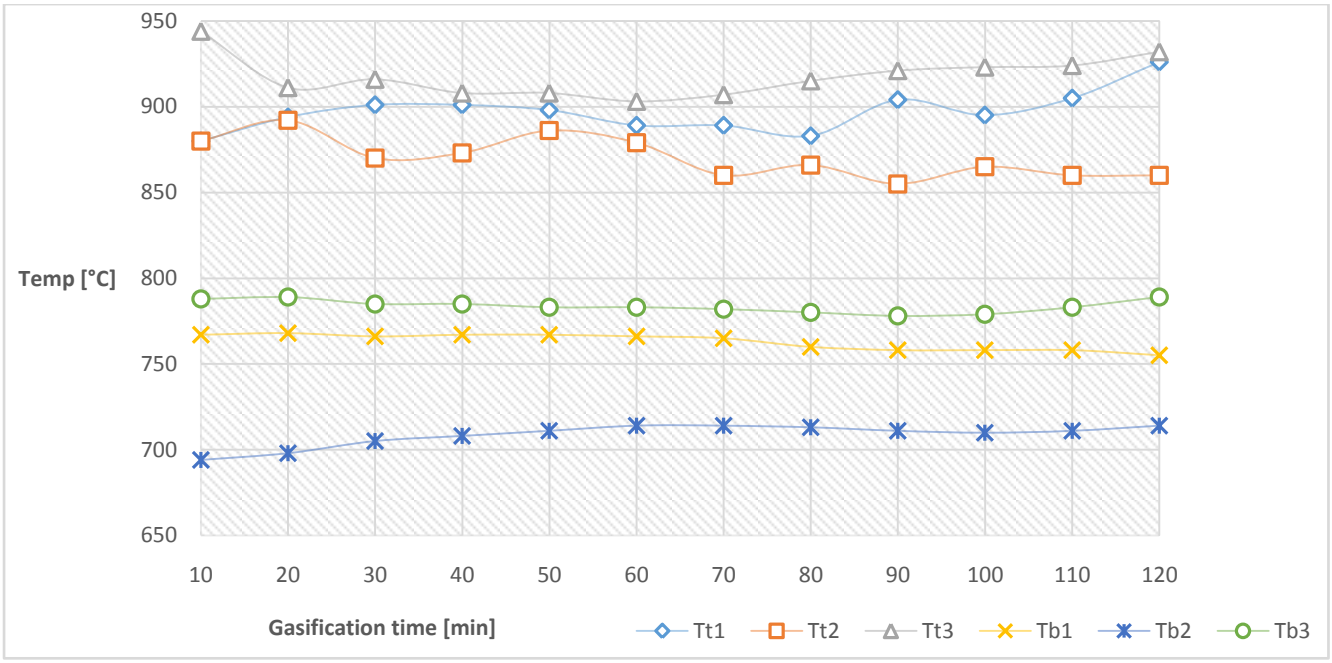

Figure 4.12 Temperature distribution as the gasifier runs on the 4KWe load for 2hrs

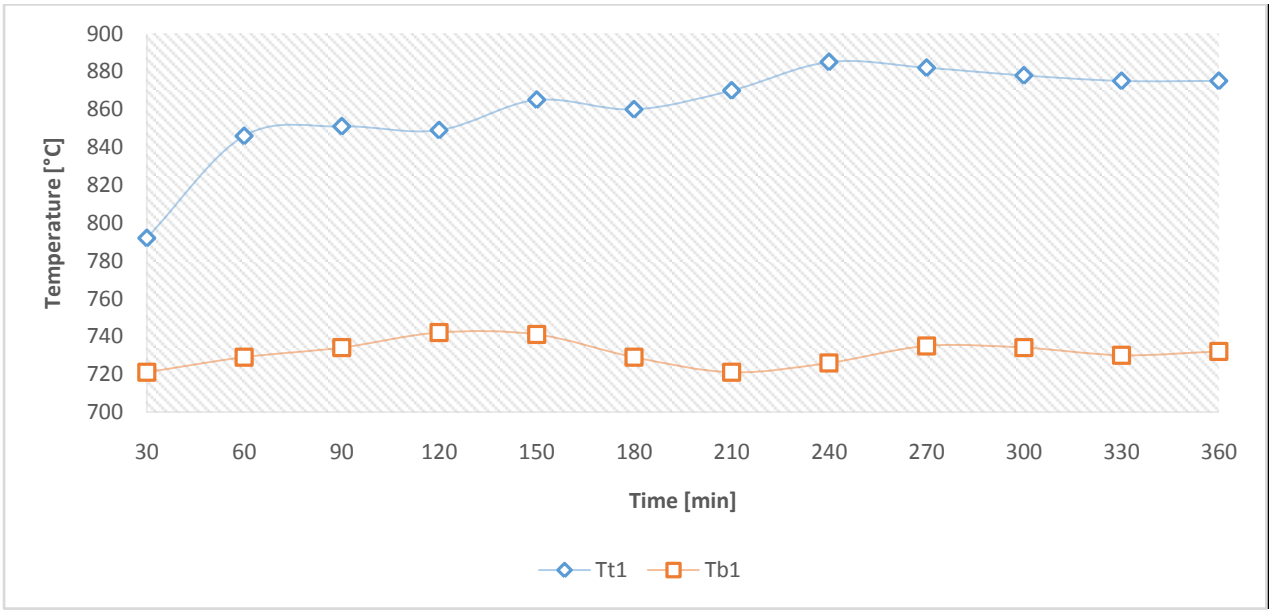

Figure 4.13 Temperature distribution as the gasifier runs on the 4KWe load for 6 hrs

4.14Variation of the exhaust stream under steady operating conditions

The composition of the engine exhaust stream was monitored under steady operating conditions to determine the composition of the exit stream escaping to the ambient and to investigate whether the power generation unit poses any serious threats to the environment. It was discovered that the exhaust stream contained mainly CO_2 at a concentration of 19.92±0.14%, and a few traces of CO, O_2 and NOx at a concentration of 0.23±0.07%, 1.22±0.68%, 146 ±51 ppm respectively as shown in Table 4.5 below. Traces of CO in the exhaust stream would be due to incomplete oxidation of producer gas from the engine. The CO_2 composition of about 20% in the exhaust stream is vented out to the ambient air. Adopting mechanisms of capturing this carboncould lessen on the effect of environmental pollution if this technology should be effectively and sustainable used by the end user.

Table 4.5 Average composition of the exhaust gas stream

Exhaust gas type	**average composition of exhaust gas**
CO_2 (% Vol)	19.92±0.14
CO (% Vol)	0.23±0.07
O_2 (% Vol)	1.22±0.68
NOx (ppm)	146±51

4.15Investigating the rate of biochar formation

From the results that summarize the amount of biochar formed (appendix A), the rate of char formation was computed based on data from four sample runs (run 10 – run 13) operated under similar conditions. From the results, the average rate of biochar formation is 0.039 ±0.004 kg/hr and the equivalent average fuel consumption rate for the four runs is 5.14±0.42 kg/hr. The rate of char formation is thus 0.75% of the fuel consumption rate which is a very low rate of char formation compared to the fuel consumption rate. This implies that majority of the char formed during pyrolysis is used up during the reduction processes to enhance producer gas formation. The option to use the gasifier for biochar production alongside electrical production is thus not economically feasible because of the insignificant amount of char that remains as part of the gasification process.

4.16 Investigating the effect of gasification time on the performance of the gasifier

The operation time is one important factor that strongly affects the product profile and overall yield achieved from thermochemical pretreatment of lignocellulosic biomass (Sievers, Kuhn, Stickel, Tucker, & Wolfrum, 2016). It is one important measure of reactor performance and provides a metric to use when evaluating changes in reactor design and operating parameters. Thus, the gasifier was run at three different operation time regimes to investigate a variation in product composition.

4.16.1 Effect of FCR with operation time

In order to investigate the effect of gasification time on the performance of the gasifier, three different sets of gasification times at higher operation time (HOT), medium operation time (MOT) and lower operation time (LOT) were considered and experiments were conducted in triplicate at all these gasification times to monitor the fuel consumption rate of the gasifier (FCR), ER, gas composition, cold gas efficiency (CGE), Carbon conversion efficiency (CCE), gas calorific value and gasifier temperature. According to the results summarized in Tables 4.6- 4.8.The average gasification times for HOT, MOT and LOT were 6.56±0.17hrs, 3.47±0.058hrs and 1.62±0.204hrs respectively. The fuel consumption of the biomass inside the gasifier increased with gasification time because more fuel would be burnt to sustain the gasification process inside the gasifier for the duration of the experiment. Autothermal gasifiers are thus sustained by the exothermic heat generated from the combustion of biomass and thus would demand more fuel to sustain these reactions.

Subsequently, the FCR of the gasifier was 5.47±0.2kg/hr, 5.27±0.14kg/hr and 4.89±0.071kg/hr for HOT, MOT and LOT respectively. A decrease of gasification time from HOT to MOT and HOT to LOT decreased the FCR by 3.65% and 10.6% respectively. It appeared that the highest FCR of 5.47±0.2kg/hr was observed at HOT of 6.56±0.17hrs of gasification compared to 5.27±0.14kg/hr and 4.89±0.071kg/hr at 3.47±0.058hrs and 1.62±0.204hrs respectively because the gasifier achieves and maintains steady state conditions for longer hours at HOT.

Steady state conditions maintained for longer hours increase on the rate of accumulation of heat inside the gasifier which increases on the rate of drying of the incoming biomass and subsequently expedites the combustion and pyrolysis reactions inside the gasifier leading to the gasification of drier biomass hence increasing on the rate of biomass consumption rate as the reactor gets hotter.Table 4.6-4.8 Effect of gasification time on the gasification performance of the reactor

Table 4.6. Effect of Higher Operation Time (HOT) on the gasification performance of the reactor

Higher Operation Time (HOT) - 6.56±0.17hrs				
	Rep 1	Rep2	Rep3	Average
Initial height (h1)/cm	10	7	5.5	
Final height (h2)/cm	68	70	70	
Height difference (h2-h1)/m	0.58	0.63	0.645	0.62±0.034
Hopper circular area (m^2)	0.2552	0.2552	0.2552	0.255±0
Volume of wood chips gasified	0.148	0.161	0.165	0.158±0.009
Density (kg/m^3)	227.4	227.4	227.4	227.4±0
Total Mass gasified for entire gasification time (Kg)	33.6	36.6	37.4	35.90±1.97
Total gasification time (hrs)	6.40	6.50	6.75	6.56±0.17
Mass flow rate (Kg/hr)	5.24	5.62	5.54	5.47±0.2
ER	0.256	0.239	0.242	0.245±0.009

Table 4.7 Effect of Medium Operation Time (MOT) on the gasification performance of the reactor

Medium Operation Time (MOT) - 3.47±0.058 hrs				
	Rep 1	Rep2	Rep3	
Initial (h1)/cm	42	8	35	
Final height (h2)/cm	72	40.5	67	
Height difference (h2-h1)/m	0.3	0.325	0.32	0.315±0.013
Hopper circular area (m^2)	0.2552	0.2552	0.2552	0.2552±0
Volume of wood chips gasified	0.077	0.083	0.082	0.0804±0.003
Density (kg/m^3)	227.4	227.4	227.4	227.4±0
Total Mass gasified for entire gasification time (Kg)	17.41	18.86	18.57	18.28±0.77
Total gasification time	3.4	3.5	3.5	3.47±0.058
Mass flow rate (Kg/hr)	5.12	5.39	5.31	5.27±0.14
ER	0.262	0.249	0.253	0.255±0.007

Table 4.8 Effect of Lower Operation Time (LOT) on the gasification performance of the reactor

Lower Operation Time (LOT) - 1.62±0.204 hrs				
	Rep 1	Rep2	Rep3	
Initial (h_1)/cm	40	55	58	
Final height (h_2)/cm	55	69	70	
Height difference (h_2-h_1)/m	0.15	0.14	0.12	0.137±0.015
Hopper circular area (m^2)	0.2552	0.2552	0.2552	0.255176±0
Volume of wood chips gasified	0.03828	0.03572	0.03062	0.035±0.004
Density (kg/m^3)	227.4	227.4	227.4	227.4±0
Total Mass gasified for entire gasification time (Kg)	8.70	8.12	6.96	7.93±0.9
Total gasification time	1.8	1.667	1.4	1.62±0.204
Mass flow rate (Kg/hr)	4.84	4.87	4.97	4.89±0.071
ER	0.277	0.275	0.270	0.274±0.004

4.16.2 Effect of operation time with temperature

The gasification temperature of the reactor was monitored during the duration of the experiment for HOT, MOT and LOT. Temperature results for the last one hour of operation were recorded to depict the variation in the temperature trends as shown in Figure 4.14. It was observed that all the gasification temperatures for HOT, MOT and LOT were between 850-950 ºC. The increase in gasification temperature was in the order HOT>MOT>LOT. The longer the gasifier is maintained under the state of thermodynamic equilibrium, the higher the accumulation of heat and its distribution within the gasifier due to biomass combustion, pyrolysis and gasification respectively. Hence, the gasifier becomes hotter at HOT due to the cumulative generation of heat that distributes within the gasifier. This makes the gasifier more stable while operating under steady conditions. Thus, HOT registered the highest temperatures because it was operated for longer hours and produced significantly higher cumulative temperatures. Allowing the gasifier to run for longer operation times ensures complete devolatilization of biomass (Gable & Brown, 2016).Subsequently, the formed char is further gasified to produce heat and accompanying gases.

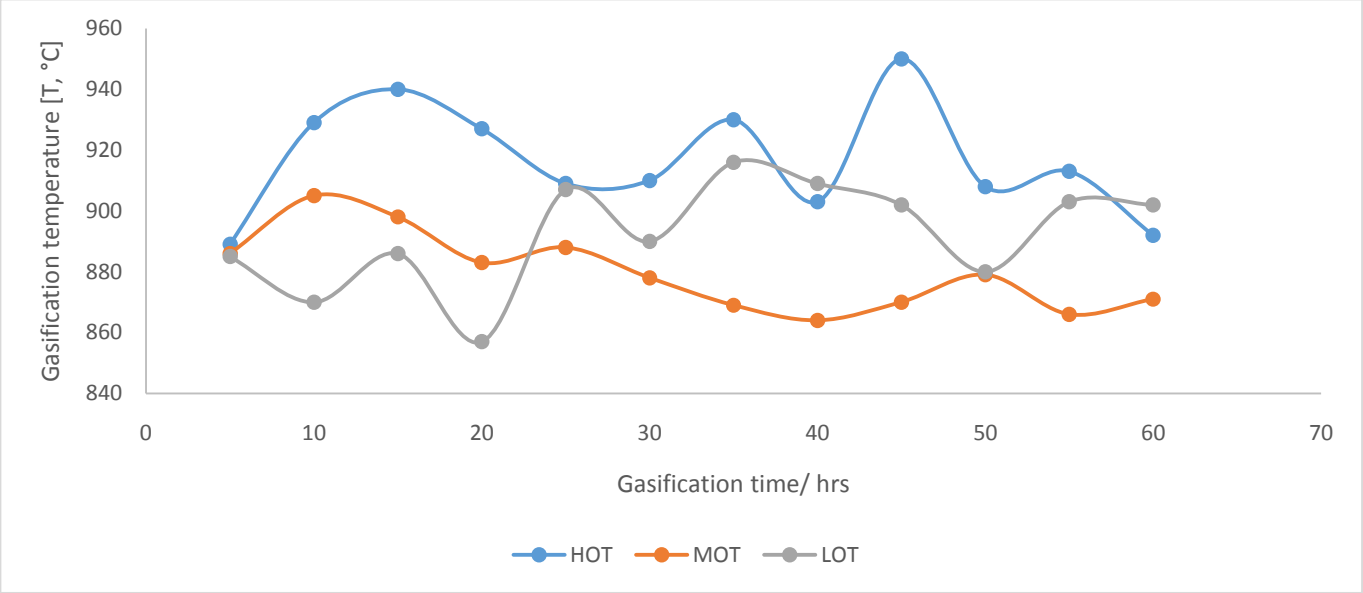

Figure 4.14 Temperature distribution of the gasifier at LOT, MOT and HOT

4.17Effect of variation in moisture content to the overall gasification performance of the gasifier

Woodchips of varying moisture contents were classified into three grades of Low moisture content (LMC) witha corresponding moisture content value of 6.4±2.4% (Table 4.9), Medium Moisture Content (MMC) with moisture content 13.73± 0.6% (Table 4.10) and High moisture content (HMC) with moisture content of 17.5±0.3%(Table 4.11) and were gasified in the downdraft gasifier at a constant load of 2KWe to investigate the overall gasification performance in terms of fuel consumption rate (FCR), reaction temperatures,equivalence ratio,producer gas composition, carbon conversion efficiency, as well as gas yield. The experiments for each set of moisture content were done in triplicate to investigate the extent of data replicability whose findings are summarized in Tables 4.9-4.11. The gasifier's maximum moisture content tolerance was 30 % but from the practical experimental performance of the gasifier, wood chips of such moisture content could not easily be used inside the gasifier as it takes long to start when used with woodchips of wet

moisture content (upto 30%) alongside other challenges such as the possibility of high tar formation due to the low temperatures reported inside the gasifier arising from high moisture content. Choice of the moisture content range was thus considered on the basis of allowing a quick start and to simulate real case scenarios within which the gasifier can operate from based upon the end user's ease of adaptation.

4.17.1 Effect of moisture content on the FCR

When the gasifier was operated with wood chips from LMC –MMC- HMC as shown in Tables 4.9-4.11 at nearly similar gasification timesof 2.17±0.058hrs, 1.83 ±0.18hrs, 2.6±0.13 hrs for LMC, MMC and HMC respectively, the fuel consumption rate (FCR) of the gasifier decreased from 5.58±0.08kg/hr at LMC, to 4.86±0.025 kg/hr at MMC and to 4.61±0.05kg/hr at HMC. The decrease in FCR is attributed by the increase in the amount of moisture present in woodchips. When the amount of moisture present in woodchips increases, more heat is required to drive off the water vapour and part of the heat is lost during the heating up process which leads to the loss of the heat that would otherwise have been used to gasify the wood chips. The decline in the amount of heat due to drying of biomass woodchips thus reduces on the amount of the overall heat available to convert woodchips to gas and thus reducing the rate of biomass consumption and its subsequent conversion into gasification products. The findings from this research at a moisture content of6.4±2.4% provide the highest fuel consumption rate of upto 5.58±0.08kg/hr compared to 4.86±0.025kg/hr and 4.61±0.053kg/hr at MMC and HMC respectively. These findings thus confirm that drier woodchips should be used during biomass gasification because they contribute to a higher FCR.

Table 4.9 Variation of fuel consumption rate at a Lower moisture content 6.4±2.4% at 2kW

	Replicate 1	**Replicate 2**	**Replicate 3**	Average
MC %	6.4±2.4	6.4±2.4	6.4±2.4	
Initial height (h1)/cm	7	5.5	5	
Final height (h2)/cm	27	26	26	
Height difference (h2-h1)/m	0.2	0.215	0.21	0.208±0.0076
Hopper circular area (m^2)	0.2552	0.2552	0.2552	0.25518
Volume of wood chips gasified	0.051	0.055	0.054	0.053±0.0019
Density (kg/m^3)	227.4	227.4	227.4	227.4±0
Total Mass gasified for entire gasification time (Kg)	11.6	12.5	12.2	12.1±0.44
Total gasification time	2.1	2.2	2.2	2.17±0.058
Mass flow rate (Kg/hr)	5.53	5.67	5.54	5.58±0.08

Table 4.10 Variation of fuel consumption rate at a medium moisture content (MMC) 13.73± 0.6% at 2kW

	Replicate1	**Replicate 2**	**Replicate 3**	**Average**
MC%	14.2±1.7	13.9±1.4	13.1±1.1	
	2	3	1	
Initial height (h1)/cm	55	35	40	
Final height (h2)/cm	69	52	55	
Height difference (h2-h1)/m	0.14	0.17	0.15	0.15±0.0153
Hopper circular area (m^2)	0.2552	0.2552	0.2552	0.2552
Volume of wood chips gasified	0.036	0.043	0.038	0.039±0.004
Density (kg/m^3)	227.4	227.4	227.4	227.4
Total Mass gasified for entire gasification time (Kg)	8.12	9.86	8.70	8.90±0.9
Total gasification time (hrs)	1.7	2.02	1.8	1.83 ±0.18
Mass flow rate (Kg/hr)	4.87	4.88	4.84	4.86±0.025

Table 4.11 Variation of fuel consumption rate at a Higher moisture content (HMC) 17.5±0.3%at 2kW

	Replicate1	**Replicate 2**	**Replicate 3**	**Average**
MC %	17.8 ± 2.14	17.2±1.5	17.5±1.2	
Initial height (h1)/cm	10	35	52	
Final height (h2)/cm	32	55	72	53
Height difference (h2-h1)/m	0.22	0.2	0.2	0.207±0.012
Hopper circular area (m^2)	0.2552	0.2552	0.2552	0.2552
Volume of wood chips gasified	0.056	0.051	0.051	0.053±0.003
Density (kg/m^3)	227.4	227.4	227.4	227.4
Total Mass gasified for entire gasification time (Kg)	12.77	11.60	11.60	12.00±0.67
Total gasification time	2.75	2.5	2.55	2.6±0.13
Mass flow rate (Kg/hr)	4.64	4.64	4.55	4.6±0.053

4.17.2 Effect of biomass moisture content with ER

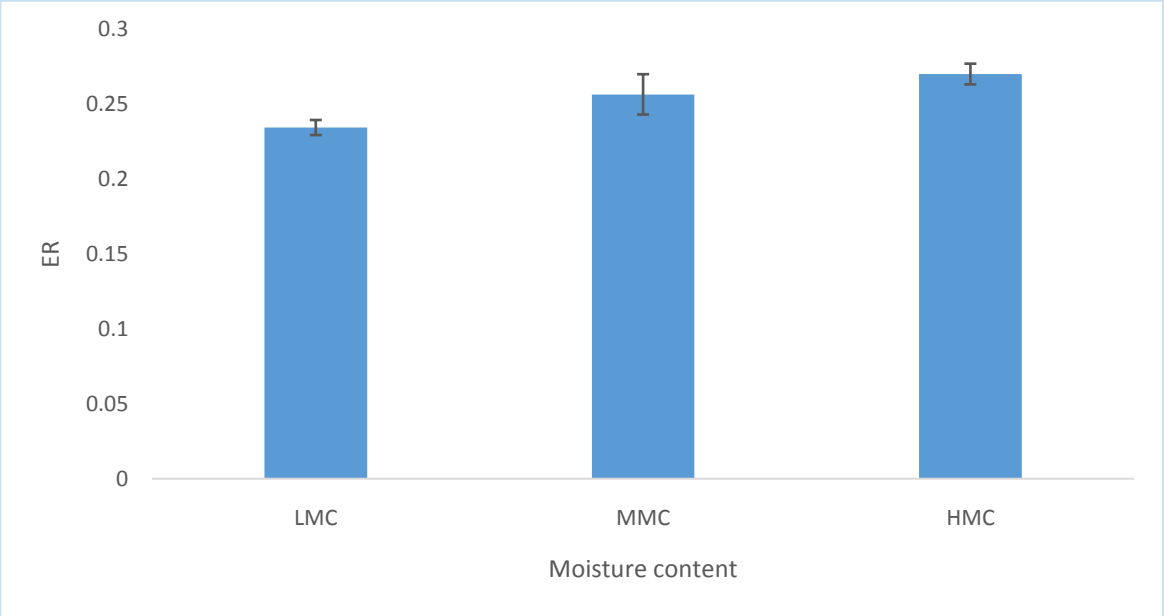

Figure 4.15 Variation of moisture content with ER

As observed in Figure 4.15, increase in moisture content from LMC-MMC –HMC increased the ER from 0.240 - 0.2788 – 0.2946 respectively. At LMC, wood chips are drier and are gasified with generation of more heat as compared to wet or moist woodchips. Increase in the gasification temperature increases the FCR of the gasifier, the increase in ER was due to the increase in temperature.

4.17.3 Effect of moisture content on the quality of syngas production

As the moisture content was varied from LMC –MMC-HMC with their corresponding moisture content values of 6.4±2.4%, 13.73± 0.6% and 17.5±0.3% respectively, it was observed that the overall composition of the major components of producer gas of CO, H_2, and CH_4varied significantly with increase in moisture content. The individual composition

ofgases such as CO decreased from 25.3±0.48% (at LMC) to 21.3±1.06% (at MMC) and to 19.4±0.11% (at HMC). The decrease of CO is justified by the decrease in gasification temperatures as moisture content increases. Generally, higher CO formation are favored by increase in temperature (Lahijani & Zainal, 2011) and any drop in the gasification temperature such as that observed during increase in moisture content would decrease the composition of CO. Subsequently, the composition of H_2 decreased from 18.1± 1.19 % (at LMC) to 17.562±1.26% (at MMC) and increased to 19.9±0.60% (at HMC). The details of the trend of gas compositions are shown in Tables 4.12-4.14. CH_4 decreased from 2.2±0.05%(at LMC) to 1.9±0.47% (at MMC) and increased to 2.4± 0.18 % (at HMC). The composition of CO_2 increased with increase in moisture content from 2.4±0.20 (at LMC) to 3.7±0.55% (at MMC) and 10.9±5.31% (at HMC). The increase in the composition of H_2, $CH_4$and CO_2 with increase in moisture content could be explained by the steam gasification reactions that take place in the reduction zone (equations 4.1-4.3) (Atnaw, Sulaiman, & Yusup, 2014)as justified by the equations below

$$C + H_2O \rightarrow CO + H_2 \qquad \Delta H = \frac{119kJ}{mol} \ldots\ldots\ldots\ldots\ldots\ldots\ldots\ldots\ldots\ldots\ldots\ldots\ldots\ldots\ldots\ldots (4.1)$$

$$C + 2H_2O \rightarrow CO_2 + 2H_2 \qquad \Delta H = \frac{75kJ}{mol} \ldots\ldots\ldots\ldots\ldots\ldots\ldots\ldots\ldots\ldots\ldots\ldots\ldots\ldots\ldots\ldots (4.2)$$

$$C + 2H_2 \rightarrow CH_4 \qquad \Delta H = \frac{-87kJ}{mol} \ldots\ldots\ldots\ldots\ldots\ldots\ldots\ldots\ldots\ldots\ldots\ldots\ldots\ldots\ldots\ldots (4.3)$$

From the equations above (equations 4.1-4.3), the composition of CO , CO_2 and H_2 is supposed to yield a significant increase with increase in moisture content but according to equations 4.1 and 4.2, the formation of the gasification products is favored endothermically and would depend on the gasification temperature for such a significant increase to happen.

However, the temperature of the downdraft autothermal gasifier doesn't increase with addition of more moist woodchips but instead drops. Thus justifies the slight increases in the gas composition of CO, CO_2 and CH_4 as the moisture content increases. It should however be noted that the concentration of CO and H_2 would equally be enhanced by the cracking of tars which would only take place at high temperatures. Wood chips of high moisture content don't favor high temperature formation for the case of autothermal gasifiers and are thus constrained in terms of tar cracking hence making less contribution to the addition of H_2 and CO formation when more moist woodchips are used. In conclusion, the formation of CO and H_2 in downdraft autothermal gasifiers largely depends on the reactions that take place in the reduction zone inside the gasifier and the temperature of the gasifier. The higher the attained temperatures, the higher the CO and H_2 concentration and could only be favored when dry woodchips are used for gasification.

4.17.4 Effect of moisture content on the calorific value of the producer gas fuel

It is important to determine the effect of themoisture content of woodchips on the fuel heating value of the producer gas so as to evaluate its performance in the engine.Variation of the moisture content of woodchips from LMC –MMC-HMC with their corresponding moisture content values of6.4±2.4%, 13.73± 0.6% and 17.5±0.3% respectively had a bearing on the heating value of the fuel. The lower heating value (LHV) of producer gas generally decreased from 6.4±0.19MJ/$m^3$to 5.3±0.19MJ/m^3 with a slight increase of 3.2% upto 5.47±0.01MJ/m^3 when woodchips moisture content was varied from LMC –MMC-HMC. The increase of upto 3.2% from MMC-HMC is not significant but in general, the variation of LHV of the fuel from LMC –HMC decreased by 14.53% which is a significant decrease. To further test the effect of moisture content on LHV, moisture content data was statistically tested with one

way anova with detailed results for the variation of moisture content shown in Appendix A3. Results showed a significant impact of change in moisture content with both LHV and HHV as the F_{stat} is greater than the F_{crit} for both cases. The heating value of the syngas generally decreases as moisture content increases. The decrease in the heating value of syngas is attributed to the decrease in the concentration of CO which is temperature dependent and would decrease as moisture content increases as part of heat is lost during quenching. The heating value of the producer gas obtained is in the range of 5-6MJ/m^3 as shown in Tables 4.12-4.14 and in agreement with the expected LHV between (4–6 MJ/Nm^3)for the heating values from theair gasification of woody biomass (Zainal et al., 2002a). Moist woodchips thus need to be dried within acceptable moisture content tolerance to produce synthesis of recommended and acceptable heating values. Drying of woodchips not only improves on the fuel heating value but also improves on the quality of synthesis gas that goes to the engine which improves the engine performance and combustion efficiency. Low temperatures arising from moist wood chips would affect the gasification efficiency, energy conversion efficiency as well as compromising on the yield of syngas. It can be observed from Tables 4.12-4.14 that an increase in moisture content from LMC-MMC-HMC also decreased the CGE by 12 %, which affected the whole gasifier performance. In addition, McKendry, (2002) observed that biomass of moisture content above 30% is difficult to ignite. Therefore, biomass samples should be dried to a moisture level no higher than 20% not to compromise the gasifier performance, gas quality and energy conversion efficiency.

Table 4.12 Effect of moisture content on the gas composition at LMC

Average gas composition (% v/v)	CO	CO_2	CH_4	H_2	O2	N_2	MC% wc	LHV/MJ/m^3	HHV/MJ/m^3	CGE, %	Y (m^3/kg)
Rep1	24.859	2.491	2.271	18.024	1.444	50.909	6.4±2.4	5.898	6.347	67.857	2.115
Rep2	25.315	2.448	2.17	16.988	2.323	50.747	6.4±2.4	5.813	6.234	70.985	2.245
Rep3	25.826	2.118	2.205	19.355	2.069	48.424	6.4±2.4	6.145	6.613	88.568	2.649
Average at MC 6.4±2.4%,	25.3±0.48	2.4±0.20	2.2±0.05	18.1±1.19	1.9±0.45	50.0±1.39	6.4±2.4	6.0±0.17	6.4±0.19	75.80±11.16	2.34±0.29

Table 4.13 Effect of moisture content on the gas composition at MMC

Average gas composition (% v/v)	CO	CO_2	CH_4	H_2	O_2	N_2	MC%wc	LHV/MJ/m^3	HHV/MJ/m^3	CGE, %	Y (m^3/kg)
Rep1	20.469	3.748	1.977	16.163	0.688	56.952	14.2±1.7	5.039	5.438	63.344	2.310
Rep2	20.889	4.153	2.261	17.918	2.440	52.336	13.9±1.4	5.395	5.828	74.990	2.555
Rep3	22.478	3.059	1.340	18.603	0.366	54.151	13.1±1.1	5.355	5.750	62.490	2.145
Average gas composition (% v/v) at MC 13.73±0.6%	21.3±1.06	3.7±0.55	1.9±0.47	17.6±1.3	1.26±1.12	54.5±2.32	13.7±0.6	5.3±0.19	5.7±0.21	66.94±6.98	2.3±0.21

Table 4.14 Effect of moisture content on the gas composition at HMC

	CO	CO_2	CH_4	H_2	O_2	N_2	MCwc	LHV/MJ/m^3	HHV/MJ/m^3	CGE, %	Y (m^3/kg)
Rep 1	19.381	13.985	2.518	19.562	1.358	43.194	17.8 ±2.14	5.468	5.950	68.839	2.314
Rep 2	19.554	14.001	2.516	19.517	1.356	43.053	17.2±1.5	5.484	5.965	69.061	2.315
Rep3	19.359	4.801	2.212	20.543	0.105	52.978	17.5±1.2	5.464	5.951	62.357	2.097
Average (% v/v) at MC 17.5±0.3%	19.4±0.11	10.9±5.31	2.4±0.18	19.9±0.60	0.9±0.72	46.4±5.67	17.5±0.3	5.47±0.01	5.96±0.009	66.75±3.81	2.24±0.13

4.17.5 Effect of moisture content on gasification temperature

The variation of woodchips from LMC –MMC-HMC, with corresponding moisture content of 6.4±2.4%, 13.73±0.6% and 17.5±0.3% respectively was recorded against their corresponding gasification temperature. The gasifier had two sets of thermocouples that could report the temperatures of the gasifier at the top (Tt) and bottom (Tb) of the reduction zone. The initials Tt_red_LMC,Tt_red_MMC, Tt_red_HMC, Tb_red_LMC, Tb_red_MMC, and Tb_red_HMC, were used to represent the temperatures at the top and bottom of the reduction zone for LMC, MMC and HMC respectively. Average results of the respective data sets at LMC, MMC and HMC were computed to depict the relationship between temperature and moisture content. It was observed from this study that the higher the woodchips moisture content, the lower were the gasifier reaction temperatures. Drier woodchips (LMC) recorded the highest temperatures of 918.8±14.71ºCat the top of the reduction zone and 782.3±3.74ºC at the bottom of the reduction zone compared to 848.8 ±6.73ºC at MMC and 804.5 ±17.54ºC at HMC of the top of the reduction zone and 757.6±5.93 at MMC, 707.6±7.41 at the bottom of the reduction zone for MMC and HMC respectively. It can be further confirmed from Figure 4.16 that the gasification temperatures nearly remained constant after attaining steady state conditions. Details of the trend of gasification temperatures are summarized in the Figure 4.16 with detailed results in appendix section A6. The decrease in temperatures as moisture content increases may be justified by the loss of heat in form of biomass drying. Heat is loss in form of vapour while driving off the moisture content present in woody biomass and this affects the overall gasification temperatures.

For drier wood chips, there is little or no heat lost as part of removing moisture and all the

available heat is used to initiate the combustion reactions as well as expedite the gasification reactions within the gasifier.

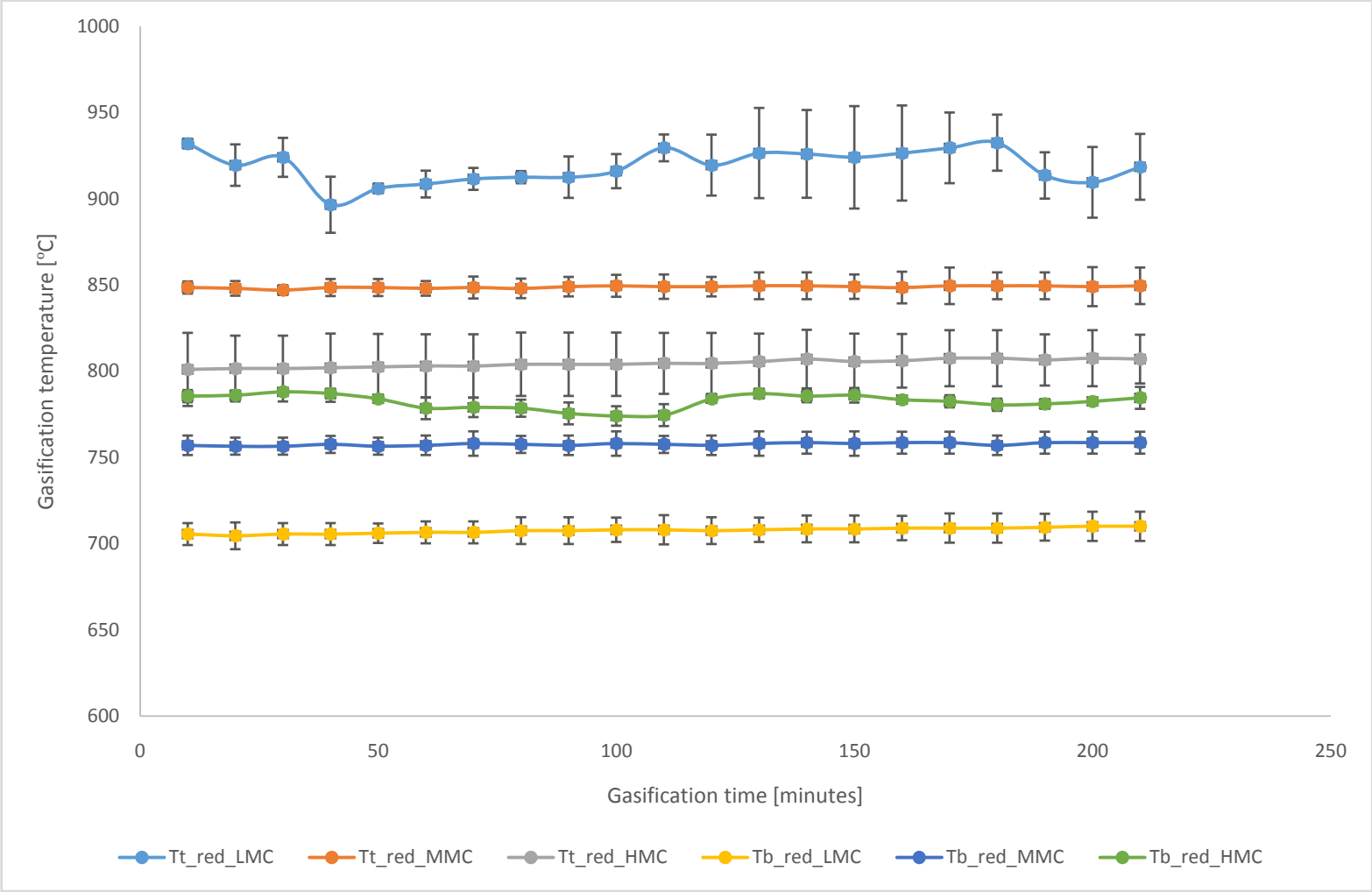

Figure 4.16 Effect of moisture content on the gasification temperature

4. 18 Investigating the production potential of the maximum rated power from the gasifier

In order to investigate the actual possible power production potential of the gasifier, a set of experiments were conducted with application of different rated resistive loads while recording the actual power output from the gasifier as detailed in Table 4.15.

Table 4. 15 Variation of Power with connection load

Imposed Rated Load(IRL/kW)	Parameter	Rep 1	Rep 2	Rep 3	Average
0	V	268.4	268.2	268.5	268.4±0.15
	I	0	0	0	0
	F	59.79	60.95	59.7	60.1±0.70
	P_{actual}	0	0	0	0
2	V	227.9	227.3	229	228.1±0.86
	I	8.731	8.750	8.885	8.8±0.084
	F	46.83	46.89	47.31	47.0±0.26
	P_{actual}	5.969	5.988	6.123	6.0±0.08
4	V	192.89	192.77	191.30	192.3±0.9
	I	7.134	7.137	7.087	7.1±0.032
	F	41.29	41.26	41.09	41.2±0.11
	P_{actual}	4.196	4.186	4.132	4.2±0.03

Where V, I, F, P is voltage, current, frequency and power respectively

As observed from the above experimental tests in Table 4.15, the load was varied from 0-4kWe while recording the values for current, voltage, frequency and power without adjusting the throttle nob for the change in frequency. It was observed from all various load connections [0-4kWe] that the current, voltage, frequency and power varied as the loads were varied. When the engine was not connected to any load, there was no current passing through the system, while a voltage of 268.4±0.15V and frequency 60.1±0.70Hz was recorded. This frequency of 60 Hz corresponds to the maximum rated for the generator and could be achieved at no connection load and was seen to significantly decrease as the load increased. Subsequently, there was no power generated from the engine when the engine was not connected to any load. Increasing the connection load from 2-4 kWe decreased current from 8.8±0.084 - 7.1±0.032 ampires, voltage decreased from 228.1±0.86 - 192.3±0.9 Volts, frequency decreased from 47.0±0.26 - 41.2±0.11 Hz and subsequently power decreased from 6.0±0.08 - 4.2±0.03 kWe respectively. An increase in the applied load decreased the frequency of the gasifier and subsequently the power if the throttle is not increasingly adjusted. At higher frequency, the engine can produce much power than the load can consume thus a throttle can be adjusted in a decreasing or increasing mode to increase or decrease power. These results implied that an increase in the applied connection load from 2 - 4kWe increased the generator frequency and a general power production output. The relative decrease in power production with increasing load could be justified by the reduction in the speed of rotation of the generator coils which reduces on the maximum possible conversion of mechanical energy to electrical energy arising from the variable ER ratios for both the gasifier and the engine. Thus to produce more power from the gasifier, the frequency was increased by adjusting the throttle valve. Adjusting to increase the speed of rotation could in turn produce more mechanical energy which in turn yields more power coming from the engine. Thus, the throttle valve was increased to generate more power arising from the

increased frequency. Results for power generated at varying frequency settings are summarized in Tables 4.16 - 4.18 and interpreted in Figures 4.16-4.19.

Table 4.16 Variation of power with frequency at 35 HZ

Time	Frequency (Hz)	Voltage (V)	Current (I)	Power (Kwe)	Load
10	34.98	206.9	4.727	1.67	10
20	35	203.9	4.689	1.63	10
30	34.9	203.5	4.685	1.6681	10
40	35.2	203.5	4.663	1.6855	10
50	35.13	206.5	4.753	1.702	10
60	35.1	205.3	4.709	1.675	10
Av	35.052	204.933	4.704	1.672	10
SD	0.111	1.525	0.0323	0.024	0

Table 4.17 Variation of power with frequency at 30 HZ

Time	Frequency (Hz)	Voltage (V)	Current (I)	Power (Kwe)	Load
0	29.67	130.85	3.05	0.6691	10
30	29.66	130.39	2.997	0.667	10
60	29.54	127.3	2.933	0.642	10
90	29.77	129.13	2.972	0.6349	10
120	29.15	125.69	2.861	0.627	10
Av	29.558	128.672	2.963	0.648	10
SD	0.242	2.161	0.071	0.019	0

Table 4.18 Variation of power with frequency at 40 HZ

Time	Frequency (Hz)	Voltage (V)	Current (I)	Power (Kwe)	Load
10	40.17	324.3	7.38	4.261	10
20	39.8	324.7	7.514	4.085	10
30	40.44	324.4	7.442	4.158	10
40	40.3	325.5	7.45	4.167	10
50	40.2	318	7.284	4.167	10
60	39.62	317.7	7.287	4.027	10
Av	40.088	322.433	7.393	4.144	10
SD	0.313	3.576	0.093	0.080	0

Table 4.19 Variation of power with frequency at 52 HZ

Time	Frequency (Hz)	Voltage (V)	Current (I)	Power (Kwe)	Load
10	51.77	438.7	10.054	7.64	10
20	52.4	437.2	10	7.557	10
30	51.8	437.5	10.1	7.543	10
Av	51.99	437.8	10.051	7.58	10
SD	0.355	0.794	0.050	0.052	0

In order to further confirm the maximum possible power output from the gasifier, the generator was connected to a 10kW resistive load while the frequency variedfrom 30Hz – 35Hz – 40Hz to 52 Hz by adjusting the throttle valveof the engine and noting changes in current, voltage, power as well as their corresponding values of incoming air in order to evaluate their respective ER due to the changes in frequency.

Increase in frequency from 30Hz – 35Hz – 40Hz to 52 Hz increased linearly with voltage, current, power and air flow rate with an R square value of 0.9665, 0.9666, 0.9849 and 0.9955 respectively as shown in Figures 4.17- 4.20. Increasing frequency by 73% (30Hz – 52 Hz) power produced from the gasifier increased by a factor of 1066% (0.65KWe -7.58KWe). It was further heard that as the frequency increased, the sound coming from the engine also

increased. This might be due to higher vibrations from the engine as the frequency increased. The engine noise went so high as the frequency approached 52Hz and appeared to be unbearable under practical operating conditions. This might be justified by the fact the engine could not work beyond the maximum rated capacity. Further research is needed to reflect the change in sound pitch with frequency in terms of decibels to confirm if this passes the in-house pitch as per occupational standards. When the engine frequency was tempted to increase beyond 52 Hz, the gasifier shut off with production of a very loud noise which might have been due to improper fuel – air mixing ratios as frequency increased. Thus, the maximum possible attained power from the gasifier was 7.58KW produced at 52 Hz. The recommended frequency of 60Hz to reflect a power output of 10KWe could not be achieved under real practical operating conditions as the gasifier was seen to shut off whenever frequency exceeded 52Hz and made a very loud noise at higher frequency settings which most likely could not pass the recommended maximum in house pitch. Based on Figure 4.18, the relationship between power generated against frequency was achieved and according to the equation of the line, (Y=0.3201X-9.0205), a substitution of the recommended maximum frequency of 60Hz corresponds to a maximum 10kWe which is said to be the maximum attainable power from the gasifier but according to the findings from this experimental set up, this only appears to be in theory.

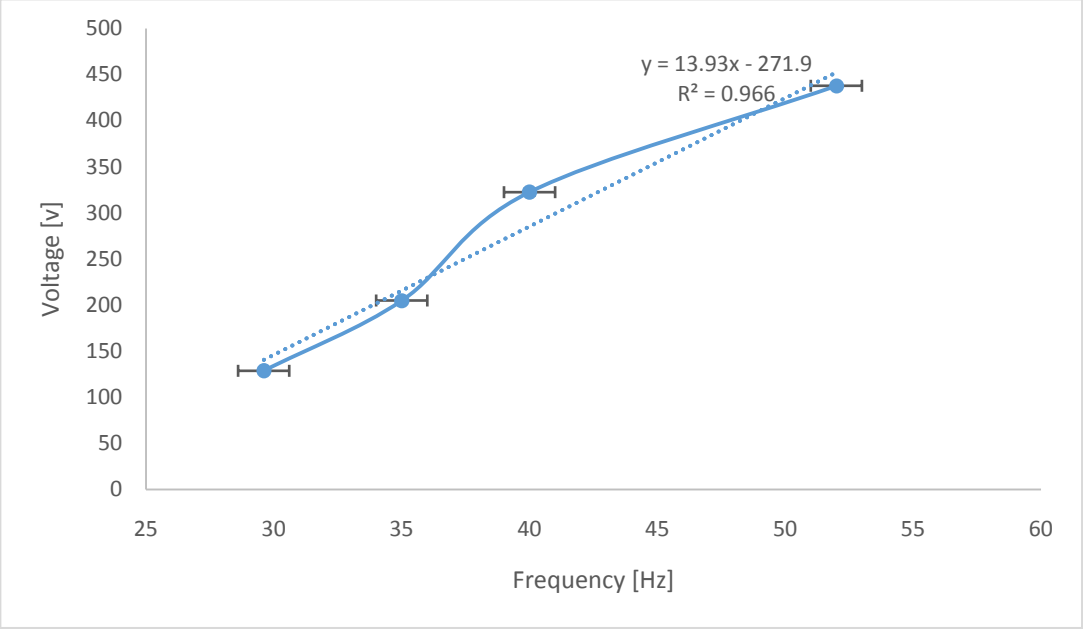

Figure 4.17 Variation of measured output voltage with frequency

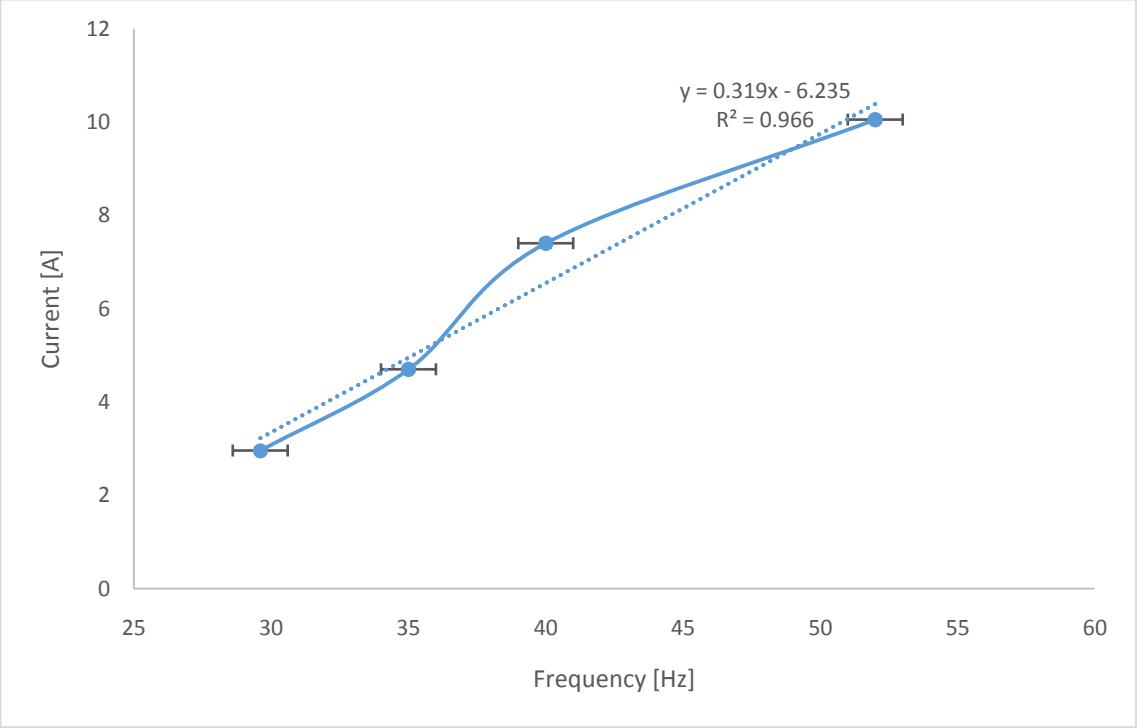

Figure 4.18 Variation of measured frequency with output current

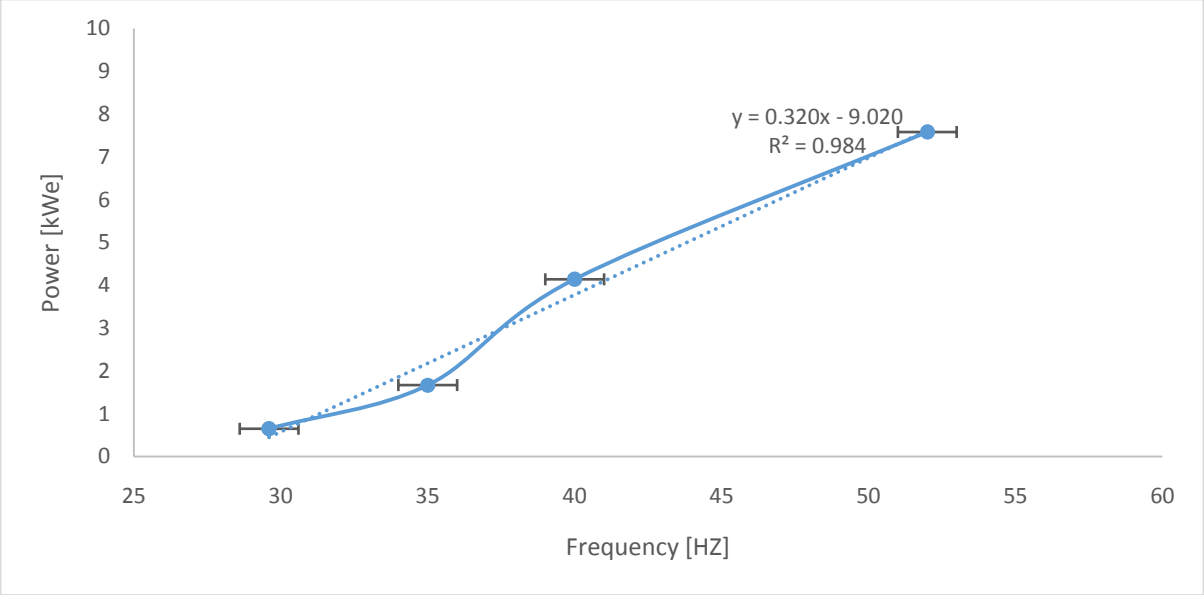

Figure 4.19 Variation of measured frequency with output power

4.19 Variation of Frequency with Fuel Consumption Rate

In addition, increasing the frequency from (30Hz – 52 Hz) resulted in an increase in the incoming air velocity from 0.3m/s to 1.1 m/s as shown in Figure 4.19. This implied that the engine was operating at a faster rate to produce the required fuel to sustain the power supply.

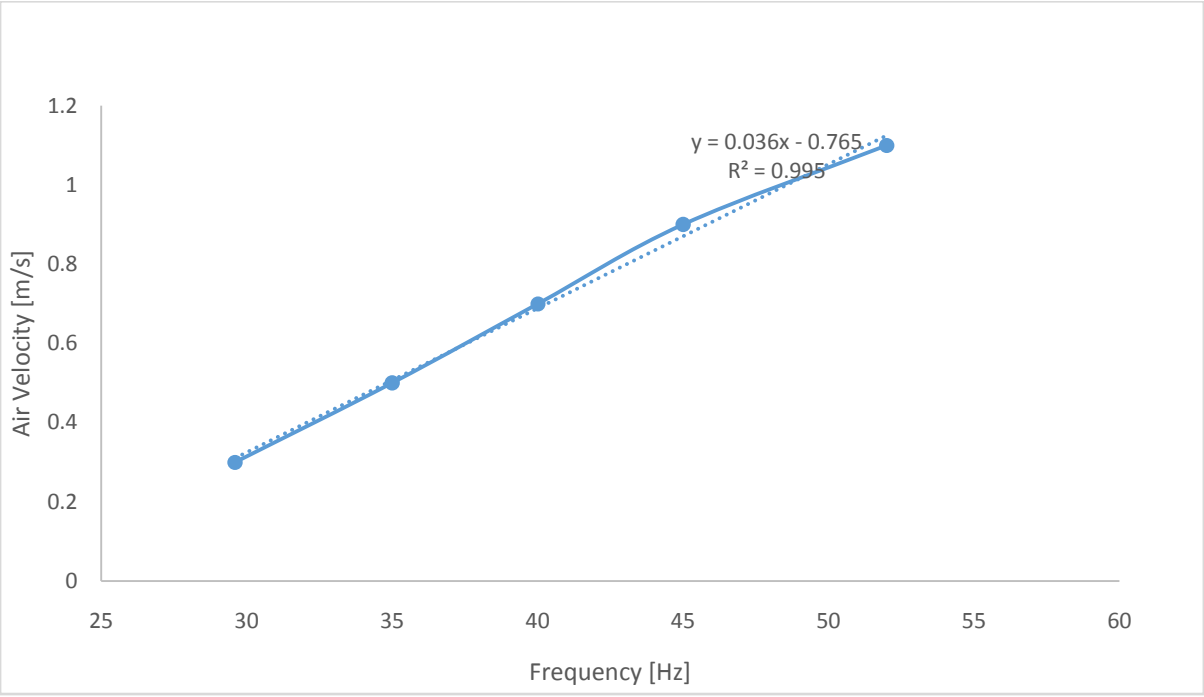

Figure 4.20 Variation of frequency with incoming air velocity

The ER value above 0.3 for the frequency above 45 Hz arose is due to the high frequency operation of the gasifier which is accompanied with higher air flow rates and shorter gas residence times inside the gasifier. The higher the gasifier efficiency, the higher the incoming airflow rate and the higher the ER.

Table 4.20 Frequency Variation with Fuel Consumption Rate

	Run 1	Run 2	Run 3
Initial height (h1)/cm	19	8	6
Final height (h2)/cm	43	70	60
Height difference (h2-h1)/m	0.24	0.62	0.54
Hopper circular area (m^2)	0.25518	0.25518	0.25518
Volume of wood chips gasified	0.061	0.158	0.138
Density (kg/m^3)	227.4	227.4	227.4
Total Mass gasified for entire gasification time (Kg)	13.9	36.0	31.3
Total gasification time	2.9	6.7	5.583
Mass flow rate (Kg/hr)	4.80	5.37	5.61
Frequency(HZ)	40	45	52
Air flow	0.7	0.9	1.1
ER	0.279	0.321	0.376
Power (KW)	4.14±0.080	5.384±0.06	7.58±0.052

CHAPTER 5

5.0 Development of equilibrium modeling of producer gas product composition in a conventional downdraft gasifier

5.1Summary

An equilibrium model is developed to establish the composition of theproducer gasproduced in a downdraft gasifier to establish a thorough understanding of the gasification process in the downdraft gasifier as well as generate reliable modeling data that can be used to benchmark the success of experimental works. Therefore, raw biomass data for wood gasification was established from the experiments conducted and partly outsourced from secondary sources in order to complete the model. The model was further validated with the experimental results obtained from the wood gasification in a downdraft gasifier which gave a better understanding for the gasification process. . The thermodynamic equilibrium model yielded a gas composition of 25.99%, 23.92%, and 0.42% for CO, H_2 and CH_4 respectively that was in good agreement with the experimental results at 850 ºC and ER of 0.27. Similarly, the modeled gasification temperature of 870.85ºC corresponds with a minor deviation of 2.5% with the experimental gasification temperature of 850ºC. The agreement between experimental and modelling results reveals that the thermodynamic equilibrium model can be used to predict the composition of producer gas from downdraft gasifiers. The results obtainedare important in the optimization of the operating conditions at the equilibrium state and also provide a simple tool to estimate the gasification performance for preliminary technical analysis of the whole process. Further still, a thermodynamic equilibrium model that predicts the composition of producer gas based on their elemental composition mitigates on the use of feedstocks that would yield low amounts of producer gas. The optimized producer gas can later be channeled to the engine for electrical power generation

Key words: thermodynamic model, equilibrium, char, producer gas, power generation

5.2Introduction

The use of models to predict gasification performance is a promising tool which can be used to deduce a number of gasifier outputs as well as optimize gasifier performance.The use of models to predict the performance of the gasifier is less economic and less labor intensive compared to experimental works. As such, models such as kinetic, transient, semi transient, steady – state and equilibrium models have been developed to predict producer gas composition during biomass gasification. Models based on thermodynamic equilibrium have been used widely, and they are convenient enough for process studies on the influence of the most important waste and process parameters(Zainalet al.,2002)(Schuster, Löffler, Weigl, & Hofbauer, 2001). Models based on thermodynamic equilibrium are more accurate when the reaction temperature is sufficiently higher. In real practice, it may not be very possible to achieve the results as obtained from modeling and such results would be the maximum obtainable during gasification experiments. Researchers have expressed varying opinions on the choice of major independent reactions for inclusion in establishing a thermodynamic equilibrium for producer gas production in a downdraft gasifier as shown in reaction equations (5)-(9). While some authors assert that char is part of the gasification product at equilibrium (ChristusJeya et al., 2014)(Azzone et al., 2012; Roy, Datta, & Chakraborty, 2009) ,(Huang & Ramaswamy, 2009) others believe that char is not part of the gasification products (Balu & Chung, 2012; Zainal et al., 2001)(Dutta et al., 2014)(Jarungthammachote & Dutta, 2007). Such a variation in assumption and the lack of agreement yields differing results in terms of composition and this need to be investigated. Therefore, biomass data from secondary sources is used to perform a thermodynamic equilibrium model that includes both cases. This will give a better understanding of the gasification process and assists to carry out design, simulation, and optimization of gasifiers and perform process analysis as part of the solid carbon mayremain when the reaction temperature is low due to limited gasification

processes. The thermodynamic equilibrium model is advantageous due to its ability to predict the maximum possible conversion of biomass during gasification and the theoretical efficiency(Huang & Ramaswamy, 2009). In addition, an approach that predicts the composition of producer gas based on their elemental composition is important because it helps to know the possible energetic potential of a particular feedstockand mitigates the use of those feedstocks that would otherwise yield low amounts of producer gas. It is also important in the optimization of the operating conditions at the equilibrium state and also being a simple tool to estimate the gasification performance for preliminary techno-economic analysis of the whole process. Although different authors have proposed models that could lead to this conclusion, controversy still exists on whether char remains as part of the gasification product or is completely used up during the entire reduction process as mentioned above. A thermochemical equilibrium model with a comparative approach for biomass gasification with and without char is developed and used to predict the gas composition as well as its associated calorific values. In addition, the effect of ultimate analysis on the fuel calorific value is studied. Results arising from this model are compared with the conducted experimental data as well as with data from others to ascertain their validity.

5.3 General empirical formula of wood chips

In order to establish the stoichiometric global equation for complete gasification of woodchips to be used for estimating the ER, it is important to determine the empirical formula for woodchips so that its general formula can be computed based on the average composition. The mole ratio formula, based on the ratio of C,H,O,S and N gives the workable formula for most biomass that can be used in writing conventional equations (Saravanakumar

et al., 2007). A typical composition of various wood chips is gathered from literature and a general equation can be established. From literature, the composition of Nitrogen and Sulphur in the woodchips is very small and was ignored in this calculation (Zainal et al, 2001);(Ahmed et al., 2011).A detailed empirical formula calculation is shown in Table 5.0

Table 5.0: Typical composition of spartanspruce as obtained during the experiment.

		Elemental analysis of wood chips				
	Rep	**C**	**H**	**O**	**N**	**Ash**
spartanspruce	1	46.62	6.42	46.42	0.52	0.02
	2	46.69	6.05	46.69	0.56	0.02
	3	46.81	6.34	46.43	0.41	0.02
Average		46.7±0.09	6.3±0.20	46.5±0.15	0.5±0.08	0.02±0

Thus the general formula of wood chips can be computed as follows.

$$Consider\ the\ equation\ of\ woodchips\ as\ CxHyOz\ where\ x, y, and\ z\ are\ subscripts.$$

$$Assume\ x = 1\ and\ by\ using\ the\ formula$$

$$y = \frac{mass\ fraction\ of\ Hydrogen \times Molecular\ weight\ of\ Carbon}{mass\ fraction\ of\ carbon\ \times Molecular\ weight\ of\ Hydrogen}$$

$$y = \frac{6.0 \times 12}{47\ \times 1} = 1.5$$

$$z = \frac{mass\ fraction\ of\ Oxygen \times Molecular\ weight\ of\ Carbon}{mass\ fraction\ of\ carbon\ \times Molecular\ weight\ of\ Oxygen}$$

$$z = \frac{46 \times 12}{47 \times 16} = 0.7$$

The general formula for wood chips is thus $CH_{1.5}O_{0.7}$

5.4Model development and choice of independent reactions

The following assumptions were used based on Balu& Chung(2012) and were the bases for solving the generated equations.

1. The gasification reactor is in the state of thermodynamic equilibrium.
2. The gasification process is completely adiabatic at equilibrium. In the energy equation there is no heat loss term assuming that the system is perfectly insulated and there is no parasitic influence on the system
3. Only C, H, O contents of the feedstock were chosen so other mineral contents were not considered because of their negligible amounts present.
4. The energy input provided for start-up of the combustion reaction is not accounted for in the steady state overall energy balance. Charcoal added during the start-up of the experiment is intended to get the combustion process going as well as to heat up the entire system from room temperature to the gasification temperature. As the gasification process reaches the steady state, part of the feedstock is consumed as the fuel in the combustion zone for a continuous gasification process.
5. That all the Cs (solid carbon) is converted to producer gas species and there is no solid carbon left after the gasification and the exit producer gas is composed only of H_2, CO, CO_2, H_2O, CH_4 and N_2. Other higher hydocarbons are neglected. The composition gases are modelled to exhibit ideal behaviour irrespective of the high operating temperatures in the gasifier.
6. The producer gas composition estimated is free of any O_2 from the supplied air since the amount of air supplied is constrained using the intake valve, making it a partial oxidation process and all the O_2 is consumed during the combustion reaction.

7. It is assumed that there is no soot formation and all the biomass is converted to the exit gas composition under a high temperature with no tar in the downdraft gasifier.
8. The pyrolysis product burns and achieves equilibrium in the reduction zone before exiting the gasifier.
9. The equilibrium model assumes that all the reactions are in thermodynamic equilibrium.
10. All the reagents enter the gasifier at the same temperature and pressure
11. The formation of tar was neglected in thermodynamic calculations because of its low concentrations especially in downdraft gasifiers. This puts a limitation to the use of this model for other gasifier designs such as the updraft gasifiers where tar is not cracked down and is part of the gasification products. The results of this model can thus not be used for such gasifiers.

The global equation for the air gasification of biomass in a downdraft gasifier can thus follow the equation below which considers the major elements present in biomass as C, H, O and omits the other elements such as N, S and traces of metal elements where x andy represent the numbers of atoms of H and O respectively. The composition of individual elements can be determined from the biomass ultimate analysis.

$$CH_{1.5}O_{0.7}+wH_2O +c(O_2+ 3.76N_2) = x_1CO+ x_2CO_2 +x_3CH_4+ x_4H_2 +x_5H_2O+x_6C+3.76cN_2 \quad (5.1)$$

where *x* and*y* are numbers of atoms of hydrogen and oxygen per one atom of carbon in the feedstock and *w* and*c* are the amounts of moisture, air per one kmol of feedstock, xi refers to the mole fraction of the respective gases respectively. By determining the ultimate analysis of the feedstock, values of subscripts x and y can be generated. The *w value* is determined using the moisture content (MC) in the feedstock computed as below

$$w = \frac{MW_{biomass} \times MC}{MW_{H2O} \times (1-MC)} \quad (5.2)$$

Where $MW_{biomass}$ is the relative molecular mass of the biomass feedstock, MW_{H2O} is the relative molecular weight of water and MC is the moisture content of the biomass feedstock. There are a total of 6 unknowns in Eq. (5)if there is no carbon (ie C=0) and the equilibrium calculations carried out with H_2, CO, CO_2, H_2O, and CH_4 as the exit producer gas components along with N_2.Whereas the downdraft gasifier consists of the four zones of drying for removal of moisture, pyrolysis of biomass into oil, char and volatiles, oxidation of the volatile products of pyrolysis and gasification of char from pyrolysis, this research considers only the reaction zone and is simulated by the thermodynamic equilibrium model. For the development of an equilibrium model approach, the number of independent reactions has to be determined by applying the phase rule, (Tassios, 1993). Only two independent reactions need to be considered for the equilibrium equations in the case where no solid carbon remains in the equilibrium state while three independent reactions have to be considered in the equilibrium calculations if some solid carbon remains. Although Schuster et al.,(2001) considered the water gas reaction along with the methane decomposition reaction,Zainal et al, (2001)selected one reaction resulting from the combination of the Boudouard equilibrium and heterogeneous water gas reaction and the hydrogenating gasification as the main gasification reactions but according to the thermodynamic theory of independent reaction selection (Tassios, 1993), there is no significant difference between the above reported modelling efforts. The only point that differentiates the equilibrium reactions is that the methane decomposition reaction is favored in the case of steam gasification (high feed moisture content) and not in the case of the conventional gasification process(Mountouris, Voutsas, & Tassios, 2006). Mountouris et al., (2006) further asserted that as far as the gasification temperature is concerned, the equilibrium is not achieved when

the gasification temperature is sufficiently below 800°C (common gasifiers). The following simplified chemical conversion formulas (Table 5.1) describe the basic gasification process(Schuster et al., 2001) above 800°C.

Table 5.1 Major reactions in the reduction zone at 800°C

Equation	**Nature of reaction**	**MJ/kg mole**	**Equation number**
$C + CO_2 \leftrightarrow 2CO$	Boudouard equilibrium (endothermic)	- 164.9	5.3
$C + H_2O \leftrightarrow CO + H_2$	Heterogeneous water gas shift reaction (endothermic)	-122.6	5.4
$C + 2H_2 \leftrightarrow CH_4$	Hydrogenating gasification (exothermic)	+ 75	5.5
$CH_4 + H_2O \leftrightarrow CO + 3H_2$	Methane decomposition (endothermic)	-205.9	5.6
$CO + H_2O \leftrightarrow CO_2 + H_2$	Water gas shift reaction (exothermic)	+ 42.3	5.7

Zainal et al, (2001) and Higman and van der Burgt, (2003) presented that Eqs. (5.3) and (5.4) can be combined to give the water–gas shift reaction (equation 5.7) by subtracting Eq. (5.3) from Eq. (5.4).Considering equilibrium to be achieved when no solid carbon remains, the equilibrium state is taken care by only two reactions called Water-gas shift and Hydrogenating gasification(Dutta et al., 2014)(Zainal et al., 2001). Thus, the two independent reactions with no carbon left after gasification are equation (5.5) and (5.7).

Hydrogenating gasification (exothermic) (R1) : $C + 2H_2 \leftrightarrow CH_4$ (5.5)

Water – Gas shift reaction (R2) : $CO + H_2O \leftrightarrow CO_2 + H_2$ (5.7)

If there is no carbon left after gasification, (ie C=0), there are a total of 6 unknowns in equation (5.1) and the equilibrium calculations were carried out with H_2, CO, CO_2, H_2O, and CH_4 as the exit syngas components along with N_2. For solving the 6 unknowns, 6 simultaneous equations were formed using the data available from the global equation and the 2 independent reactions. Using the C, H, O balance of the global equation (5.1) followed by the rate constant equation for the 2 independent chemical equations considered and finally

carrying out the energy balance for the whole system, the equations required for the numerical analysis are formulated.

Carbon Balance:

$$1 = x1 + x2 + x3 \tag{5.8}$$

Hydrogen Balance:

$$1.5 + 2w = 4x3 + 2x4 + 2x5 \tag{5.9}$$

Oxygen Balance:

$$0.7 + w + 2c = x1 + 2x2 + x5 \tag{5.10}$$

By considering the independent reactions which are a function of temperature, partial pressures (P) and the moles of the respective species (xi) and Po is the standard pressure (1atm). The equilibrium expressions then become

The equilibrium constant for hydrogenating gasification [K1],

$$K1 = \frac{\left[\frac{P_{CH4}}{P_O}\right]}{\left[\frac{P_{H2}}{P_O}\right]^2}$$

$$K1 = \frac{[x3]}{[x4]^2} \tag{5.11}$$

Similarly, the equilibrium constant for water gas shift reaction can be written as (K_2),

$$K2 = \frac{\left[\frac{P_{CO2}}{P_O}\right]\left[\frac{P_{H2}}{P_O}\right]}{\left[\frac{P_{CO}}{P_O}\right]\left[\frac{P_{H2O}}{P_O}\right]}$$

$$K2 = \frac{[x2][x4]}{[x1][x5]} \tag{5.12}$$

Where x_i the mole fraction of the compound i in the gas mixture, $x_i = \frac{n_i}{\sum_1^6 ni}$ (5.13)

But the relationship between the free energy of the reaction at any moment in time (ΔG) and the standard-state free energy of reaction (ΔG°) as defined by (Koroneos & Lykidou, 2011)is described by the following equation.

$$\Delta G = \Delta G^{\circ} + RTlnQ \quad (5.14)$$

where, *R* is the ideal gas constant in J/mol-K, *T* is the temperature in kelvin, *ln* represents a logarithm to the base *e*, and *Q* is the reaction quotient at that moment in time. When the reaction is at equilibrium, the driving force behind a chemical reaction is zero($\Delta G = 0$), hence deriving a general equation for establishing the equilibrium constant (K).

$$\Delta G^{\circ} = -RTlnK \; or \; K = e^{\frac{-\Delta G^{O}}{RT}} \quad (5.15)$$

This equation allows us to calculate the equilibrium constant for any reaction from the standard-state free energy of reaction, or vice versa. The detailed computation of the values for K1 and K2 is detailed in the appendix section A4 where equations 5.16- 5.31 follow and the finalized equations 5.25 and 5.31 for the generation of equilibrium constant are computed.

$$[\boldsymbol{lnK_1}] = \frac{\mathbf{7082.848}}{\boldsymbol{T}} - \mathbf{6.567}\boldsymbol{lnT} + \mathbf{3.733}\boldsymbol{x}\mathbf{10}^{-\mathbf{3}}\boldsymbol{T} - \mathbf{3.6067}\boldsymbol{x}\mathbf{10}^{-\mathbf{7}}\boldsymbol{T}^{\mathbf{2}} + \frac{\mathbf{35050}}{\boldsymbol{T}^{\mathbf{2}}} + \mathbf{32.52} \quad (5.25)$$

and

$$[\boldsymbol{lnK2}] = \frac{\mathbf{5870.06}}{\boldsymbol{T}} + \mathbf{1.86}\ \boldsymbol{lnT} - \mathbf{2.69}\boldsymbol{x}\mathbf{10}^{-\mathbf{4}}\boldsymbol{T} - \frac{\mathbf{58200}}{\boldsymbol{T}^{\mathbf{2}}} - \mathbf{18.0081} \quad (5.31)$$

Since the gasification process is assumed to be adiabatic (Zainal et al, 2001),(Koroneos& Lykidou, 2011), with no carbon formation (C=0), then the energy balance of the gasification reaction leads to a new set of equation, which can determine the final temperature of the system with the reference temperature as 298.15 K and pressure of 1 atm.

5.5Establishing the Energy Balance of the gasifier

After the system has attained a state of thermodynamic equilibrium, the gasification process is assumed to behave adiabatically. By considering the temperature in gasification zone as T and the temperature at inlet state as 298.15K (25 °C), the enthalpy balance for this process can be written as follows.

$$\sum_i n_i \left[{H^o}_{fi} + \Delta {H_{298.15}}^T\right]_{ireactants} = \sum_i m_i \left[{H^o}_{fi} + \Delta {H_{298.15}}^T\right]_{iproducts} \quad (5.34)$$

$$H^o{}_{fwoodc\ hips} + w\left(H^o{}_{fH2O(l)} + H_{vap}\right) + cH^o{}_{fO2} + 3.76cH^o{}_{fN2} + \Delta T'(cCp_{O2} + 3.76cCp_{N2}$$

$$=$$

$$x_1H^o{}_{fco} + x_2H^o{}_{fco2} + x_3H^o{}_{fCH4} + x_4H^o{}_{fH2} + x_5H^o{}_{fH2Ovap} + 3.76cH^o{}_{fN2} + \Delta T(x_1Cp_{co} +$$

$$x_2Cp_{co2} + x_3Cp_{CH4} + x_4Cp_{H2} + x_5Cp_{H20} + 3.76cCp_{N2})$$

Where

T_1 = temperature of the inlet,

T_2 = temperature of the reduction zone

T'_2 = air inlet temperature

${H^o}_{fi}$ is the enthalpy of formation in kJ/kmol and its value is zero for all chemical elements at reference state,

H_{vap} is the heat of vaporization of water,

$H^{o}{}_{fH2o(l)}$ is the heat of formation of water,

$\Delta T = T_2 - T_1$ and $\Delta T' = T'2 - T1$

$\Delta H_{298}{}^{T}$ represents the enthalpy difference between any given temperature state (T) and at reference state (298 K, 1 atm) (Jarungthammachote & Dutta, 2007).

H_f and h_f are the enthalpy of formation of biomass and species respectively in kJ/kmol.

C_p is the molar specific heat of species at constant pressure in kJ/kmol K and is a function of temperature. But since the enthalpy of formation for $H^{o}{}_{fH2}, H^{o}{}_{fN2}, H^{o}{}_{fO2}$ are zero at ambient temperature, the above equation (5.34) reduces to

$$H^{o}{}_{fwoodc\ hips} + w\left(H^{o}{}_{fH2o(l)} + H_{vap}\right)$$

$$= x_1 H^{o}{}_{fco} + x_2 H^{o}{}_{fco2} + x_3 H^{o}{}_{fCH4} + x_5 H^{o}{}_{fH2Ovap} + \Delta T(x_1 Cp_{co} + x_2 Cp_{co2} + x_3 Cp_{CH4} + x_4 Cp_{H2} + x_5 Cp_{H20} + 3.76 c Cp_{N2}) \quad (5.35)$$

$$H^{o}{}_{fwoodc\ hips} + w\left(H^{o}{}_{fH2O(l)} + H_{vap}\right) + cH^{o}{}_{fO2} + 3.76 cH^{o}{}_{fN2} + \Delta T'(cCp_{O2} + 3.76 c Cp_{N2}$$

$$= x_1 H^{o}{}_{fco} + x_2 H^{o}{}_{fco2} + x_3 H^{o}{}_{fCH4} + x_4 H^{o}{}_{fH2} + x_5 H^{o}{}_{fH2Ovap} + 3.76 cH^{o}{}_{fN2} + \Delta T(x_1 Cp_{co} + x_2 Cp_{co2} + x_3 Cp_{CH4} + x_4 Cp_{H2} + x_5 Cp_{H20} + 3.76 c Cp_{N2})$$

Thus

$$T_2 = T_1 + \frac{\left\{H^{o}{}_{fwoodc\ hips} + w\left(H^{o}{}_{fH2O(l)} + H_{vap}\right) + cH^{o}{}_{fO2} + 3.76 cH^{o}{}_{fN2} + \Delta T'(cCp_{O2} + 3.76 c Cp_{N2}\right\} - \left\{x_1 H^{o}{}_{fco} + x_2 H^{o}{}_{fco2} + x_3 H^{o}{}_{fCH4} + x_4 H^{o}{}_{fH2} + x_5 H^{o}{}_{fH2Ovap} + 3.76 cH^{o}{}_{fN2}\right\}}{\{x_1 Cp_{co} + x_2 Cp_{co2} + x_3 Cp_{CH4} + x_4 Cp_{H2} + x_5 Cp_{H20} + 3.76 c Cp_{N2}\}} \quad (5.36)$$

The procedure for the computation of the LHV of biomass and its heat of formation is detailed in appendix A5.De Souza-Santos (2004) proposed the relationship for finding the enthalpy of formation for solid fuel in reactant as

$$h_{f,fuel} = LHV + \sum_{k=prod}\left[n_k\left(h_f\right)_k\right] \quad (5.37)$$

The heat of formation of biomass is required, which is derived according to the formula by (Schuster et al., 2001).

$$h^f_{biomass} = ph^f_{CO_2} + qh^f_{H_2O} - (LHV + rh^f_{O_2}) \quad (5.38)$$

a, b, c are coefficients from combustion calculations

From the stoichiometric equation for complete combustion of woodchips ($CH_{1.5}O_{0.7}$), values of a, b and c can be got according to the equation below.

$$CH_{1.5}O_{0.7} + 1.025(O_2 + 3.76N_2) \rightarrow CO_2 + 0.75H_2O + 1.025(3.76N_2) \quad (5.39)$$

According to the above equation, r= 1.025, p= 1 and q= 0.75 and hence $h^f_{woodc\ hips}$ can be got

$$\text{as } h^f_{CO_2} = -\frac{393.5\text{kJ}}{\text{mol}}, h^f_{H_2O} = -\frac{241.82\text{kJ}}{\text{mol}}, h^f_{O_2} = \frac{0kJ}{mol}$$

$$h^f_{woodc\ hips} = -\frac{393.5\text{kJ}}{\text{mol}} - \frac{241.82\text{kJ}}{\text{mol}} - (\frac{470.041\text{KJ}}{\text{mol}} + \frac{0kJ}{mol}$$

$$h^f_{woodc\ hips} = -810{,}238.6\text{kJ/mol}$$

Subsequently, the specific heat of various substances was computed based on the formula

$$\Delta h_T = \int_{298}^{T} Cp\,(T)dT \qquad (5.40)$$

Cp can be defined by the empirical equation below

$$Cp(T) = a + bT + cT^2 + dT^3 \qquad (5.41)$$

where T is the temperature in Kelvin, K and

$$\int_{298}^{T} Cp\,(T)dT = aT + \frac{b}{2}T^2 + \frac{c}{3}T^3 + \frac{d}{4}T^4 + k \qquad (5.42)$$

where κ is a constant of integration and a, b, c, and d are the specific gas species coefficients, which are shown in Table 5.2 below

Table 5.2.The Coefficients of specific heat for the empirical equation (Cengel, 2002)

Gas species	***a***	***b***	***c***	***d***	**Temperature range (K)**
Hydrogen	29.11	-0.1916×10^{-2}	0.4003×10^{-5}	-0.8704×10^{-9}	273–1800
Carbon monoxide	28.16	0.1675×10^{-2}	0.5372×10^{-5}	-2.222×10^{-9}	273–1800
Carbon dioxide	22.26	5.981×10^{-2}	-3.501×10^{-5}	-7.469×10^{-9}	273–1800
Water vapour	32.24	0.1923×10^{-2}	1.055×10^{-5}	-3.595×10^{-9}	273–1800
Methane	19.89	5.204×10^{-2}	1.269×10^{-5}	-11.01×10^{-9}	273–1500
Nitrogen	28.90	-0.1571×10^{-2}	0.8081×10^{-5}	-2.873×10^{-9}	273–1800

Detailed results are summarized in appendix B2 and a summary of results shown in Table 5.3 below.

5.6Calculation procedure for determination of producer gas composition from modeling

To establish the actual values of producer gas composition, values of w and c are specified. The major equations (a combination of linear and non linear), equations, 5.8, 5.9, 5.10, 5.11, 5.12, 5.25, 5.31 and 5.35 with unknowns (x_1-x_5, k1 and K2 and gasification temperature T_2, weresolvedwithMatLab software (R2016a) using Fsolver, trust region reflective algorithm. To complete this computation, an initial gasification temperature (T_2) and gas composition (x_1-x_5) was assumed and used to calculate the equilibrium constants K_1 &K_2 using generic equations derived from major equations from the gasification processand new values of $x_1, x_2, x_3, x_4, x_5$of gas composition and gasification temperature $T_2$are obtained with convergenceafter iterations with the solver. Detailed results that show convergence with iterations and the Matlab script are shown in the Appendix section with a summary of results here below.

5.7 Results from Modelling work.

5.7.1 Modelling variation of producer gas composition with moisture content

The equilibrium model described above is used to predict the composition of producer gas at varying operating conditions. It can be observed from Figure 5.1 below that as the moisture content was varied from 5% to 50 %, the composition of major gases varied accordingly. Carbon monoxide decreased from 29.33% to 3.59 % at ER of 0.24. This pattern for the decrease in the composition of CO was the same for all other ER between 0.24 – 0.45.However, the composition of Hydrogen increases 25.45% to 25.93% as moisture content changes from 5% to 20% but then drops from 25.15% to 17.4% as the moisture content

increases from 30% to 50%. This trend in the increase and decrease of Hydrogen content with increase in moisture content at increasing ER is maintained as shown in Table 5.3. Methane was significantly low for the entire range of moisture content (5% to 50%) and decreased with increasing ER. Subsequently, the composition of water vapor increased from 5.23 % to 30.9 % as moisture content increased from 5% to 50%. Such a trend in the variation of gas composition with increase in moisture is expected as justified in equations 4.1 – 4.3.The increase in the composition of H_2, $CH_4$and CO_2 with increase in moisture content arises due to steam gasification reactions that take place in the reduction zone as the moisture content increases.(Atnaw, Sulaiman, & Yusup, 2014). A similar trend in the variation of producer gas with moisture content has been observed by other researchers. Li-ping et al., (2010) similarly concluded that the contents of CO_2, CH_4, and H_2 in gas, lower heating value (LHV) of gas and aqueous yield increased with increase in moisture content, while content of CO and tar yield decreased. It should be noted that, the gasifier was assumed to be completely adiabatic as part of the modelling work, therefore, to sustain the high temperatures, more air need to be supplied to maintain the higher gasification temperatures otherwise the gasification temperatures would in practice drop as the moisture content of the feed increases without increasing the air flow rate.

5.7.2Modelling variation of moisture content with gasification temperature

Temperature is one of the major factors determining the composition and quality of producer gas. For autothermal gasifiers, the gasification temperature is dependent on the operating ER of the gasifier. As part of modelling, the ER was maintained constant as the moisture content was varied. It can be shown in Figure 5.2, that as moisture content increased from 5% to 50%, the gasification temperature dropped from 812.85ºC to592.5ºC at ER= 0.24,

from1006.4ºC–649.2ºC at ER= 0.3, 1165.9ºC - 702.4ºC at ER=0.35 , 1450.6ºC - 844.9ºC at ER =0.45.For all the ER (0.24-0.45), the temperature of the gasifier decreased as the moisture content increased as part of the heat is lost during evaporation as moisture content continues to increase. For drier biomass, lesser heat is lost during evaporation as the amount of water vapor present is less. For autothermal gasifiers, a drop in gasification temperature due to moisture content would imply supplying more air to increase the exothermicity of the reactions and raise the gasification temperature to sustain the state of thermodynamic equilibrium otherwise the gasification temperatures drop significantly as moisture contents in the biomass increase. Consequently, the temperature of the gasifier increases as the operating equivalence ratio of the gasifier increases at varying moisture content levels. This increase in temperature with ER is due to the supplier of more air which increases the extent of exothermicity for the reactions.

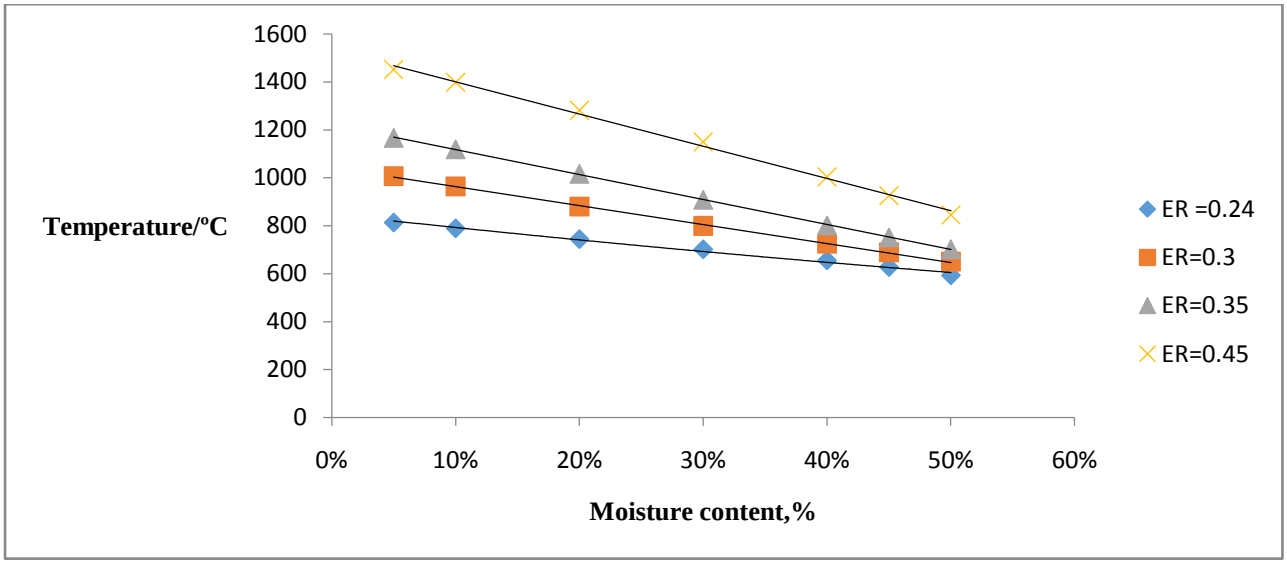

Figure 5.1 Variation of moisture content with gasification temperature at varying ER

5.7.3 Validation of the model

To further validate the model, the obtained results from the equilibrium model are compared with the experimental works done as part of this research, as well as compared with other models that were previously developed by other researchers. The results arising are summarized in the Table 5.3 below. The biomass used in this study is spartan spruce of composition 46.7%, 6.3%, 46.5%, 0.48% and 0.02 % for C, H, O, N and ash respectively. It should be noted that, the results out of the model are influenced by the composition and nature of the biomass used as well as influenced by the amount of air and moisture content during gasification. Models worked out under conditions that are of close range are expected to relate if the differences in operating conditions are not significantly large.

A comparison of modelling results for the effect of moisture content with experimental results reveals that, as the experimental moisture content was varied from 6.4±2.4%, 13.73± 0.6% and 17.5±0.3% respectively, it was observed that the overall composition of the major components of producer gas of CO, H_2, and CH_4varied significantly with increase in moisture content. The individual composition of gases such as CO decreased from 25.3±0.48% at 6.4±2.4%, to 21.3±1.06% at 13.73% and to 19.4±0.11% at 17.5±0.3%. The decrease of CO is justified by the decrease in gasification temperatures as moisture content increases. Generally, higher CO formation are favored by increase in temperature (Lahijani & Zainal, 2011) and any drop in the gasification temperature such as that observed during increase in moisture content for both experimental and modelling results would decrease the composition

of CO. Thus, the CO composition and variation trend is in the order of the same magnitude for both experimental and modelling results.

Subsequently, the composition of H_2 decreased from 18.1± 1.19 % (at 6.4±2.4 %,) to 17.562±1.26% at13.73% and increased to 19.9±0.60% at 17.5±0.3%. A similar observation is made in the composition of hydrogen content from modelling as it initially increases with increase in moisture content but then decreases with increase in moisture content as detailed in Table 5.3. CH_4 decreased from 2.2±0.05 % at 6.4±2.4% to 1.9±0.47% at 13.73% and increased to 2.4± 0.18 % (at 17.5±0.3%. The composition of CO_2 increased with increase in moisture content from 2.4±0.20 at 6.4±2.4%to 3.7±0.55% at 13.73% and 10.9±5.31% (at 17.5±0.3%. Similarly, Carbondioxide from modelling increased with increase in moisture content for all sets of ER. For experiments done with nearly the same moisture content (10% with modelling and 6.4±2.4% with experiment and ER of 0.27, a comparison of results reveals that, the composition of CO is 25.99% for modelling while its 25.3±0.48% from experiment, which leaves a deviation of 2.6% between results. This minor deviation shows a great deal of relationship between results. By comparing this with the results from other researchers, this composition relates well with the experimental results from Zainal et al., (2001). The deviations of the modeled results from other researchers, such as the CO composition of 18.3 % (Jayah et al., 2003), may be due to the difference in the air to fuel ratio as well as the working moisture contents.

Generally, there is a close match between the results from the modelling study with the experimental works done as part of this research as well as a close correlation with other

researchers, for results obtained at nearly similar operating conditions as summarized in Table 5.3 below.

An operating equivalence ratio of 0.27 and moisture content of 10% was used to provide a baseline comparison between the modelling and experimental results.The thermodynamic equilibrium model yielded a gas composition of 25.99%, 23.92%, and 0.42% for CO, H_2 and CH_4 respectively that was in good agreement with the experimental results at 850 ºC and ER of 0.27. Similarly, the modeled gasification temperature of 870.85ºC corresponds with a minor deviation of 2.5% with the experimental gasification temperature of 850ºC. The agreement between experimental and modelling results reveals that the thermodynamic equilibrium model can be used to predict the composition of producer gas from downdraft gasifiers.Thus, the composition and variation trend of all major gases from both experiment and modelling is in the order of the same magnitude.

Table 5.3 Modelling Producer gas composition at varying moisture content

	Modelling results from this research							Experimental work from this research	Modelling results for Zainal et al (2001)	Modelling results from Jayah et al (2003)
MC	5%	10%	20%	30%	40%	45%	50%	**6.4±2.4**	20%	14.7%
ER	0.24	0.24	0.24	0.24	0.24	0.24	0.24	**0.27±0.01**		0.38
VOL %										
CO	29.33	26.75	21.19	15.17	9.03	6.14	3.59	**25.3±0.48**	19.61	18.30
CO_2	6.39	7.87	10.99	14.14	16.84	17.74	18.09	**2.4±0.20**	12.01	11.10
CH_4	0.72	0.95	1.58	2.51	3.80	4.60	5.51	**2.2±0.05**	0.64	1.1
H_2	25.45	25.75	25.93	25.15	22.74	20.54	17.40	**18.1±1.19**	21.06	16.4
H_2O	5.23	6.57	9.83	14.30	20.83	25.29	30.89	**50.0**	46.7	53.2
N_2	32.88	32.10	30.47	28.72	26.77	25.70	24.52			
										na
TG/ºC	812.9	788.9	743.8	701.2	654.9	627	592.5	**850**	800	
MC	5%	**10%**	20%	30%	40%	45%	50%			
ER	0.27	**0.27**	0.27	0.27	0.27	0.27	0.27			
VOL %										
CO	28.21	**25.99**	21.09	15.61	9.78	6.92	4.30			
CO_2	6.22	**7.46**	10.17	13.06	15.73	16.74	17.30			
CH_4	0.30	**0.42**	0.82	1.53	2.65	3.39	4.26			
H_2	23.49	**23.92**	24.49	24.25	22.49	20.71	18.04			

H_2O	6.54	**7.83**	10.85	14.89	20.76	24.78	29.86			
N_2	35.25	**34.38**	32.57	30.66	28.59	27.46	26.25			
TG/ºC	905.7	**871**	805.1	745.2	687.5	656.3	620.4			
MC	5%	10%	20%	30%	40%	45%	50%			
ER	0.3	0.3	0.3	0.3	0.3	0.3	0.3			
VOL %										
CO	27.00	25.10	20.82	15.88	10.41	7.63	4.99			
CO_2	6.21	7.20	9.52	12.12	14.71	15.79	16.52			
CH_4	0.09	0.17	0.38	0.85	1.74	2.39	3.196			
H_2	21.26	21.71	22.59	22.92	21.92	20.56	18.36			
H_2O	7.87	9.18	12.05	15.70	20.92	24.53	29.09			
N_2	37.57	36.63	34.65	32.54	30.3	29.11	27.84			
TG/ºC	1006.4	963.4	879	798.5	724.6	688.4	649.4			
MC	5%	10%	20%	30%	40%	45%	50%			
ER	0.35	0.35	0.35	0.35	0.35	0.35	0.35			
VOL %										
CO	24.98	23.42	19.95	15.89	11.15	8.58	5.99			
CO_2	6.28	7.07	8.84	10.91	13.23	14.34	15.24			
CH_4	0.03	0.05	0.10	0.27	0.73	1.17	1.79			
H_2	17.53	17.99	18.99	19.93	20.15	19.57	18.22			
H_2O	9.99	11.28	14.09	17.37	21.69	24.64	28.44			
N_2	41.18	40.19	38.02	35.63	33.05	31.70	30.31			

TG/ºC	1165.9	1118.3	1016.2	908	801.6	751.5	702.5			
MC	5%	10%	20%	30%	40%	45%	50%			
ER	0.45	0.45	0.45	0.45	0.45	0.45	0.45			
VOL %										
CO	20.975	19.87	17.42	14.59	11.25	9.34	7.26			
CO_2	7.0056	7.50	8.58	9.85	11.34	12.19	13.05			
CH_4	0.0046	0.006	0.012	0.03	0.09	0.17	0.35			
H_2	11.543	11.93	12.78	13.74	14.77	15.20	15.37			
H_2O	13.1207	14.38	17.18	20.40	24.17	26.38	29.01			
N_2	47.351	46.31	44.02	41.40	38.38	36.72	34.96			
TG/ºC	1450.6	1397.3	1280.6	1149.5	1003	924.6	845			

na; not available

5.7.4 Modelling the variation of producer gas composition with equivalence ratio

Equivalence ratio is one key factor that determines the quality of producer gas and its composition. It subsequently determines the extent of gasification temperature for autothermal gasifiers. As the moisture content was maintained constant at 10%, and the ER varied from 0.24 – 0.45, the composition of CO decreased from26.75% to 19.87%, Hydrogen decreased from 25.75% to 11.93 %, while methane decreased from 0.95% to 0.006%. Carbondioxide decreased from 7.87% to 7.07% between ER of 0.24 -0.35 and then increased to 7.50% as ER increased to 0.45. The increase in CO_2 is due to increased temperature which increases the rate of oxidation of carbon. Increase in ER corresponds with supply of more air which leads to the increased oxidation of carbon hence more Carbondioxide in the mixture and subsequently the increase in the gasification temperature as the ER increases.

Table 5.5 Modelling producer gas composition at varying equivalence ratio

MC	**10%**	**10%**	**10%**	**10%**	**10%**
ER	0.24	0.27	**0.3**	**0.35**	0.45
VOL %					
CO	26.75	25.99	25.10	23.42	19.87
CO_2	7.87	7.46	7.20	7.07	7.50
CH_4	0.95	0.42	0.17	0.05	0.01
H_2	25.75	23.92	21.71	18.00	11.93
H_2O	6.57	7.83	9.18	11.28	14.38
N_2	32.10	34.38	36.63	40.19	46.31
TG/ºC	788.9	871	963.4	1118.3	1397.3

Chapter 6

6.0 CONCLUSIONS AND RECOMMENDATIONS

6.1 Conclusions

As part of the review of this thesis, this work discussed the process of biomass power generation from the start of the gasification process (cradle) till the end of energy recovery (grave) which provide an understanding on the suitability and application of this technology to satisfy the end user requirement. Most theories in literature report findings on the laboratory scale with less data on pilot energy systems thus experimental findings arising from this research cleared the doubts on the possibility of gasification to provide alternative renewable energy and provide a basis as promising bioenergy systems and assist to provide sustainable energy solutions on a practical basis especially for the rural communities.

Biomass gasification is one promising avenue for clean energy production that combats the effects of global warming and subsequently climate change. Gasification temperature, ER, fuel moisture content, have been found to have significant effects on the quality of produced producer gas while ER determines the gasification temperature for autothermal gasifiers.

The gasifier stably and optimally operates with woodchips of moisture content less than 10% to produce an energy rich gas for gasification times longer than six hours to yield a gas rich in Hydrogen (H_2), Carbon monoxide (CO) and methane (CH_4) at a respective concentration of upto 18.1±1.19%, 25.3±0.48% and 2.2±0.05% with a corresponding Higher Heating Value (HHV), Cold Gas Efficiency (CGE) and gas production rate of 6.4±0.19MJ/m^3, 75.8±11.16%

and 2.34±0.29m^3/kg respectively. The reactor takes longer time to attain thermodynamic equilibrium once operated with woodchips of moisture content above 15%. This subsequently affects the quality of producer gas yielding a gas of low calorific value with a less combustion efficiency. The moisture content of the wood chips was found to play a very significant role in determining the values of temperatures attained and subsequently determining the quality of producer gas produced. The gasifier was found to produce the required energy with a possibility of generation upto the design capacity required for very many industrial applications. Increasing the engine throttle valve increased the frequency of the engine and subsequently the voltage.

Increase in moisture content decreased the gasification temperature and also decreased the composition of CO in the mixture but increased the composition of hydrogen. The thermodynamic equilibrium model yielded a gas composition of 25.99%, 23.92%, and 0.42% for CO, H_2 and CH_4 respectively that was in good agreement with the experimental results at 850 ºC and ER of 0.27. Similarly, the modeled gasification temperature of 870.85ºC corresponds with a minor deviation of 2.5% with the experimental gasification temperature of 850ºC.

The exhaust stream composition contained Carbondioxide (CO_2) of upto 20% which is on the higher side if the gasifier is to be adopted as a sustainable renewable energy system. Higher values of CO_2 were due to the complete oxidation of hydrocarbons during engine performance. The gasifier was found to operate better with wood chips in the size range between 1.3cm – 4.0cm as very fine wood chips would block the flow of air hence compromising on the sustainability of the exothermic reactions and bigger wood chip

particles would not be easily broken down by the auger hence resisting the flow of the woodchips into the reactor. Operating the gasifier at optimal conditions yields a gas of high calorific value good enough to make it a reliable standalone that could be integrated into sustainable bioenergy systems. The maximum possible attained power from the gasifier was 7.58KW produced at 52 Hz. The recommended frequency of 60Hz to reflect a power output of 10KWe could not be achieved under real practical operating conditions as the gasifier was seen to shut off whenever frequency exceeded 52Hz and made a very loud noise at higher frequency settings which most likely could not pass the recommended maximum in house pitch. Increasing a connection load to the genset decreased the maximum possible power output while increasing the frequency to generate more power works within a maximum threshold of 52 Hz and makes too much noise which could affect the eardrum. However, based on Figure 4.19, the relationship between power generated against frequency was achieved and according to the equation of the line, (Y=0.3201X-9.0205), a substitution of the recommended maximum frequency of 60Hz corresponds to a maximum 10KWe which is said to be the maximum attainable power from the gasifier but according the findings from this experimental set up, this only appears to be in theory.

6.2 Limitations and Future research needs

i. While operating the gasifier at higher frequency, the gasifier produces a louder noise that requires to be lowered down to conform to the regulatory safety noise requirements. Further research is needed to reflect the change in sound pitch with frequency in terms of decibels to confirm if operating the gasifier at higher frequencies passes the in-house pitch as per occupational standards.

ii. The gasifier should be operated with drier woodchips to enable a quick start of the gasification reactions which would subsequently assist in the quicker attainment of thermodynamic equilibrium to produce a clean gas that would contain the required energy used to run the engine and produce the necessary energy.

iii. There is also a need to test and optimize the performance of different small scale bioenergy systems on different biomass feedstocks and match their performance with the needs of the end user.

iv. There is a need to develop a mechanical loading system to replace the manual loading mechanism which is labor intensive and compromises safety standards

v. There is need to develop a centralized control panel to increase on the system automation so that the system can be run by less operators. The current system arrangement demands that atleast two or more operators need to be present if a successful run must be completed

vi. There is need to build and integrate a sieving mechanism to the gasifier to reduce on the much time spent when sieving non uniform solid biomass samples, as well as eliminate any dust which would create resistance to the flow of incoming air.

vii. There is need to build and integrate a crusher to the gasifier to increase its acceptation tolerance and ease the feeding sysem. This will reduce on the much challenges of auger failure due to bigger particles, increase the gasification efficiency due to

uniformity of the fed crushed biomass as well as reduce on the operation time of running the gasifier

viii. There is still a need to understand the economics involved per unit cost of energy producedin comparison with other alternative energy options to strongly come up with informed economic decisions

ix. The gasifier in its present form can not be used as a bioenergy –biochar system because of the insignificant amounts of biochar produced and further modifications deserve to be made if biochar could be produced alongside energy generation

x. It is important to rebuild the hopper in a more transparent form to monitor the flow of the feedstock during the process of gasification

xi. The gasifier needs to be configured with wheels to ease its mobility from place to place

xii. The gasifier deserves to be rebuilt with a stepping ladder to ease its process of fuel feeding and loading

xiii. The heat that escapes in the exhaust can be recovered and further converted into electricity using thermo electric generators

xiv. There is need to integrate the airal gasification with compressed steam to increase on the fuel energy density and the overall gasification performance

xv. There is a need to build an enclosed jacked around the engine, to reduce on the inhouse noise arising from the gasifier

6.3 Main contributions of this research

i. This research provides a technical analysis on the possibility of power generation from wood.

ii. The biomass gasification was successful (with CGE, ~ 70% but the efficiency significantly decreased with conversion to electricity (eff~20%) due to low thermal efficiency of the SIE and low HHV of the gas

iii. The findings and recommendations if implemented increase on the competitiveness of the power pallet as well as making the rig more applicable to many parts of the World which have no access to power

iv. Notwithstanding, this is a promising technology of harnessing power for places which are not grid connected.

7. Appendix

Appendix A1: Biomass samples used

Figure A1.1 Woodchips before sieving

Appendix A2: Calculations

A2.1 Bulk density calculation

	R1	R2	R3
Wo	212.83	212.83	212.83
W1	636.3	535.8	458.5
V(ml)	2000	1400	1000
g/cm^3	0.211735	0.230693	0.24567
kg/m^3	211.735	230.6929	245.67
Average bulk density (kg/m^3)	229±10.6		

	Determination of biochar bulk density		
	Trial 1	Trial 2	Trial 3
W2/g	569.21	556.79	576.4
W1/g	410.9	410.9	410.9
W2-W1/g	158.31	145.89	165.5
Volume of cylinder (cc)	750	750	750
Density of biochar g/cc	0.21108	0.19452	0.220667
Average density kg/m^3	208.76±13.227		

Biochar collection				
	run10	run11	run12	run13
W1/g	23.5	120.4	391.4	139.8
W2/g	361.3	376	596.44	408
(W2-W1)/kg	0.3378	0.2556	0.20504	0.2682
Gasification time (GT)/hrs	7.75	6.916	6.083	6.5
Rate of char formation(kg/hr)	0.044	0.037	0.034	0.041
Average(kg/hr)	0.039 ±0.004			

A2.2 Analysis of the moisture content

From the moisture content analsysis of woodchips, the wood chips used for gasification had an average moiture content of 14% ±4.58%. This moisture content fits well in the tolerance level of the gasifier (Moisture content of < 30%).

Sample moisture content analysis of wood chips

Sample number	1	2	3	4	5	6	7	8	9	10	Average
Moisture %	15	14	20	11	14	18	18	8	16	8	14.20±4.13

A2.3 Calculation of the heating value of the biomass fuel

From the ultimate analysis of woodchips, the heating value of the fuel can be determined as

	C	H	O	N	S
Ultimate analysis %	48.7	6.0	42.1	0.0	0.0
$LHV_{woodchips(MJ/Kg)} = 34.835x_C + 93.870x_H - 10.800x_O + 0.628x_N + 10.465x_S$	19.9980				
$HHV_{biomass\ (MJ/Kg)} = LHV + 21.978H$	21.3167				

Appendix A3

Table A-3-1 Temperature distribution of the gasifier on a 2 KW electrical load

	2KW					
Time/min	Tt 1-2	Tt2-2	Tt3-2	Tb1-2	Tb2-2	Tb3-2
5	880	944	880	788	767	741
10	892	911	880	789	768	752
15	870	916	901	785	766	761
20	873	908	901	785	767	760
25	886	908	898	783	766	763
30	879	903	889	783	765	761
35	860	907	899	782	760	760
40	866	915	883	780	758	763
45	855	921	904	778	758	763
50	865	923	895	779	758	761
55	860	924	905	783	755	759
60	860	932	926	789	758	761

Table A-3-2 Temperature distribution of the gasifier on a 4 KW electrical load

Time	Tt1	Tt2	Tt3	Tb1	Tb2	Tb3
5	889	895	886	760	789	763
10	885	928	905	819	805	764
15	870	932	898	830	805	767
20	886	885	883	827	803	769
25	857	904	888	830	803	773
30	907	914	878	839	805	774
35	890	916	869	836	813	775
40	916	910	864	836	815	775
45	909	904	870	835	816	771
50	902	909	879	832	817	770
55	880	935	866	823	804	770
60	903	907	871	822	798	768

Table A.3-3 Temperature distribution of the gasifier on a 10 KW electrical load

Time/min	Tt2-10	Tt3-10	Tb2-10	Tb3-10
5	877	877	745	734
10	882	836	764	742
15	861	879	747	722
20	871	903	747	717
25	923	914	761	727
30	895	920	763	746
35	944	922	758	742
40	885	924	751	747
45	902	942	752	739
50	874	949	740	746
55	880	940	736	716
60	896	924	740	723

Table A2 Temperature distribution of the gasifier on a 4 KW electrical load for 2hr

Time	Tt1	Tt2	Tt3	Tb1	Tb2	Tb3
10	880	880	944	767	694	788
20	894	892	911	768	698	789
30	901	870	916	766	705	785
40	901	873	908	767	708	785
50	898	886	908	767	711	783
60	889	879	903	766	714	783
70	889	860	907	765	714	782
80	883	866	915	760	713	780
90	904	855	921	758	711	778
100	895	865	923	758	710	779
110	905	860	924	758	711	783
120	926	860	932	755	714	789

Table A3 Temperature distribution of the gasifier on a 4 KW electrical load for 6 hrs

Time/min	Tt1	Tb1
30	792	721
60	846	729
90	851	734
120	849	742
150	865	741
180	860	729
210	870	721
240	885	726
270	882	735
300	878	734
330	875	730
360	875	732

Table A4 Incoming air velocity profile distribution of the gasifier at varying electrical loads

Time/min	V4kw	V2kw	V2kw
5	0.7	0.8	0.8
10	0.7	0.9	0.8
15	0.7	0.9	0.8
20	0.7	0.9	0.8
25	0.7	0.9	0.8
30	0.6	0.8	0.9
35	0.6	1.1	0.8
40	0.6	1.1	0.8
45	0.6	1.0	0.8
50	0.6	0.9	0.8
55	0.6	0.8	0.8
60	0.6	0.8	0.8

Table A.5.1 Sample ER computation for run 1

Time/min	Interval/S	Velocity m/s	Temp air /°C	Density, D(Kg/m^3)	Q (m^3/s)=UA	Mass flow [kg]= Qxdensityxtime
30	1800	0.8	22.4	1.1777	0.002065	4.377358
60	1800	0.8	26.2	1.1777	0.002065	4.377358
90	1800	0.9	27.8	1.1777	0.002323	4.924528
120	1800	0.8	30.8	1.1777	0.002065	4.377358
Average Temperature (TºC)			26.8			
Sum of air (Kg)						18.0566
Volume of air (m^3)				0.119		
A/F(m^3/kg) at ER = 1				4.84		
ER		0.27				

Table A.5.2 Sample ER computation for run 3

Time/min	Interval/S	Velocity m/s	Temp air /C	Density, D(Kg/m^3)	Q (m^3/s)=UA	Mass flow [kg]= Qxdensityxtime
30	1800	0.8	22.4	1.1777	0.002065	4.377358
60	1800	0.8	26.2	1.1777	0.002065	4.377358
90	1800	0.8	27.8	1.1777	0.002065	4.377358
120	1800	0.8	30.8	1.1777	0.002065	4.377358
Average Temperature (TºC)			26.8			
Sum of air (Kg)						17.50943
Volume of air (m^3)				0.119		
A/F(m^3/kg) at ER = 1				4.84		
ER		0.26				

Table A.5.3 Sample ER computation for run 8

Time/min	Interval/S	Velocity m/s	Temp air /C	Density, D(Kg/m^3)	Q (m^3/s)=UA	Mass flow [kg]= Qxdensityxtime
30	1800	0.8	28.2	1.1726	0.002065	4.358402
60	1800	0.7	27.8	1.1726	0.001807	3.813602
90	1800	0.7	27.9	1.1726	0.001807	3.813602
120	1800	0.7	29.7	1.1726	0.001807	3.813602
150	1800	0.6	29.1	1.1726	0.001549	3.268802
180	1800	0.6	29.1	1.1726	0.001549	3.268802
210	1800	0.6	28.6	1.1726	0.001549	3.268802
240	1800	0.6	26.7	1.1726	0.001549	3.268802
270	1800	0.6	27.2	1.1726	0.001549	3.268802
300	1800	0.6	26.8	1.1726	0.001549	3.268802
330	1800	0.6	27.2	1.1726	0.001549	3.268802
360	1800	0.6	27	1.1726	0.001549	3.268802
375	900	0.6	27	1.1726	0.001549	1.634401
Average Temperature (TºC)			27.94167			
Sum of air (Kg)						43.58402
Volume of air (m^3)				0.12		
A/F(m^3/kg) at ER = 1				4.86		
ER		0.227				

Table A.5.4 Variation of velocity with connection load

Time/min	V2kw	V2kw	V4kw	V4KW	V10KW	V10KWe
5	0.9	0.8	0.8	0.8	0.7	0.7
10	0.9	0.9	0.7	0.9	0.7	0.6
15	0.9	0.9	0.7	0.8	0.6	0.6
20	0.9	0.9	0.7	0.8	0.6	0.6
25	0.9	0.9	0.7	0.7	0.6	0.6
30	0.9	0.8	0.7	0.6	0.6	0.6
35	0.9	0.9	0.7	0.6	0.6	0.6
40	0.9	0.9	0.7	0.6	0.6	0.6
45	0.9	0.9	0.7	0.6	0.6	0.6
50	0.9	0.9	0.7	0.6	0.6	0.6
55	0.8	0.8	0.7	0.6	0.6	0.6
60	0.8	0.8	0.7	0.6	0.5	0.6

Table A.5.5 Sample ER computation for run 9

Time/min	Interval/S	Velocity m/s	Temp air /C	Density, D (Kg/m^3)	Q (m^3/s) =UA	Mass flow [kg]= Qxdensityxtime
30	1800	1.2	28.9	1.1704	0.003097	6.525338
60	1800	1.1	26.2	1.1704	0.002839	5.98156
90	1800	1	25.8	1.1704	0.002581	5.437781
120	1800	0.7	31	1.1704	0.001807	3.806447
150	1800	0.7	29.1	1.1704	0.001807	3.806447
180	1800	0.7	29.7	1.1704	0.001807	3.806447
210	1800	0.7	28.4	1.1704	0.001807	3.806447
240	1800	0.7	27.9	1.1704	0.001807	3.806447
270	1800	0.7	28	1.1704	0.001807	3.806447
300	1800	0.7	27.7	1.1704	0.001807	3.806447
330	1800	0.7	29	1.1704	0.001807	3.806447
360	1800	0.7	29.9	1.1704	0.001807	3.806447
Average Temperature (TºC)			28.46667			
Sum of air (Kg)						52.2027
Volume of air (m^3)				0.120226		
A/F(m^3/kg) at ER = 1				4.87		
ER		0.27				

Table A6 Producer gas composition against various electrical loads

Average gas composition (% v/v)	**CO**	**CO_2**	**CH_4**	**H_2**	**O_2**	**LHV(kCal/m^3)**
Run 1 (2KWe load)	22.48±1.99	3.06±0.95	1.34±0.26	18.60±0.86	0.37± 0.13	5.36±0.14
Run 2 (2KWe load)	20.47±1.60	1.75±0.63	1.98± 0.35	16.16±0.97	0.69± 0.14	5.04±0.14
Run 3 (2KWe load)	20.89±1.14	4.15±0.46	2.26±0.24	17.92±0.51	2.44±0.25	5.40± 0.14
Run 4 (no load)	21.28±1.48	1.18±0.45	1.16±0.19	17.70±0.59	0.15±0.14	5.04±0.17
Run 5 (4KWe load)	21.24±1.30	10.73±1.12	2.27±0.25	17.42±0.40	2.17±0.13	5.38±0.16
Run 6 (4KWe load)	21.18±1.34	10.33±2.03	2.25±0.25	17.45±0.40	2.20±0.18	5.36±0.17
Run 7 (4KW) for 6 hrs	19.55±1.56	14.00±1.09	2.52±0.25	19.52±0.41	1.36±0.11	5.48±0.20

Table A7- Variation of moisture content with temperature at the top of the reduction zone

Time/ Min	T_tred1-6.4	T_tred2-6.4	Average T_tred_LMC	SD	T_tred1-13	T_tred2-13	Average_13	SD	T_tred1-17	T_tred2-17	Average _HMC	SD
10	930	934	932	2.82	851	846	848.5	3.53	786	816	801	21.21
20	928	911	919.5	12.02	851	845	848	4.24	788	815	801.5	19.09
30	932	916	924	11.31	849	845	847	2.82	788	815	801.5	19.0
40	885	908	896.5	16.26	852	845	848.5	4.94	788	816	802	19.79
50	904	908	906	2.82	852	845	848.5	4.94	789	816	802.5	19.09
60	914	903	908.5	7.77	851	845	848	4.24	790	816	803	18.38
70	916	907	911.5	6.36	853	844	848.5	6.36	790	816	803	18.38
80	910	915	912.5	3.53	852	844	848	5.65	791	817	804	18.38
90	904	921	912.5	12.02	853	845	849	5.65	791	817	804	18.38
100	909	923	916	9.89	854	845	849.5	6.36	791	817	804	18.38
110	935	924	929.5	7.77	854	844	849	7.07	792	817	804.5	17.67
120	907	932	919.5	17.67	853	845	849	5.65	792	817	804.5	17.67
130	908	945	926.5	26.16	855	844	849.5	7.77	794	817	805.5	16.26
140	908	944	926	25.45	855	844	849.5	7.77	795	819	807	16.97
150	903	945	924	29.69	854	844	849	7.07	794	817	805.5	16.26
160	907	946	926.5	27.57	855	842	848.5	9.19	795	817	806	15.55
170	915	944	929.5	20.50	857	842	849.5	10.60	796	819	807.5	16.26

180	921	944	932.5	16.26	855	844	849.5	7.77	796	819	807.5	16.26
190	923	904	913.5	13.43	855	844	849.5	7.77	796	817	806.5	14.84
200	924	895	909.5	20.50	857	841	849	11.31	796	819	807.5	16.26
210	932	905	918.5	19.09	857	842	849.5	10.60	797	817	807	14.14

Table A8- Variation of moisture content with temperature at the bottom of the reduction zone

Time	T_bred1-17	T_bred2_17	Average @MMC	SD	T_bred1_13	T_bred2_13	Average @MMC	SD	T_bred1_6.4	T_bred2_6.4	Average @LMC	SD
10	701	710	705.5	6.36	753	761	757	5.65	788	783	785.5	3.53
20	699	710	704.5	7.77	753	760	756.5	4.94	788	784	786	2.82
30	701	710	705.5	6.36	753	760	756.5	4.94	789	787	788	1.41
40	701	710	705.5	6.36	754	761	757.5	4.94	785	789	787	2.82
50	702	710	706	5.65	753	760	756.5	4.94	785	783	784	1.41
60	702	711	706.5	6.36	753	761	757	5.65	783	774	778.5	6.36
70	702	711	706.5	6.36	753	763	758	7.07	783	775	779	5.65
80	702	713	707.5	7.77	754	761	757.5	4.94	782	775	778.5	4.94
90	702	713	707.5	7.77	753	761	757	5.65	780	771	775.5	6.36
100	703	713	708	7.07	753	763	758	7.07	778	770	774	5.65
110	702	714	708	8.48	754	761	757.5	4.94	779	770	774.5	6.36
120	702	713	707.5	7.77	753	761	757	5.65	783	785	784	1.41
130	703	713	708	7.07	753	763	758	7.07	789	785	787	2.82
140	703	714	708.5	7.77	754	763	758.5	6.36	788	783	785.5	3.53
150	703	714	708.5	7.77	753	763	758	7.07	789	783	786	4.24
160	704	714	709	7.07	754	763	758.5	6.36	785	782	783.5	2.12

170	703	715	709	8.48	754	763	758.5	6.36	785	780	782.5	3.53
180	703	715	709	8.48	753	761	757	5.65	783	778	780.5	3.53
190	704	715	709.5	7.77	754	763	758.5	6.36	783	779	781	2.82
200	704	716	710	8.48	754	763	758.5	6.36	782	783	782.5	0.70
210	704	716	710	8.48	754	763	758.5	6.36	780	789	784.5	6.36

Table B1. Specific enthalpy and entropy of some gases at 25 °C, 1 atm(Cengel, 2002)

Gas	h_0 (kJ kmol^{-1})	s_0 (kJ kmol^{-1} K^{-1})
N_2	8669	191.502
O_2	8682	205.033
H_2	8468	130.574
CO	8669	197.543
CO_2	9364	213.685
CH_4	–	–

Table B2**.**The Coefficients of specific heat for the empirical equation (Cengel, 2002)

Gas species	***a***	***b***	***c***	***d***	**Temperature range (K)**
H_2	29.11	-0.1916×10^{-2}	0.4003×10^{-5}	-0.8704×10^{-9}	273–1800
CO	28.16	0.1675×10^{-2}	0.5372×10^{-5}	-2.222×10^{-9}	273–1800
CO_2	22.26	5.981×10^{-2}	-3.501×10^{-5}	-7.469×10^{-9}	273–1800
$H_2O(g)$	32.24	0.1923×10^{-2}	1.055×10^{-5}	-3.595×10^{-9}	273–1800
CH_4	19.89	5.204×10^{-2}	1.269×10^{-5}	-11.01×10^{-9}	273–1500
N_2	28.90	-0.1571×10^{-2}	0.8081×10^{-5}	-2.873×10^{-9}	273–1800

Appendix A3: Statistical analysis of results

Variation of velocity with connection load

Anova: Single Factor.						
SUMMARY						
Groups	*Count*	*Sum*	*Average*	*Variance*		
V2kw	12	10.6	0.883333	0.001515		
V2kw	12	10.4	0.866667	0.002424		
V4kw	12	8.5	0.708333	0.000833		
V4KW	12	8.2	0.683333	0.012424		
V10KW	12	7.3	0.608333	0.002652		
V10KWe	12	7.3	0.608333	0.000833		
ANOVA						
Source of Variation	*SS*	*df*	*MS*	*F*	*P-value*	*F crit*
Between Groups	0.892361	5	0.178472	51.77656	1.56E-21	2.353809
Within Groups	0.2275	66	0.003447			
Total	1.119861	71				

Variation of reduction zone temperature (top) with load

Anova: Single Factor						
SUMMARY						
Groups	*Count*	*Sum*	*Average*	*Variance*		
877	11	9813	892.0909	580.8909		
889	11	9805	891.3636	324.8545		
880	11	9566	869.6364	139.4545		
ANOVA						
Source of Variation	*SS*	*df*	*MS*	*F*	*P-value*	*F crit*
Between Groups	3581.636	2	1790.818	5.140121	0.012035	3.31583
Within Groups	10452	30	348.4			
Total	14033.64	32				

Variation of reduction zone temperature (bottom) with load

Anova: Single Factor						
SUMMARY						
Groups	*Count*	*Sum*	*Average*	*Variance*		
Tb10	12	8801	733.4167	139.3561		
Tb4	12	9239	769.9167	15.90152		
Tb2	12	9105	758.75	39.84091		
ANOVA						
Source of Variation	*SS*	*df*	*MS*	*F*	*P-value*	*F crit*
Between Groups	8394.889	2	4197.444	64.54347	3.93E-12	3.284918
Within Groups	2146.083	33	65.03283			
Total	10540.97	35				

Anova: Single Factor : Effect of Moisture content on LHV of fuel						
SUMMARY						
Groups	*Count*	*Sum*	*Average*	*Variance*		
LMC	3	17.85727	5.952423	0.029764		
MMC	3	15.79089	5.263631	0.037959		
HMC	3	16.41692	5.472307	0.00011		
ANOVA						
Source of Variation	*SS*	*df*	*MS*	*F*	*P-value*	*F crit*
Between Groups	0.748491	2	0.374246	16.55151	0.003613	5.143253
Within Groups	0.135666	6	0.022611			
Total	0.884157	8				
Results for HHV of the fuel						
LMC	MMC	HMC				
6.347688	5.438355	5.950238				
6.234815	5.82883	5.965808				
6.61388	5.750612	5.951119				
Anova: Single Factor : : Effect of Moisture content on LHV of fuel						
SUMMARY						
Groups	*Count*	*Sum*	*Average*	*Variance*		
LMC	3	19.19638	6.398794	0.037881		
MMC	3	17.0178	5.672599	0.042682		
HMC	3	17.86717	5.955722	7.65E-05		
ANOVA						
Source of Variation	*SS*	*df*	*MS*	*F*	*P-value*	*F crit*
Between Groups	0.803831	2	0.401916	14.95219	0.004667	5.143253
Within Groups	0.16128	6	0.02688			
Total	0.965112	8				

Appendix A4

Thus

$$K_1 = e^{\frac{-\Delta G^o{}_1}{8.314T}} \qquad (5.16)$$

$$and$$

$$K_2 = e^{\frac{-\Delta G^o{}_2}{8.314T}} \qquad (5.17)$$

Therefore, the K values are now written in terms of the unknown values as per definition, and the Gibbs free energy technique is used to set up the variables in terms of the equilibrium constants. The dependence of ΔG^0 with temperature *T* can be written as follows (Koroneos & Lykidou, 2011):

$$\frac{d}{dT}\left[\frac{\Delta G^O}{RT}\right] = -\frac{\Delta H^o}{RT^2}(23) \text{ But} \qquad \Delta G^\circ = -RTlnK$$

Thus substitutingΔG° in the above the equation below

$$\frac{d}{dT}[lnK] = \frac{\Delta H^o}{RT^2} \qquad (5.18)$$

The above generates the relationship between temperature T and the equilibrium constant K. If ΔH^o is exothermic (negative enthalpy change), the equilibrium constant will be reduced if the temperature increases. The equilibrium constant K, increases with temperature, for an endothermic reaction. By integrating the above equation on both sides generates the equation below, where y is the constant of integration.

$$[lnK] = \int \frac{\Delta H^o}{RT^2} dT + y \quad (5.19)$$

According to (Perry, Green, & Maloney, 1997)

$$\frac{\Delta H^o}{R} = \frac{J}{R} + \Delta AT + \frac{\Delta B}{2}T^2 + \frac{\Delta C}{3}T^3 - \frac{\Delta D}{T} \quad (5.20)$$

Where J is a constant and $\Delta A, \Delta B, \Delta C, \Delta D$ are the coefficients for determining the specific heat. By combining the above two equations and integrating the product generates an overall equation as

$$[lnK] = -\frac{J}{RT} + \Delta AlnT + \frac{\Delta B}{2}T + \frac{\Delta C}{6}T^2 + \frac{\Delta D}{2T^2} + y \quad (5.21)$$

Substituting $\Delta G^\circ = -RTlnK$ into the above equation generates an equation that can be used to establish the equilibrium constant at any temperature T

$$[\Delta G^o] = J - RT\left(\Delta AlnT + \frac{\Delta B}{2}T + \frac{\Delta C}{6}T^2 + \frac{\Delta D}{2T^2} + y\right) \quad (5.22)$$

Where constants J and y can be determined. When the enthalpy change ΔH^o is known at T = 298K, the value of J can be established while the value of y can be obtained at known values of $[\Delta G^o]$ or $\ln K$ of normally at 298K using the equations above. Under the assumption of no char formation, two values of K1 and K2 must be obtained. The equations leading to their calculations are derived from their equations of reaction.

For K_1

Hydrogenating gasification (exothermic) $C + 2H_2 \leftrightarrow CH_4$ (5.5)

Thus, the above equation can be used to make the required calculations and generate the values of$\Delta A, \Delta B, \Delta C, \Delta D$ expressed as

$$\Delta A = A_{CH4} - A_C - 2A_{H2}(29)$$

$$\Delta B = B_{CH4} - B_C - 2B_{H2} \quad (5.23)$$

$$\Delta C = C_{CH4} - C_C - 2C_{H2} \quad (5.24)$$

$$\Delta D = D_{CH4} - D - 2D_{H2} \quad (5.25)$$

Table 5.2. Heat capacities (values of species A, B, C, D) (Perry et al., 1997)

Chemical species	**Formula**	**Tmax**	**A**	**B**	**C**	**D**
Methane	CH_4	1500	1.702	0.009081	-2.164x10^{-6}	
Hydrogen	H_2	3000	3.249	0.000422		8300
Carbonmonoxide	CO	2500	3.376	0.000557		-3100
Carbondioxide	CO_2	2000	5.457	0.001047		-115700
Nitrogen	N_2	2000	3.28	0.000593		4000
Water	H_2O	2000	3.47	0.00145		12100
Carbon	C	2000	1.771	0.000771		-86700
			ΔA	**ΔB**	**ΔC**	**ΔD**
Change of species based on Hydrogenating gasification $C + 2H_2 \leftrightarrow CH_4$			-6.567	0.007466	-0.000002164	70100
Change of species based on water gas shift reaction $CO + H_2O \leftrightarrow CO_2 + H_2$			1.86	-0.000538	0	-116400
$C + H_2O \leftrightarrow CO + H_2$			1.384	-0.001242	0	79800
$CH_4 + H_2O \leftrightarrow CO + 3H_2$			7.951	-0.008708	0.000002164	9700

Thus, the calculation of J and y values requires enthalpy values of $\Delta H^o_{298.15}$ and $\Delta G^o_{298.15}$ which is obtained from the available data summarized in Table 3.

$$\Delta H^o_{298.15} = \Delta H^o_{298.15\,CH4} - \Delta H^o_{298.15\,C} - 2\Delta H^o_{298.15\,H2}$$

$$\Delta H^o_{298.15} = -74520 - 0 - 2(0) = -74520\ \text{J/mol}$$

$$\Delta G^{o}_{298.15} = \Delta G^{o}_{298.15\,CH4} - \Delta G^{o}_{298.15\,C} - 2\Delta G^{o}_{298.15\,H2}$$

$$\Delta G^{o}_{298.15} = -50460 - 0 - 0 = -50460\text{J/mol}$$

Thus substituting the above values in the equation (5.20) below at T= 298.15K

$$\frac{\Delta H^{o}}{R} = \frac{J}{R} + \Delta A T + \frac{\Delta B}{2}T^{2} + \frac{\Delta C}{3}T^{3} - \frac{\Delta D}{T}$$

$$\frac{-74520}{8.314} = \frac{J}{8.314} + (-6.567x298.15) + (\frac{0.007466}{2})x298.15^{2}$$

$$+ \frac{(-0.000002164)}{3}x298.15^{3} - \frac{70100}{298.15}$$

And by calculation, J $= -58886.8$

Table 5.3. Values of Heat of formation ΔH^{o}_{298} and Gibb's free energy ΔG^{o}_{298} at 298.15K (Perry et al., 1997)

Chemical species	**Formula**	**phase**	$\Delta H^{o}_{298.15}$ **(KJ/Kmol)**	$\Delta G^{o}_{f298.15}$ **KJ/Kmol**
Methane	CH_4	g	-74520	-50460
Oxygen	O_2	g	0	0
Nitrogen	N_2	g	0	0
Hydrogen	H_2	g	0	0
Carbonmonoxide	CO	g	-110525	-137169
Carbondioxide	CO_2	g	-393509	-394359
Carbon	C	s	0	0
Water	H_2O	g	-241818	-228572
Water	H_2O	l	-285830	-237129

Thus, substituting the values of J in the equation (5.22) below, the values of y can be established. Thus, when T = 298.15

$$[\Delta G^{o}] = J - RT(\Delta A lnT + \frac{\Delta B}{2}T + \frac{\Delta C}{6}T^{2} + \frac{\Delta D}{2T^{2}} + y)$$

$$[-50460] = -58886.8 - ((8.314x298.15)(-6.567ln298.15 + \frac{0.007466}{2}x298.15 + \frac{-0.000002164}{6}x298.15^2 + \frac{70100}{2x298.15^2} + y)$$

$$y = 32.52$$

Therefore, the general equation for establishing the equilibrium constant K1 at any temperature T becomes

$$[\boldsymbol{lnK_1}] = \frac{\mathbf{7082.848}}{\boldsymbol{T}} - \mathbf{6.567}\boldsymbol{lnT} + \mathbf{3.733}\boldsymbol{x}\mathbf{10}^{-\mathbf{3}}\boldsymbol{T} - \mathbf{3.6067}\boldsymbol{x}\mathbf{10}^{-\mathbf{7}}\boldsymbol{T}^{\mathbf{2}} + \frac{\mathbf{35050}}{\boldsymbol{T}^{\mathbf{2}}} + \mathbf{32.52} \quad (5.25)$$

Similarly, through the same calculation steps, the equilibrium constant K_2 can be computed based on the major equation below.

$$CO + H_2O \leftrightarrow CO_2 + H_2 \quad (5.7)$$

From the above equation,

$$\Delta A = (A_{CO2} + A_{H2}) - (A_{co} + A_{H2O}) \quad (5.26)$$

$$\Delta B = (B_{CO2} + B_{H2}) - (B_{co} + B_{H2O}) \quad (5.27)$$

$$\Delta C = (C_{CO2} + C_{H2}) - (C_{co} + C_{H2O}) \quad (5.28)$$

$$\Delta D = (D_{CO2} + D_{H2}) - (D_{co} + D_{H2O}) \quad (5.29)$$

Through calculations, results of change in species are summarized in the table above as

$$\Delta A = 1.86, \Delta B = -0.000538, \Delta C = 0, \Delta D = -116400$$

Subsequently, calculation of their corresponding enthalpy change and Gibb's free energy at standard conditions follows

$$\Delta H^o_{298} = (\Delta H^o_{298_{Co2}} + \Delta H^o_{298_{H2}}) - (\Delta H^o_{298_{Co}} + \Delta H^o_{298_{H2O}} \quad (5.30)$$

$$\Delta H^o_{298} = -41154 \frac{J}{mol}$$

Thus substituting the above values in the equation below at T= 298.15K

$$\frac{-41154}{8.314} = \frac{J}{R} + 1.86x298.15 + \frac{-0.000538}{2} x298.15^2 + \frac{0}{3} x298.15^3 - \frac{-116400}{298.15}$$

$$\frac{J}{R} = -5870.06 \; or \; J = -5870.06 \; R$$

$$\Delta G^o_{298} = (\Delta G^o_{298_{Co2}} + \Delta G^o_{298_{H2}}) - (\Delta G^o_{298_{Co}} + \Delta G^o_{298_{H2O}})$$

$$\Delta G^o_{298} = -28618 \frac{J}{mol}$$

Also,

$$[\Delta G^o] = J - RT(\Delta A lnT + \frac{\Delta B}{2} T + \frac{\Delta C}{6} T^2 + \frac{\Delta D}{2T^2} + y)$$

$$-28618 = (-5870.06 \; x8.314) - (8.314x298.15)(1.86 \; ln298.15 + \frac{-0.000538}{2} x298.15 + \frac{0}{6} x298.15^2 + \frac{-116400}{2x298.15^2} + y)$$

$$y = -18.0081$$

Thus, K2 can be expressed according to the general equation below

$$\boldsymbol{[lnK2] = \frac{5870.06}{T} + 1.86 \; lnT - 2.69x10^{-4}T - \frac{58200}{T^2} - 18.0081} \quad (5.31)$$

Appendix A5: Matlab code used for generation of modelling results

```
functionsy_gas

clc
% General formular of biomass CxHyOz (Spartanspruce used)
Mw_bio=24.7; % molecular weight of wood
bio_comp = [46.7,6.3,46.5,0.48,0.02 ]; % comp_spartanspruce

mc=0.05; % moisture content
c=0.27; % amnt of air per kmol feedstock
w=(Mw_bio*mc)./(18*(1-mc)); % amnt of moisture per kmol feedstock
%w=0.1525

%% Assume x=1 kmol of C
%x=1; % kmol of C
y=(bio_comp(2)*12)/(bio_comp(1)*1); % kmol of H/kmol of C
z=(bio_comp(3)*12)/(bio_comp(1)*16); % kmol of O/kmol of C


%% Calculate equilibrium constants for gasification and water gas shift
%% rxns. According to Perry
% In K =INTEGRAL(DH/RT^2) dT + yy ; yyconst of integr
% DH/R=J/R + DA/T +DB T^2/2 + DC T^3/3 -DD/T; J constant n DA, DB ,..
coeffs
% for determining specific heat.
%% Function to determine the syngas composition from the biomass elemental
%% composition and Temperature (gasification)
%% disp('elemental composition should be of the form [C, H, O, N, Ash]');

% DG= J - RT( DA In T + DB T/2 + DC T^2/6 + DD/(2T^2) + yy)
% In K =-J/RT + DA In T + DB T/2 + DC T^2/6 + DD/(2T^2) + yy
% For known DH, calculate J at known T=298.15K.
% Then for known DG J T, calculate yy.
A=[7082.85; 5870.06]; % A=-J/R
B=[-6.567; 1.86]; C=[3.733E-03; -2.69E-04];
D=[-3.6067E-07;0]; E=[35050; -58200];
yy=[32.52;-18.0081];

%KK =A./T + B.*log(T)+ C.*T + D.*T^2 + E./(T^2) + yy;

% Molecular weights
Mw_co=28;Mw_co2=44;Mw_ch4=16;Mw_h2=2; Mw_h2o=18;
Mw_o2=32;Mw_n2=28;

% Heats of formation in KJ/kmol
H_co=-110525; H_co2=-393509; H_ch4=-74520; H_h2=0; H_h2o=-241818;
H_vap=40650;H_o2=0; H_n2=0;
H_bio =-104822; % KJ/kmol
```

```
% coeff for determining Cp in KJ/kmol
coeff_co=[28.16 0.1675e-02 0.5372e-05 -2.222e-09];
coeff_co2=[22.26 5.981e-02 -3.501e-05 -7.469e-09];
coeff_ch4=[19.89 5.204e-02 1.269e-05 -11.01e-09];
coeff_h2=[29.11 -0.1916e-02 0.4003e-05 -0.8704e-09];
coeff_h2o=[32.24 0.1923e-02 1.055e-05 -3.595e-09];
coeff_n2=[28.9 -0.1571e-02 0.8081e-05 -2.873e-09];

coeff=[coeff_co;coeff_co2; coeff_ch4;coeff_h2;coeff_h2o;coeff_n2];


%% solve for syngas mole fractions x1 - x6
% x1-C0; x2-C02; x3-CH4 x4-H2; x5-H2O x6-Tg;

x0=[0.5 0.5 0.5 0.5 0.5 1200]'; % Guess


function f=syngas(x)
% Function F(x) to solve for x1-x6.

% Functions linear
f_1=1-(x(1)+x(2)+x(3)); % carbon balance
      f_2=(y + 2*w)-(4*x(3) +2*x(4) +2*x(5)); % hydrogen balance
      f_3=(z+w +2*c)-(x(1) +2*x(2) +x(5)); % oxygen balance

% Equilibrium constants
      KK =A./x(6) + B.*log(x(6))+ C.*(x(6)) + D.*(x(6))^2 + E./((x(6))^2) +
yy;
K =exp(KK);

% Nonlinear functions for equilibrium constants
f_4=x(3) - K(1)*x(4)^2 ;
      f_5=(x(2)*x(4) - K(2)*x(1)*x(5));

%% Energy balance

% Evaluating Integrals for sensible heats for the gases to
% gasification temp Tg (x(6))
sens_heat=quadv(@sensible,298,x(6));


      LHS=(H_bio + w*(H_h2o - H_vap));

      RHS=(x(1)*(H_co+sens_heat(1)) + x(2)*(H_co2+sens_heat(2)) +...
      x(3)*(H_ch4+sens_heat(3))+ x(4)*(H_h2+sens_heat(4)) +...
      x(5)*(H_h2o+sens_heat(5)) + 3.76*c*(sens_heat(6)));

      f_6=LHS-RHS; % Function for energy balance


      f=[f_1;f_2;f_3;f_4;f_5; f_6]; % Function F(x)

end


%% Solving F(x)
```

```
options = optimset('Display','iter','Algorithm','trust-region-
reflective','MaxFunEvals',10000);
x=fsolve(@syngas,x0,options); % fsolve solver used to find F(x)=0
residual =feval(@syngas,x) %

mol_frac_co=x(1)
mol_frac_co2=x(2)
mol_frac_ch4=x(3)
mol_frac_h2=x(4)
mol_frac_h20=x(5)
Temp_gasification=x(6)


vol=x(1:5).*1000*8.314*x(6)./101325;

n2_out=3.76*c;
vol_n2=n2_out*1000*8.314*x(6)./101325;

total_vol=(sum(vol)+vol_n2);

vol_per=100*vol./total_vol;
vol_per_n2=100*vol_n2./total_vol;

vol_per=[vol_per; vol_per_n2]




functiondh=sensible(T)
dh=coeff(:,1)+coeff(:,2).*T + coeff(:,3).*T.^2 + coeff(:,4).*T.^3;

end







end
```

A.5.1 Sample results from modelling

Iteration	Func-count	f(x)	Norm of step	First-order optimality
0	7	2.75155e+10		5.92e+10
1	14	164109	10	1.45e+08
2	21	5073.77	10.385	2.55e+07
3	28	6.69273e-06	0.183671	701
4	35	1.74385e-06	0.143295	42.8
5	42	1.72952e-06	2.82884e-10	0.00107

Equationsolved, inaccuracypossible.

The vector of function values is near zero, as measured by the default value

of the function tolerance. However, the last step was ineffective.

<stopping criteria details>

residual =

-0.0001

0.0000

-0.0003

-0.0001

0.0013

-0.0000

```
mol_frac_co =

    0.8119


mol_frac_co2 =

    0.1799


mol_frac_ch4 =

    0.0084


mol_frac_h2 =

    0.6773


mol_frac_h20 =

    0.1877


Temp_gasification =   1.1793e+03

vol_per =

28.1887
    6.2443
    0.2901
   23.5141
    6.5157
   35.2471


>>
```

8. References

Abuadala, a., & Dincer, I. (2010). Efficiency evaluation of dry hydrogen production from biomass gasification. *Thermochimica Acta*, *507–508*, 127–134. https://doi.org/10.1016/j.tca.2010.05.013

Ahmed, I. I., Nipattummakul, N., & Gupta, a. K. (2011). Characteristics of syngas from co-gasification of polyethylene and woodchips. *Applied Energy*, *88*(1), 165–174. https://doi.org/10.1016/j.apenergy.2010.07.007

Alarcon, D., Joehnk, T. F., & Koch, B. (2013). Global food security index 2013: An annual measure of the state of global food security, 1–44.

Andri, F., Reni, V.R., Lars, W., Eva, O., Andri, O.F., Advan, W and Wim, T. (1997). Gasification of Biomass wastes and residues for electricity production. *Biomass and Bioenergy*, *12*(6).

Arroyo, J., Moreno, F., Muñoz, M., & Monné, C. (2013). Efficiency and emissions of a spark ignition engine fueled with synthetic gases obtained from catalytic decomposition of biogas. *International Journal of Hydrogen Energy*, *38*(9), 3784–3792. https://doi.org/10.1016/j.ijhydene.2013.01.087

ASTM. D1762-84. (2013). Standard Test Method for Chemical Analysis of Wood Charcoal. *ASTM International, West Conshohocken*. Retrieved from http://www.astm.org/Standards/D1762.htm

Atnaw, S. M., Sulaiman, S. A., & Yusup, S. (2014). Influence of fuel moisture content and reactor temperature on the calorific value of Syngas resulted from gasification of oil palm fronds. *The Scientific World Journal*, *2014*. https://doi.org/10.1155/2014/121908

Augusto, L., Nogueira, H., & Capaz, R. S. (2013). Biofuels in Brazil : Evolution , achievements and perspectives on food security. *Global Food Security*, *2*(2), 117–125. https://doi.org/10.1016/j.gfs.2013.04.001

Aziz, M. (2015). Integrated supercritical water gasification and a combined cycle for microalgal utilization. *Energy Conversion and Management*, *91*, 140–148. https://doi.org/10.1016/j.enconman.2014.12.012

Azzone, E., Morini, M., & Pinelli, M. (2012). Development of an equilibrium model for the simulation of thermochemical gasification and application to agricultural residues. *Renewable Energy*, *46*, 248–254. https://doi.org/10.1016/j.renene.2012.03.017

Balu, E., & Chung, J. N. (2012). System characteristics and performance evaluation of a trailer-scale downdraft gasifier with different feedstock. *Bioresource Technology*, *108*, 264–73. https://doi.org/10.1016/j.biortech.2011.12.105

Barisano, D., Canneto, G., Nanna, F., Villone, a., Alvino, E., Carnevale, M., & Pinto, G. (2014). Production of gaseous carriers via biomass gasification for energy purposes. *Energy Procedia*, *45*, 2–11. https://doi.org/10.1016/j.egypro.2014.01.002

Bauen, A., Berndes, G., Junginger, M., Vuille, F., & Londo, M. (2009). Bioenergy – a Sustainable. *Structure*, 1–108.

Bharathiraja, B., Chakravarthy, M., Kumar, R. R., Yogendran, D., Yuvaraj, D., Jayamuthunagai, J., … Palani, S. (2015). Aquatic biomass (algae) as a future feed stock for bio-re fi neries : A review on cultivation , processing and products. *Renewable and Sustainable Energy Reviews*, *47*, 634–653. https://doi.org/10.1016/j.rser.2015.03.047

Bhattacharjee, S., & Dey, A. (2014). Techno-economic performance evaluation of grid

integrated PV-biomass hybrid power generation for rice mill. *Sustainable Energy Technologies and Assessments*, *7*, 6–16. https://doi.org/10.1016/j.seta.2014.02.005

Bilgen, S; Kaygusuz, K; Sari, A. (2004). Second law analysis of various types of coal and woody biomass in Turkey. *Energy Sources*, *26*, 1083–1094.

Bini, R., & Prima, M. D. I. (2010). Organic Rankine Cycle (Orc) in Biomass Plants : an Overview on Different Applications, 9.

Boateng, a. a., Walawender, W. P., Fan, L. T., & Chee, C. S. (1992). Fluidized-bed steam gasification of rice hull. *Bioresource Technology*, *40*(3), 235–239. https://doi.org/10.1016/0960-8524(92)90148-Q

Boloy, R. A. M., Silveira, J. L., Tuna, C. E., Coronado, C. R., & Antunes, J. S. (2011). Ecological impacts from syngas burning in internal combustion engine: Technical and economic aspects. *Renewable and Sustainable Energy Reviews*, *15*(9), 5194–5201. https://doi.org/10.1016/j.rser.2011.04.009

Brammer, J. G., & Bridgwater, A. V. (2002). The in uence of feedstock drying on the performance and economics of a biomass gasiÿer – engine CHP system, *22*, 271–281.

Bruun, S., Jensen, L. S., Khanh Vu, V. T., & Sommer, S. (2014). Small-scale household biogas digesters: An option for global warming mitigation or a potential climate bomb? *Renewable and Sustainable Energy Reviews*, *33*, 736–741. https://doi.org/10.1016/j.rser.2014.02.033

Buckee, G. (1996). Determination of total nitrogen in barley and malt by combustion method — collaborative trial Submitted on Behalf of the Analysis Committee of EBC By Claes-Goran Johansson. A combustion method , relying on the Dumas principle, for the determination off to, *102*, 249–250.

Bullock, D. S., & Olfert, J. S. (2014). Size, volatility, and effective density of particulate emissions from a homogeneous charge compression ignition engine using compressed natural gas. *Journal of Aerosol Science*, *75*, 1–8. https://doi.org/10.1016/j.jaerosci.2014.04.005

Canan, Acar and Ibrahim, D. (2015). A review on clean energy solutions for better sustainability. *International Journal of Energy Research*, *39*, 585–606.

Cha, H., Eom, T., Song, S., & Min, K. (2015). Journal of Natural Gas Science and Engineering An experimental study on the fuel conversion ef fi ciency and NO x emissions of a spark-ignition gas engine for power generation by fuel mixture of methane and model syngas (H 2 / CO). *Journal of Natural Gas Science and Engineering*, *23*(x), 517–523. https://doi.org/10.1016/j.jngse.2015.03.004

Channiwala, S. a., & Parikh, P. P. (2002). A unified correlation for estimating HHV of solid, liquid and gaseous fuels. *Fuel*, *81*, 1051–1063. https://doi.org/10.1016/S0016-2361(01)00131-4

Channiwala, S. A., & Parikh, P. P. (2002). A unified correlation for estimating HHV of solid, liquid and gaseous fuels. *Fuel*, *81*(8), 1051–1063. https://doi.org/10.1016/S0016-2361(01)00131-4

Chaves, L. I., da Silva, M. J., de Souza, S. N. M., Secco, D., Rosa, H. A., Nogueira, C. E. C., & Frigo, E. P. (2016a). Small-scale power generation analysis: Downdraft gasifier coupled to engine generator set. *Renewable and Sustainable Energy Reviews*, *58*, 491–498. https://doi.org/10.1016/j.rser.2015.12.033

Chaves, L. I., da Silva, M. J., de Souza, S. N. M., Secco, D., Rosa, H. A., Nogueira, C. E. C.,

& Frigo, E. P. (2016b). Small-scale power generation analysis: Downdraft gasifier coupled to engine generator set. *Renewable and Sustainable Energy Reviews*, *58*, 491–498. https://doi.org/10.1016/j.rser.2015.12.033

Chawdhury, M. a., & Mahkamov, K. (2010). Development of a Small Downdraft Biomass Gasifier for Developing Countries. *Journal of Scientific Research*, *3*(1). https://doi.org/10.3329/jsr.v3i1.5613

Chen, H., & Zhang, Y. P. (2015). New biore fi neries and sustainable agriculture : Increased food , biofuels , and ecosystem security, *47*, 117–132. https://doi.org/10.1016/j.rser.2015.02.048

Chen, J.-S., & Gunkel, W. W. (1987). Modeling and simulation of co-current moving bed gasification reactors — Part II. A detailed gasifier model. *Biomass*, *14*(2), 75–98. https://doi.org/10.1016/0144-4565(87)90012-6

Chiang, K., Lu, C., Lin, M., & Chien, K. (2013). Reducing tar yield in gasification of paper-reject sludge by using a hot-gas cleaning system. *Energy*, (1–7). https://doi.org/10.1016/j.energy.2012.12.010

Cho, M., Choi, Y., & Kim, J. (2015). Air gasification of PVC (polyvinyl chloride) - containing plastic waste in a two-stage gasi fi er using Ca-based additives and Ni-loaded activated carbon for the production of clean and hydrogen-rich producer gas, 1–8. https://doi.org/10.1016/j.energy.2015.05.026

Cho, M. H., Mun, T. Y., & Kim, J. S. (2013). Production of low-tar producer gas from air gasification of mixed plastic waste in a two-stage gasifier using olivine combined with activated carbon. *Energy*, *58*, 688–694. https://doi.org/10.1016/j.energy.2013.06.021

Chris Higman and Maarten van der Burgt. (2003). Gasification. *Gulf Professional Pub USA*.

ChristusJeya Singh, V., Joseph Sekhar, S., & Thyagarajan, K. (2014). Performance studies on downdraft gasifier with biomass energy sources available in remote villages. *American Journal of Applied Sciences*, *11*(4), 611–622. https://doi.org/10.3844/ajassp.2014.611.622

Chutichai, B., Tiraset, S., & Assabumrungrat, S. (2012). Analysis of Biomass Gasification and PEMFC Integrated Systems for Power Generation : A Combined Heat and Power Approach, *29*, 283–288. https://doi.org/10.3303/CET1229048

Colpan, C. O., Hamdullahpur, F., Dincer, I., & Yoo, Y. (2010). Effect of gasification agent on the performance of solid oxide fuel cell and biomass gasification systems. *International Journal of Hydrogen Energy*, *35*(10), 5001–5009. https://doi.org/10.1016/j.ijhydene.2009.08.083

Corella, Â., Aznar, P., Caballero, M. A., & Gil, J. (1999). Biomass gasi ® cation in atmospheric and bubbling ¯ uidized bed : E € ect of the type of gasifying agent on the product distribution, *17*, 0–14.

Dasappa, S., Subbukrishna, D. N., Suresh, K. C., Paul, P. J., & Prabhu, G. S. (2011). Operational experience on a grid connected 100kWe biomass gasification power plant in Karnataka, India. *Energy for Sustainable Development*, *15*(3), 231–239. https://doi.org/10.1016/j.esd.2011.03.004

De Kam, M. J., Vance Morey, R., & Tiffany, D. G. (2009). Biomass Integrated Gasification Combined Cycle for heat and power at ethanol plants. *Energy Conversion and Management*, *50*(7), 1682–1690. https://doi.org/10.1016/j.enconman.2009.03.031

Declercq, ir. D. (2006). Power cycles Principles of combustion cycles and efficient concepts

This contribution is based on the EC BREF- document Reference Document on Best Available Techniques for, (July), 1–34.

Dejtrakulwong, C., & Patumsawad, S. (2014). Four Zones Modeling of the Downdraft Biomass Gasification Process: Effects of Moisture Content and Air to Fuel Ratio. *Energy Procedia*, *52*, 142–149. https://doi.org/10.1016/j.egypro.2014.07.064

Dentice d'Accadia, M., Sasso, M., Sibilio, S., & Vanoli, L. (2003). Micro-combined heat and power in residential and light commercial applications. *Applied Thermal Engineering*, *23*(10), 1247–1259. https://doi.org/10.1016/S1359-4311(03)00030-9

Dewulf, J., & Van Langenhove, H. (2005). Integrating industrial ecology principles into a set of environmental sustainability indicators for technology assessment. *Resources, Conservation and Recycling*, *43*(4), 419–432. https://doi.org/10.1016/j.resconrec.2004.09.006

Deydier, A., Marias, F., Bernada, P., Couture, F., & Michon, U. (2010). Equilibrium model for a travelling bed gasifier, *5*. https://doi.org/10.1016/j.biombioe.2010.08.022

Doherty, W., Reynolds, A., & Kennedy, D. (2009). The Effect of Air Preheating in a Biomass CFB Gasifier using ASPEN Plus Simulation The effect of air preheating in a biomass CFB gasifier using ASPEN Plus simulation. https://doi.org/10.1016/j.biombioe.2009.05.004.This

Dou, B., Wang, C., Chen, H., Song, Y., Xie, B., Xu, Y., & Tan, C. (2012). Research progress of hot gas filtration, desulphurization and HCl removal in coal-derived fuel gas: A review. *Chemical Engineering Research and Design*, *90*(11), 1901–1917. https://doi.org/10.1016/j.cherd.2012.04.009

Drift, B. Van Der. (2013). Allothermal gasification for co-firing, (July).

Du, L., Yao, J. Z., & Lin, W. G. (2005). Experimental study of particle flow in a gas-solid separator with baffles using PDPA. *Chemical Engineering Journal*, *108*(1–2), 59–67. https://doi.org/10.1016/j.cej.2004.12.043

Dutta, P. P., Pandey, V., Das, a. R., Sen, S., & Baruah, D. C. (2014). Down Draft Gasification Modelling and Experimentation of Some Indigenous Biomass for Thermal Applications. *Energy Procedia*, *54*(3712), 21–34. https://doi.org/10.1016/j.egypro.2014.07.246

El-Emam, R. S., & Dincer, I. (2015). Thermal modeling and efficiency assessment of an integrated biomass gasification and solid oxide fuel cell system. *International Journal of Hydrogen Energy*, *40*(24), 7694–7706. https://doi.org/10.1016/j.ijhydene.2015.02.061

Enders, A., Hanley, K., Whitman, T., Joseph, S., & Lehmann, J. (2012). Characterization of biochars to evaluate recalcitrance and agronomic performance. *Bioresource Technology*, *114*, 644–53. https://doi.org/10.1016/j.biortech.2012.03.022

EPM. (2015). Continuous Emissions Monitoring Systems (CEMS).

Erkiaga, A., Lopez, G., Amutio, M., Bilbao, J., & Olazar, M. (2014). Influence of operating conditions on the steam gasification of biomass in a conical spouted bed reactor. *Chemical Engineering Journal*, *237*, 259–267. https://doi.org/10.1016/j.cej.2013.10.018

Ewing, M., & Msangi, S. (2009). Biofuels production in developing countries : assessing tradeoffs in welfare and food security, *12*, 520–528. https://doi.org/10.1016/j.envsci.2008.10.002

Ferrer, Y., Templier, J. C., Gonthier, Y., & Bernis, a. (2000). Study of filter cake formation mechanisms during tangential filtration of dust-laden gases at high temperature. *Powder*

Technology, *113*(1–2), 197–204. https://doi.org/10.1016/S0032-5910(00)00343-0

Figiel, A., & Tajner-Czopek, A. (2006). The effect of candy moisture content on texture. *Journal of Foodservice*, *17*(4), 189–195. https://doi.org/10.1111/j.1745-4506.2006.00037.x

Formosa, F., & Despesse, G. (2010). Analytical model for Stirling cycle machine design. *Energy Conversion and Management*, *51*(10), 1855–1863. https://doi.org/10.1016/j.enconman.2010.02.010

Fournel, S., Marcos, B., Godbout, S., & Heitz, M. (2015). Bioresource Technology Predicting gaseous emissions from small-scale combustion of agricultural biomass fuels. *Bioresource Technology*, *179*, 165–172. https://doi.org/10.1016/j.biortech.2014.11.100

Gable, P., & Brown, R. C. (2016). Effect of biomass heating time on bio-oil yields in a free fall fast pyrolysis reactor, *166*, 361–366. https://doi.org/10.1016/j.fuel.2015.10.073

Gallagher, C., & Murphy, J. D. (2013). What is the realistic potential for biomethane produced through gasification of indigenous Willow or imported wood chip to meet renewable energy heat targets? *Applied Energy*, *108*, 158–167. https://doi.org/10.1016/j.apenergy.2013.03.021

Gao, N., Li, a, Quan, C., & Gao, F. (2008). Hydrogen-rich gas production from biomass steam gasification in an updraft fixed-bed gasifier combined with a porous ceramic reformer. *International Journal of Hydrogen Energy*, *33*(20), 5430–5438. https://doi.org/10.1016/j.ijhydene.2008.07.033

Garcia, L., Salvador, M.L., Arauzo,J and Bilbao, R. (2001) CO_2 as a gasifying agent for gas production from pine sawdust at low temperatures using a Ni/Al coprecipitated catalyst. *Fuel Processing Technology*, 69, 157–174

Ghassemi, H., & Shahsavan-markadeh, R. (2014). Effects of various operational parameters on biomass gasification process ; a modified equilibrium model. *Energy Conversion and Management*, *79*, 18–24. https://doi.org/10.1016/j.enconman.2013.12.007

González, J. F., Román, S., Bragado, D., & Calderón, M. (2008). Investigation on the reactions influencing biomass air and air/steam gasification for hydrogen production. *Fuel Processing Technology*, *89*(8), 764–772. https://doi.org/10.1016/j.fuproc.2008.01.011

Guan, R., Li, W., Chen, H., & Li, B. (2005). Effects of Fe- and Ca-based additives on NO emission during gasification of N-containing model compound under different atmospheres. *Fuel*, *84*(17), 2178–2183. https://doi.org/10.1016/j.fuel.2005.05.006

Guangul, F. M., Sulaiman, S. a., & Ramli, A. (2012). Gasifier selection, design and gasification of oil palm fronds with preheated and unheated gasifying air. *Bioresource Technology*, *126*, 224–232. https://doi.org/10.1016/j.biortech.2012.09.018

Guangul, F. M., Sulaiman, S. a., & Ramli, A. (2014). Study of the effects of operating factors on the resulting producer gas of oil palm fronds gasification with a single throat downdraft gasifier. *Renewable Energy*, *72*, 271–283. https://doi.org/10.1016/j.renene.2014.07.022

Guizani, C., Escudero Sanz, F. J., & Salvador, S. (2015). Influence of temperature and particle size on the single and mixed atmosphere gasification of biomass char with H2O and CO2. *Fuel Processing Technology*, *134*, 175–188. https://doi.org/10.1016/j.fuproc.2015.01.031

Güngören Madenoğlu, T., Sağlam, M., Yüksel, M., & Ballice, L. (2013). Simultaneous effect

of temperature and pressure on catalytic hydrothermal gasification of glucose. *Journal of Supercritical Fluids*, *73*, 151–160. https://doi.org/10.1016/j.supflu.2012.10.004

Guo, X., Xiao, B., Liu, S., Hu, Z., Luo, S., & He, M. (2009). An experimental study on air gasification of biomass micron fuel (BMF) in a cyclone gasifier. *International Journal of Hydrogen Energy*, *34*(3), 1265–1269. https://doi.org/10.1016/j.ijhydene.2008.11.107

Hanaoka, T., Inoue, S., Uno, S., Ogi, T., & Minowa, T. (2005). Effect of woody biomass components on air-steam gasification. *Biomass and Bioenergy*, *28*(1), 69–76. https://doi.org/10.1016/j.biombioe.2004.03.008

Hau, J. L., & Ray, R. (2008). Athermodynamic model of the outputs of gasification of Solid Waste.International journal of chemical reactor engineering, *6*.https://www.escholar.manchester.ac.uk/api/datastream?publicationPid=uk-ac-man-scw:103487&datastreamId=post-peer-review-publishers.pdf (accessed June 2016)

Heidenreich, S. (2013). Hot gas filtration - A review. *Fuel*, *104*, 83–94. https://doi.org/10.1016/j.fuel.2012.07.059

Hernández, J. J., Ballesteros, R., & Aranda, G. (2013). Characterisation of tars from biomass gasification: Effect of the operating conditions. *Energy*, *50*, 333–342. https://doi.org/10.1016/j.energy.2012.12.005

Howaniec, N., & Smoliński, A. (2014). Effect of fuel blend composition on the efficiency of hydrogen-rich gas production in co-gasification of coal and biomass. *Fuel*, *128*, 442–450. https://doi.org/10.1016/j.fuel.2014.03.036

Huang, H. J., & Ramaswamy, S. (2009). Modeling biomass gasification using thermodynamic equilibrium approach. *Applied Biochemistry and Biotechnology*, *154*, 193–204. https://doi.org/10.1007/s12010-008-8483-x

Huber, G. W., Iborra, S., & Corma, A. (2006). Synthesis of transportation fuels from biomass: Chemistry, catalysts, and engineering. *Chemical Reviews*, *106*(9), 4044–4098. https://doi.org/10.1021/cr068360d

Huynh, C. Van, & Kong, S.-C. (2013). Combustion and NOx emissions of biomass-derived syngas under various gasification conditions utilizing oxygen-enriched-air and steam. *Fuel*, *107*, 455–464. https://doi.org/10.1016/j.fuel.2012.12.016

IEA. (2006). *Warning: Please note that this PDF is subject to specific restrictions that limit its use and distribution. The terms and conditions are available online at www.iea.org/w/bookshop/pricing.html*. *World energy outlook*.

IEA. (2012). Future Biomass-based Transport Fuels Summary and Conclusions from the. In *Future Biomass-based Transport Fuels Summary and Conclusions from the IEA Bioenergy ExCo67 Workshop*.

Irfan, M., Riaz, M., Saleem, M., Muhammad, S., Saleem, F., & Berg, L. Van Den. (2014). Estimation and characterization of gaseous pollutant emissions from agricultural crop residue combustion in industrial and household sectors of Pakistan. *Atmospheric Environment*, *84*, 189–197. https://doi.org/10.1016/j.atmosenv.2013.11.046

Isaksson, J., Pettersson, K., Mahmoudkhani, M., Åsblad, A., & Berntsson, T. (2012). Integration of biomass gasification with a Scandinavian mechanical pulp and paper mill – Consequences for mass and energy balances and global CO2 emissions. *Energy*, *44*(1), 420–428. https://doi.org/10.1016/j.energy.2012.06.013

Jaojaruek, K., Jarungthammachote, S., Kathrina, M., Gratuito, B., & Wongsuwan, H. (2011). Bioresource Technology Experimental study of wood downdraft gasification for an

improved producer gas quality through an innovative two-stage air and premixed air / gas supply approach, *102*, 4834–4840. https://doi.org/10.1016/j.biortech.2010.12.024

Jarungthammachote, S., & Dutta, a. (2007). Thermodynamic equilibrium model and second law analysis of a downdraft waste gasifier. *Energy*, *32*, 1660–1669. https://doi.org/10.1016/j.energy.2007.01.010

Jeong, H. J., Park, S. S., & Hwang, J. (2014). Co-gasification of coal-biomass blended char with CO2 at temperatures of 900-1100 C. *Fuel*, *116*, 465–470. https://doi.org/10.1016/j.fuel.2013.08.015

Jeschke, M. R., & Heggenstaller, A. (2012). Sustainable Corn Stover Harvest for Biofuel Production. *Crop Insights*, *22*(5), 1–6.

Josef Schmidhuber. (2007). *Biofuels : An emerging threat to Europe ' s Food Security ? Biofuels : An emerging threat to Europe ' s Food Security ? Impact of an increased biomass use on*.

Kalinci, Y., Hepbasli, A., & Dincer, I. (2010). Efficiency assessment of an integrated gasifier/boiler system for hydrogen production with different biomass types. *International Journal of Hydrogen Energy*, *35*(10), 4991–5000. https://doi.org/10.1016/j.ijhydene.2009.08.079

Karmakar, M. K., Mandal, J., Haldar, S., & Chatterjee, P. K. (2013). Investigation of fuel gas generation in a pilot scale fluidized bed autothermal gasifier using rice husk. *Fuel*, *111*, 584–591. https://doi.org/10.1016/j.fuel.2013.03.045

Karp, A., & Richter, G. M. (2011). eXtra Botany Meeting the challenge of food and energy security, 1–9. https://doi.org/10.1093/jxb/err099

Khatiwada, D., Seabra, J., Silveira, S., & Walter, A. (2012). Power generation from sugarcane biomass – A complementary option to hydroelectricity in Nepal and Brazil. *Energy*, *48*(1), 241–254. https://doi.org/10.1016/j.energy.2012.03.015

Kim, I., Seo, Y. H., Kim, G.-Y., & Han, J.-I. (2015). Co-production of bioethanol and biodiesel from corn stover pretreated with nitric acid. *Fuel*, *143*, 285–289. https://doi.org/10.1016/j.fuel.2014.11.031

Kongtragool, B., & Wongwises, S. (2003). A review of solar-powered Stirling engines and low temperature differential Stirling engines. *Renewable and Sustainable Energy Reviews*, *7*(2), 131–154. https://doi.org/10.1016/S1364-0321(02)00053-9

Kongtragool, B., & Wongwises, S. (2006). Thermodynamic analysis of a Stirling engine including dead volumes of hot space, cold space and regenerator. *Renewable Energy*, *31*(3), 345–359. https://doi.org/10.1016/j.renene.2005.03.012

Koroneos, C., & Lykidou, S. (2011). Equilibrium modeling for a downdraft biomass gasifier for cotton stalks biomass in comparison with experimental data. *Journal of Chemical Engineering and Materials Science*, *2*(April), 61–68.

Kumar, A., Demirel, Y., Jones, D. D., & Hanna, M. a. (2010). Optimization and economic evaluation of industrial gas production and combined heat and power generation from gasification of corn stover and distillers grains. *Bioresource Technology*, *101*(10), 3696–3701. https://doi.org/10.1016/j.biortech.2009.12.103

Kumar, A., Eskridge, K., Jones, D. D., & Hanna, M. a. (2009). Steam-air fluidized bed gasification of distillers grains: Effects of steam to biomass ratio, equivalence ratio and gasification temperature. *Bioresource Technology*, *100*(6), 2062–8. https://doi.org/10.1016/j.biortech.2008.10.011

Kumar, A., Jones, D. D., & Hanna, M. a. (2009). Thermochemical Biomass Gasification: A Review of the Current Status of the Technology. *Energies*, *2*(3), 556–581. https://doi.org/10.3390/en20300556

Lahijani, P., & Zainal, Z. A. (2011). Gasification of palm empty fruit bunch in a bubbling fluidized bed: a performance and agglomeration study. *Bioresource Technology*, *102*(2), 2068–76. https://doi.org/10.1016/j.biortech.2010.09.101

Le, C. D., Kolaczkowski, S. T., & McClymont, D. W. J. (2015). Using quadrupole mass spectrometry for on-line gas analysis – Gasification of biomass and refuse derived fuel. *Fuel*, *139*, 337–345. https://doi.org/10.1016/j.fuel.2014.09.010

Li-ping, X. I. E., Tao, L. I., Jian-dong, G. A. O., Xue-ning, F. E. I., Xia, W. U., & Yuan-guang, J. (2010). Effect of moisture content in sewage sludge on air gasification. *Journal of Fuel Chemistry and Technology*, *38*(5), 615–620. https://doi.org/10.1016/S1872-5813(10)60048-5

Liang, C., Chen, X., Xu, P., Liu, B., Zhao, C., & Xu, C. (2011). Effect of moisture content on conveying characteristics of pulverized coal for pressurized entrained flow gasification. *Experimental Thermal and Fluid Science*, *35*(6), 1143–1150. https://doi.org/10.1016/j.expthermflusci.2011.03.009

Lin Wei, Lester O Pordesimo, Filip S. D To, James Wooten, Agus Haryanto, E. P. C. (2009). Effects of Feedstock Properties on the Performance of A Downdraft Gasifier. *American Society of Agricultural and Biological Engineers*. Retrieved from https://elibrary.asabe.org/abstract.asp?aid=27211

Liu, L., Ye, J., Zhao, Y., & Zhao, E. (2015). The plight of the biomass power generation industry in China – A supply chain risk perspective. *Renewable and Sustainable Energy Reviews*, *49*, 680–692. https://doi.org/10.1016/j.rser.2015.04.151

Liu, X., Gao, S., & Li, J. (2005). Characterizing particle clustering behavior by PDPA measurement for dilute gas-solid flow. *Chemical Engineering Journal*, *108*(3), 193–202. https://doi.org/10.1016/j.cej.2005.01.012

Liu, Y., Jia, W., Guo, Q., & Ryu, H. (2014). Effect of Gasifying Medium on the Coal Chemical Looping Gasification with CaSO4 as Oxygen Carrier. *Chinese Journal of Chemical Engineering*, *22*(11–12), 1208–1214. https://doi.org/10.1016/j.cjche.2014.09.011

Lombardi, L., Carnevale, E., & Corti, A. (2012). Analysis of energy recovery potential using innovative technologies of waste gasification. *Waste Management*, *32*(4), 640–652. https://doi.org/10.1016/j.wasman.2011.07.019

Lonati, G., & Zanoni, F. (2013). Monte-Carlo human health risk assessment of mercury emissions from a MSW gasification plant. *Waste Management*, *33*(2), 347–355. https://doi.org/10.1016/j.wasman.2012.10.015

Luan, Y. T., Chyou, Y. P., & Wang, T. (2013). Numerical analysis of gasification performance via finite-rate model in a cross-type two-stage gasifier. *International Journal of Heat and Mass Transfer*, *57*(2), 558–566. https://doi.org/10.1016/j.ijheatmasstransfer.2012.10.026

Lucas, C., Szewczyk, D., Blasiak, W., & Mochida, S. (2004). High-temperature air and steam gasification of densified biofuels. *Biomass and Bioenergy*, *27*(6), 563–575. https://doi.org/10.1016/j.biombioe.2003.08.015

Lucquiaud, M., & Gibbins, J. (2011). Steam cycle options for the retrofit of coal and gas

power plants with postcombustion capture. *Energy Procedia*, *4*, 1812–1819. https://doi.org/10.1016/j.egypro.2011.02.058

Luo, S., Xiao, B., Hu, Z., Liu, S., Guan, Y., & Cai, L. (2010). Influence of particle size on pyrolysis and gasification performance of municipal solid waste in a fixed bed reactor. *Bioresource Technology*, *101*(16), 6517–6520. https://doi.org/10.1016/j.biortech.2010.03.060

Lv, P. M., Xiong, Z. H., Chang, J., Wu, C. Z., Chen, Y., & Zhu, J. X. (2004). An experimental study on biomass air-steam gasification in a fluidized bed. *Bioresource Technology*, *95*(1), 95–101. https://doi.org/10.1016/j.biortech.2004.02.003

Mac an Bhaird, S. T., Hemmingway, P., Walsh, E., Maglinao, A. L., Capareda, S. C., & McDonnell, K. P. (2015). Bubbling fluidised bed gasification of wheat straw–gasifier performance using mullite as bed material. *Chemical Engineering Research and Design*, *97*, 36–44. https://doi.org/10.1016/j.cherd.2015.03.010

Macías-Machín, a., Socorro, M., Verona, J. M., & Macías, M. (2006). New granular material for hot gas filtration: Use of the "Lapilli." *Chemical Engineering and Processing: Process Intensification*, *45*(9), 719–727. https://doi.org/10.1016/j.cep.2006.02.009

Mahapatra, S., & Dasappa, S. (2014). Influence of surface area to volume ratio of fuel particles on gasification process in a fixed bed. *Energy for Sustainable Development*, *19*(1), 122–129. https://doi.org/10.1016/j.esd.2013.12.013

Mainali, B., & Silveira, S. (2015). Using a sustainability index to assess energy technologies for rural electrification. *Renewable and Sustainable Energy Reviews*, *41*, 1351–1365. https://doi.org/10.1016/j.rser.2014.09.018

Makwana, J. P., Joshi, A. K., Athawale, G., Singh, D., & Mohanty, P. (2015). Air gasification of rice husk in bubbling fluidized bed reactor with bed heating by conventional charcoal. *Bioresource Technology*, *178*, 45–52. https://doi.org/10.1016/j.biortech.2014.09.111

Manyà, J. J., Sánchez, J. L., Ábrego, J., Gonzalo, A., & Arauzo, J. (2006). Influence of gas residence time and air ratio on the air gasification of dried sewage sludge in a bubbling fluidised bed. *Fuel*, *85*(14–15), 2027–2033. https://doi.org/10.1016/j.fuel.2006.04.008

Martínez, J. D., Mahkamov, K., Andrade, R. V., & Silva Lora, E. E. (2012). Syngas production in downdraft biomass gasifiers and its application using internal combustion engines. *Renewable Energy*, *38*(1), 1–9. https://doi.org/10.1016/j.renene.2011.07.035

McKendry, P. (2002). Energy production from biomass (Part 3): Gasification technologies. *Bioresource Technology*, *83*(1), 55–63. Retrieved from http://www.ncbi.nlm.nih.gov/pubmed/12058831

Mendiara, T., Izquierdo, M. T., Abad, A., Diego, L. F. De, Gayán, P., & Adánez, J. (2014). International Journal of Greenhouse Gas Control Release of pollutant components in CLC of lignite. *International Journal of Greenhouse Gas Control*, *22*, 15–24. https://doi.org/10.1016/j.ijggc.2013.12.013

Meng, X., De Jong, W., Pal, R., & Verkooijen, A. H. M. (2010). In bed and downstream hot gas desulphurization during solid fuel gasification: A review. *Fuel Processing Technology*, *91*(8), 964–981. https://doi.org/10.1016/j.fuproc.2010.02.005

Moldavsky, L., Gutfinger, C., Oron, A., & Fichman, M. (2013). Effect of sonic waves on gas filtration by granular beds. *Journal of Aerosol Science*, *57*, 125–130. https://doi.org/10.1016/j.jaerosci.2012.10.002

Moroń, W., & Rybak, W. (2015). NOx and SO2 emissions of coals, biomass and their blends

under different oxy-fuel atmospheres. *Atmospheric Environment*, *116*, 65–71. https://doi.org/10.1016/j.atmosenv.2015.06.013

Mountouris, a., Voutsas, E., & Tassios, D. (2006). Solid waste plasma gasification: Equilibrium model development and exergy analysis. *Energy Conversion and Management*, *47*, 1723–1737. https://doi.org/10.1016/j.enconman.2005.10.015

Mun, T. Y., Kim, J. O., Kim, J. W., & Kim, J. S. (2011). Influence of operation conditions and additives on the development of producer gas and tar reduction in air gasification of construction woody wastes using a two-stage gasifier. *Bioresource Technology*, *102*(14), 7196–7203. https://doi.org/10.1016/j.biortech.2011.04.068

Mun, T. Y., & Kim, J. S. (2013). Air gasification of dried sewage sludge in a two-stage gasifier. Part 2: Calcined dolomite as a bed material and effect of moisture content of dried sewage sludge for the hydrogen production and tar removal. *International Journal of Hydrogen Energy*, *38*(13), 5235–5242. https://doi.org/10.1016/j.ijhydene.2013.02.073

Mun, T. Y., Seon, P. G., & Kim, J. S. (2010). Production of a producer gas from woody waste via air gasification using activated carbon and a two-stage gasifier and characterization of tar. *Fuel*, *89*(11), 3226–3234. https://doi.org/10.1016/j.fuel.2010.05.042

Mustafi, N. N., Raine, R. R., & Verhelst, S. (2013). Combustion and emissions characteristics of a dual fuel engine operated on alternative gaseous fuels. *Fuel*, *109*, 669–678. https://doi.org/10.1016/j.fuel.2013.03.007

Ndibe, C., Grathwohl, S., Paneru, M., Maier, J., & Scheffknecht, G. (2015). Emissions reduction and deposits characteristics during cofiring of high shares of torrefied biomass in a 500kW pulverized coal furnace. *Fuel*, *156*, 177–189. https://doi.org/10.1016/j.fuel.2015.04.017

Ngo, S. I., Lim, Y.-I., Song, B.-H., Lee, U.-D., Lee, J.-W., & Song, J.-H. (2015). Effects of fluidization velocity on solid stack volume in a bubbling fluidized-bed with nozzle-type distributor. *Powder Technology*, *275*, 188–198. https://doi.org/10.1016/j.powtec.2015.02.017

Ngo, S. I., Nguyen, T. D. B., Lim, Y. Il, Song, B. H., Lee, U. Do, Choi, Y. T., & Song, J. H. (2011). Performance evaluation for dual circulating fluidized-bed steam gasifier of biomass using quasi-equilibrium three-stage gasification model. *Applied Energy*, *88*(12), 5208–5220. https://doi.org/10.1016/j.apenergy.2011.07.046

Nisamaneenate, J., Atong, D., & Sornkade, P. (2015). Fuel gas production from peanut shell waste using a modular downdraft gasi fi er with the thermal integrated unit. *Renewable Energy*, *79*, 45–50. https://doi.org/10.1016/j.renene.2014.09.046

Nsamba, H. K., Hale, S. E., Cornelissen, G., & Bachmann, R. T. (2015). Sustainable Technologies for Small-Scale Biochar Production — A Review, (March), 10–31.

Núñez-Regueira, L. (2001). Determination of calorific values of forest waste biomass by static bomb calorimetry. *Thermochimica Acta*, *371*(1–2), 23–31. https://doi.org/10.1016/S0040-6031(01)00421-X

Obernberger, I., & Thek, G. (2008). Combustion and gasification of solid biomass for heat and power production in Europe-State of the art and relevant future development. *8th European Conference on Industrial Furnaces and Boilers*, (April 2008), 1–24. https://doi.org/978-972-99309-3-5

Okigbo, B. N. (1980). Nutritional implications of projects giving high priority to the

production of staples of low nutritive quality: The Case for Cassava (Manihot esculenta, Crantz) in the Humid Tropics of West Africa. *Africa*, *4*(3), Accessed 08.09.09.

Okudoh, V., Trois, C., Workneh, T., & Schmidt, S. (2014). The potential of cassava biomass and applicable technologies for sustainable biogas production in South Africa : A review. *Renewable and Sustainable Energy Reviews*, *39*, 1035–1052. https://doi.org/10.1016/j.rser.2014.07.142

Olgun, H., Ozdogan, S., & Yinesor, G. (2010). Results with a bench scale downdraft biomass gasifier for agricultural and forestry residues, *5*(1). https://doi.org/10.1016/j.biombioe.2010.10.028

Paethanom, A., Nakahara, S., Kobayashi, M., Prawisudha, P., & Yoshikawa, K. (2012). Performance of tar removal by absorption and adsorption for biomass gasification. *Fuel Processing Technology*, *104*, 144–154. https://doi.org/10.1016/j.fuproc.2012.05.006

Papagiannakis, R. G., Rakopoulos, C. D., Hountalas, D. T., & Rakopoulos, D. C. (2010). Emission characteristics of high speed, dual fuel, compression ignition engine operating in a wide range of natural gas/diesel fuel proportions. *Fuel*, *89*(7), 1397–1406. https://doi.org/10.1016/j.fuel.2009.11.001

Parikh, J., Channiwala, S., & Ghosal, G. (2005). A correlation for calculating HHV from proximate analysis of solid fuels. *Fuel*, *84*(5), 487–494. https://doi.org/10.1016/j.fuel.2004.10.010

Pattanotai, T., Watanabe, H., & Okazaki, K. (2015). Effects of particle aspect ratio on pyrolysis and gasification of anisotropic wood cylinder. *Fuel*, *150*, 162–168. https://doi.org/10.1016/j.fuel.2015.02.017

Pérez, J. F., Melgar, A., & Nel, P. (2012). Effect of operating and design parameters on the gasification / combustion process of waste biomass in fixed bed downdraft reactors : An experimental study, *96*, 487–496. https://doi.org/10.1016/j.fuel.2012.01.064

Perry, R., Green, D., & Maloney, J. (1997). *Perry's chemical engineers' handbook*. *Journal of Chemical Education*. Retrieved from http://pubs.acs.org/doi/pdf/10.1021/ed027p533.1%5Cnhttp://www.lavoisier.fr/livre/notice.asp?ouvrage=1037804

Pighinelli, A. L. M. T., Boateng, A. a., Mullen, C. a., & Elkasabi, Y. (2014a). Evaluation of Brazilian biomasses as feedstocks for fuel production via fast pyrolysis. *Energy for Sustainable Development*, *21*, 42–50. https://doi.org/10.1016/j.esd.2014.05.002

Pighinelli, A. L. M. T., Boateng, A. a., Mullen, C. a., & Elkasabi, Y. (2014b). Evaluation of Brazilian biomasses as feedstocks for fuel production via fast pyrolysis. *Energy for Sustainable Development*, *21*, 42–50. https://doi.org/10.1016/j.esd.2014.05.002

Plis, P., & Wilk, R. K. (2011). Theoretical and experimental investigation of biomass gasification process in a fixed bed gasifier. *Energy*, *36*(6), 3838–3845. https://doi.org/10.1016/j.energy.2010.08.039

Popp, J., Lakner, Z., Harangi-rákos, M., & Fári, M. (2014). The effect of bioenergy expansion : Food , energy , and environment. *Renewable and Sustainable Energy Reviews*, *32*, 559–578. https://doi.org/10.1016/j.rser.2014.01.056

Prins, M. J. (2005). *Thermodynamic analysis of biomass gasification and torrefaction*. *Library*.

Rakopoulos, C. D., Kosmadakis, G. M., Demuynck, J., De Paepe, M., & Verhelst, S. (2011). A combined experimental and numerical study of thermal processes, performance and

nitric oxide emissions in a hydrogen-fueled spark-ignition engine. *International Journal of Hydrogen Energy*, *36*(8), 5163–5180. https://doi.org/10.1016/j.ijhydene.2011.01.103

Raman, P., & Ram, N. K. (2013a). Design improvements and performance testing of a biomass gasifier based electric power generation system. *Biomass and Bioenergy*, *56*, 555–571. https://doi.org/10.1016/j.biombioe.2013.06.004

Raman, P., & Ram, N. K. (2013b). Performance analysis of an internal combustion engine operated on producer gas, in comparison with the performance of the natural gas and diesel engines. *Energy*, *63*, 317–333. https://doi.org/10.1016/j.energy.2013.10.033

Ran, J., & Li, C. (2012). High temperature gasification of woody biomass using regenerative gasifier. *Fuel Processing Technology*, *99*, 90–96. https://doi.org/10.1016/j.fuproc.2012.01.002

Rao, S. G. (2003). Experiments and modelling studies of producer gas based spark-ignited reciprocating engines [. *PhD thesis.Indian Institute of Science, Bangalore, INDIA*.

Rapagnà, S., Gallucci, K., Di Marcello, M., Foscolo, P. U., Nacken, M., Heidenreich, S., & Matt, M. (2012). First Al2O3 based catalytic filter candles operating in the fluidized bed gasifier freeboard. *Fuel*, *97*, 718–724. https://doi.org/10.1016/j.fuel.2012.02.043

Rapagnà, S., Gallucci, K., Di Marcello, M., Matt, M., Nacken, M., Heidenreich, S., & Foscolo, P. U. (2010). Gas cleaning, gas conditioning and tar abatement by means of a catalytic filter candle in a biomass fluidized-bed gasifier. *Bioresource Technology*, *101*(18), 7134–41. https://doi.org/10.1016/j.biortech.2010.03.139

Reed, T.B. and Das, A. (1988). Downdraft Gasifier Engine Systems Handbook of Biomass, (March). Retrieved from http://www.nrel.gov/docs/legosti/old/3022.pdf

Roethlisberger, R. P., & Favrat, D. (2002). Comparison between direct and indirect (prechamber) spark ignition in the case of a cogeneration natural gas engine,. *Applied Thermal Engineering*, *22*(11), 1231–1243. https://doi.org/10.1016/S1359-4311(02)00041-8

Rosillo-Calle, F. (2012). Food versus Fuel Toward a New Paradigm—The Need for a Holistic Approach.

Roy, P. C., Datta, A., & Chakraborty, N. (2009). Modelling of a downdraft biomass gasifier with finite rate kinetics in the reduction zone, (December 2008), 833–851. https://doi.org/10.1002/er

Ryu, C., Yang, Y. Bin, Khor, A., Yates, N. E., Sharifi, V. N., & Swithenbank, J. (2006). Effect of fuel properties on biomass combustion: Part I. Experiments—fuel type, equivalence ratio and particle size. *Fuel*, *85*(7–8), 1039–1046. https://doi.org/10.1016/j.fuel.2005.09.019

Sánchez, J. L., Murillo, M. B., Rodríguez, E., & Gea, G. (2014). Air – steam gasification of sewage sludge in a fluidized bed . Influence of some operating conditions. *CHEMICAL ENGINEERING JOURNAL*, *248*, 373–382. https://doi.org/10.1016/j.cej.2014.03.055

Saravanakumar, a., Haridasan, T. M., Reed, T. B., & Bai, R. K. (2007). Experimental investigation and modelling study of long stick wood gasification in a top lit updraft fixed bed gasifier. *Fuel*, *86*(17–18), 2846–2856. https://doi.org/10.1016/j.fuel.2007.03.028

Sarkar, M., Kumar, A., Tumuluru, J. S., Patil, K. N., & Bellmer, D. D. (2014). Gasification performance of switchgrass pretreated with torrefaction and densification. *Applied Energy*, *127*, 194–201. https://doi.org/10.1016/j.apenergy.2014.04.027

Sarker, S., Bimbela, F., Luis, J., & Kofoed, H. (2015). Characterization and pilot scale fluidized bed gasification of herbaceous biomass : A case study on alfalfa pellets. *Energy Conversion and Management*, *91*, 451–458. https://doi.org/10.1016/j.enconman.2014.12.034

Sarker, S., & Nielsen, H. K. (2015). Assessing the gasification potential of five woodchips species by employing a lab-scale fixed-bed downdraft reactor. *Energy Conversion and Management*, *103*, 801–813. https://doi.org/10.1016/j.enconman.2015.07.022

Scheffknecht, G., & Ndibe, C. (2015). Biomass and Bioenergy Combustion , co fi ring and emissions characteristics of torre fi ed biomass in a drop tube reactor. https://doi.org/10.1016/j.biombioe.2015.05.010

Schmieder, H., Abeln, J., Boukis, N., Dinjus, E., Kruse, A., Kluth, M., … Schacht, M. (2000). Hydrothermal gasification of biomass and organic wastes. *The Journal of Supercritical Fluids*, *17*(2), 145–153. https://doi.org/10.1016/S0896-8446(99)00051-0

Schoeters, J., Maniatis, K., & Buekens, A. (1989). The fluidized-bed gasification of biomass: Experimental studies on a bench scale reactor. *Biomass*, *19*(1–2), 129–143. https://doi.org/10.1016/0144-4565(89)90011-5

Schuster, G., Löffler, G., Weigl, K., & Hofbauer, H. (2001). Biomass steam gasification - An extensive parametric modeling study. *Bioresource Technology*, *77*, 71–79. https://doi.org/10.1016/S0960-8524(00)00115-2

Seggiani, M., Puccini, M., Raggio, G., & Vitolo, S. (2012). Effect of sewage sludge content on gas quality and solid residues produced by cogasification in an updraft gasifier. *Waste Management*, *32*(10), 1826–1834. https://doi.org/10.1016/j.wasman.2012.04.018

Senapati, P. K., & Behera, S. (2012). Experimental investigation on an entrained flow type biomass gasification system using coconut coir dust as powdery biomass feedstock. *Bioresource Technology*, *117*, 99–106. https://doi.org/10.1016/j.biortech.2012.04.049

Service, F., Nicholls, D., & Zerbe, J. (2012). Cofiring Biomass and Coal for Fossil Fuel Reduction and Other Benefits — Status of North American Facilities in 2010.

Shadloo, M. S., Poultangari, R., Abdollahzadeh Jamalabadi, M. Y., & Rashidi, M. M. (2015). A new and efficient mechanism for spark ignition engines. *Energy Conversion and Management*, *96*, 418–429. https://doi.org/10.1016/j.enconman.2015.03.017

Sharma, A., Takanohashi, T., & Saito, I. (2008). Effect of catalyst addition on gasification reactivity of HyperCoal and coal with steam at 775 – 700 ° C, *87*, 2686–2690. https://doi.org/10.1016/j.fuel.2008.03.010

Sheth, P. N., & Babu, B. V. (2009). Experimental studies on producer gas generation from wood waste in a downdraft biomass gasifier. *Bioresource Technology*, *100*(12), 3127–3133. https://doi.org/10.1016/j.biortech.2009.01.024

Sibanda, V., Greenwood, R. W., & Seville, J. P. K. (2001). Particle separation from gases using cross-flow filtration. *Powder Technology*, *118*(1–2), 193–202. https://doi.org/10.1016/S0032-5910(01)00311-4

Sibanda, V., Greenwood, R. W., Seville, J. P. K., Ding, Y., & Iyuke, S. (2010). Predicting particle segregation in cross-flow gas filtration. *Powder Technology*, *203*(3), 419–427. https://doi.org/10.1016/j.powtec.2010.03.039

Siedlecki, M., de Jong, W., & Verkooijen, A. H. M. (2011). Fluidized bed gasification as a mature and reliable technology for the production of bio-syngas and applied in the production of liquid transportation fuels-a review. *Energies*, *4*(3), 389–434.

https://doi.org/10.3390/en4030389

Sievers, D. A., Kuhn, E. M., Stickel, J. J., Tucker, M. P., & Wolfrum, E. J. (2016). Online residence time distribution measurement of thermochemical biomass pretreatment reactors. *Chemical Engineering Science*, *140*, 330–336. https://doi.org/10.1016/j.ces.2015.10.031

Simanjuntak, J. P., & Zainal, Z. a. (2015). Experimental study and characterization of a two-compartment cylindrical internally circulating fluidized bed gasifier. *Biomass and Bioenergy*, *77*, 147–154. https://doi.org/10.1016/j.biombioe.2015.03.023

Singh, A., & Madhoolika, A. (2008). Acid rain and its ecological consequences, *29*(x), 15–24.

Singh, R. K., Murty, H. R., Gupta, S. K., & Dikshit, A. K. (2012). An overview of sustainability assessment methodologies. *Ecological Indicators*, *15*(1), 281–299. https://doi.org/10.1016/j.ecolind.2011.01.007

Skoulou, V., Koufodimos, G., Samaras, Z., & Zabaniotou, a. (2008). Low temperature gasification of olive kernels in a 5-kW fluidized bed reactor for H2-rich producer gas. *International Journal of Hydrogen Energy*, *33*(22), 6515–6524. https://doi.org/10.1016/j.ijhydene.2008.07.074

Son, Y.-I., Yoon, S. J., Kim, Y. K., & Lee, J.-G. (2011). Gasification and power generation characteristics of woody biomass utilizing a downdraft gasifier. *Biomass and Bioenergy*, *35*(10), 4215–4220. https://doi.org/10.1016/j.biombioe.2011.07.008

Soundararajan, R., Anantharaman, R., & Gundersen, T. (2014). Design of Steam Cycles for Oxy-combustion Coal based Power Plants with Emphasis on Heat Integration. *Energy Procedia*, *51*(1876), 119–126. https://doi.org/10.1016/j.egypro.2014.07.013

Splitter, D. a., & Reitz, R. D. (2014). Fuel reactivity effects on the efficiency and operational window of dual-fuel compression ignition engines. *Fuel*, *118*, 163–175. https://doi.org/10.1016/j.fuel.2013.10.045

Sprouse, C., & Depcik, C. (2013). Review of organic Rankine cycles for internal combustion engine exhaust waste heat recovery. *Applied Thermal Engineering*, *51*(1–2), 711–722. https://doi.org/10.1016/j.applthermaleng.2012.10.017

Stine, W. B. (1994). 8 . 5 Stirling Engines Thermodynamic Implementation of the Stirling Cycle. *Energy Conversion*, *1872*, 67–76.

Stolarski, M. J., Krzyżaniak, M., Łuczyński, M., Załuski, D., Szczukowski, S., Tworkowski, J., & Gołaszewski, J. (2015a). Lignocellulosic biomass from short rotation woody crops as a feedstock for second-generation bioethanol production. *Industrial Crops and Products*. https://doi.org/10.1016/j.indcrop.2015.04.025

Stolarski, M. J., Krzyżaniak, M., Łuczyński, M., Załuski, D., Szczukowski, S., Tworkowski, J., & Gołaszewski, J. (2015b). Lignocellulosic biomass from short rotation woody crops as a feedstock for second-generation bioethanol production. *Industrial Crops and Products*. https://doi.org/10.1016/j.indcrop.2015.04.025

Sutton, D., Kelleher, B., Doyle, A., & Ross, J. R. H. (2001). Investigation of nickel supported catalysts for the upgrading of brown peat derived gasi ® cation products, *80*, 111–116.

Tahani, M., Javan, S., & Biglari, M. (2013). A comprehensive study on waste heat recovery from internal combustion engines using organic rankine cycle. *Thermal Science*, *17*(2), 611–624. https://doi.org/10.2298/TSCI111219051T

Tan, Z., Liu, S., Bliss, N., & Tieszen, L. L. (2012). Current and potential sustainable corn

stover feedstock for biofuel production in the United States. *Biomass and Bioenergy*, *47*, 372–386. https://doi.org/10.1016/j.biombioe.2012.09.022

Tao, J., Lu, Q., Dong, C., Du, X., & Dahlquist, E. (2015). Effects of electric current upon catalytic steam reforming of biomass gasification tar model compounds to syngas. *Energy Conversion and Management*, *100*, 56–63. https://doi.org/10.1016/j.enconman.2015.05.003

Tassios, D. (1993). Applied chemical engineering thermodynamics. *Springer-Verlag*.

Tay, H. L., Kajitani, S., Zhang, S., & Li, C. Z. (2013). Effects of gasifying agent on the evolution of char structure during the gasification of Victorian brown coal. *Fuel*, *103*, 22–28. https://doi.org/10.1016/j.fuel.2011.02.044

Teir, S. (2002). Basics of Steam Generation.

Thomas. B. Reed, Mike Markson, S. E. R. I. (1983). A Predictive Model for Stratified Downdraft Gasification of Biomass. *Solar Energy Research Institute*,.

Tinaut, F. V, Melgar, A., Pérez, J. F., & Horrillo, A. (2008). Effect of biomass particle size and air superficial velocity on the gasification process in a downdraft fixed bed gasifier . An experimental and modelling study. *Fuel Processing Technology*, *89*(11), 1076–1089. https://doi.org/10.1016/j.fuproc.2008.04.010

Tinwala, F., Mohanty, P., Parmar, S., Patel, A., & Pant, K. K. (2015). Intermediate pyrolysis of agro-industrial biomasses in bench-scale pyrolyser: Product yields and its characterization. *Bioresource Technology*, *188*, 258–264. https://doi.org/10.1016/j.biortech.2015.02.006

Tryner, J., Willson, B. D., & Marchese, A. J. (2014). The effects of fuel type and stove design on emissions and efficiency of natural-draft semi-gasifier biomass cookstoves. *Energy for Sustainable Development*, *23*, 99–109. https://doi.org/10.1016/j.esd.2014.07.009

Tsiakmakis, S., Mertzis, D., Dimaratos, A., Toumasatos, Z., & Samaras, Z. (2014). Experimental study of combustion in a spark ignition engine operating with producer gas from various biomass feedstocks. *Fuel*, *122*, 126–139. https://doi.org/10.1016/j.fuel.2014.01.013

Tyndall, J. C., Berg, E. J., & Colletti, J. P. (2011). Corn stover as a biofuel feedstock in Iowa's bio-economy: An Iowa farmer survey. *Biomass and Bioenergy*, *35*(4), 1485–1495. https://doi.org/10.1016/j.biombioe.2010.08.049

United Nations. (2007). *Indicators of Sustainable Development : Guidelines and Methodologies*. *New York*.

US DOE. (2004). Biomass Cofiring in Coal-Fired Boilers, 40.

Vaja, I., & Gambarotta, A. (2010). Internal Combustion Engine (ICE) bottoming with Organic Rankine Cycles (ORCs). *Energy*, *35*(2), 1084–1093. https://doi.org/10.1016/j.energy.2009.06.001

Van Paasen SVB, Rabou LPLM, B. R. (2004). Tar removal with a wet electrostatic precipitator (esp); a parametric study, (May), 1–8.

Vinterbäck, J. (2010). versus Food and Feed ,.

Wang, C., Zhang, L., Chang, Y., & Pang, M. (2015). Biomass direct-fired power generation system in China: An integrated energy, GHG emissions, and economic evaluation for Salix. *Energy Policy*, *84*, 155–165. https://doi.org/10.1016/j.enpol.2015.04.025

Wang, Y., Yoshikawa, K., Namioka, T., & Hashimoto, Y. (2007). Performance optimization

of two-staged gasification system for woody biomass. *Fuel Processing Technology*, *88*(3), 243–250. https://doi.org/10.1016/j.fuproc.2006.10.002

Wu, M.-H., Lin, C.-L., & Zeng, W.-Y. (2014). Effect of waste incineration and gasification processes on heavy metal distribution. *Fuel Processing Technology*, *125*, 67–72. https://doi.org/10.1016/j.fuproc.2014.03.027

Xiao, R., Jin, B., Zhou, H., Zhong, Z., & Zhang, M. (2007). Air gasification of polypropylene plastic waste in fluidized bed gasifier. *Energy Conversion and Management*, *48*(3), 778–786. https://doi.org/10.1016/j.enconman.2006.09.004

Xiao, R., Zhang, M., Jin, B., Huang, Y., & Zhou, H. (2006). High-temperature air/steam-blown gasification of coal in a pressurized spout-fluid bed. *Energy and Fuels*, *20*(2), 715–720. https://doi.org/10.1021/ef050233h

Xiong, S., Zhuo, J., Zhang, B., & Yao, Q. (2013). Journal of Analytical and Applied Pyrolysis Effect of moisture content on the characterization of products from the pyrolysis of sewage sludge. *Journal of Analytical and Applied Pyrolysis*, *104*, 632–639. https://doi.org/10.1016/j.jaap.2013.05.003

Xu, Z. R., Zhu, W., & Li, M. (2012). Influence of moisture content on the direct gasification of dewatered sludge via supercritical water, *7*(1), 0–8. https://doi.org/10.1016/j.ijhydene.2012.01.086

Yaliwal, V. S., Banapurmath, N. R., Gireesh, N. M., & Tewari, P. G. (2014). Production and utilization of renewable and sustainable gaseous fuel for power generation applications: A review of literature. *Renewable and Sustainable Energy Reviews*, *34*, 608–627. https://doi.org/10.1016/j.rser.2014.03.043

Yamazaki, T., Kozu, H., Yamagata, S., Murao, N., Ohta, S., Shiya, S., & Ohba, T. (2005). Effect of Superficial Velocity on Tar from Downdraft Gasification of Biomass, (17), 1186–1191.

Yang, J., & Chen, B. (2014). Emergy analysis of a biogas-linked agricultural system in rural China - A case study in Gongcheng Yao Autonomous County. *Applied Energy*, *118*, 173–182. https://doi.org/10.1016/j.apenergy.2013.12.038

Yang, W., Ponzio, A., Lucas, C., & Blasiak, W. (2006). Performance analysis of a fixed-bed biomass gasifier using high-temperature air. *Fuel Processing Technology*, *87*(3), 235–245. https://doi.org/10.1016/j.fuproc.2005.08.004

Yang, Y. B., Yamauchi, H., Nasserzadeh, V., & Swithenbank, J. (2003). Effects of fuel devolatilisation on the combustion of wood chips and incineration of simulated municipal solid wastes in a packed bed. *Fuel*, *82*(18), 2205–2221. https://doi.org/10.1016/S0016-2361(03)00145-5

Yao, Y., Tsai, J., & Wang, I. (2013). Emissions of gaseous pollutant from motorcycle powered by ethanol – gasoline blend. *Applied Energy*, *102*, 93–100. https://doi.org/10.1016/j.apenergy.2012.07.041

Yin, R., Liu, R., Wu, J., Wu, X., Sun, C., & Wu, C. (2012). Influence of particle size on performance of a pilot-scale fixed-bed gasification system. *Bioresource Technology*, *119*, 15–21. https://doi.org/10.1016/j.biortech.2012.05.085

Yoon, S. J., Son, Y.-I., Kim, Y.-K., & Lee, J.-G. (2012). Gasification and power generation characteristics of rice husk and rice husk pellet using a downdraft fixed-bed gasifier. *Renewable Energy*, *42*, 163–167. https://doi.org/10.1016/j.renene.2011.08.028

Yoshiie, R., Taya, Y., Ichiyanagi, T., Ueki, Y., & Naruse, I. (2013). Emissions of particles

and trace elements from coal gasification. *Fuel*, *108*, 67–72. https://doi.org/10.1016/j.fuel.2011.06.011

Yuntenwi, E. a. T., MacCarty, N., Still, D., & Ertel, J. (2008). Laboratory study of the effects of moisture content on heat transfer and combustion efficiency of three biomass cook stoves. *Energy for Sustainable Development*, *12*(2), 66–77. https://doi.org/10.1016/S0973-0826(08)60430-5

Zainal, Z. ., Rifau, A., Quadir, G. ., & Seetharamu, K. . (2002a). Experimental investigation of a downdraft biomass gasifier. *Biomass and Bioenergy*, *23*(4), 283–289. https://doi.org/10.1016/S0961-9534(02)00059-4

Zainal, Z. A., Ali, R., Lean, C. H., & Seetharamu, K. N. (2001). Prediction of performance of a downdraft gasi ® er using equilibrium modeling for di € erent biomass materials, *42*.

Zainal, Z. A., Rifau, A., Quadir, G. A., & Seetharamu, K. N. (2002b). Experimental investigation of a downdraft biomass gasiÿer, *23*(May), 283–289.

ZEF. (2014). In Focus: Biomass and Energy, (29).

Zhu, C., Liu, S., Liu, H., Yang, J., Liu, X., & Xu, G. (2015). NOx emission characteristics of fluidized bed combustion in atmospheres rich in oxygen and water vapor for high-nitrogen fuel. *Fuel*, *139*, 346–355. https://doi.org/10.1016/j.fuel.2014.08.058